Palladium-Catalyzed
Amide Formation via Masked Isocyanates

By

David Brzezinski

Thesis submitted to the University of Ottawa in partial fulfillment of the requirements for the M. Sc. Degree in Chemistry and Biomolecular Sciences

Department of Chemistry and Biomolecular Sciences
Faculty of Science
University of Ottawa

Candidate	Supervisor
David Brzezinski	Prof. André M. Beauchemin

Abstract

Amides are one of the most common functional groups in biological systems and in bioactive molecules. Arguably the most direct way to form amides is via the condensation of an amine onto a carboxylic acid. This reaction is notoriously difficult and has stimulated much development, including the developments of new reagents and catalysts to perform this transformation under milder conditions. More broadly, amide formation continues to be of high importance and the incorporation of emerging transformations utilizing new disconnections are complimentary to existing routes.

Isocyanates are the simplest electrophiles containing the desired *NCO* motif and have a large presence in the polymer (e.g. polyurethane) and paint industries. In addition, isocyanates have been utilized for amide formation with various nucleophiles in a stoichiometric and catalytic fashion, but the inherent functional group intolerance associated with the high reactivity of isocyanate largely remains. Efforts have been made to address such limitations of isocyanates, including the use of a blocking group which allow for *in situ* release of the isocyanate while using a bench stable masked (blocked) isocyanate precursor. Changes to the blocking group structure have direct correlations to the stability and reactivity of the precursor, which helps in suppressing common side reactions observed with free isocyanates such as polymerization or oligomerization.

Incorporation of a blocking group strategy in catalytic amide forming reactions has the power to unlock the potential of isocyanates with reactivity that would not be attainable with free isocyanates. Reports imparting this strategy exemplify the power of a blocking group with increased applicability and functional group tolerance compared to reactions with the free isocyanate counterpart. The implementation of this strategy for catalytic amide formation is sparse including only two reports with a rhodium catalyst. Utilization of different metals could broaden the scope of reactivity allowing for extensions that the rhodium (I) catalyst cannot do.

The development of a palladium-catalyzed amide synthesis via masked isocyanates was targeted (Chapter 2). Indeed, implementation of a blocking group strategy with alkyl and aryl isocyanates allowed for efficient synthesis of amides with electron rich and mildly deficient aryl boroxine nucleophiles. Catalysis was achieved with 1 mol% of $Pd(OAc)_2$ and 2 mol% of SPhos at 50 °C with Et_3N to aid in the deblocking of the isocyanate. Several control experiments were

conducted to obtain mechanistic insight including what mechanism may be operative as well as the necessity of this blocking group strategy. Kinetic studies were performed using the variable time normalization analysis method and have yielded the following information: 1) the presence of catalyst decomposition, 2) that the rate determining step involved the catalyst, boroxine, and masked isocyanate, and 3) that the rate determining step is likely the insertion into the isocyanate.

In summary, palladium catalysts can achieve catalysis with masked isocyanates to facilitate amide formation under appropriate conditions. With limited reports of masked isocyanates in catalysis, this reactivity could act as a steppingstone for developments of reactivity that are held back with the use of free isocyanates.

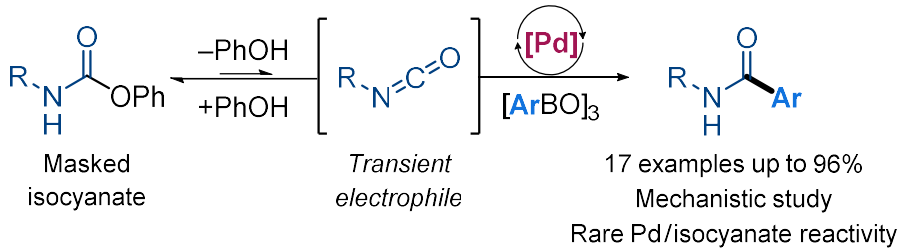

Acknowledgements

First and foremost, I would like to thank Dr. André Beauchemin for taking me into his lab back in May 2017. He has been a staple in my success as an emerging chemist by supporting me, guiding me, and pushing me to meet deadlines. His contagious positive attitude towards chemistry and high optimism helps make anything feel like it is possible.

I would like to thank Josh for laying the foundation of the Pd project and giving me guidance as this project was evolving into what it is now. His unprecedented knowledge in catalysis helped in the determination of many of the side products that were obtained throughout this study. Furthermore, even after graduating, he had aided in the kinetic studies that turned into a large undertaking that I couldn't do on my lonesome.

The welcoming nature all the members of the Beauchemin group has allowed to me develop friendships which in turn have extended past the boundaries of the lab to include many excursions that have made this time that much more enjoyable. I would like to thank William for supporting my wellbeing by always sharing his food with me. Meredith, Ryan, Dilan, and Jasper for always being there to brainstorm and get to the root of the problem at hand and tell me all about their projects and how passionate they are about them. I would also like to thank Neda, Alshimaa, and Frédéric that have accompanied me through this journey and to all the undergraduate students that have passed through the lab.

The consequence of being in a small department such as chemistry has allowed me to get to know a good chunk of the community and develop deep rooted friendships with many more people than only the people that are in the Beauchemin group. These friendships have exposed me to many different types of chemistry that are not just organic chemistry. I also need to thank some of the faculty members that have helped me towards the end of my MSc degree. Dr. Keillor has served a huge role in crunching the numbers obtained from the kinetic study as well as helping interpret the meanings behind them. Dr. Facey and Dr. Pallister were always there to help with deconvoluting the data I had obtained from NMR experiments and had helped in the NMR experiments I had to do. Dr. Newman, Dr. Pratt, and Dr. Richeson have served as people that I can go to talk to about chemistry and talk to about current events.

Table of Contents

Abstract ii
Acknowledgements iv
List of Figures viii
List of Schemes ix
List of Tables xi
List of Abbreviations xii
Statement of Contributions xvi
Chapter 1 : Introduction 1
1.1 : Amide Synthesis 2
1.1.1 : Activated Ester Formation 3
1.1.2 : Acid Chloride Formation 4
1.1.3 : Coupling via acid anhydride 5
1.1.4 : Amide formation with carbon monoxide 6
1.1.5 : Methyl esters as electrophilic partners for synthesis of amides 6
1.2 : Isocyanates 7
1.2.1 : Masked Isocyanates 8
1.3 : Amide Syntheses with Isocyanates 9
1.3.1 : Carboxylic acid addition to isocyanates 9
1.3.2 : Stoichiometric carbon-based nucleophilic addition to isocyanates 10
1.3.3 : Catalytic carbon-based nucleophilic addition to isocyanates 12
1.4 : Palladium-catalyzed heterocumulene addition 15
1.4.1 : Carbon dioxide fixation with palladium 16
1.4.2 : Palladium-catalyzed additions to isocyanates 18
1.5 : Catalytic approaches with masked isocyanates 24

1.5.1 : Heteroatom-based additions to masked isocyanates 25
1.5.2 : Carbon-based additions to masked isocyanates 26
1.6 : Project goals 29
Chapter 2 : 31
2.1 : Towards a palladium-catalyzed activation of blocked isocyanates 32
2.1.1 : Preliminary studies into the palladium project 32
2.1.2 : Optimization study 34
2.1.3 : Surveying the applicability of the palladium-catalyzed reaction 39
2.2 : Investigation into the mechanism 42
2.2.1 : Investigation into a Pd(0)/(II) type mechanism 43
2.2.2 : Proposal of a Pd(II) mechanism 46
2.2.3 : Attempts to further probe the mechanism 48
2.3 : Kinetic studies 56
2.3.1 : Kinetically probing the catalyst 60
2.3.2 : Kinetically probing the reaction order in carbamate reagent 66
2.3.3 : Kinetically probing the reaction order in boroxine reagent 68
2.3.4 : Tracing the kinetic results to the mechanism 69
Chapter 3 : 71
Chapter 4 : 74
4.1 : General information 75
4.2 : Supporting information for Chapter 2 75
4.2.1 : Starting material synthesis 76
4.2.2 : Supplementary optimization data 82
4.2.3 : Synthesis of substrates from tables Table 2-6 and Table 2-7 84

4.2.4 : Supplemental data for kinetic studies 95

Appendix I 104

Claims to Original Research 105

Presentations from this work 105

Spectra 106

List of Figures

Figure 1-1: Amine addition to activated carboxylic acid derivative..... 2

Figure 1-2: Carbodiimide coupling agents 3

Figure 1-3: Reagents used for acid chloride formation 4

Figure 1-4: Major resonance structures of isocyanates..... 7

Figure 2-1: Early studies visually showing the order in $Pd(OAc)_2$ (upper) and **1g** (lower) both being zero..... 60

Figure 2-2: Experiments probing if catalyst decomposition (upper) or product deactivation (lower) is present..... 62

Figure 2-3: Determining the kinetic profile of the catalyst using the VTNA approach including 0 (upper), 0.5 (middle), and 1 (lower) as possible orders..... 64

Figure 2-4: Analyzing the reaction profile of the catalyst using VTNA with Dr. Keillor's mathematical algorithm 66

Figure 2-5: Analyzing the reaction order for the carbamate reagent (**1g**) using VTNA contrasting between a visual (upper) and mathematical (lower) approach 67

Figure 2-6: Analyzing the reaction order for the boroxine reagent (**2a**) using VTNA contrasting between a visual (upper) and mathematical (lower) approach 69

Figure 3-1: Summary of Project 72

Figure 4-1: Order in catalyst with points omitted..... 103

List of Schemes

Scheme 1-1: Carbodiimide-mediated amidation pathways 3

Scheme 1-2: DMF catalyzed acid chloride formation via thionyl chloride 4

Scheme 1-3: Mechanism of Vilsmeier reagent generation 5

Scheme 1-4: Carbonic acid anhydride formation via EEDQ 6

Scheme 1-5: Palladium-catalyzed benzylic aminocarbonylation 6

Scheme 1-6: Nickel-catalyzed amide formation with heteroaromatic esters 7

Scheme 1-7: Deblocking temperatures of isocyanates 8

Scheme 1-8: Oligomerization products of isocyanates 9

Scheme 1-9: Carboxylic acid addition to isocyanates 9

Scheme 1-10: Proposed decarboxylation mechanistic pathway 10

Scheme 1-11: Grignard addition to isocyanates 11

Scheme 1-12: Amidation of electron rich arene 11

Scheme 1-13: Intramolecular Friedel-Crafts reaction with an isocyanate 11

Scheme 1-14: Seminal report of the addition of benzene to phenyl isocyanate 12

Scheme 1-15: Rh(III) Aminocarbonylation with isocyanates 13

Scheme 1-16: Rhodium-catalyzed organostannane addition to isocyanates 13

Scheme 1-17: Rhodium-catalyzed organoboron addition to isocyanates 14

Scheme 1-18: Titanium-catalyzed Grignard addition to isocyanates 15

Scheme 1-19: Palladium mediated telomerization of 1,3-butadiene with CO_2 16

Scheme 1-20: Palladium-catalyzed addition of organozinc reagents to CO_2 17

Scheme 1-21: Pd(II)-catalyzed carboxylation of alkenyl C-H bonds with CO_2 17

Scheme 1-22: Palladium-catalyzed ring-expansion of epoxides 19

Scheme 1-23: Palladium-catalyzed three-component amide formation 20

Scheme 1-24: Heterocycle formation through a bis-allyl palladacycle intermediate 20

Scheme 1-25: Bimetallic catalytic system for synthesis of N-(alkoxycarbonyl)indole subunits . 22

Scheme 1-26: Murakami's work with 2(alkynyl)phenyl isocyanates 23

Scheme 1-27: Palladium-catalyzed organoboron addition to isocyanates..... 23

Scheme 1-28: Palladium-catalyzed 5-exo dig cyclization with isocyanates 24

Scheme 1-29: Palladium-catalyzed unsymmetrical urea formation via sodium cyanate 25

Scheme 1-30: Palladium oxidative addition complex for cross-linking of peptides and proteins 26

Scheme 1-31: Rhodium-catalyzed direct amidation of carbamate protected amines with proposed mechanism 28

Scheme 1-32: Rhodium-catalyzed amidation of masked isocyanates 29

Scheme 2-1:Formation of biaryl product..... 42

Scheme 2-2: Carbamate oxidative addition pathways..... 43

Scheme 2-3: Probing the carbamate oxidative addition pathway..... 44

Scheme 2-4: Possible Pd(0)/(II) type catalytic cycle..... 45

Scheme 2-5: Proposed oxidation of Pd(0) with isocyanates..... 46

Scheme 2-6: Oligomerization control experiments 47

Scheme 2-7: Proposed Pd(II) catalytic cycle..... 48

Scheme 2-8: Scale-up reaction with phenyl isocyanate..... 53

Scheme 2-9: Conditions for kinetic study..... 58

List of Tables

Table 2-1: Initial optimization for the Pd-catalyzed system[a] 33

Table 2-2: Base screen[a] 35

Table 2-3: Effect of solvent [a] 36

Table 2-4: Palladium precatalyst screen[a] 37

Table 2-5: Second ligand scan[a] 38

Table 2-6: Scope of aryl boroxines[a] 40

Table 2-7: Scope of blocked isocyanates[a] 41

Table 2-8: Exploring different organoboron reagents[a] 50

Table 2-9: Control reactions on free isocyanate[a] 52

Table 2-10: Exploring different blocking group[a] 54

Table 2-11: More blocking groups[a] 56

Table 4-1: Boron equivalent[a] 83

Table 4-2: Temperature dependence[a] 83

Table 4-3: Supplemental data for Figure 2-1 95

Table 4-4: Raw data for inhibition studies (Figure 2-2)[a] 96

Table 4-5: Raw data for determination of the order in catalyst (Figure 2-3) 97

Table 4-6: Raw data for determination of order in **1g** (Figure 2-5) 99

Table 4-7: Raw data for determination of order in **2a** (Figure 2-6) 100

List of Abbreviations

acac	Acetylacetone
Ar	Aryl
atm	Atmosphere
Bn	Benzyl
Boc	*tert*-Butoxycarbonyl
br.	Broad
Bu	Butyl
cat.	Catalytic
$CDCl_3$	Deuterochloroform
$CHCl_3$	Chloroform
Cbz	Carboxybenzyl
cod	1,5-cyclooctadiene
cp	Cyclopentyl
Cy	Cyclohexyl
°C	Degree Celsius
δ	Chemical shift in parts per million
d	Doublet
dba	Dibenzylideneacetone
DBU	1,8-Diazabicyclo[5.4.0]undec-7-ene
dd	Doublet of doublets
DCC	*N,N'*-Dicyclohexylcarbodiimide
DCM	Methylene chloride

DIPEA	Diisopropyl ethylamine
DMF	Dimethyl formamide
DMSO	Dimethyl sulfoxide
EDC	(1-Ethyl-3-(3'-dimethylaminopropyl)-carbodiimide hydrochloride
EEDQ	2-Ethoxy-1-ethoxycarbonyl-1,2-dihydroquinoline
EI	Electron impact
Elim.	Elimination
EtOAc	Ethyl acetate
EtOH	Ethanol
Et_2O	Diethyl ether
Et_3N	Triethylamine
eq. or equiv.	Equivalent
ESI-TOF	Electron spray ionization time of flight
Et	Ethyl
FG	Functional group
h	Hour
HCl	Hydrochloric acid
HOBt	1-Hydroxybenzotriazole
HRMS	High-resolution mass spectrometry
Hz	Hertz
i-Pr	Isopropyl
IR	Infrared
J	Coupling constant

LG	Leaving group
L	Ligand
M	Molar
m	Multiplet
Me	Methyl
MeOH	Methanol
MeCN	Acetonitrile
mg	Milligram
mL	Milliliter
mmol	Millimole
Nuc	Nucleophile
NMR	Nuclear magnetic resonance
OAc	Acetate
o.n.	Overnight
Ph	Phenyl
PhOH	Phenol
PivCl	Pivaloyl chloride
pKa	Acid dissociation constant
ppm	Parts per million
R	Carbon-based substituent
RPKA	Reaction profile kinetic analysis
r.t.	Room temperature
$SOCl_2$	Thionyl chloride

t	Tertiary
TFA	Trifluoroacetic acid
THF	Tetrahydrofuran
TLC	Thin layer chromatography
TMS	Trimethylsilane
Tol	Toluene
Ts	*para*-Toluenesulfonyl
VTNA	Variable time normalization analysis

Statement of Contributions

Over the course of my time as a graduate student in the Beauchemin lab, I had the opportunity to collaborate with my fellow graduate students as well as undergraduate students. Herein I will layout my contributions to the project described in this thesis.

At the beginning of my studies, I collaborated with Mr. Joshua Derasp for four months, who served as my immediate supervisor during our developments of a palladium-catalyzed amide formation via masked isocyanates. Mr. Joshua Derasp came up with the hypothesis where he obtained the first hit (Table 2-1) when he was nearing the conclusion of his rhodium-catalyzed amide formation via masked isocyanates project. The results outlined in Table 2-1 are the sole results obtained by Mr. Joshua Derasp before I started working on this project.

The optimization study of this reaction was largely a collaborative effort, although just beginning as a graduate student, Mr. Joshua Derasp governed the paths that were taken towards the optimized conditions. Surveying the applicability and scale-up of this transformation was largely my work with only a few entries obtained by Mr. Joshua Derasp (indicated as a footnote in Table 2-6 and Table 2-7). At this time, control reactions outlined in Scheme 2-6, Scheme 2-8 and Table 2-9 were conducted by Mr. Joshua Derasp which were performed to better understand the mechanism.

Following this, kinetic studies using the variable time normalization analysis methodology were performed where from Mr. Joshua Derasp could provide guidance remotely, as he had performed similar studies for his Rh work, but did not engage in this work since he has been a postdoctoral fellow since June 2019. With the limited conclusions drawn from the kinetic study, we sought the expertise of Prof. Jeffrey Keillor to elucidate the short comings of the analysis. This sprouted a collaboration with Prof. Jeffrey Keillor to process the data that was obtained experimentally which was in turn used to draw some of the conclusion outlined in this thesis.

Chapter 1: Introduction

1.1: Amide Synthesis

Amides are among some of the most prevalent functional groups in chemistry and their synthesis accounts for approximately 16% of all reactions carried out in medicinal chemistry laboratories.[1] The most direct way of forming this bond is by the condensation of a carboxylic acid and an amine extruding a molecule of water, but this method does require very forcing conditions (>100 °C) limiting the compatibility with chemical complexity.[1] To mitigate this problem, acid activation (Figure 1-1) is required to promote the coupling with less forcing conditions that are compatible with more complex molecules.[1] One of the most prevalent methods of amide formation is with a carbodiimide coupling agent, although these reactions have been designed to be very efficient, there is a vast amount of waste produced.[1] More modern methodologies of forging amides are through catalytic reactions (Figure 1-1) which have the opportunity to enable cleaner chemistry by the reduction of stoichiometric waste. Because this thesis focuses on amide formation using a palladium-catalyzed amide synthesis using masked isocyanates, the relevant context on amide syntheses, acid activation and isocyanate addition will be provided in the introduction chapter (Figure 1-1).

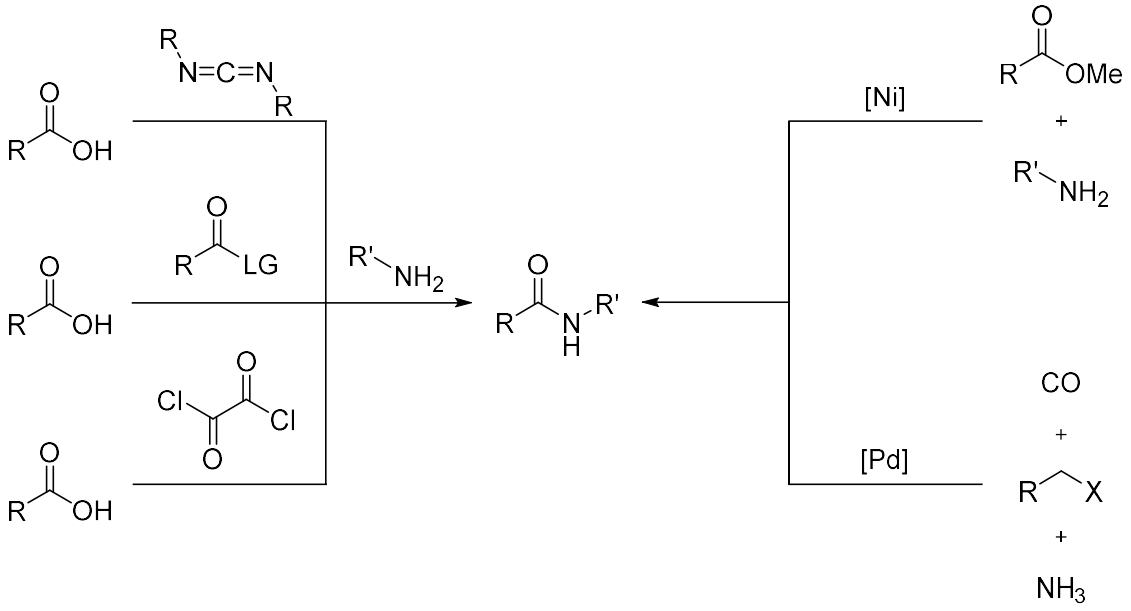

Figure 1-1: Amine addition to activated carboxylic acid derivative

[1] Dunetz, J. R.; Magano, J.; Weisenburger, G. A. *Org. Process Res. Dev.* **2016,** *20*, 140.

1.1.1: Activated Ester Formation

Activated ester formation is one of the most widely used methods in process chemistry to form an amide bond.[1] This primarily involves the use of a coupling agent such as (1-ethyl-3-(3'-dimethylaminopropyl)-carbodiimide hydrochloride (EDC) and *N,N'*-dicyclohexylcarbodiimide (DCC) shown in Figure 1-2. These coupling reagents are required to be used in stoichiometric

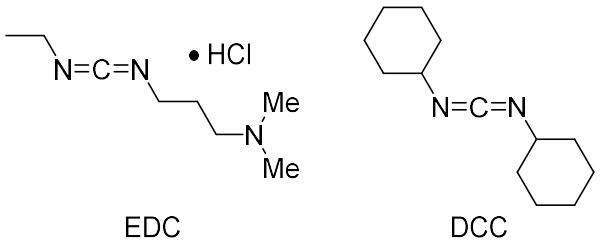

Figure 1-2: Carbodiimide coupling agents

amount and give urea by-products. EDC is the most widely used carbodiimide for the synthesis of drug candidates primarily because the urea by-product is water-soluble and can be removed during the aqueous workup.[1]

The coupling reaction starts with the formation of an ion pair between the carbodiimide and the acid that forms *O*-acylisourea which is an activated electrophile (Scheme 1-1). This intermediate can undergo various reactions that can lead to both the desired amide as well as unwanted side products. The major unwanted pathway is the rearrangement of the *O*-acylisourea into an *N*-acylurea which is an irreversible reaction. The first desired reaction is the reaction with

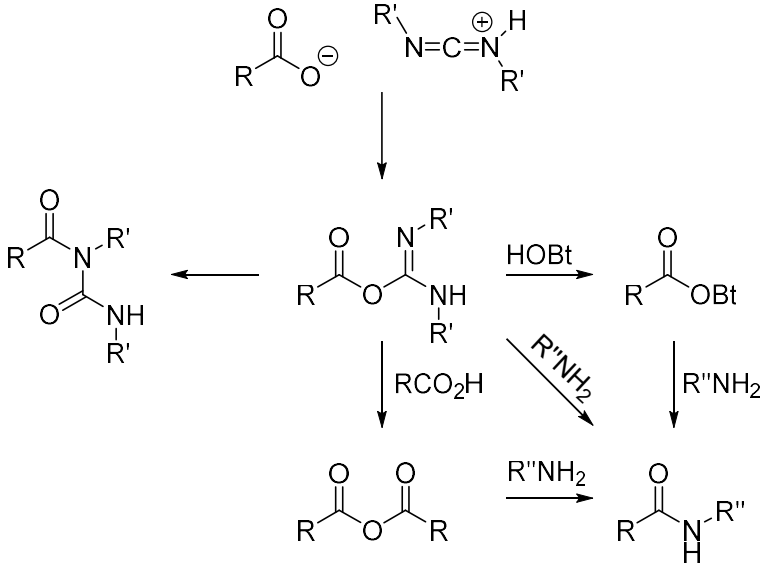

Scheme 1-1: Carbodiimide-mediated amidation

the amine which results in the desired amide. The presence of a second equivalent of the acid gives rise to the possibility for anhydride formation, followed by the addition of the amine to again form the desired amide. An additive such as HOBt can be used to help mitigate side product formation by adding more productive pathways for this coupling to undergo.

1.1.2: Acid Chloride Formation

Another widely used method of amide bond formation is through the conversion of the carboxylic acid into the corresponding acid chloride. There are several reagents that have been employed for such transformations, namely thionyl chloride, oxalyl chloride, phosphorous oxychloride, and the Vilsmeier-Haak reagent (Figure 1-3). The Vilsmeier reagent was first

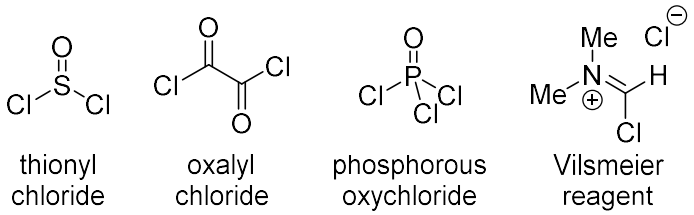

Figure 1-3: Reagents used for acid chloride formation

synthesized in 1927 by using *N*-methylformanilide and phosphorous oxychloride.[2] These reagents have all been employed on large scale but thionyl chloride and oxalyl chloride are the most widely used in process chemistry.[1] One drawback when using this methodology is that an equivalent of HCl is produced in the amide bond formation which can lead to incompatibility with acid-sensitive groups. An aqueous base can be used in tandem to neutralize the formation of the acid produced. A catalytic amount of DMF is often used in tandem with thionyl chloride, oxalyl chloride, and phosphorous oxychloride to serve as a catalyst for acid chloride formation (Scheme 1-2). The use of DMF allows for the generation of the Vilsmeier intermediate which regenerates the DMF and forms the acid chloride.[1] The Vilsmeier reagent can also be purchased, but the high cost makes it

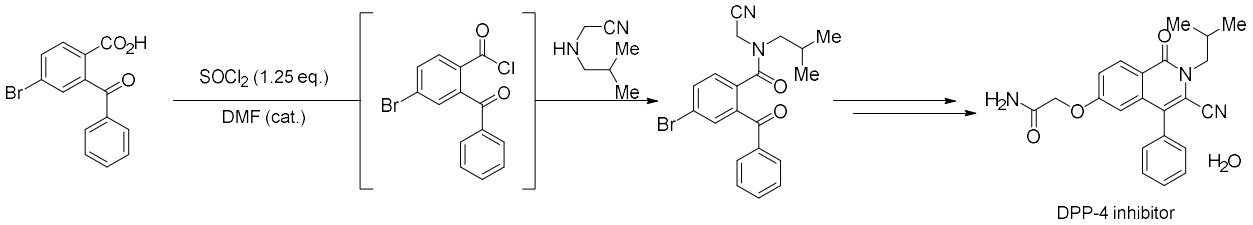

Scheme 1-2: DMF catalyzed acid chloride formation via thionyl chloride

[2] Vilsmeier, A.; Haack, A. *Ber.* **1927,** *60*, 119.

not viable on large scale.[1] A recent example of using this process on kilogram scale is shown in Scheme 1-2.[3]

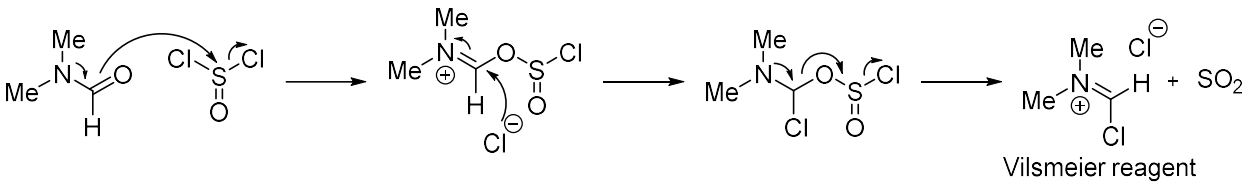

Scheme 1-3: Mechanism of Vilsmeier reagent generation

1.1.3: Coupling via acid anhydride

This methodology uses an activating agent that allows formation of either a mixed carboxylic acid anhydride or carbonic acid anhydride as an intermediate which can then be attacked by an amine to enable the coupling.[1] Mixed carboxylic acid anhydrides can be formed with use of reagents such as acetic anhydride[4] or pivaloyl chloride,[5] while carbonic acid anhydrides are formed using reagents such as ethyl chloroformate,[6] Boc anhydride,[7] and EEDQ.[8] The former method suffers from regiochemical control which can be avoided by increasing the steric bulk of the reagent that is used to form the mixed anhydride.[1] PivCl targets the regiochemical problem because it imposes enough steric bulk to reduce this problem and is often used on large scale because of its relatively low cost and wide availability. The latter method relies on the relative electrophilicity of the two carbonyls that are generated to dictate regiochemistry in Scheme 1-4. Ethyl chloroformate has been used on large scale, but usage is sparse compared to isobutyl chloroformate due to its toxicity and volatility.[1] The by-products of these reactions are easily removed which makes these reactions quite desirable.

---

[3] Sera, M.; Yamashita, M.; Ono, Y.; Tabata, T.; Muto, E.; Ouchi, T.; Tawada, H. *Org. Process Res. Dev.* **2014,** *18*, 446.
[4] Hoekstra, M. S.; Sobieray, D. M.; Schwindt, M. A.; Mulhern, T. A.; Grote, T. M.; Huckabee, B. K.; Hendrickson, V. S.; Franklin, L. C.; Granger, E. J.; Karrick, G. L. *Org. Process Res. Dev*. **1997,** *1*, 26.
[5] Li, B.-F.; Hughes, R. M.; Le, J.; McGee, K.; Gallagher, D. J.; Gross, R. S.; Provencal, D.; Reddy, J. P.; Wang, P.; Zegelman, L.; Zhao, Y.; Zook, S. E. *Org. Process Res. Dev*. **2009,** *13*, 463.
[6] Hirokawa, Y.; Horikawa, T.; Noguchi, H.; Yamamoto, K.; Kato, S. *Org. Process Res. Dev*. **2002,** *6*, 28.
[7] Patterson, D. E.; Powers, J. D.; LeBlanc, M.; Sharkey, T.; Boehler, E.; Irdam, E.; Osterhout, M. H. *Org. Process Res. Dev.* **2009,** *13*, 900.
[8] Ormerod, D.; Willemsens, B.; Mermans, R.; Langens, J.; Winderickx, G.; Kalindjian, S. B.; Buck, I. M.; McDonald, I. M. *Org. Process Res. Dev.* **2005,** *9*, 499.

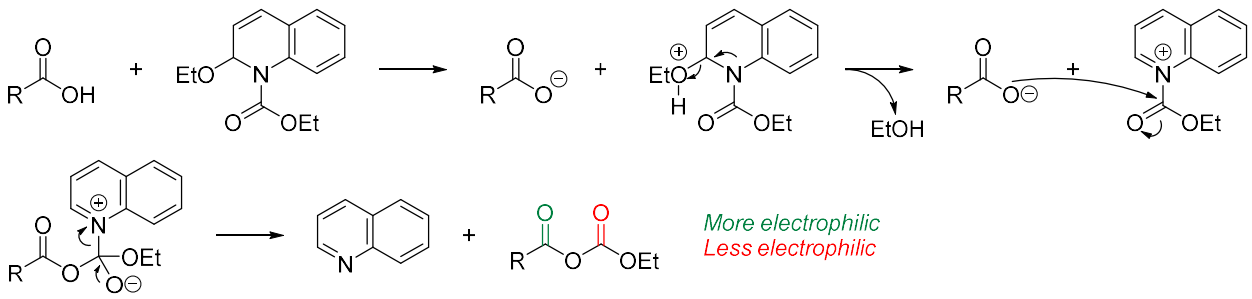

Scheme 1-4: Carbonic acid anhydride formation via EEDQ

1.1.4: Amide formation with carbon monoxide

Aminocarbonylation is the use of carbon monoxide as a carbonyl source in combination with an amine nucleophile.[9] This process requires a catalyst to allow for this transformation to occur and the first example of this was a palladium-catalyzed aminocarbonylation of aryl halides and vinyl halides by Schoenberg and Heck.[10] Compared to methods aforementioned, this does not require the use of a carboxylic acid but rather a halide functionalized substrate. Although, aminocarbonylation requires an atmosphere of carbon monoxide which does have its inherent safety concerns dealing with the toxicity of carbon monoxide. Beller and co-workers[11] communicated the palladium-catalyzed aminocarbonylation of benzyl chlorides using ammonia which opens the door for sp^3 halides rather than being limited to sp^2 halides (Scheme 1-5).

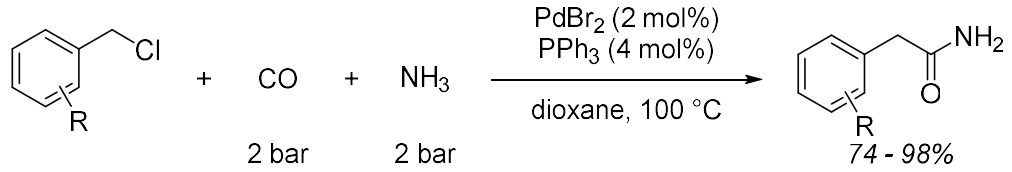

Scheme 1-5: Palladium-catalyzed benzylic aminocarbonylation

1.1.5: Methyl esters as electrophilic partners for synthesis of amides

Methyl esters are derivatives of carboxylic acids and are deemed less electrophilic owing to the higher pKa of leaving group. With the reduced electrophilicity of the carbonyl carbon, researchers often hydrolyze the methyl ester to the corresponding acid to then do acid activation to reach an even more electrophilic species. However, reaching the desired amide can be achieved

[9] Allen, C. L.; Williams, J. M. J. *Chem. Soc. Rev.* **2011,** *40*, 3405.
[10] Schoenberg, A.; Heck, R. F. *J. Org. Chem.* **1974,** *39*, 3327.
[11] Wu, X.-F.; Schranck, J.; Neumann, H.; Beller, M. *ChemCatChem* **2012,** *4*, 69.

by either activation of the ester with a Lewis acid[12] or using an organometallic base[13] to activate the amine. A recent example of nickel-catalyzed activation of a methyl ester to allow for amide synthesis was reported by Zheng and Newman (2019).[14] The ligands used enabled nickel to do an oxidative insertion into the C-O bond which does further chemistry with the amine to produce the desired amide product. Various ligands were screened, and a handful of privileged ligands were attained and were found to be suitable in this synthesis. Heteroaromatic esters as well as primary and secondary amines were found to be competent coupling partners under the reaction conditions.

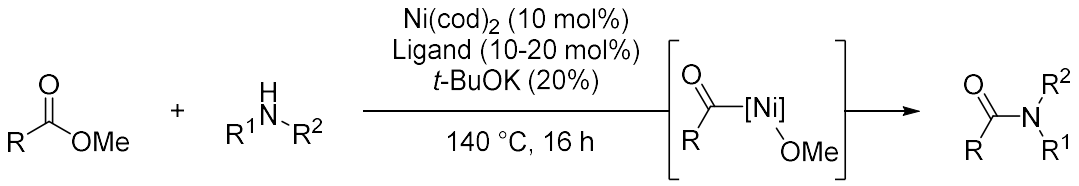

Scheme 1-6: Nickel-catalyzed amide formation with heteroaromatic esters

1.2: Isocyanates

Isocyanates were first discovered by Wurtz[15] in 1849 and consist of the *NCO* motif which has resonance structures that are shown in Figure 1-4 illustrating its ambiphilic nature. Isocyanates are very reactive species which are very important bulk chemicals that have many applications

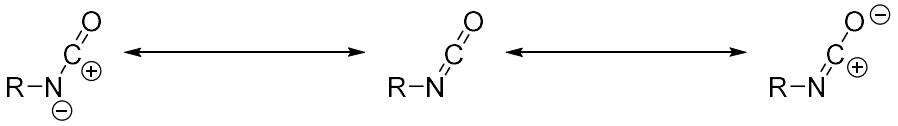

Figure 1-4: Major resonance structures of isocyanates

among coatings, paint, and polymer industries like DuPont and Bayer.[16] The synthesis of polyurethanes via the reaction of a polyester diol with diisocyanates made them one of the major chemicals produced in the world.[19] Since these species are so reactive, they do come with inherent safety concerns that affect worker health in the polymer industry. Isocyanates are powerful irritants to the mucous membranes of the eyes and gastrointestinal and respiratory tracts.[17] A famous

[12] Han, C.; Lee, J. P.; Lobkovsky, E.; Porco, J. A., Jr. *J. Am. Chem. Soc.* **2005,** *127*, 10039.
[13] Wang, W. Bo. Roskamp, E. J. *J. Org. Chem.* **1992,** *57*, 6101.
[14] Zheng, Y.-L.; Newman, S. G. *ACS Catal.* **2019,** *9*, 4426.
[15] Wurtz, A. *Justus Liebigs Ann. Chem.* **1849,** *71*, 326.
[16] Richter, F. (2012). *Ullmann's Encyclopedia of Industrial Chemistry*. Leverkusen, Germany: Bayer AG.
[17] The National Institute for Occupational Safety and Health (NIOSH)
https://www.cdc.gov/niosh/topics/isocyanates/default.html

example of the danger of these chemicals was illustrated by the tragedy at the Bhopal Union carbide plant in 1984 with methyl isocyanate.[18] Following the accident, exposure of methyl isocyanate killed thousands of people and affected the community in Bhopal for generations with mutations and birth defects. Preventing exposure to isocyanates is a critical step in eliminating the health hazard. Isocyanates have limited functional group tolerance which greatly reduces the functional groups that can be tethered on these substrates including Lewis basic entities. An effort in development for safer alternatives is in progress and an example of this is the use of masked (blocked) isocyanate reagents.

1.2.1: Masked Isocyanates

Masked isocyanates have been developed to mitigate exposure to the harmful nature of isocyanates as well as allowing for isocyanates that would not typically be available. This is done

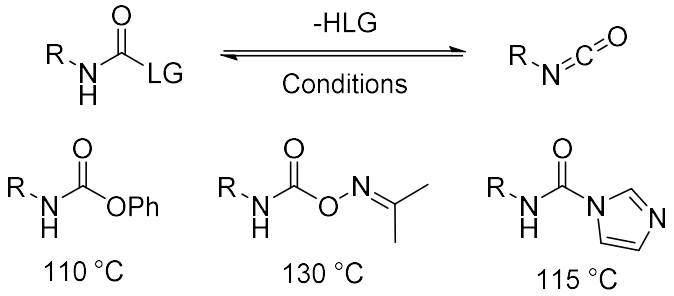

Scheme 1-7: Deblocking temperatures of isocyanates

by the release of the reactive isocyanate *in situ* by the loss of a leaving group. Various blocking groups can be used for masked isocyanates including alcohols, oximes, and amines which will generate the desired isocyanate upon heating or with basic or acidic catalysis (Scheme 1-7).[20] The deblocking temperature is the point at which the concentration of the isocyanate is no longer zero.[19] Deblocking temperatures typically have a range when they are reported because they depend highly on the R group as well as the solvent at which it is being measured in. In general, blocked aromatic isocyanates deblock at lower temperatures than blocked aliphatic isocyanates because the isocyanate is conjugated, it is picking up stability as the reaction proceeds, leading to milder conditions.[20] Other than safety, masked isocyanates are often used to reduce side reactions

[18] Broughton, E. *Environ. Health: Global Access Sci. Source* **2005,** *4,* No. 6.
[19] Delebecq, E.; Pascault, J.-P.; Boutevin, B.; Ganachaud, F. *Chem. Rev.* **2013,** *113*, 80.
[20] Wicks, D. A.; Wicks, Z. W., Jr. *Prog. Org. Coat.* **1999,** *36*, 148.

(Scheme 1-8) by limiting their concentration in solution. Uretdione and isocyanurate are the dimers and trimers of the isocyanate respectively whereas the allophanate and biuret products derive from the blocking group attacking the uretdione dimer.[20] A blocking group strategy reduces the opportunity for an isocyanate to come in contact with another equivalent of itself hence reducing undesired by-products. This can be accomplished by substrate engineering to control the rate of release as well as the temperature at which the isocyanate is released.[20]

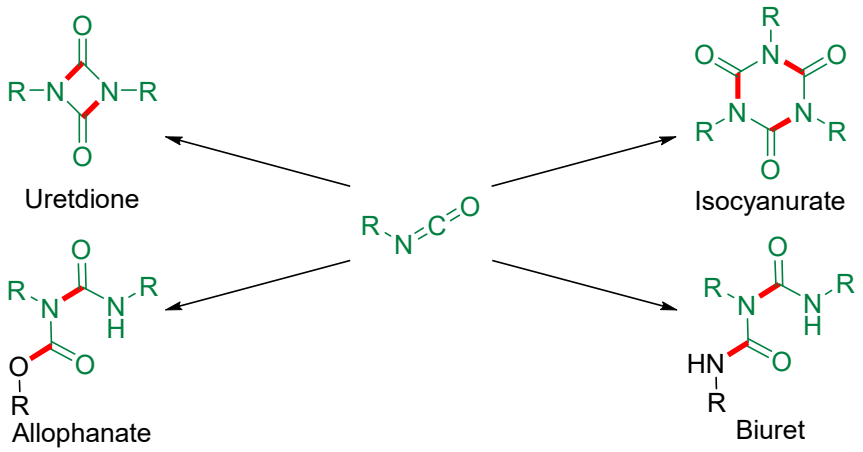

Scheme 1-8: Oligomerization products of isocyanates

1.3: Amide Syntheses with Isocyanates

Aforementioned methods assemble the carbon-nitrogen bond as a way of synthesizing the desired amide whereas an isocyanate already has the carbon-nitrogen bond present, which opens up a different disconnection for synthesis. Using isocyanates to synthesize amides would require a carbon-based nucleophile, or an equivalent thereof, to furnish the desired carbon-carbon bond.

1.3.1: Carboxylic acid addition to isocyanates

The addition of a carboxylic acid to an isocyanate would form a mixed anhydride followed by decarboxylation to furnish the desired amide (Scheme 1-9). An early example of a carboxylic

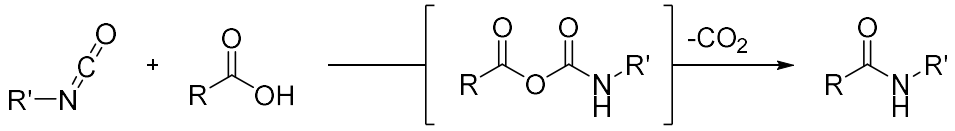

Scheme 1-9: Carboxylic acid addition to isocyanates

acid addition to an isocyanate in dry toluene at 60 °C was documented by Scott and co-workers[21] in 1986. No mechanism for the decarboxylation step was provided but it has since been documented that the carbon atom that is lost is the sp carbon of the isocyanate. The mechanism was later explained computationally to go through a pseudo-1,3 alkyl shift via a four-membered ring intermediate followed by the decarboxylation to form the desired amide (Scheme 1-10).[22] Since carboxylic acids do not have the greatest nucleophilicity, other functional groups can outcompete leading to undesired reactivity and limited functional group tolerance.[23]

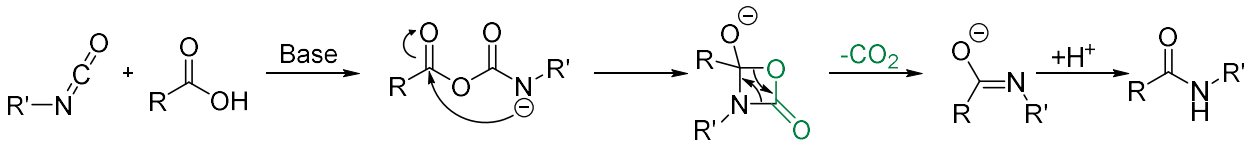

Scheme 1-10: Proposed decarboxylation mechanistic pathway

1.3.2: Stoichiometric carbon-based nucleophilic addition to isocyanates

Isocyanates are very electrophilic species which makes them suitable electrophiles for amide surrogates. Nucleophiles can vary from organometallics such as Grignard reagents or electron rich aromatics accessed by Friedel-Crafts or C-H functionalization reactions.

Grignard reagents were first described to add to isocyanates by Blaise[24] (1901) and a few accounts have been documented since then, including an example Singleton and co-workers[25] (1938) where Grignard reagents could add to isocyanates at 50 °C. Further advancements by Bode[26] enabled the Grignard addition to sterically encumbered isocyanates at 0 °C (Scheme 1-11). This procedure has been developed to require equal equivalents of each reagent and allows access to hindered amide substrates which would have otherwise been unattainable with previously described methods.

---

[21] Blagbrough, I. S.; Mackenzie, N. E.; Ortiz, C.; Scott, A. I. *Tetrahedron Lett.* **1986,** *27*, 1251.
[22] Jiang, Y.-Y.; Liu, T.-T.; Zhang, R.-X.; Xu, Z.-Y.; Sun, X.; Bi, S. *J. Org. Chem.* **2018,** *83*, 2676.
[23] Sasaki, K.; Crich, D. *Org. Lett.* **2011,** *13*, 2256. (See references cited therein for more examples of this type of reaction)
[24] Blaise, E. E. *Compt. Rend.* **1901,** *132*, 38.
[25] Singleton, H. M.; Edwards, W. R., Jr. *J. Am. Chem. Soc.* **1938,** *60*, 540.
[26] Schäfer, G.; Matthey, C.; Bode, J. W. *Angew. Chem. Int. Ed.* **2012,** *51*, 9173.

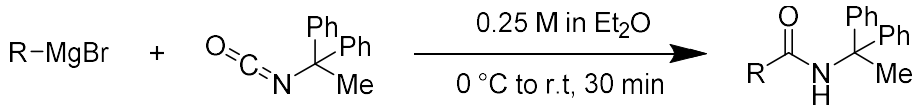

Scheme 1-11: Grignard addition to isocyanates

Friedel-Crafts reactions are as class of reactions that proceed through an electrophilic aromatic substitution allowing for the synthesis of monoacylated products. These reactions usually only do monoacylation because the product is too deactivated to do a second acylation since an electron rich arene is the required. Most Friedel-Crafts reactions require a stoichiometric amount

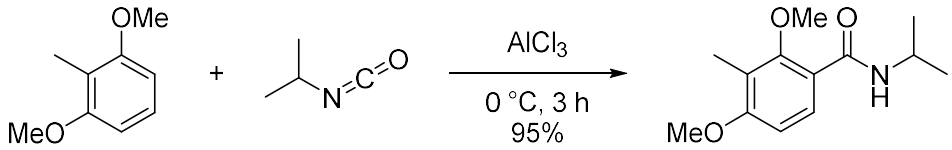

Scheme 1-12: Amidation of electron rich arene

of a Lewis acid catalyst is such as $AlCl_3$ and $FeCl_3$ and the partner is traditionally an acyl chloride, formation of an acylium ion, which is quite electrophilic. This type of reaction makes sense to work with an isocyanate because of how electrophilic they are. This has been shown by Franck[27] (2014) where they were able to do a Friedel-Crafts reaction with isopropyl isocyanate and an electron rich arene on the way to an analogue of the natural product epicocconone (Scheme 1-12).

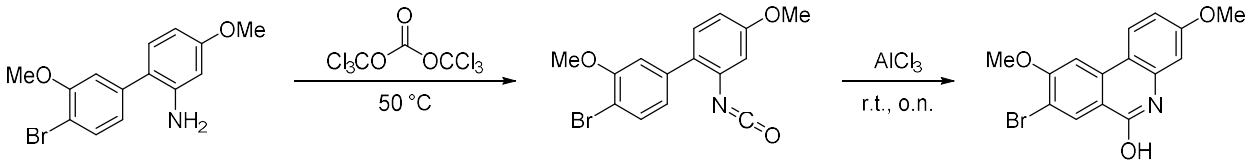

Scheme 1-13: Intramolecular Friedel-Crafts reaction with an isocyanate

This method allows for the direct addition of this amide to the most electron rich site which is *ortho* to the methoxy group. This is an example of an intermolecular coupling, but the substrate can be engineered to do the intramolecular reaction as shown in Scheme 1-13.[28] Liverton and co-workers[28] used a substrate with a pendant amine that was converted to an isocyanate with triphosgene followed by activation with Friedel-Crafts conditions allowing for the intramolecular cyclization to get their desired product.

---

[27] Piexoto, P. A.; Boulangé, A. Ball, M.; Naudin, B.; Alle, T.; Cosette, P.; Karuso, P.; Franck, X. *J. Am. Chem. Soc.* **2014,** *136*, 15248.

[28] Rudd, M.; McCauley, J.; Romano, J.; Butcher, J.; Bush, K.; McIntyre, C.; Nguyen, K.; Gilbert, K.; Lyle, T.; Holloway, M.; Wan, B.; Vacca, J.; Summa, V.; Harper, S.; Rowley, M.; Carroll, S.; Burlein, C.; DiMuzio, J.; Gates, A.; Graham, D.; Huang, Q.; Ludmerer, S.; McClain, S.; McHale, C.; Stahlhut, M.; Fandozzi, C.; Taylor, A.; Trainor, N.; Olsen, D., Liverton, N. *Bioorg. Med. Chem. Lett.* **2012,** *22*, 7201.

In contrast with use of a carboxylic acid as a nucleophile in section 1.3.1, the nucleophiles described herein can allow for more complex substrates to be attained due to their higher selectivity and milder conditions required.

1.3.3: Catalytic carbon-based nucleophilic addition to isocyanates

Isocyanates are isoelectronic to carbon dioxide, which adds value as they can be used in place of carbon dioxide where there is much less chemical diversity.[29] Methodologies of using isocyanates to add the amide functional group catalytically would target some of the *12 principles of green chemistry*.[30] Doing this reaction catalytically reduces waste and reduces derivatization. In 1978, Hong and co-workers[31] were able to devise a method that allowed for the direct addition of benzene to phenyl isocyanate to synthesize benzanilide in 41% yield under quite harsh conditions (Scheme 1-14).

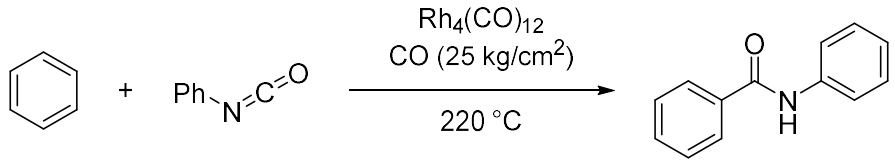

Scheme 1-14: Seminal report of the addition of benzene to

The mastery of C-H functionalization has grown in the last few decades, allowing for milder conditions to do this transformation. Rhodium has opened up the door for catalytic transformations involving the installation of an amide through the use of an isocyanate.[29] A recent example by the Wang group in 2018 displays this by a Rh(III) C(sp^3)-H bond aminocarbonylation with isocyanates.[32] This reaction shows the versatility of this approach by enabling reactivity with both aryl and alkyl isocyanates under mild conditions (Scheme 1-15). This was done by activating the C(sp^3)-H of 8-methylquinoline that can then insert into the isocyanate followed by protodemetallation. This methodology does require the coordination of the cationic rhodium with the nitrogen of the quinoline system which would limit substrate scope because this nitrogen is necessary for the reaction to proceed. Examples using a rhodium catalyst to do this transformation do require some sort of directing group to allow for the metal center to get into close proximity for

[29] Hummel, J. R.; Boerth, J. A.; Ellman, J. A. *Chem. Rev.* **2017,** *117*, 9163.
[30] Sheldon, R. A. *Chem. Soc. Rev.* **2012,** *41*, 1437.
[31] Hong, P.; Yamazaki, H.; Sonogashira, K.; Hagihara, N. *Chem. Lett.* **1978,** *7*, 535.
[32] Zhao, H.; Zho, X.; Li, b.; Liu, X.; Guo, N.; Lu, Z.; Wang, S. *J. Org. Chem.* **2018,** *83*, 4153.

the C-H functionalization step.[29] Metals including iridium, rhenium, ruthenium, cobalt, and manganese have also been shown to allow for the addition of isocyanates in a C-H functionalization type reaction.[29]

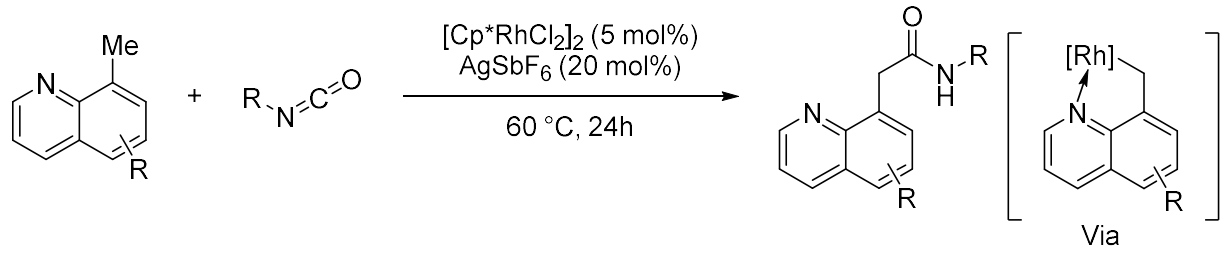

Scheme 1-15: Rh(III) Aminocarbonylation with isocyanates

Organometallic catalysts have also been used in conjunction with organostannane reagents, boronic acids, and Grignard reagents to add to isocyanates.[33] An example by Mori and co-workers[34] devised a method that allowed for the rhodium-catalyzed arylation and alkenylation of isocyanates with organostannane reagents (Scheme 1-16). It is worth noting that phenol was used in conjunction with the reaction mixture of the organostannane. The authors realized the ability of the phenol to act as a blocking group of the isocyanate and it was found that increasing the ratio of the phenol resulted in lower yields where their optimized ratio was 2:1 isocyanate:phenol.[34] The use of phenol was also found to be crucial for protoderhodation to regenerate the active catalyst.[34]

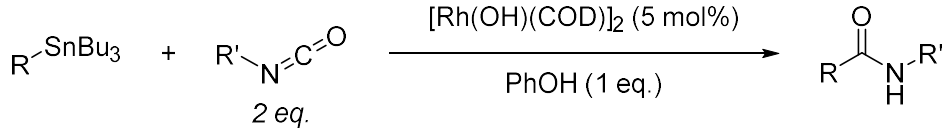

Scheme 1-16: Rhodium-catalyzed organostannane addition to

To further expand on the organometallic reagents used for the addition to isocyanates, Murakami and co-workers[35] employed organoboron reagents. The use of organoboron reagents is desirable because of their commercial availability and decreased toxicity when compared to organostannane reagents. Since organoboron reagents are widely available, the need for preparative methods involving Grignard and organolithium reagents is reduced. The use of organoboron reagents in this instance allowed for the reduction of temperature as well as the

[33] Serrano, E.; Martin, R. *Eur. J. Org. Chem.* **2018,** *2018*, 3051.
[34] Koike, T.; Takahashi, M.; Arai, N.; Mori, A. *Chem. Lett.* **2004,** *33*, 1364.
[35] Miura, T.; Takahashi, Y.; Murakami, M. *Chem. Commun.* **2007,** 3577.

loading of the rhodium catalyst (Scheme 1-17). It is also worth noting that the use of phenol was not necessary for this reaction whereas it was necessary in the organostannane reaction described above.[34]

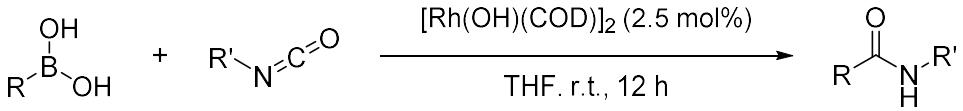

Scheme 1-17: Rhodium-catalyzed organoboron addition to

As previously described,[26] the synthesis of hindered and electron-deficient secondary amide from isocyanates with Grignard reagents (Scheme 1-11). However, before Bode reported this in 2012, Zhang reported the titanium catalyzed addition of branched and linear alkyl Grignard reagents to phenyl isocyanate at -10 ℃ (Scheme 1-18) but due to the high reactive nature of Grignard reagents, substances possessing sensitive functional groups were precluded.[36] Additionally, since titanium catalysts prefer a less sterically encumbered state, only the linear products were obtained as titanium can do β-hydride elimination followed by the reinsertion to get the less sterically encumbered linear product. The active catalyst is likely being formed by the reducing the Ti (IV) with the Grignard reagent. The following year, Zhang reported[37] that at higher temperatures, urea products could be obtained by Cp_2TiH reducing the isocyanate to a secondary amine which could then attack another equivalent of the isocyanate.

[36] Zhang, Y.; Jiang, J.; Chen. Y. *Tetrahedron Lett.* **1987,** *28*, 3815.
[37] Zhang, Y.; Jiang, J.; Zhang, Z. *Tetrahedron Lett.* **1988,** *29*, 651.

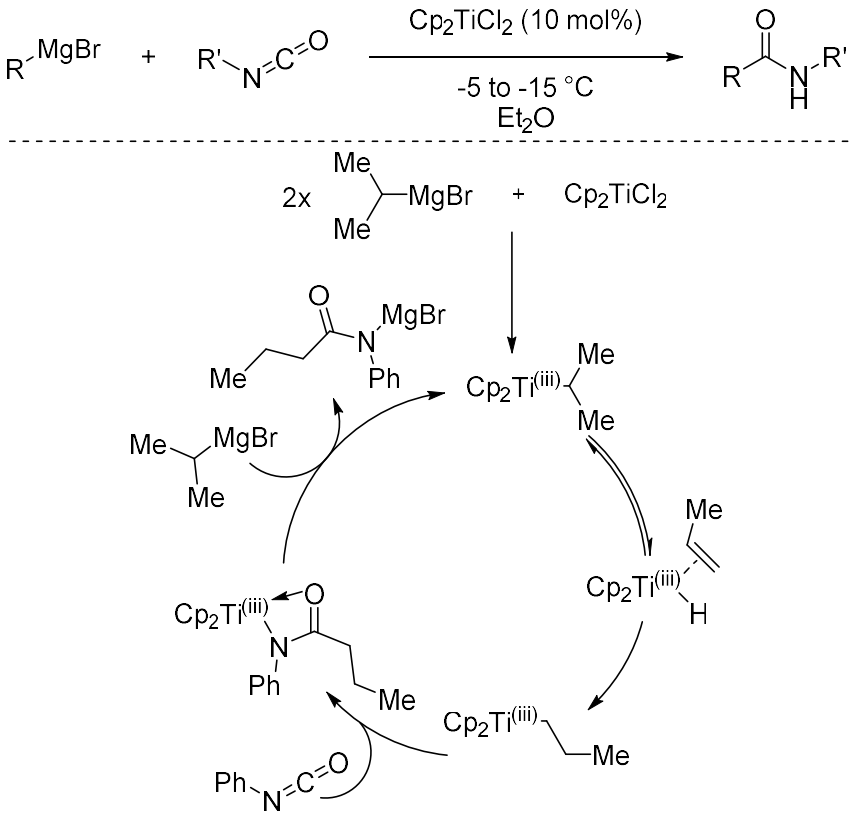

Scheme 1-18: Titanium-catalyzed Grignard addition to

1.4: Palladium-catalyzed heterocumulene addition

A cumulene is hydrocarbon with two or more consecutive double bonds. A heterocumulene like the name suggests is a cumulene that has one of the doubly bonded carbon atoms being replaced with a heteroatom. Heterocumulenes encompass isocyanates and carbon dioxide because they include an array of 3 atoms doubly bonded to each other. Isocyanates are isoelectronic to CO_2 which could lead one to believe that modern catalytic carboxylation reactions could be transcribed to isocyanates for the formation of amides. Although other metals have been seen to enable this transformation, palladium will be the general focus of this section as this is largely the core of this study.

1.4.1: Carbon dioxide fixation with palladium

Carbon dioxide has had a steady increase as a component in greenhouse gases since pre-industrial times.[38] This increase in CO_2 concentration is largely due to the combustion of fossil fuels, which are required to meet the world's energy demand.[38] Since CO_2 is so abundant, the need to reduce concentration has never been so great. CO_2 has the potential to be used for its carbon atom for the ability to create new C-C bonds with carbon nucleophiles. However, activation of CO_2 is difficult because this is the most oxidized form of carbon which makes it relatively inert for use in mild transformations.[38] To create new C-C bonds with CO_2, the use of carbon nucleophiles is limited to organolithium and Grignard reagents due to their strong nucleophilic character.[38]

Pathways that palladium can go through to make new C-C bonds with carbon dioxide include oxidative cyclometallation, nucleophilic carboxylation, nucleophilic carbonylation. Oxidative cyclometallation pathways are typically limited to systems with extended π systems such as dienes and diynes.[38] Behr and co-workers[39] communicated the reaction of butadiene in the presence of solid CO_2 and a catalyst system of $Pd(acac)_2/P(i\text{-}Pr)_3$ to synthesize various lactones (Scheme 1-19). Mechanistic studies suggested that the product shown in Scheme 1-19 was isomerizing to give the side-products obtained and that the δ-lactone could be isomerized selectively to the γ-lactone.[39]

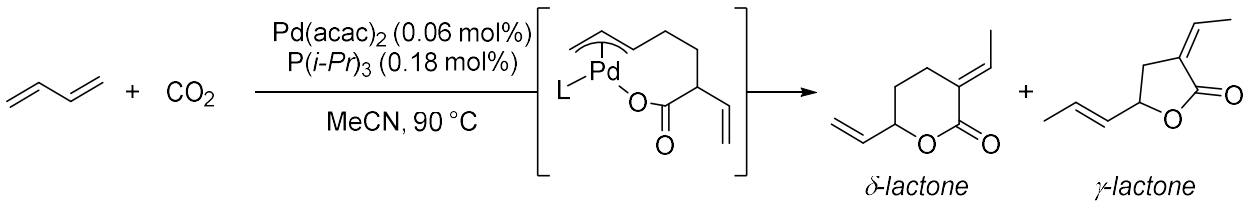

Scheme 1-19: Palladium mediated telomerization of 1,3-butadiene with CO_2

A more recent example of palladium being used to catalyze C-C bond formation with CO_2 was communicated by Dong and co-workers[40] where organozinc reagents were added to CO_2 to form carboxylic acids (Scheme 1-20). This research was inspired by the Aresta complex (Ni(η^2-

[38] Liu, Q.; Wu, L.; Beller, M. *Nat. Commun.* **2015,** *6*, 5933.
[39] Behr, A.; Juszak, K.-D. *J. Organomet. Chem.* **1983,** *255*, 263.
[40] Yeung, C. S.; Dong, V, M. *J. Am. Chem. Soc.* **2008,** *130*, 7826.

CO_2)(PCy_3)$_2$) which was the first metal-CO_2 complex to be isolated and characterized.[41] The authors thought this complex would readily undergo transmetallation with organozinc reagents followed by reductive elimination to furnish the desired C-C bond. Dong and co-workers[40] were able to extend this chemistry to work with palladium salts, namely $Pd(OAc)_2$ with PCy_3 as a ligand, allowing for reactivity with both electron poor and rich organozinc arenes.

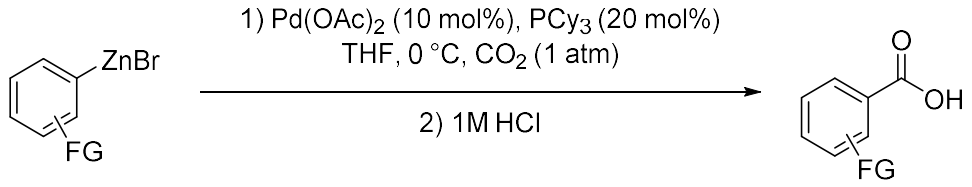

Scheme 1-20: Palladium-catalyzed addition of organozinc reagents to CO_2

Traditionally, carbonylation reactions utilize the high reactivity of phosgene as a carbonylative reagent, but in light of the development of transition metal catalysis, phosgene has been mostly replaced with the use of carbon monoxide.[42] Carbonylation reactions traditionally utilize CO for constructing a synthetically versatile carbonyl group with high efficiency and selectivity.[43] However, CO is highly toxic which causes safety issues as well as high cost.[43] CO_2 has been employed to allow for advances in this area as a formyl carbonylation reagent either by decarboxylation or reduction *in situ*.

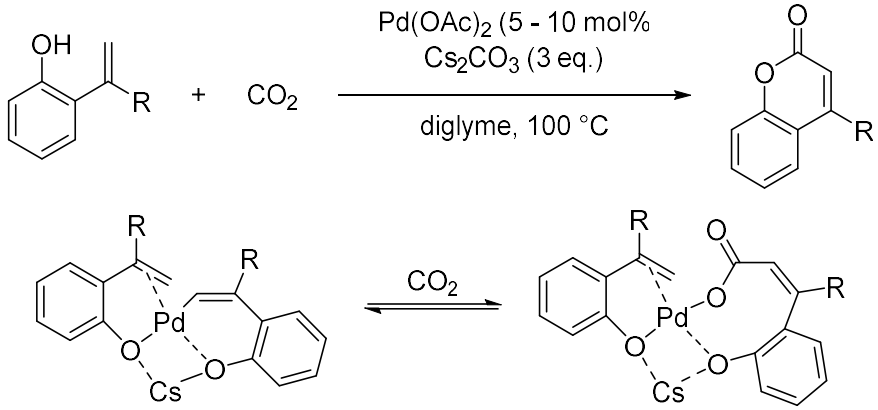

Scheme 1-21: Pd(II)-catalyzed carboxylation of alkenyl C-H bonds with CO_2

[41] Aresta, M.; Nobile, C. F.; Albano, V. G.; Forni, E.; Manassero, M. *J. Chem. Soc., Chem. Commun*. **1975,** *15*, 636.
[42] Song, L.; Jiang, Y.-X.; Zhang, Z.; Gui, Y.-Y.; Zhou, X.-Y.; Yu, D.-G. *Chem. Commun.* **2020,** *56*, 8355.
[43] Wu, L.; Fang, X.; Liu, Q.; Jackstell, R.; Beller, M.; Wu, X.-F. *ACS Catal.* **2014,** *4*, 2977.

The use of CO_2 as a carbonyl source has been recently reported by Iwasawa and co-workers[44] with the palladium(II)-catalyzed direct carboxylation of alkenyl C-H bonds with CO_2 (Scheme 1-21). This methodology was found to hinge on the need for a palladium catalyst as well as Cs_2CO_3. Extensive mechanistic studies were performed suggesting that there was a carboxylation-decarboxylation equilibrium that favored the carboxylation side which was attributed to formation of a lactone.[44] The intermediate with CO_2 coordinated reacts with another molecule of the 2-hydroxystyrene derivative and base to give the product as well as regeneration of the alkenyl palladium(II) intermediate (Scheme 1-21).[44]

1.4.2: Palladium-catalyzed additions to isocyanates

Palladium is a commonly used catalyst to insert into double bonds to perform Heck-type[45] chemistry as well as Tsuji-Trost[46] chemistry. The Heck reaction is often described as a vinylation or arylation of olefins under palladium catalysis with a basic solvent.[45] This is an important reaction because of its simplicity, high efficiency, and as well as its high chemoselectivity.[45] The Tsuji-Trost reaction is a palladium-catalyzed reaction that often requires an activated allylic substrate and a nucleophile.[46] The activated allylic substrate is often an allylic alcohol protected as an acetate or an ester, allowing the oxygen atom to act as a leaving group.[46] This type of reaction has gained traction in asymmetric allylic alkylations in complex total syntheses.[47] Palladium has also been seen to insert polarized π bonds such as ketones, aldimines, isocyanides, and nitriles.[29] The use of a palladium catalyst inserting into an isocyanate, however, is quite underdeveloped and includes just a few examples and could be due to the notion that palladium has been seen to catalyze oligomerization products shown in Scheme 1-8.[48]

The earliest example of palladium being used in tandem with isocyanates was reported by Trost[49] in 1987. This type of chemistry follows π allyl type chemistry where the substrate has an activated allyl moiety that can act as a leaving group for the palladium catalyst to insert into. This

---

[44] Sasano, K.; Takaya, J.; Iwasawa, N. *J. Am. Chem. Soc.* **2013,** *135*, 10954.
[45] Jagtap, S. *Catalysis* **2017,** *7*, 267.
[46] Butt, N. A.; Zhang, W. *Chem. Soc. Rev.* **2015,** *44*, 7929.
[47] Trost, B. M.; Crawley, M. L. *Chem. Rev.* **2003,** *103*, 2921.
[48] (a) Paul, F.; Mouline, S.; Piechaczyk, O.; Floch, P. L.; Osborn, J. A. *J. Am. Chem. Soc.* **2007,** *129*, 7294. (b) Lee, S. G.; Choi, K.-Y.; Kim, Y.-J.; Park, S.; Lee, S. W. *Dalton Trans.* **2015,** *44*, 6537. (c) Choi, J.-H.; Jung, K.-Y.; Kim, Y.-J.; Lee, S. W. *Polyhedron* **2016,** *117*, 283.
[49] Sudhakar, A. R.; Trost, B. M. *J. Am. Chem. Soc.* **1987,** *109*, 3792.

was shown by Trost where a vinyl epoxide can ring open due to the strained nature of the epoxide (Scheme 1-22). This species can then do a nucleophilic attack on the isocyanate giving the intermediate shown in Scheme 1-22 which can then close the ring to give the cyclic carbamate product. Enantioselective variants as well as a decarboxylative method of this cycloaddition reaction have been developed by other groups further exploring this type of chemistry.[50]

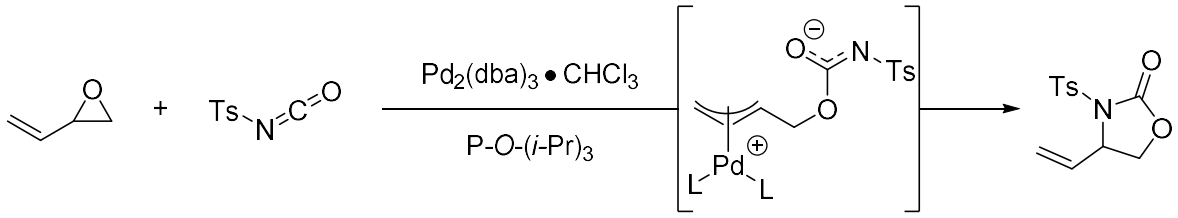

Scheme 1-22: Palladium-catalyzed ring-expansion of epoxides

An early example of using a catalytic amount of palladium with an isocyanate was reported by Szabó and co-workers[51] in 2001. This reaction is a three-component palladium catalyzed amide formation with allyl stannanes and allyl chlorides with toluenesulfonyl isocyanate (Scheme 1-23). The authors noted that special care had to be taken when looking at the temperature and the reaction. When R^1 and $R^2 \neq H$, a longer time and a higher reaction temperature had to be employed otherwise there would be a considerable amount of the mono-allylated product recovered after work-up. It is worth noting mixtures of regioisomers and homo-coupled products could be attained if there weren't alkyl substituents at C1 and C3 positions of the allyl chloride.[51]

[50] For selected examples see: (a) Larksarp, C.; Alper, H. *J. Am. Chem. Soc.* **1997,** *119*, 3709. (b) Zhou, H.-B.; Alper, H. *J. Org. Chem.* **2003,** *68*, 3439. (c) Trost, B.; Fandick, D. R. *J. Am. Chem. Soc.* **2003,** *125*, 11836. (d) Shintani, R.; Tsuji, T.; Park, S.; Hayashi, T. *J. Am. Chem. Soc.* **2010,** *132*, 7508.
[51] Solin, N.; Narayan, S.; Szabó, K. J. *Org. Lett.* **2001,** *3*, 909.

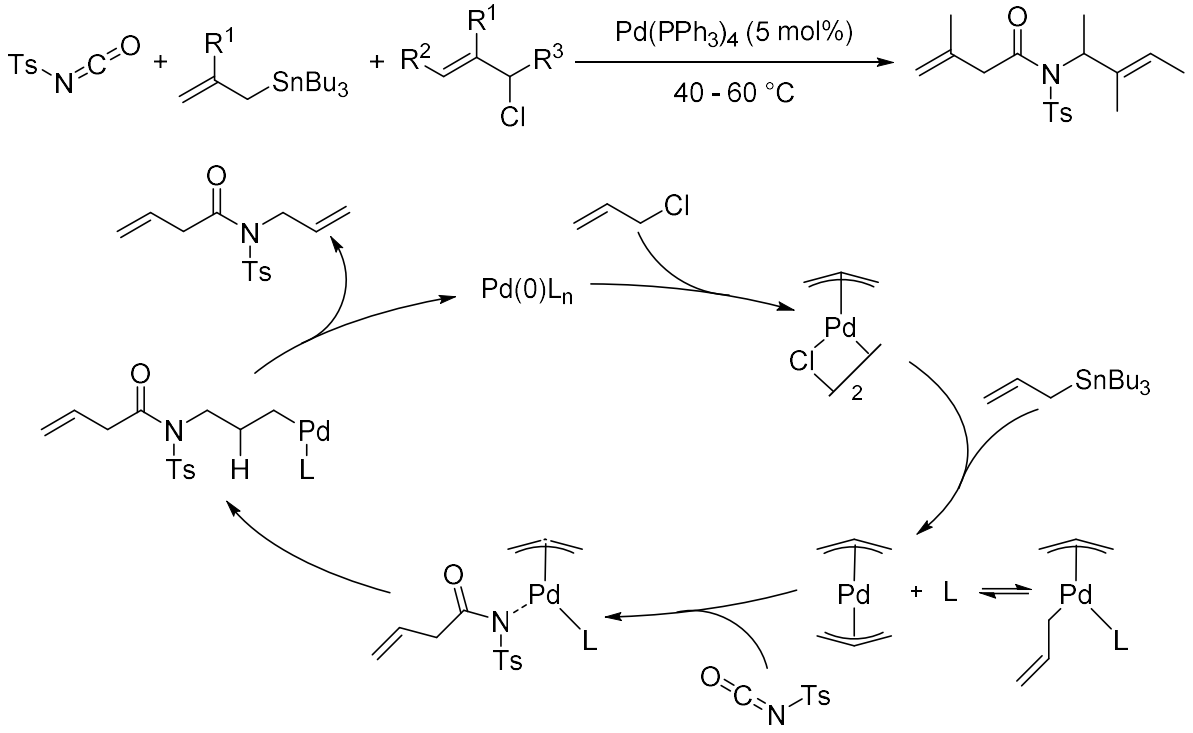

Scheme 1-23: Palladium-catalyzed three-component amide formation

Yamamoto and coworkers[52] investigated cyclization reactions with allyl palladium species in the presence of isocyanates. Palladium has been seen to do cyclometallation reactions with 1,3-butadiene to produce an electrophilic bis-allyl palladacycle intermediate (Scheme 1-23, b).[53] The authors suggested that this bis-allyl palladacycle intermediate could be accessed through a species that was already tethered shown in Scheme 1-24. This intermediate could then do a [4+2] cycloaddition to reach the divinylpiperidone product shown in Scheme 1-24.

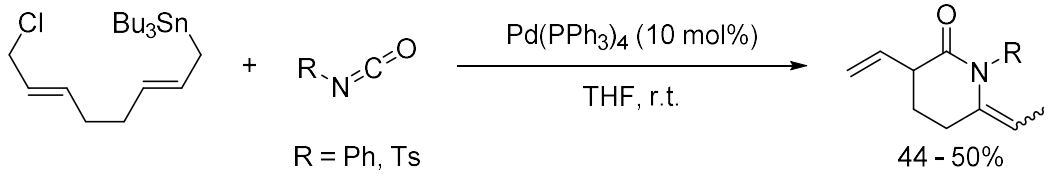

Scheme 1-24: Heterocycle formation through a bis-allyl palladacycle

[52] Nakamura, H.; Aoyagi, K.; Shim, J.-G.; Yamamoto, Y. *J. Am. Chem. Soc.* **2001,** *123*, 372.
[53] Benn, R.; Jolly, R. W.; Mynott, R.; Raspel, B.; Schenker, G.; Schick, K.-P.; Schroth, G. *Organometallics* **1985,** *4*, 1945.

Yamamoto and Kamijo[54] investigated a bimetallic and dual-role catalyst system for the synthesis of *N*-(alkoxycarbonyl)indole systems involving a palladium-copper (Scheme 1-25) and a palladium or platinum catalytic system. This methodology[54] employs a π-allyl activation with various allylcarbonates that are trapped by the palladium catalyst. This π-allylpalladium complex was proposed to insert into the isocyanate bonded to the nitrogen atom of the isocyanate which then does subsequent chemistry to reach the final product given in (Scheme 1-25). The authors noticed that both metals were required for this transformation as no product formation was seen in the absence of either metal. The use of the copper chloride was postulated to coordinatively activate the isocyanate group which was needed for the cyclization step producing the indole framework. If the copper was left out, a methoxy-allylation of the isocyanate product was isolated whereas production of this side product was limited with the use of the copper catalyst. The second transformation Yamamoto and Kamijo[54] investigated the addition of alcohols to phenyl isocyanate followed by the ring closure to give the desired indole. The palladium was found to both act as a catalyst to activated both the π and σ electrons simultaneously when an alcohol was present to do a nucleophilic attack on the activated isocyanate.[54] During the course of this research, Yamamoto and coworkers[55] also found that the coupling of 2-(alkynyl)phenyl isocyanates and terminal alkynes can take place to form oxindoles.

[54] Kamijo, S.; Yamamoto, Y. *J. Org. Chem.* **2003,** *68*, 4764.
[55] Kamijo, S.; Sasaki, Y.; Kanazawa, C.; Schüßeler, T.; Yamamoto, Y. *Angew. Chem. Int. Ed.* **2005,** *44*, 7718.

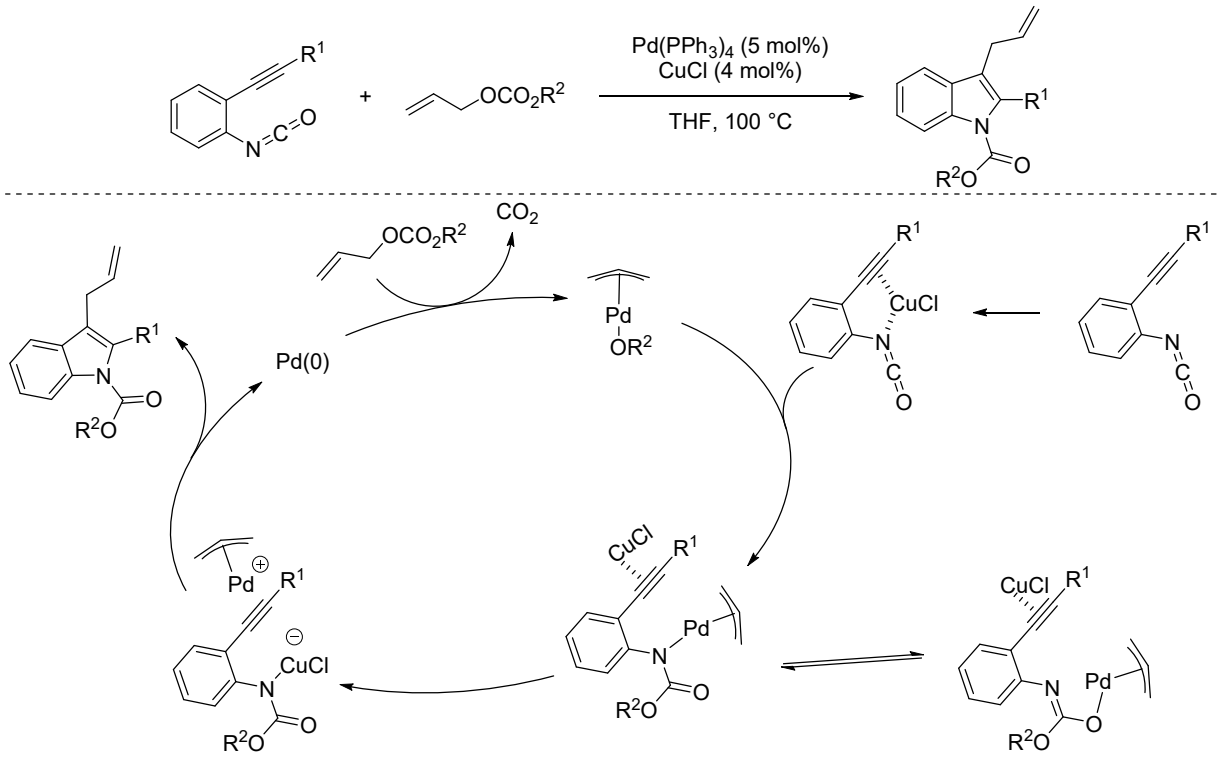

Scheme 1-25: Bimetallic catalytic system for synthesis of N-(alkoxycarbonyl)indole subunits

After the two examples of palladium catalysis with 2-(alkynyl)phenyl isocyanates by Yamamoto and coworkers,[55] Murakami's group followed this trend with various nucleophiles to reach various oxindoles (Scheme 1-26). Some of the nucleophiles they tried were boronic acids,[56a] thiols,[56d] amines,[56b] and alcohols.[56c,d] Yamamoto reported[55] the coupling with alkynyl substrates but when the arylalkyne bore a phenyl group a complex mixture was attained whereas Murakami[56a] addressed these shortcomings. The addition of amines followed the report with boron derivatives,[56a] however strongly deactivated amines were required for this transformation which can be seen by a 94% yield for *p*-toluensulfonamide and a 44% yield for aniline.[56b] The need for this decrease in nucleophilicity is attributed the urea side-product that would be attained from the direct addition to the isocyanate group. Similar conditions allowed for the addition of alkyl and aryl thiols as well as alkyl and aryl alcohols.[56d] As previously described,[56d] alcohols can be added in this system, but a side product was obtained only with benzylic alcohols and an increased

[56] (a) Miura, T.; Toyoshima, T.; Takahashi, Y.; Murakami, M. *Org. Lett.* **2008,** *10*, 4887. (b) *Org. Lett.* **2009,** *11*, 2141. (c) *Org. Lett.* **2010,** *12*, 4584. (d) Miura, T.; Toyoshima, T.; Ito, Y.; Murakami, M. *Chem. Lett.* **2009,** *38*, 1174.

temperature. This side product resulted from a 1,3-rearrangement onto the enol carbon and further optimization allowed for this product to be the sole product.[56c]

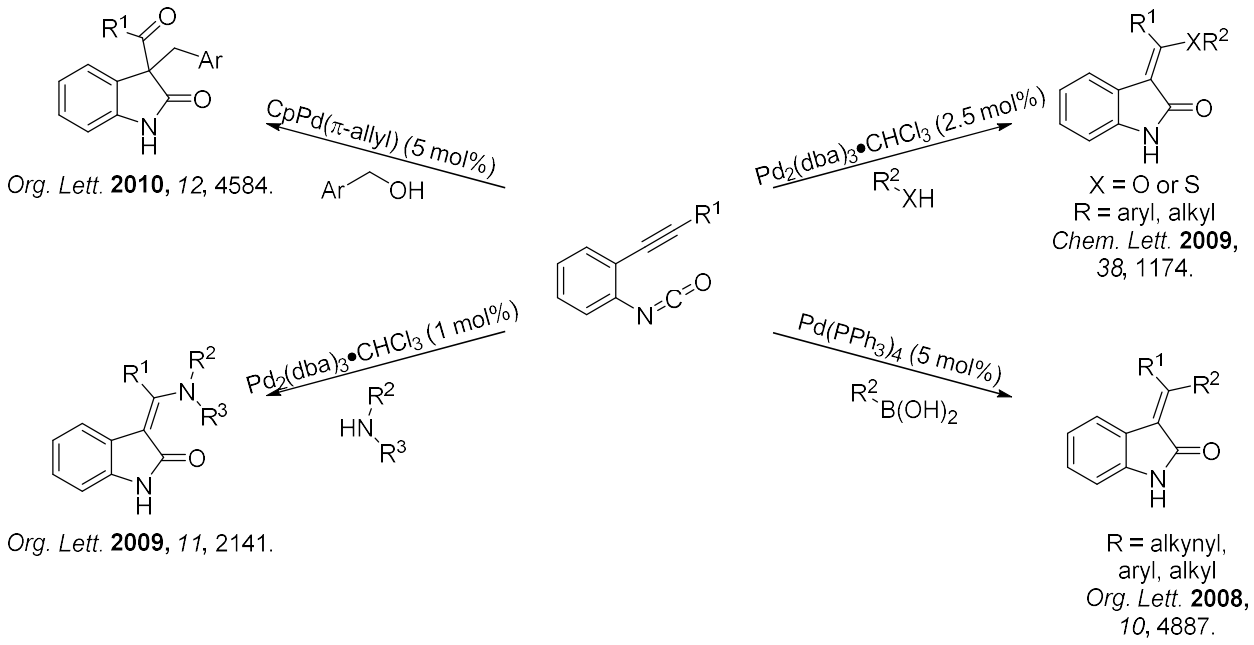

Scheme 1-26: Murakami's work with 2(alkynyl)phenyl isocyanates

Kianmehr and co-workers[57] reported the addition of aryl boronic acids to isocyanates with catalytic palladium (Scheme 1-27). This reaction isn't the most efficient because upwards of half of the boronic acid is lost to homocoupling, resulting from the aryl palladium species doing a second transmetallation followed by the reductive elimination to yield the biaryl product shown in Scheme 1-27. Because this substantial amount of biaryl formation was seen, the authors proposed a catalytic cycle that goes through a Pd(0/II) type mechanism that involves oxidative insertion into the aryl-boron bond, which is unprecedented in the literature. This mechanism was likely proposed to explain the turnover of the catalyst without having an explicit stoichiometric oxidant present.

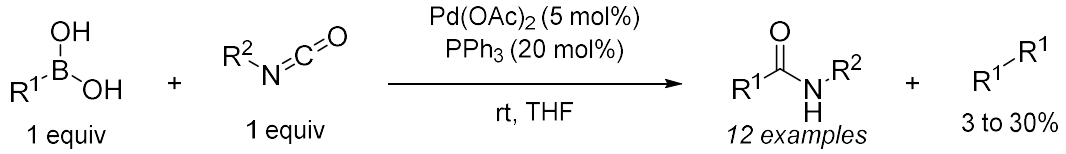

Scheme 1-27: Palladium-catalyzed organoboron addition to isocyanates

[57] Kianmehr, E.; Rajabi, A.; Ghanbari, M. *Tetrahedron Lett.* **2009,** *50*, 1687.

A recent report by Reddy et al.[58] explored the synthesis of furan and pyrrole scaffolds through a palladium-catalyzed cyclization. This methodology[58] involves a similar scaffold as exploited by Murakami[56] with alkynes and isocyanates. Differences are attained by the use internal nucleophile rather than an external nucleophile. The authors performed mechanistic experiments to probe the mechanism such as subjecting substrates that could be an intermediate in the cascade process. After these experiments, the authors proposed the mechanism in Scheme 1-28 which goes through the directed nucleopalladation with the pendant XH (O or N) group followed by the isocyanate insertion that can then release the product by protodepalladation.

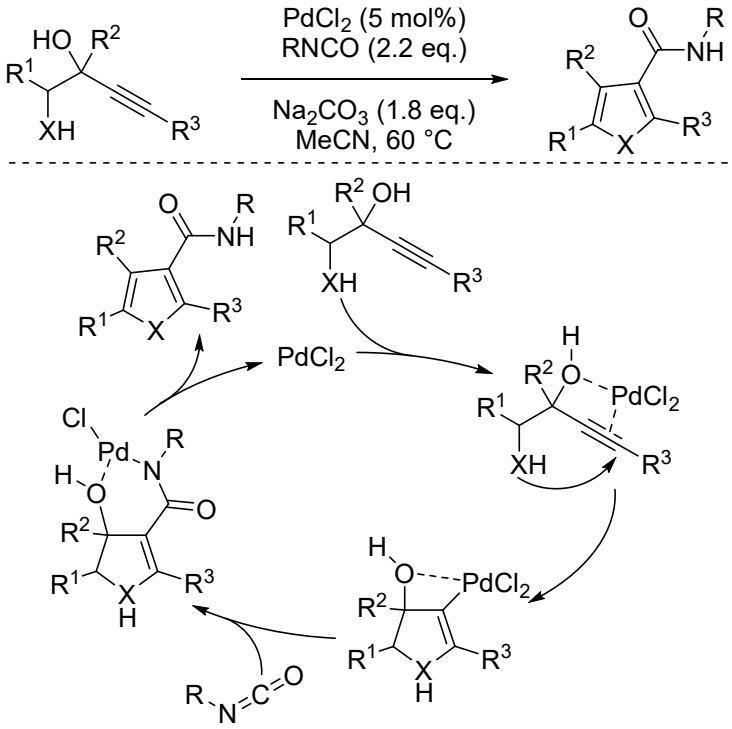

Scheme 1-28: Palladium-catalyzed 5-exo dig cyclization with isocyanates

1.5: Catalytic approaches with masked isocyanates

The type of masked isocyanate that will be discussed in this section are of the carbamate type that use an alcohol-based blocking group. Masked isocyanates in this context will be used to dampen the reactivity which can offer bench-stable precursors that can be stored for months on end.

[58] Rajesh, M.; Puri, S.; Kant, R.; Reddy, M. S. *Org. Lett.* **2016,** *18*, 4332.

1.5.1: Heteroatom-based additions to masked isocyanates

Methods exploited thus far have used a commercially available aryl or alkyl isocyanate to couple with a nucleophile, but the Buchwald group set out to use palladium to synthesize the isocyanate itself with an isocyanate salt.[59] The group initially set out to test the reductive elimination, as the initial goals of this preparation was to test the viability of the reductive elimination step to form the aryl isocyanate. This was done by reacting aryl chlorides and triflates with sodium cyanate to generate their aryl isocyanate derivatives. Using a ligand that was previously reported[60] to facilitate difficult reductive eliminations allowed for the first reported example of a successful reductive elimination from an arylpalladium species to generate an aryl

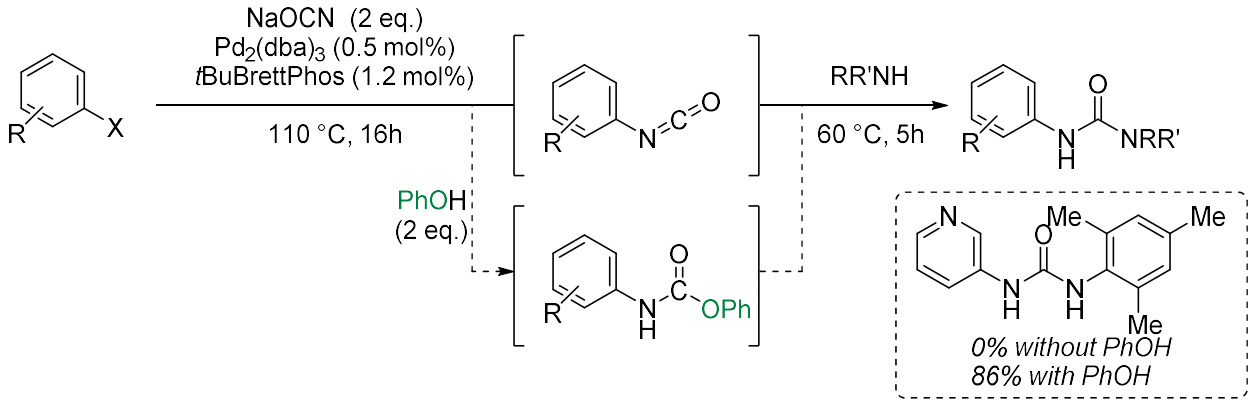

Scheme 1-29: Palladium-catalyzed unsymmetrical urea formation via sodium cyanate

isocyanate. With these results, they wanted to extend this methodology to synthesize unsymmetrical ureas (Scheme 1-29). Buchwald and co-workers[59] produced a respectable scope but there were limitations into the choice of electrophilic and nucleophilic components. To mitigate this limitation, the electrophilic isocyanate partner was targeted. The Buchwald group has previously reported[61] that the use of sodium phenoxide was beneficial in their palladium-catalyzed aminocarbonylation of aryl chlorides. It was proposed that the sodium phenoxide would form an ester by intercepting the palladium acyl species which could then interact with the amine to get to the desired amide product.[61] Phenol could be used incorporated into the sodium cyanate system by intercepting the aryl isocyanate produced from the first step forming a carbamate which in essence

[59] Vinogradova, E. V.; Fors, B. P.; Buchwald, S. L. *J. Am. Chem. Soc.* **2012,** *134*, 11132.
[60] Fors, B. P.; Buchwald, S. L. *J. Am. Chem. Soc.* **2009,** *131*, 12898.
[61] Martinelli, J. R.; Clark, T. P.; Watson, D. A.; Munday, R. H.; Buchwald, S. L. *Angew. Chem Int. Ed.* **2007,** *46*, 8460.

is a masked isocyanate. The use of phenol allowed for more sterically encumbered isocyanate as well as a wider range of function groups tolerated under the second set of optimized conditions. To illustrate the efficacy of using phenol as an additive in this system, the coupling of 3-chloropyridine which has a Lewis basic site, did not proceed without phenol but with it present proceeded with a yield of 86% (Scheme 1-29).

A follow-up report by Buchwald and co-workers[62] developed a protocol for peptide and protein cross-linking at natural amino acid residues using palladium oxidative addition complexes. This methodology uses an *O*-phenyl carbamate which has been shown to be a masked isocyanate. The *O*-phenyl carbamate can be incorporated into peptides or proteins and then the isocyanate can be intercepted by the proximal lysine residues. Synthesizing the palladium oxidative addition complex is shown in Scheme 1-30. This complex in Scheme 1-30 could be stored for several months and can readily undergo the arylation reactions that it was synthesized for.

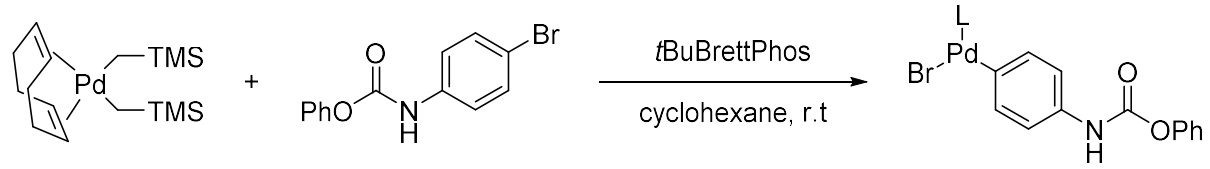

Scheme 1-30: Palladium oxidative addition complex for cross-linking of peptides and proteins

1.5.2: Carbon-based additions to masked isocyanates

With the inherent reactivity of amines, they are often protected to mitigate their nucleophilicity to prevent them from reacting in non-productive transformations. To do amide bond forming reactions, the amine often needs to be deprotected as the sp^2 carbamate amine is not nucleophilic enough to react with the desired activated electrophile for the coupling reaction to occur. The use of Boc and Cbz as protecting groups for amines is quite prevalent,[63] reducing the need for this deprotection step and using the amine in its protected state would reduce the amount of chemical waste in process chemistry. Zhang and co-workers[64] targeted the direct amidation of *N*-Boc and *N*-Cbz protected amines with a rhodium-catalyzed coupling reaction with arylboroxines

[62] Kubota, K.; Dai, P.; Pentelute, B. L.; Buchwald, S. L. *J. Am. Chem. Soc.* **2018,** *140*, 3128.
[63] Roughley, S. D.; Jordan, A. M. *J. Med. Chem.* **2011,** *54*, 3451.
[64] Lim, D. S. W.; Lew, T. T. S.; Zhang, Y. *Org. Lett.* **2015,** *17*, 6054.

(Scheme 1-31). The authors suggested that the borate salt obtained after the transmetallation was responsible for the activation of the carbamate to form the alkoxyrhodium(I) species shown in Scheme 1-31 which could then do β-alkoxy elimination to generate the coupled product. The authors initially thought there would be isocyanate intermediate as a carbamate could act as a masked isocyanate. The isocyanate intermediate was however ruled out because this intermediate was not visible on ^{1}H NMR sprectum.[64] However, the reaction was performed at 100 °C and the ^{1}H NMR was taken at room temperature 1) the formation of isocyanate is known to be temperature-dependent and possible upon heating at high temperature; 2) NMR spectroscopy may not be the method of choice to observe isocyanates; 3) that Boc and CBz are known protecting groups usually not prone to undergo nucleophilic addition, one could question the conclusion made by the authors, and thus their proposed mechanism.

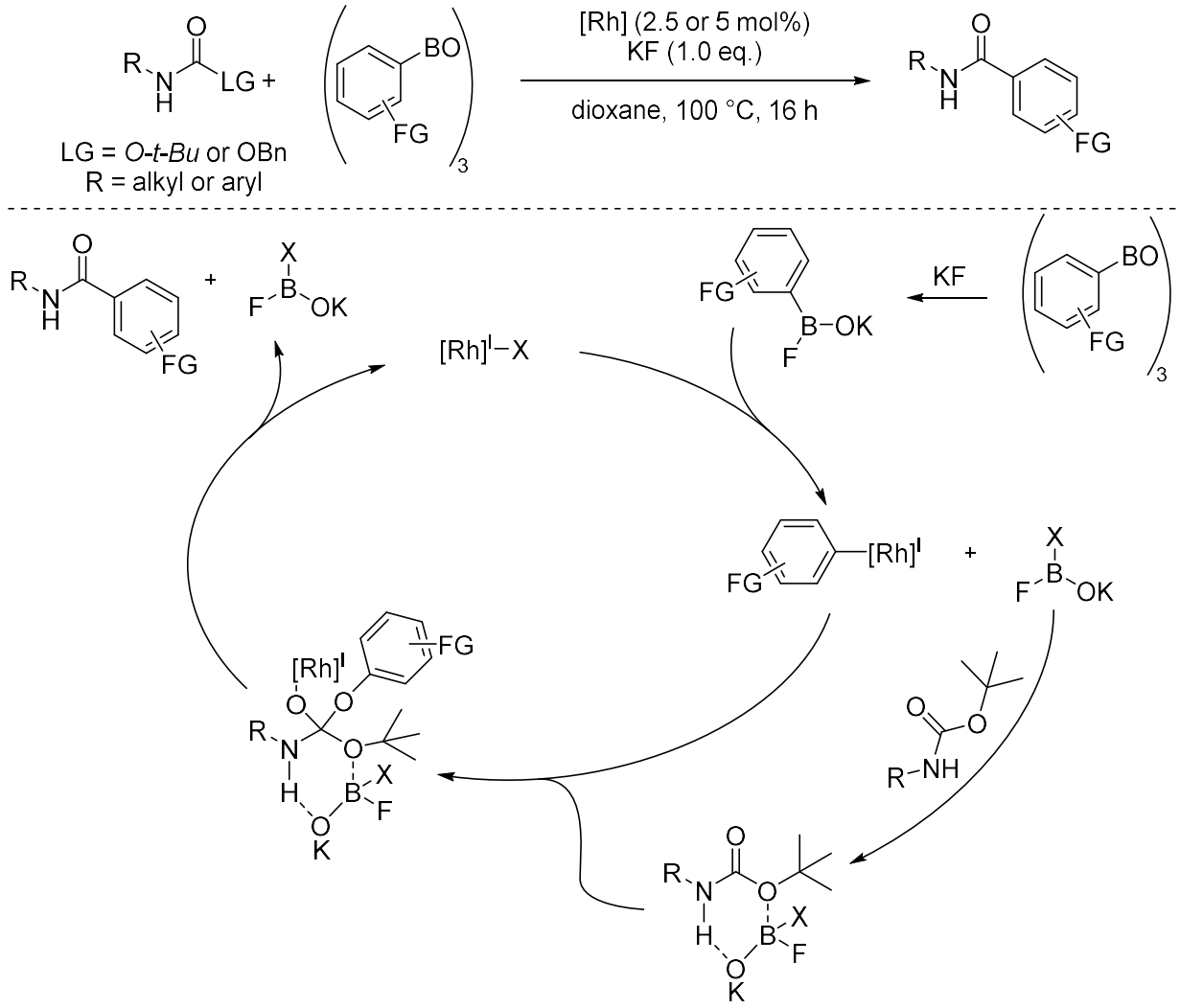

Scheme 1-31: Rhodium-catalyzed direct amidation of carbamate protected amines with proposed mechanism

A more recent report by Beauchemin and Derasp (2019)[65] built on the procedure developed by Zhang (2015)[64] that enabled the catalytic direct amidation of protected amine substrates. Zhang's work (2015)[64] uses high temperatures as well as a fluoride-based base to allow for this transformation and lacks functional group tolerance such as substrates containing Lewis basic sites. With this in mind, Beauchemin and Derasp (2019)[65] targeted these limitations by reporting a procedure that has milder conditions and takes advantage of the blocking group strategy of masked isocyanates. Pyridinic substrates were tolerated as well as substrates bearing internal nucleophiles which would not be tolerated under standard isocyanate conditions. In contrast with

[65] Derasp, J. S.; Beauchemin, A. M. *ACS Catal.* **2019,** *9*, 8104.

the catalytic cycle proposed by Zhang (2015),[64] an isocyanate intermediate is thought to be part of this catalytic cycle (Scheme 1-32) since *N*-methyl substituted masked isocyanates proved unsuitable under the reaction conditions.

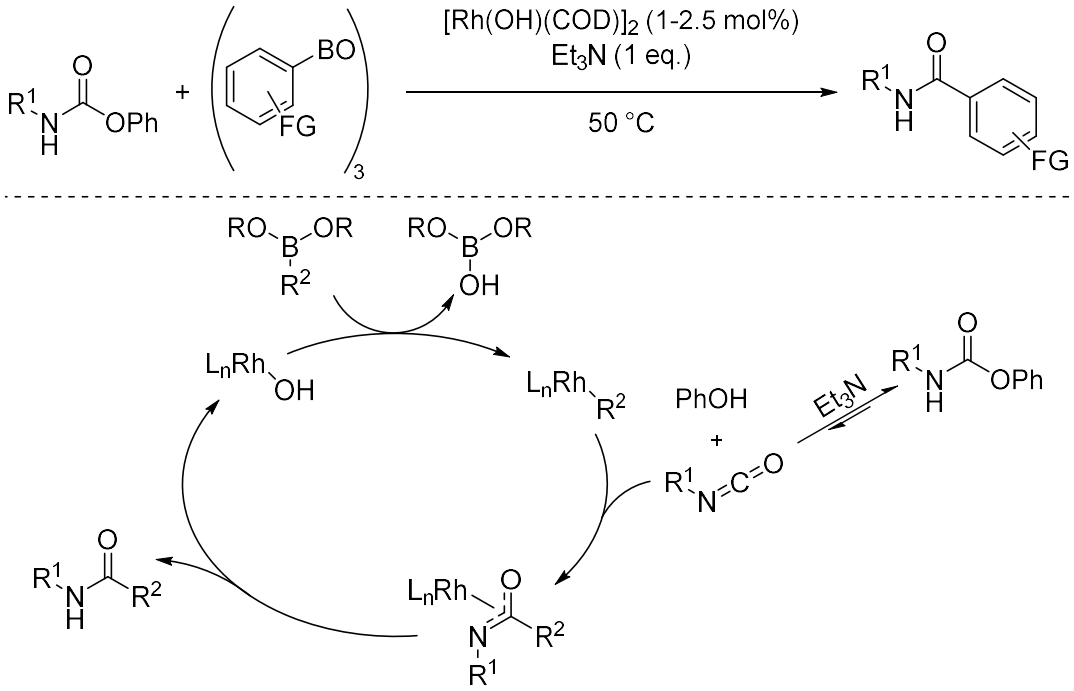

Scheme 1-32: Rhodium-catalyzed amidation of masked isocyanates

1.6: Project goals

Amide bond synthesis is one of the most sought-after chemical transformations among agrochemical, pharmaceutical, and research lab fields. Many bond disconnections have been described in sections 1.1, 1.2, and 1.5 each with their strengths and weaknesses. More modern methodologies have been introduced that target many of these limitations such as catalysis and substrate engineering. Isocyanates hold great promise for amide formation since they have wide availability and high reactivity. The high reactivity can be both a negative as well as a positive meaning that there is great functional group intolerance but the great electrophilicity reduces the need for highly reactive nucleophiles.

Masked isocyanates target many of these drawbacks by reducing oligomerization, catalyst deactivation, and functional group intolerance. The use of masked isocyanates to form ureas was elegantly shown by Buchwald and co-workers (2012)[59] where the use of phenol greatly increased functional group tolerance and increased yields in some instances. The catalytic amide formation

using blocked isocyanates for the formation of amides is sparse[64,65] and only includes the use of a rhodium-based catalyst.

As alluded to above, Rh(I) has enabled the desired amide formation reaction with masked isocyanates. As a next step, we wanted to remove the need for a boron nucleophile and target the activation of C-H bonds to address chemical waste. Rhodium has been seen to interact with a C-H bond,[66] but largely when it is the Rh(III) oxidation state whereas only Rh(I) was active in our recent work. To address this shortcoming, Pd(II) is well known to be active in C-H functionalization and was used in Kianmehr's[57] amide coupling report with isocyanates and boronic acids. Besides this key precedent, examples of Pd-catalyzed reactivity were remarkable rare. Given this, we wanted to combine the power of masked isocyanates as well as utilize the strong ligand dependence inherent with palladium to enable the desired amide synthesis via masked isocyanates and boronic acids. If this goal is met, it would expand this chemistry to other catalysts and open reactivity for palladium which could then possibly be further extended to C-H functionalization.

[66] For selected reviews on transition-metal catalyzed C-H bond functionalization see: (a) Yang, Y.; Lan, J.; You, J. *Chem. Rev.* **2017,** *117*, 8787. (b) Yeung, C. S.; Dong, V. M. *Chem. Rev.* **2011,** *111*, 1215.

Chapter 2:

Development of a palladium-catalyzed amide formation via masked isocyanates

2.1: Towards a palladium-catalyzed activation of blocked isocyanates

Given the success in developing a rhodium-catalyzed activation of blocked isocyanates for the formation of amides, further extensions with different nucleophiles was desirable.[65] The goal was to rid the rhodium-catalyzed activation methodology from a boron nucleophile with C-H as the nucleophile, although only rhodium in its 3+ oxidation state has been seen to interact with a C-H bond whereas Rh(I) was used in this case.[66] As discussed in section 1.4 and 1.5, the work done with palladium in this mode of activation is quite limited but the work by Kianmehr and co-workers[57] stood out since they disclosed a palladium-catalyzed amide formation with isocyanates and boronic acids. This work however suffered from a large production of biaryl product which could have the opportunity to be remedied through further optimization, ideally with a blocking group strategy which slows down self reactivity enabling a longer lifetime in solution.

2.1.1: Preliminary studies into the palladium project

Although the rhodium system was competent for the addition of boroxine derivatives to blocked isocyanates, the $[RhOH(cod)]_2$ catalyst[67] used is roughly ten times the cost per mmol than the $Pd(OAc)_2$ catalyst[68] which might not be sustainable for extended use. Perhaps more importantly, a palladium-catalyzed reaction variant might offer complementarity, for example by allowing reactions that are otherwise impossible to perform with a rhodium (I) catalyst. Towards this end, Joshua Derasp tested conditions using a palladium(II) catalyst and various phosphine derived ligands (Table 2-1). The rhodium system required Et_3N to promote deblocking of the isocyanate at 50 °C, so this was incorporated into the optimization study. Studies began with a combination of the catalyst system reported by Kianmehr and co-workers[57] and the rhodium study (entry 1), unfortunately, such conditions failed to produce the desired product. More traditional ligands were also screened but were also ineffective for the desired transformation (entries 2-3). Efforts continued with biaryl phosphine ligands which proved to be effective in Buchwald's system[59] (entries 4-8). Out of the ligands screened, SPhos produced the desired product with a yield of 88% (entry 6). Increasing the concentration of the reaction (entry 9) didn't have a drastic

[67] Strem Chemicals, Inc. https://www.strem.com/catalog/v/45-1000/57/rhodium_73468-85-6 (accessed Apr 15, 2020), US$ 219/mmol.
[68] Strem Chemicals, Inc. https://www.strem.com/catalog/v/46-1780/51/palladium_3375-31-3 (accessed Apr 15, 2020), US$ 21/mmol.

Table 2-1: Initial optimization for the Pd-catalyzed system[a]

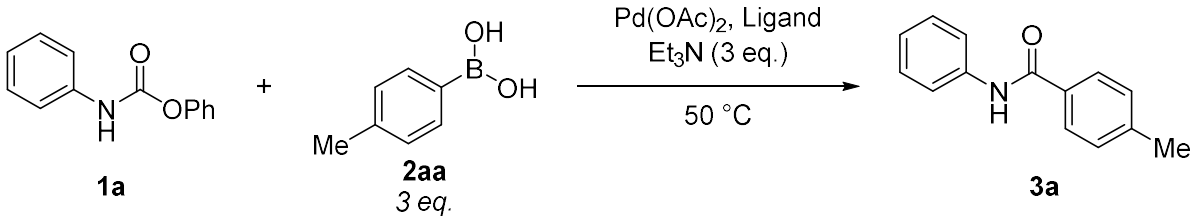

1a + **2aa** *3 eq.* → **3a**

Entry	$Pd(OAc)_2$ (mol %)	Ligand (mol %)	[THF] (M)	Time (h)	Yield (%)
1	5	PPh_3 (20)	0.1	20	0
2	5	Bipyridine (5)	0.1	20	0
3	5	Binap (5)	0.1	20	0
4	5	*t*-Bu-Josiphos (5)	0.1	20	0
5	5	XPhos (10)	0.1	20	8
6	5	SPhos (10)	0.1	20	88
7	5	*t*-Bu-XPhos (10)	0.1	20	3
8	5	DavePhos (10)	0.1	20	39
9	5	SPhos (10)	0.5	5	87
10	5	SPhos (15)	0.5	5	79
11	5	SPhos (5)	0.5	20	0
12	5	SPhos (10)	0.5	4	80
13	5	SPhos (10)	0.5	5	75
14	2.5	SPhos (5)	0.5	5	88
15	1	SPhos (2)	0.5	5	92
16[b]	0.5	SPhos (1)	0.5	24	81

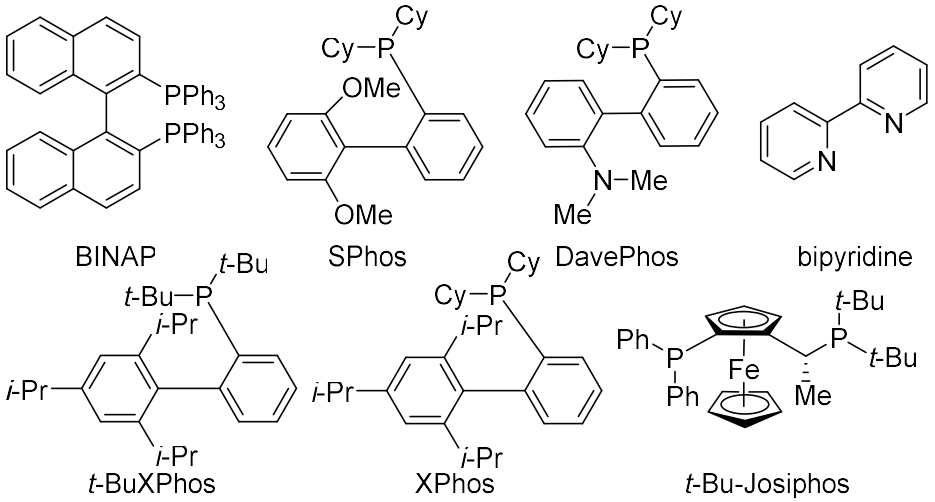

[a] Conditions: **1a** (0.1 mmol), **2aa** (0.3 mmol), Et_3N (0.3 mmol), 50 °C. ^1H NMR yield determined using 1,3,5-trimethoxybenzene as internal standard. [b] Is of isolated yield

effect on the yield. A ratio of 1:2 Pd:Ligand was found to be optimal for this transformation as a 1:1 ratio proved detrimental (entry 11) likely due in part to the phosphine ligand rendered inactive due to an oxidation to the phosphine oxide. This ratio (entry 12) was then carried forward and decreasing the catalyst loadings to 0.5 mol% didn't affect the yield (entries 13-16). Overall, the results described in Table 2-1 show the promising results obtained with palladium and what was known about this new reactivity at the start of my graduate work.

Upon joining this project, reproducing Mr. Joshua Derasp's initial result was of the utmost importance. The conditions used in Table 2-1: Entry 15 were carried forward as 1 mol% of $Pd(OAc)_2$ was more accurately weighed out than 0.5 mol%. The results were reproduceable leading to a thorough optimization study further described in section 2.1.2. Follow-up experiments including testing the loadings of the boron reagent as well as the Et_3N showed that reductions to 2 equivalents of **2aa** and 2 equivalents of Et_3N could be achieved without hampering reactivity. Although the use of the commercial boronic acid (**2aa**) gave an excellent yield, it was found that this specific boronic acid contained high amounts of the boroxine condensation by-product which was likely responsible for the desired transformation. With this, the dehydrated boronic acid (boroxine) was used moving forward.[69]

2.1.2: Optimization study

The optimization first started with a base screen for this palladium-catalyzed amidation that is shown in Table 2-2. Et_3N proved to be superior out of the bases screened to promote the desired reaction (entry 1). A stronger base such as DBU (entry 2) compared to Et_3N failed to provide the desired product. A weaker base such as *N*-methylmorpholine (entry 3) didn't produce the desired amide in even a trace amount. K_2CO_3 (entry 4) produced the amide albeit in a reduced yield possibly due to its decreased solubility. DIPEA (entry 5) which has structural similarities to Et_3N produced the desired product although in a reduced yield to that of Et_3N. Unsurprisingly, the lack of base (entry 6) resulted in a complete absence of product observed most likely due to the lack of isocyanate formation as the temperature is likely not high enough to promote isocyanate formation through thermal deblocking (≈120 °C for aryl-NHCOO-aryl).[19]

---

[69] Jung, H. H.; Buesking, A. W.; Ellman, *J.* A. *Org. Lett*. **2011**, *13*, 3912. (Boronic acid was recrystallized in water and then dehydrated under reduced pressure at 100 °C overnight.)

Table 2-2: Base screen[a]

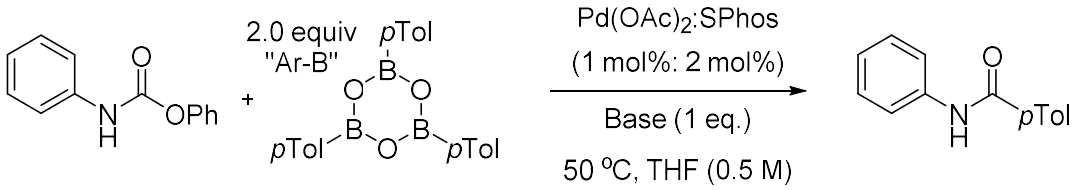

1a **2a** **3a**

Entry	Base	Yield (%)
1	Et_3N	92
2	DBU	0
3	*N*-methylmorpholine	0
4	K_2CO_3	33
5	DIPEA	47
6	none	0

[a]Conditions: **1a** (0.2 mmol), **2a** (0.13 mmol, 2.0 'Ar-B' equiv), $Pd(OAc)_2$ (1.0 mol%), SPhos (2.0 mol%), Et_3N (0.2 mmol), solvent (0.5 M), 50 °C. ^1H NMR yield determined using 1,3,5-trimethoxybenzene as internal standard.

The effects of the solvent of the desired transformation were then probed (Table 2-3). Solvents including DMF and MeCN (entries 1-2) only gave traces of product. Dichloromethane (entry 3) also failed to deliver the desired product. Toluene (entry 4) surprisingly yielded a moderate yield of the product. THF proved an ideal solvent for this transformation, similarly to the previous work by Kianmehr[57] and Derasp.[65] Dioxane (entry 6) also being an ethereal solvent was competent leading to only a slight decrease in the yield compared to THF (entry 5). Toluene, being less polar than THF, would likely limit the formation of the isocyanate because more polar solvents increase the solvated ion pair concentration.[19]

Table 2-3: Effect of solvent [a]

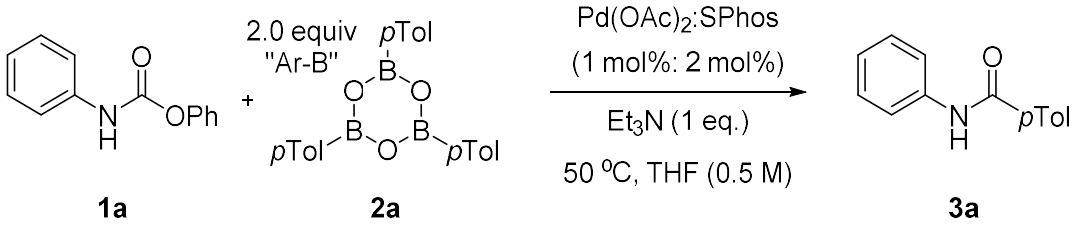

1a **2a** **3a**

Entry	Ligand	Yield (%)
1	DMF	10
2	MeCN	4
3	CH_2Cl_2	11
4	Toluene	62
5	THF	92
6	Dioxane	82

[a]Conditions: **1a** (0.2 mmol), **2a** (0.13 mmol, 2.0 'Ar-B' equiv), Pd pre catalyst (1.0 mol%), SPhos (2.0 mol%) Et_3N (0.2 mmol), THF (0.5 M), 50 °C unless indicated otherwise. ^{1}H NMR yield determined using 1,3,5-trimethoxybenzene as internal

The use of different palladium precatalysts was then evaluated (Table 2-4). Three different palladium(II) catalysts were screened (entries 1-3) affording the desired product in modest yield compared to when using $Pd(OAc)_2$. A palladium(0) catalyst (entry 4) interestingly gave the desired product even though the palladium pre catalysts screened thus far have been palladium(II). It was further found that increasing the loading of $Pd(OAc)_2$ (entries 5-6) didn't have a large effect on the efficiency of the reaction.

Table 2-4: Palladium precatalyst screen[a]

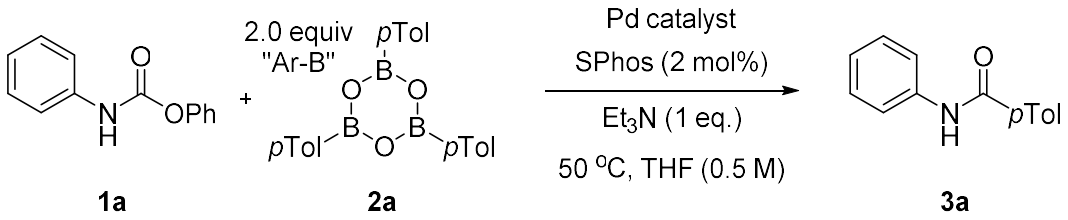

1a **2a** **3a**

Entry	Pd catalyst	Yield (%)
1	$Pd(acac)_2$ (1.0 mol%)	10
2	$PdCl_2$ (1.0 mol%)	4
3	$Pd(TFA)_2$ (1.0 mol%)	16
4	$Pd_2(dba)_3$ (0.5 mol%)	21
5[b]	$Pd(OAc)_2$ (2.0 mol%)	72
6[b]	$Pd(OAc)_2$ (3.0 mol%)	76

[a]Conditions: **1a** (0.2 mmol), **2a** (0.2 mmol, 2.0 'Ar-B' equiv), $Pd(OAc)_2$ (1.0 mol%), ligand (2.0 mol%) Et_3N (0.2 mmol), THF (0.5 M), 50 °C, unless indicated otherwise. ^1H NMR yield determined using 1,3,5-trimethoxybenzene as internal standard. [b]**2a** (0.13 mmol, 2.0 'Ar-B' equiv). [c]**2a** (0.10 mmol, 1.5 'Ar-B' equiv).

With more optimized conditions in hand, a second ligand scan (Table 2-5) was performed by Josh Derasp with the use of the boroxine derivative. Ligands screened failed to produce comparable yields to those obtained with SPhos (entries 1-10). Although, BINAP (entry 3) produced the desired amide when the boroxine (**2a**) was used whereas no trace of product was found when using the commercial boronic acid under previous conditions (Table 2-1, Entry 3). With the determined optimized conditions (entry 11), an 81% yield of the desired amide was obtained. Entries 1-11 were tested using 3 Ar-B equivalents and it was determined that this excess was found to be unnecessary as entry 12 delivered the product in a yield of 92% with only 2 equivalents of the Ar-B bonds present in the boroxine reagent. Further reduction of the loading of SPhos (entry 13) didn't hamper reactivity but increasing to 3 mol% (entry 14) had a catastrophic effect. The use of 1.5 boron equivalents (entry 15) didn't change the yield to a large degree.

Table 2-5: Second ligand scan[a]

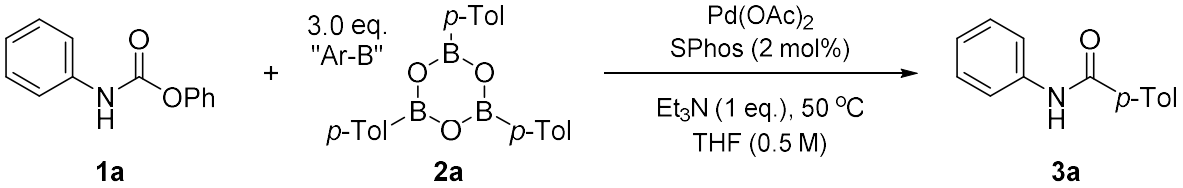

1a **2a** **3a**

Entry	Ligand	Yield (%)
1	PPh_3 (4 mol%)	0
2	PPh_3 (2 mol%)	0
3	(+/-) BINAP (1 mol%)	6
4	DPPE (1 mol%)	8
5	DPPP (1 mol %)	15
6	Bipyridine (1.0 mol%)	0
7	DavePhos (2.0 mol%)	16
8	*t*-BuXPhos (2.0 mol%)	5
9	BrettPhos (2.0 mol%)	4
10	RuPhos (2.0 mol%)	19
11	SPhos (2.0 mol%)	81
12[b]	SPhos (2.0 mol%)	92
13[b]	SPhos (1.2 mol%)	91
14[b]	SPhos (3.0 mol%)	49
15[c]	SPhos (1.2 mol%)	89

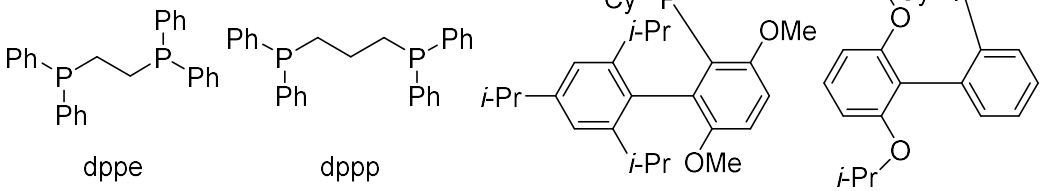

[a]Conditions: **1a** (0.2 mmol), **2a** (0.2 mmol, 3.0 'Ar-B' equiv), $Pd(OAc)_2$ (1.0 mol%), ligand (2.0 mol%) Et_3N (0.2 mmol), THF (0.5 M), 50 °C, unless indicated otherwise. ^1H NMR yield determined using 1,3,5-trimethoxybenzene as internal standard. [b]**2a** (0.13 mmol, 2.0 'Ar-B' equiv). [c]**2a** (0.10 mmol, 1.5 'Ar-B' equiv).

With the optimization nearing completion, some inconsistencies were noticed when attempting to scale-up reactions. It was found that order of addition as well as the incubation time of the catalyst solution had to be constant throughout each experiment. A study towards determining the optimal conditions to tackle each of these problems started. After crucial experiments, it became clear that if the base was added before the addition of the catalyst mixture it was detrimental to the outcome of the reaction. This could be attributed to Et_3N interacting with the masked isocyanate and liberating the isocyanate before the catalyst has an opportunity to react with it. The incubation of the catalyst solution did not have a large effect on the yield, but it was determined that a five-minute incubation time was optimal whereas longer or shorter times resulted in lower yields.

2.1.3: Surveying the applicability of the palladium-catalyzed reaction

Having the optimized conditions in hand, the next step in the process was to analyze the functional group tolerance and probe the applicability of the optimized reaction conditions. Substrates **1a** and **2a** were used in tandem with different boroxine reagents and different masked isocyanates respectively.

The impact of the aryl boroxine nucleophile on the reactivity was first evaluated. The results displayed in Table 2-6 were obtained in collaboration with Mr. Joshua Derasp. The model substrate provided the desired product **3a** in an 89% isolated yield on a 0.6 mmol scale. Boroxine derivatives possessing alkyl groups (**3a-c**) including sterically demanding substituents (**3c**) proved to be competent coupling partners. A mono-fluorinated aryl boroxine was tolerated (**3e**), as well as difluorinated aryl boroxine (**3f**) which can be a challenging partner due to its propensity to undergo fast proto-deactivation.[70] Long reaction times (**3g**) or the complete loss of reactivity (**3h**) was observed when stronger electron-withdrawing groups were present. Unfortunately, halide and heterocyclic motifs were found to be incompatible (**3i-k**) likely due to competitive oxidative addition.

[70] Kinzel, T.; Zhang, Y.; Buchwald, S. L. *J. Am. Chem. Soc.* **2010***, 132,* 14073.

Table 2-6: Scope of aryl boroxines[a]

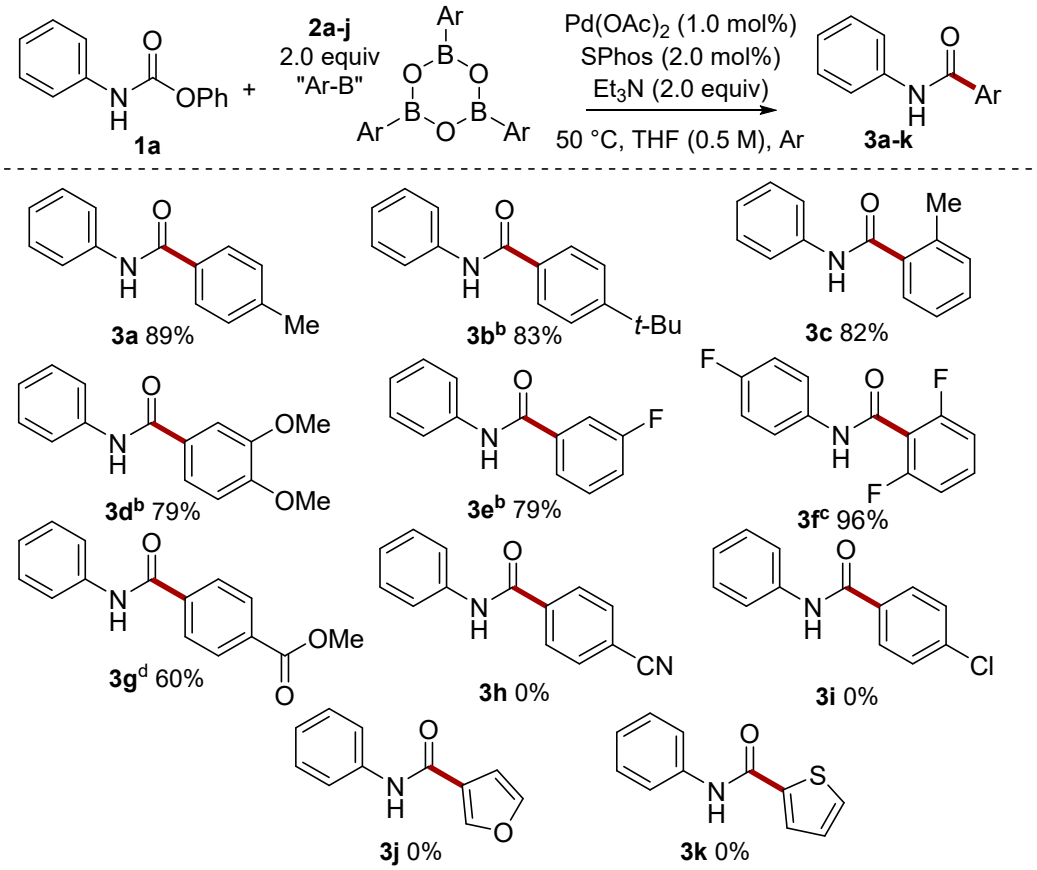

[a] Reagents and conditions: **1a** (0.600 mmol), **2a-j** (0.4 mmol), Et_3N (1.20 mmol), $Pd(OAc)_2$ (0.006 mmol), SPhos (0.012 mmol), THF (0.5 M), 50 °C, 24 h. Yields are of isolated pure material. [b] Products that were synthesized by Josh Derasp. [c] **1g** was used in place of **1a**. [d] Reaction time 48 h.

Attention was then focused on surveying structural variation on the masked isocyanate reagent (Table 2-7). Pleasingly, electron-rich aryl isocyanates were tolerated (**4a-c**) as well as masked aryl isocyanates possessing electron-withdrawing substituents (**4d**). The presence of a *p*-nitro (**4e**) substituent was tolerated, even if a higher temperature was required for the transformation. A sterically encumbered mesityl masked isocyanate (**4b**) was tolerated affording the product in 67% yield. In contrast, increased steric bulk of 2,6-diisopropyl led to a modest yield of 26% (**4c**). Alkyl isocyanates were then tested for the desired transformation. Benzylic substrates (**4g-h**) were tolerated as well as substrates derived from α-secondary amines (**4i-j**). However halogenated aryl and allyl isocyanates were unsuitable (**4k-m**), potentially due to competitive

oxidative addition into the aryl halide or competitive π allyl formation with the off cycle Pd(0) species formed.

Table 2-7: Scope of blocked isocyanates[a]

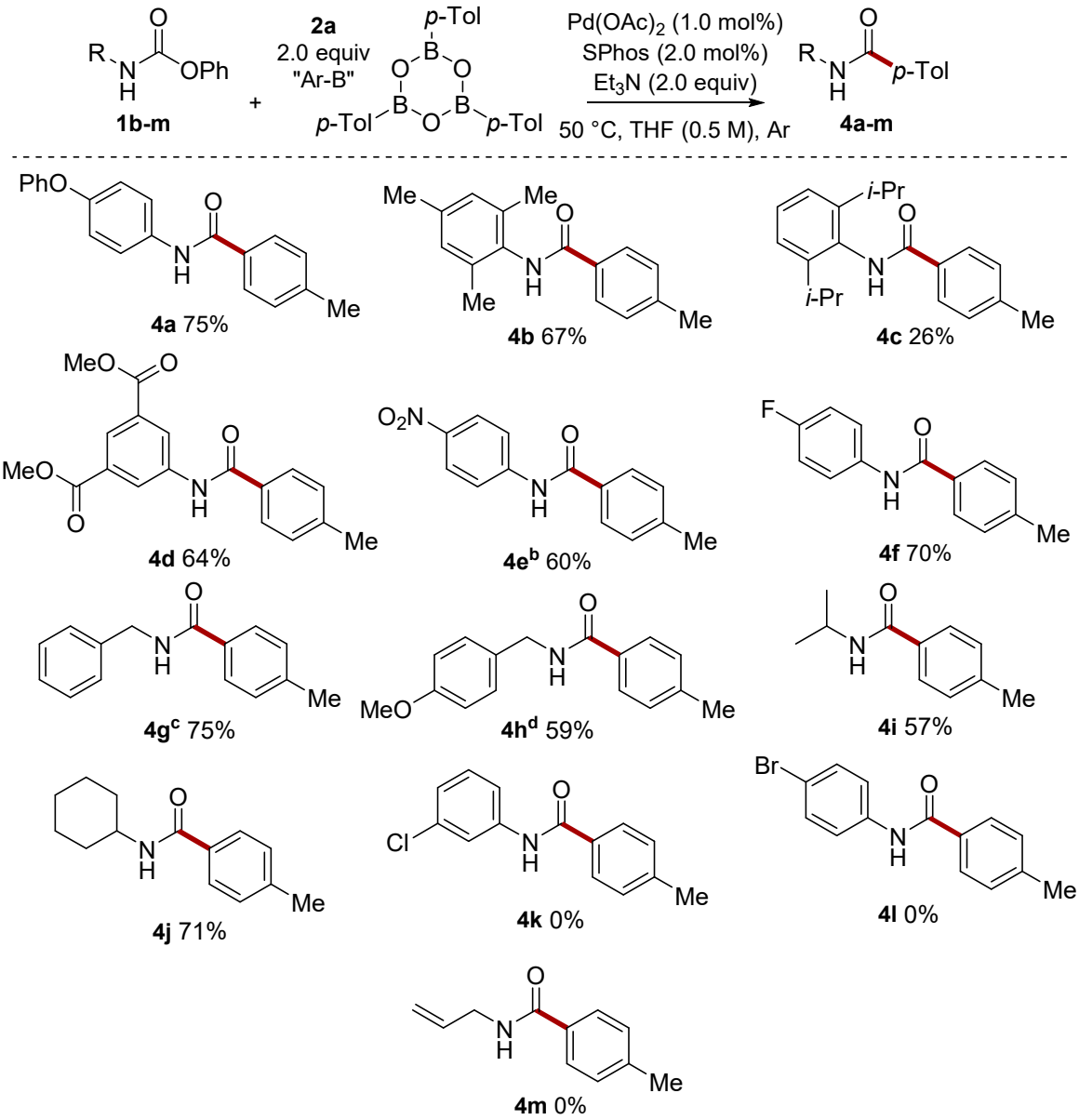

[a]Reagents and conditions: **4a-n** (0.600 mmol), **2a** (0.4 mmol), Et_3N (1.20 mmol), $Pd(OAc)_2$ (0.006 mmol), SPhos (0.012 mmol), THF (0.5 M), 50 °C, 24 h. Yields are of isolated pure material. [b]Dioxane (0.5 M), 100 °C. [c]70 °C. [d]80 °C.

While developing the scope for the aryl boroxines (Table 2-6) and blocked isocyanates (Table 2-7), by-products including homocoupled biaryl, biuret, and urea derivatives were

observed. The homocoupled biaryls likely form from palladium doing a second transmetallation with the aryl boroxine followed by a reductive elimination (Scheme 2-1). By observing this product, it would seem that some Pd(0) is being produced which could be responsible for lack of reactivity with entries **3h** and **4l**. It was postulated that Pd(II) was active during this catalytic cycle and the amount of biaryl product supersedes the amount of $Pd(OAc)_2$ that was introduced into the system. So by that logic, there must be a pathway for palladium to be reoxidized or a Pd(0) species was active like it was suggested by Kianmehr[57] (2009). However, the formation of such oligomerization products including biuret and urea type products could be responsible for the oxidation of palladium or trace oxygen that could have seeped into the system. These observations, as well as our desire to pursue more challenging palladium-catalyzed reactions such as C-H activations, provided a strong incentive to study the mechanism of this transformation.

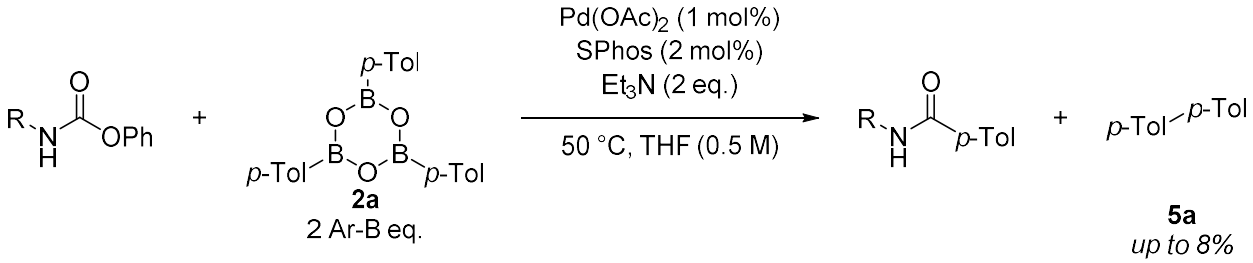

Scheme 2-1:Formation of biaryl product

2.2: Investigation into the mechanism

Stemming from the work by Kianmehr[57] (Scheme 1-27), a mechanism involving a Pd(0)/(II) catalytic cycle represents the only mechanistic proposal that have been reported for a reaction between an arylboronic acid and an isocyanate. Although a Pd(II) precatalyst was used, their reaction was plagued with the formation of a homocoupled biaryl product which would result in Pd(0) formation. For this reason, Kianmehr[57] (2009) suggested an oxidative addition into the B-O bond which would result in the Pd(II) species which would then interact with the isocyanate. As this may not be the sole mechanism that could be operative, three different modes of activation and potential catalytic cycles will be presented below for the reaction reported including oxidative addition into the C(O)-O bond, oxidative addition into the B-O bond, or redox-neutral transmetallation followed by insertion into the isocyanate.

2.2.1: Investigation into a Pd(0)/(II) type mechanism

Two options of a non-redox neutral mechanism are plausible including oxidative addition into the C(O)-O or B-O bond. Since a Pd(II) precatalyst namely $Pd(OAc)_2$ is used, reduction to the low valent species would be required to facilitate this type of non-redox neutral type mechanism. Reduction of the palladium could go through a pathway such as formation of biaryl species from the boron derivative. This is done by palladium transmetallating with two equivalents of the boron derivative followed by the reductive elimination to yield the parent biaryl species and the Pd(0) catalyst.[71] This reduced palladium catalyst could then interact with the blocked isocyanate or the boron species.

A plausible method of activation to allow for reactivity would be the oxidative addition into the C-O bond of the carbamate. The palladium mediated oxidative addition into a phenolic ester has been recently disclosed by Newman and co-workers[72] (2017) which would support the possibility of this type of mechanism being extended to carbamates. Oxidative addition using carbamate substrates has been reported albeit not into the C(O)-O bond, but rather into the distal C-O bond that would likely extrude carbon dioxide following insertion (Scheme 2-2).[73] However, this type of mechanism (Scheme 2-2) cannot be disregarded although there is a lack of literature to directly support this pathway, and that a palladium intermediate such as that shown on the left in Scheme 2-2 would be expected to eliminate Pd(0) in the absence of an oxidant. An experiment to probe this type of insertion into the C(O)-O bond of a phenyl carbamate was therefore needed, ideally on a substrate that would prevent subsequent formation of an isocyanate.

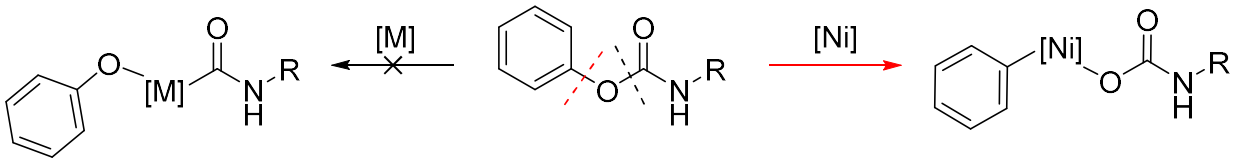

Scheme 2-2: Carbamate oxidative addition pathways

[71] Adamo, C.; Amatore, C.; Ciofini, I.; Jutand, A.; Lakmini, H. *J. Am. Chem. Soc.* **2006,** *128*, 6829.
[72] Halima, T. B.; Vandavasi, J. K.; Shkoor, M.; Newman, S. G. *ACS Catal.* **2017,** *7*, 2176.
[73] (a) Quasdorf, K. W.; Riener, M.; Petrova, K. V.; Garg, N. K. *J. Am. Chem. Soc.* **2009,** *131*, 17748. (b) Xu, L.; Li, B.-J.; Wu, Z.-H.; Lu, X.-Y.; Guan, B.-T.; Wang, B.-Q.; Zhao, K.-Q.; Shi, Z.-J. *Org. Lett.* **2010,** *12*, 884. (c) Ohtsuki, A.; Yanagisawa, K.; Furukawa, T.; Tobisu, M.; Chatani, N. *J. Org. Chem.* **2016,** *81*, 9409.

To examine this hypothesis, a methylated carbamate (**1a-Me)** was subjected to the reaction conditions (Scheme 2-3). The optimized conditions at 50 ℃ didn't produce the amide **3a-Me** to any observable yield, and consequently the temperature was increased to 100 ℃ in a follow-up experiment since this oxidative addition could require a higher activation energy. Even at 100 ℃, the amide **3a-Me** was not produced, suggesting that reactivity via insertion into the C-O bond of the carbamate is an unlikely pathway.

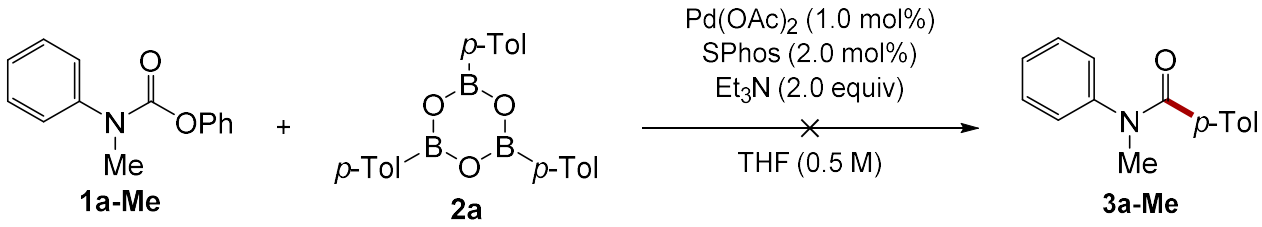

Scheme 2-3: Probing the carbamate oxidative addition pathway

Even if unlikely, Pd(0) cannot be discounted and thus, a possible catalytic cycle is given in Scheme 2-4. A method at which the palladium could be reduced is with two transmetallation events with the boron nucleophile which can then do a reductive elimination to give the biaryl product (**I'**) by a reduced palladium(0) species (**I**). At this point, an oxidative insertion step into the carbamate would occur to produce the acyl organopalladium(II) species (**II**). This species could transmetallate,[74,75] decarbonylate,[76] or β H^- eliminate[77] to lead to various products. Acyl organopalladium(II) species have been seen to transmetallate with aryl boronic acids under similar conditions although with a different palladium catalyst.[74] Wu[75] (2015) proposes a ligandless palladium that transmetallates with a boronic acid that goes through a radical-type pathway as reactivity was shut down when a radical trap was introduced suggesting this radical-type pathway. Also, this carbamoyl palladium has been seen to decarbonylate although at elevated temperatures (>100 ℃) but the need for significantly higher temperatures makes this pathway unlikely.[76] The insertion product (**II**) that is shown could do a β-hydride elimination followed by deprotonation to yield the isocyanate (**II'**) and Pd(0) which has been observed (Scheme 2-4).[77] Although, transmetallation with the aryl boroxine must occur followed by reductive elimination to yield the

[74] Yu, A.; Shen, L.; Cui, X.; Peng, D.; Wu, Y. *Tetrahedron* **2012,** *68*, 2283.
[75] Li, W.; Wu, X.-F. *Chem. Eur. J.* **2015,** *21*, 7374.
[76] Liu, C.; Szostak, M. *Org. Biomol Chem.* **2018,** *16*, 7998.
[77] Aresta, M.; Giannoccaro, P.; Tommasi, I.; Dibenedetto, A.; Lanfredi, A. M. M.; Ugozzoli, F. *Organometallics* **2000,** *19*, 3879.

desired amide product (**IV**). This transmetallation and reductive elimination event has precedence in a carbonylative palladium-catalyzed amide formation preparation involving a carbamoyl-metal intermediate (**III**) similar to the one proposed in Scheme 2-4.[75] Another possibility for a mode of activation would be through the oxidative addition into the N=C bond of the isocyanate leading to product (III'). This mode of activation has been seen in the oligomerization of isocyanates in Osborn's study.[48a] Intermediate (III') can then transmetallate with the boron reagent producing intermediate (III) which can then undergo the reductive elimination to yield the desired product. With this, a variety of pathways have been presented with their respective literature precedencies, however the experimental data presented thus far cannot fully prove the presence of these pathways and such, these pathways remain possible moving forward.

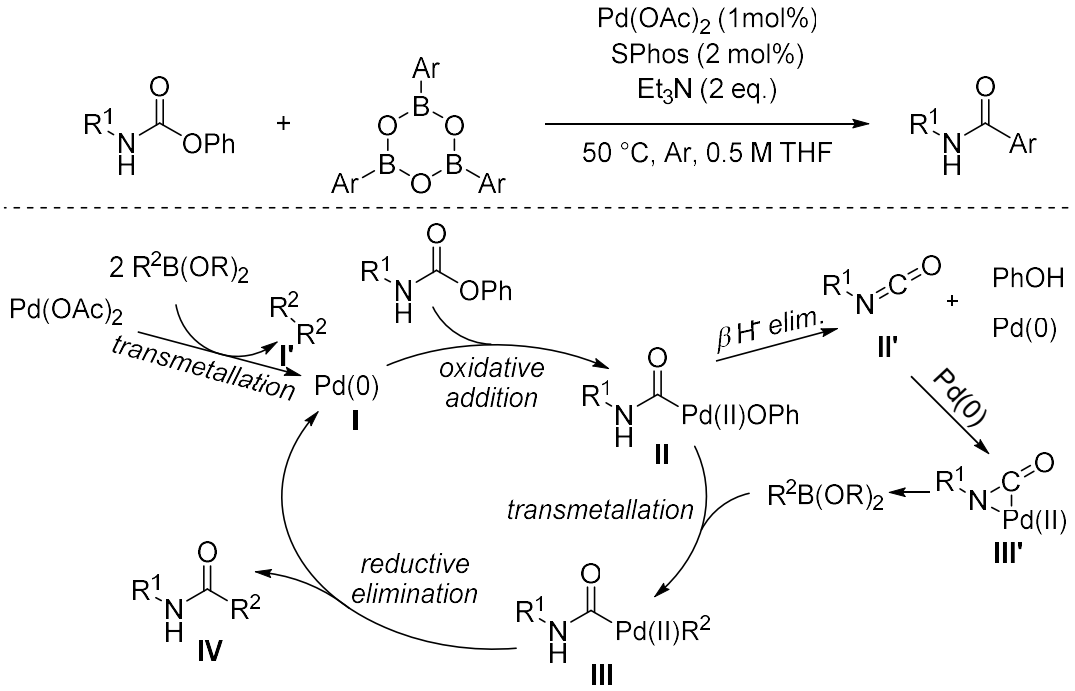

Scheme 2-4: Possible Pd(0)/(II) type catalytic cycle

Another Pd(0) pathway that must be discussed would be the type of pathway that Kianmehr[57] (2009) postulated which was the oxidative addition into the B-O bond. However, with the lack of literature precedent for an oxidative insertion into the B-O bond, this pathway was likely suggested to explain catalyst turnover without a competent oxidant. Indeed, Pd(II) generally interacts with boron derivatives to undergo a redox-neutral transmetallation to yield the organopalladium(II) and the boron salt. This chemistry has been exemplified by the development

of the Suzuki-Miyaura cross-coupling reaction and the redox neutral transmetallation step of this reaction is well established.[78] With the lack of evidence supporting this specific pathway, this type of mechanism will not be included in discussions moving forward.

2.2.2: Proposal of a Pd(II) mechanism

A redox-neutral mechanism implies that the oxidation state of the catalyst remains the same throughout the catalytic cycle thus not requiring a reagent to change the oxidation state. However, if this mechanism is operative, the formation of biaryl needs to be accounted for as well as a methodology as to how the palladium is re-oxidized. The formation of biaryl is proposed to go through the same type of mechanism as discussed (Scheme 2-4). However, the re-oxidation is more difficult to discern, the pathway could be a palladium mediated oligomerization of the isocyanate or oxidation by trace amounts of oxygen that could have been introduced into the flask. A palladium(0) catalyst has been seen to do oxidative cyclometallation reactions with isocyanates to form dimers and trimers (Scheme 2-5).[48] In this process (Scheme 2-5), there is a metallocycle that would typically do a reductive elimination to form said dimer, although the reductive elimination was favoured in Osborn's study[48a] (2007) a decarbonylative pathway could be proposed as this is a different system.

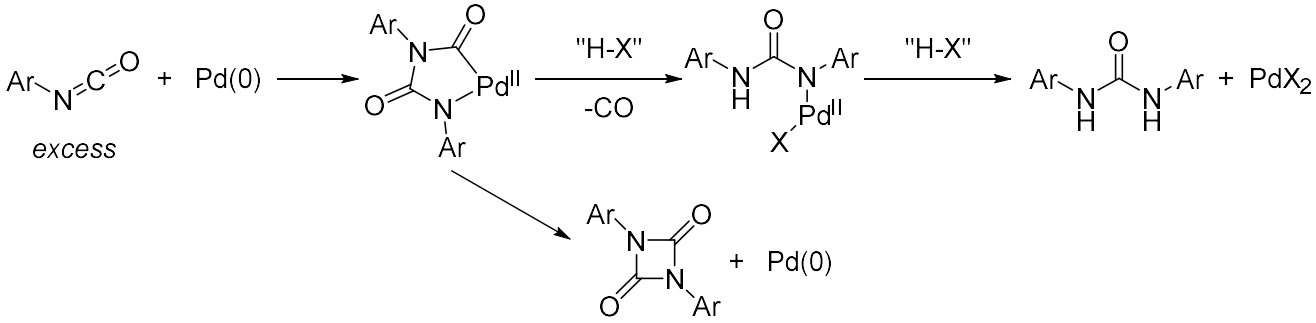

Scheme 2-5: Proposed oxidation of Pd(0) with isocyanates

The formation of cyclotrimer, urea, and biuret products during the scale-up reactions throughout the scope could be the answer to how palladium is oxidized. Control experiments were conducted by Mr. Joshua Derasp to test this hypothesis which are shown in Scheme 2-6. Conditions (**a**) in Scheme 2-6 was the first time the cyclotrimer product was isolated and was

[78] Thomas, A. A.; Denmark, S. E. *Science* **2016,** *352*, 329.

confirmed by HRMS. This trimer could however have been formed with other masked isocyanates, however the low concentration of cyclotrimer makes identification in crude ^{1}H NMR difficult. Urea formation has been more prevalent throughout developing the scope and is seen in the three conditions presented in Scheme 2-6. At the time of these experiments, the hypothesis was that palladium was catalyzing the oligomerization process, although the urea formation in both conditions (**b**) and (**c**) suggest otherwise. With conditions (**b**), urea was formed when no palladium was introduced into the system which lead to the thought that palladium might not be responsible for the by-product formation. The boroxine could catalyze such reaction with its empty *p* orbital, so the boroxine was excluded for equation (**c**). A decrease of urea formation was found when lacking the boroxine, although there was still urea formation when SPhos was present. With this, drawing the conclusion that palladium is being oxidized by the formation of oligomerization products cannot be made strongly.

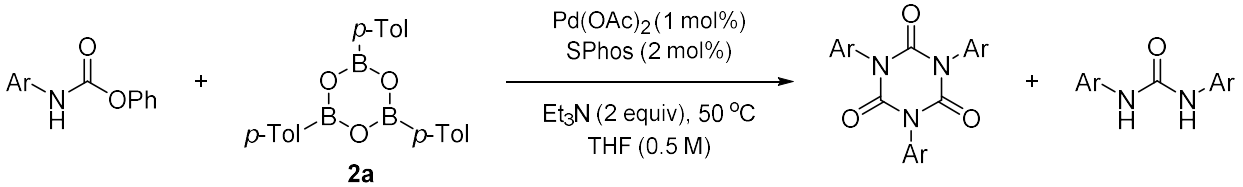

*With 3,5 dimethyl ester carbamate: 14% urea, 4% trimer (**a**)*
*With phenyl carbamate, no $Pd(OAc)_2$: 18% urea (**b**)*
*With phenyl carbamate, no boroxine, no $Pd(OAc)_2$: 9% urea (**c**)*

Scheme 2-6: Oligomerization control experiments

Although a firm reasoning for the oxidation of the palladium cannot be drawn, a redox neutral pathway could still be an option which is illustrated in Scheme 2-7. This cycle (Scheme 2-7) first does the transmetallation with the boron derivative forming the aryl-palladium species which has three possible fates. The pathways include insertion into the isocyanate, transmetallation with another equivalent of boroxine, or interaction with an oligomerization product. The productive pathway would be the insertion into the isocyanate which would lead to the desired product. The first non-productive pathway involves another transmetallation event with the boron derivative to arrive at the reduced palladium as well as the biaryl product which has been observed (Scheme 2-1). The second non-productive pathway would involve the interaction of the aryl-palladium species (Scheme 2-5) with the oligomerization products that have been observed (Scheme 2-6), but the presence of these coupled products has not been observed. The third fate would be aryl-palladium species interacting with the isocyanate, following a protodepalladation

step which would yield the desired amide product. The proton that is enabling the protodepalladation could come from two sources, the phenol that is released or another equivalent of the carbamate. With phenol having the greatest acidity of the two, it is most likely coming from the phenol that is released from isocyanate generation. The mechanism presented in Scheme 2-7 exemplifies the evidence presented thus far and will be included in discussions in subsequent sections.

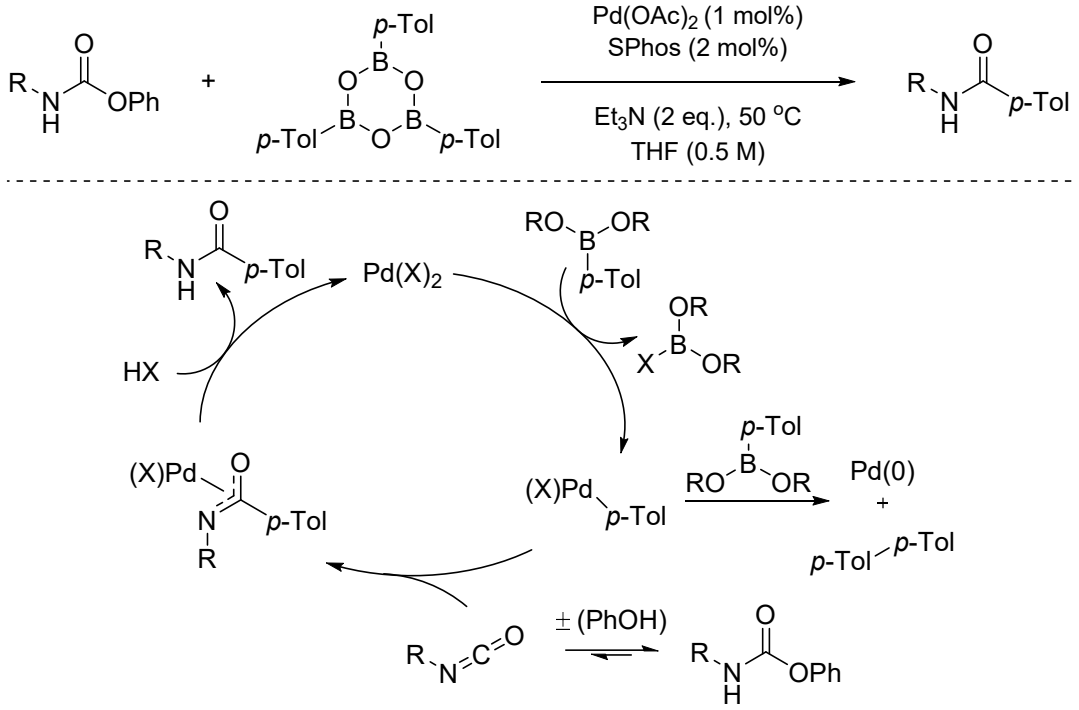

Scheme 2-7: Proposed Pd(II) catalytic cycle

2.2.3: Attempts to further probe the mechanism

In parallel efforts to understand the mechanism, other strategies were explored to circumvent by-product formation. The first method was trying to use different boron derivatives in hopes to slow the unwanted second transmetallation step. The second method was testing whether or not the blocking group strategy was necessary to promote reactivity. The third method was testing different blocking groups which would impact the rate of isocyanate formation.

The underlying hypothesis was that changing the structure of the organoboron reagent would change the relative rate of transmetallation steps, which in turn could have effects on the formation of the low valent palladium species. Indeed, while both steps could be slower, using more hindered boron reagents could be less likely to undergo the second transmetallation.

Different boron esters were subjected to the optimized reaction conditions at both 50 and 70 °C shown in Table 2-8. Substrate **1g** was used in this instance in order to visualize a more noticeable change on the outcome of the reaction since the optimized yield of this substrate (entry 1) was lower than the optimal substrate **1a** (89 %). With the exception of entry 4 at 70 °C which gave a modest amount of the amide, all of the tested organoboron reagents completely suppressed the formation of the desired products. This suggests that this modification prevented facile transmetallation since only traces of reactivity were observed, thus accounting for the formation of oligomerization product **5b** (Table 2-8).

Table 2-8: Exploring different organoboron reagents[a]

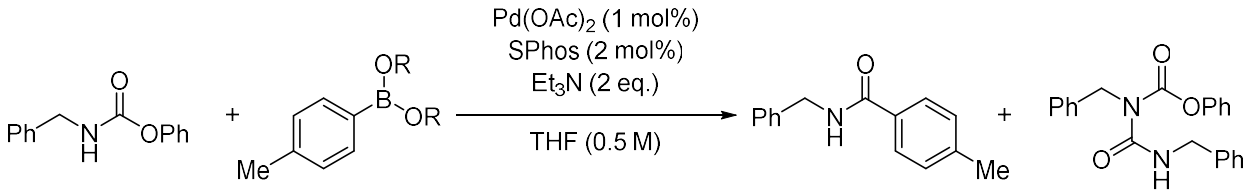

1g **2aa-ae** **4g** **5b**

Entry	Organoboron	50 °C		70 °C	
		Yield **4g** (%)	Yield **5b** (%)	Yield **4g** (%)	Yield **5b** (%)
1	Boroxine	57	-	75[b]	-
2	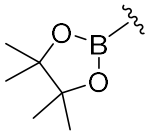	0	3	0	3
3	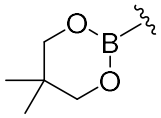	0	17	0	32
4	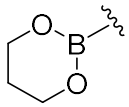	0	7	0	20
5	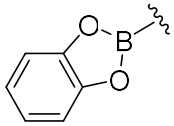	0	4	13	6

[a] Conditions: **1g** (0.2 mmol), **2aa-ae** (0.4 mmol), $Pd(OAc)_2$ (1 mol%), SPhos (2 mol%), Et_3N (0.4 mmol), THF (0.5 M), 50 °C unless otherwise indicated. ^1H NMR yield determined using 1,3,5-trimethoxybenzene as internal standard. [b] 80 °C.

A blocking group strategy proved to be effective in the Rh-catalyzed amide formation methodology recently disclosed,[65] to probe the efficacy of this strategy for this Pd-catalyze amide formation methodology, control reactions involving the free phenyl isocyanate were ran (Table 2-9). To quantify the remaining isocyanate, methanol was used to quench the reaction to form

product **6a** which can be analyzed via ^{1}H NMR spectroscopy. Control reactions 1 and 2 in Table 2-9 tested the applicability of the optimized reaction conditions on the phenyl isocyanate. The trace amount of product (**3a**) shows the necessity of the blocking group since having too much of the isocyanate in solution is detrimental for the outcome of the reaction. The addition of base (entry 3) increased product formation slightly whereas when the isocyanate was just exposed to base, although almost complete consumption of the isocyanate to oligomerization products was observed. This reinforces the power of a blocking group strategy which can mitigate these oligomerization products. When using the catalytic system developed by Kianmehr[57] but with boroxine as a nucleophile as opposed to the boronic acid (entry 5), the desired amide product was obtained where it was completely inactive when the masked isocyanate was used (Table 2-1, entry 1). Furthermore, the use unaltered commercially available boronic acid did boost the yield to 28% from 14%, but the reported 64% could not be reproduced. Although the use of a blocking group still allowed for formation of the biaryl product, this was greatly reduced from the 30% Kianmehr[57] (2009) reported to about 4% under the optimized reaction conditions described above. The results obtained here suggest that the overall performance of this reactions hinges on the use of a blocking group.

Table 2-9: Control reactions on free isocyanate[a]

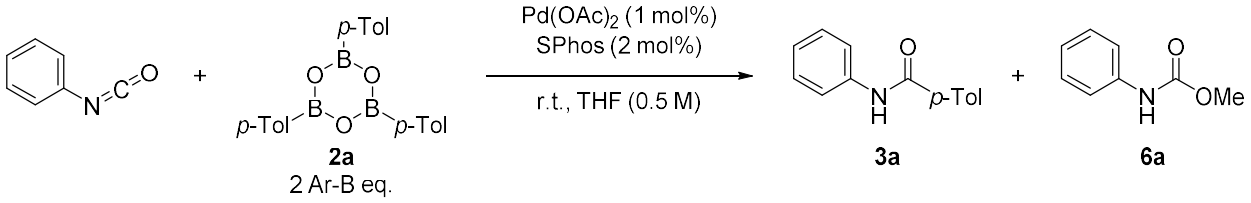

Entry	Deviation for conditions	**3a** Yield (%)	**6a** Yield (%)[b]
1	None	6	79
2	50 °C	6	74
3	2 eq. Et_3N at 50 °C	17	21
4[c]	2 eq. Et_3N at 50 °C, No Pd/SPhos/Boroxine	0	5
5	[Pd] (5 mol%), PPh_3 (20 mol%) 0.33 eq. $[RBO]_3$ "Kianmehr conditions"	14	42
6[d]	[Pd] (5 mol%), PPh_3 (20 mol%) 1 eq. $RB(OH)_2$	28	68

[a]Conditions: Phenyl isocyanate (0.2 mmol), **2a** (0.13 mmol), $Pd(OAc)_2$ (1.0 mol%), SPhos (2.0 mol%), Et_3N (0.4 mmol), THF (0.5 M), 50 °C unless otherwise noted. ^1H NMR yield determined using 1,3,5-trimethoxybenzene as internal standard. [b]Reactions were quenched with MeOH and stirred at room temperature for 1 h. Presence of **6a** is assumed to represent remaining starting material. [c]Crude NMR matched literature reports of phenyl isocyanurate. [d]Commercially available boronic acid used directly.

To see how a blocking group strategy effects the generation of the biaryl product **5a**, a larger scale reaction was performed (Scheme 2-8) to allow for the this product to be isolated. Testing the $Pd(OAc)_2$/SPhos system with the free isocyanate (Scheme 2-8) produced the desired amide in a yield of 17% as well as the biaryl product to 23% whereas it was 8% when using the blocking group. In contrast with Kianmehr's conditions[57] which had triphenylphosphine as a ligand, the use of SPhos could increase the congestion around the palladium center making it more selective for the isocyanate than the boroxine. But as seen from the results obtained from Scheme

2-8, this did not prohibit the undesired reactivity. It can be further reinforced from these results that a blocking group strategy has a positive effect on the outcome of the reaction.

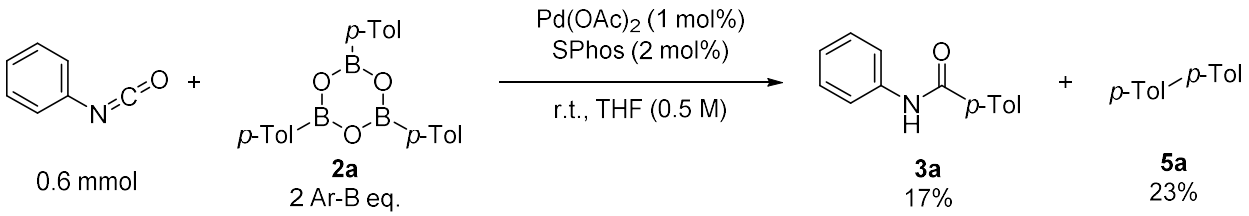

Scheme 2-8: Scale-up reaction with phenyl isocyanate

Changing the blocking group would likely affect the rate of isocyanate formation, the position of the equilibrium as well as impact the protodepalladation event if the blocking group is responsible for this step. Table 2-10 illustrates various blocking groups screened with the optimized conditions including an amine (entry 1), an oxime (entry 2), and phenolic substrates (entries 3-4). Deblocking can be affected by the temperature as well as the nature of the blocking group such as acidity and steric encumbrance. Amines are not frequently used as blocking groups because of the rapid rate of the reverse reaction being the reformation of the urea which results in a low effective concentration of isocyanate.[20] The greater basicity of amines would have a positive affect on the protodepalladation step. Increasing the temperature to 80 °C for entry 1 promoted reactivity whereas 50 °C completely suppressed product formation as only starting material was recovered. With this, manipulating the equilibrium in disfavour of the forward reaction greatly reduces performance of the reaction. Oximes are widely used in industry due to their low deblocking temperatures and can be highly dependant on steric effects which can allow for optimization.[20] Entry 2 produced the amide although with a poor yield. Increasing the effective concentration of isocyanate greatly reduced the performance of the reaction. The effect of increasing the steric bulk is known to enable rapid deblocking, however 2,6-dimethylphenol was found to deblock at much higher temperatures suggesting that the steric effect is overshadowed by the electronic effect.[20] Increasing the steric bulk on the aromatic group (entry 3) provided the amide in a poor yield at 50 °C whereas increasing the temperature resulted in the decomposition of the blocked isocyanate. This result could offer support of an oxidative insertion pathway as increasing the steric bulk around the C-O bond would make this step less favourable however results from Scheme 2-3 suggest this pathway is still unlikely. The increase of deblocking rate can also be corelated to the presence of electron withdrawing substituent.[20] An electron donating group present

on the phenol was competent under the reaction conditions at 50 °C although a reduction in reactivity was found when increasing the temperature to 80 °C. From the results in Table 2-10, the increased lability of the blocking group was found to detrimental to the performance of the reaction. With this, it would appear that groups that are somewhat between these two extremes are necessary to promote reactivity which can be seen from modest product formation resulting from entries 3 and 4.

Table 2-10: Exploring different blocking group[a]

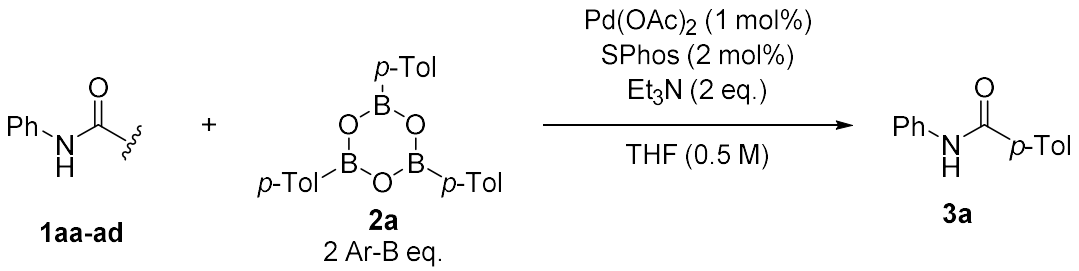

Entry	Blocking group	50 °C Yield **3a** (%)	80 °C Yield **3a** (%)
1	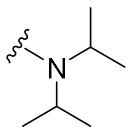	0	8
2	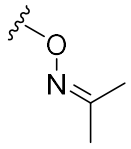	3	2
3	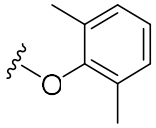	46	2
4	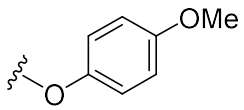	75	17

[a] Conditions: **1aa-ad** (0.2 mmol), **2a** (0.4 mmol), $Pd(OAc)_2$ (1 mol%), SPhos (2 mol%), Et_3N (0.4 mmol), THF (0.5 M), 50 °C unless otherwise indicated. ^1H NMR yield determined using 1,3,5-trimethoxybenzene as internal standard.

A follow-up study linked to results illustrated in Table 2-10 was performed to gain further insight into how the blocking group affects the reaction. This included addressing the innocence

of the blocking groups from substrates **1aa** and **1ab** as well as more phenolic and alkyl substrates. To probe the innocence of diisopropylamine and acetone oxime as blocking groups, a control experiment with substrate **1a** with one equivalent of diisopropylamine and acetone oxime was done. Doping the reaction with diisopropylamine resulted in the quantitative formation of the unsymmetrical urea **1aa**. Doping the reaction with acetone oxime resulted in complete inhibition of the desired reaction. The blocking groups that were tested included *o*-cresol, *p*-cresol, and *p*-fluorophenol probe both the steric and electronic effects of the blocking group. Increasing the steric hinderance with substrate **1ae** did not affect the performance of the reaction at both 50 and 80 ℃ suggesting that electronic effect gained overshadows the steric effect of deblocking. The use of mildly donating (**1af**) and withdrawing (**1ag**) phenolic substrates had minimal effects on the overall performance of the reaction at 50 ℃. Although with an increased temperature, the yield dropped suggesting that the forward reaction of deblocking has a negative impact. Alkyl alcohols (**1ah** and **1ai**) contrasted with aryl alcohols deblock at higher temperatures likely due to the increased pKa of the conjugate base. Using trifluoroethanol (**1ah**) as a blocking group resulted in reduced yields which would be expected as alkyl blocking groups require higher temperatures for deblocking. The CF_3 group is strongly electron withdrawing which favours the forward reaction increasing the effective concentration of the isocyanate in solution. Increasing the temperature to 70 ℃ had a positive effect on the outcome of the reaction with a greater yield of the desired product. The use of *tert*-butanol as a blocking group was incompatible with the reaction conditions as only the unreacted *boc* protected aniline was recovered at the end of the reaction. This suggests that a higher reaction temperature is required to enable reactivity as 100 ℃ when a rhodium catalyst was used in a similar transformation.[64] Concluding these studies, it was found the amine and oxime blocking groups were not innocent and didn't enable the desired reactivity. Limiting the steric encumbrance of the blocking group with *o*-cresol showed that the steric effects were overshadowing the electronic effects.

Table 2-11: More blocking groups[a]

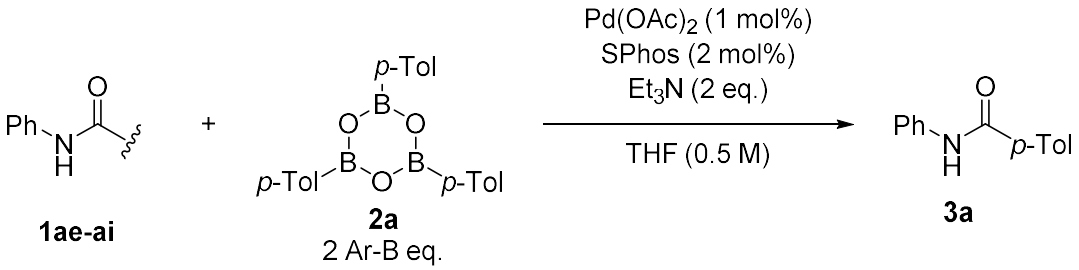

Entry	Blocking group	50 °C Yield **3a** (%)	80 °C Yield **3a** (%)
1	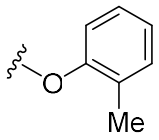	87	80
2	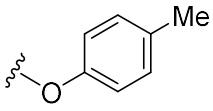	81	51
3	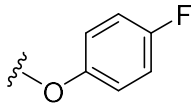	73	22
4	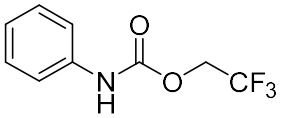	47	66
5	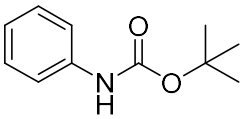	0	0

[a] Conditions: **1ae-ai** (0.2 mmol), **2a** (0.4 mmol), $Pd(OAc)_2$ (1 mol%), SPhos (2 mol%), Et_3N (0.4 mmol), THF (0.5 M), 50 °C unless otherwise indicated. ^1H NMR yield determined using 1,3,5-trimethoxybenzene as internal standard.

2.3: Kinetic studies

With many unanswered questions from the experiments carried out from sections 2.1 and 2.2, a kinetic study was done to gain further insight into the mechanism of the reaction. Variable

time normalization analysis (VTNA) was developed by Prof. Jordi Burés[79] (2016, 2019) which utilizes conversion over time data that can obtained in a non-continuous manner. Another type of kinetic analysis namely reaction progress kinetic analysis (RPKA) was popularized by Prof. Blackmond[80] is an exhaustive method involving continuous analysis gathering the instantaneous reaction rate at all points during the reaction. As VTNA involves the gathering of non-continuous data, implementing this analysis would require minimal changes to the overall procedure and was used moving forward. The mathematical basis of VTNA lies in the comparison of the concentration of a single reagent with all other conditions remaining the same. For example, doubling the concentration of one component would offer a different reaction profile that could be faster or slower in comparison to the control reaction. However, if the two experiments were normalized with the trapezoid rule (Equation 2-1), overlay can occur with manipulation of an exponent (α). The greatest overlay in this analysis would suggest the order of the respective reagent being analyzed.

$$f(t) = \int_0^t [A]^\alpha dt \approx \sum_{i=1}^{n} \left(\frac{[A]_i + [A]_{i-1}}{2}\right)^\alpha (t_i - t_{i-1})$$

Equation 2-1: Trapezoid rule

In order to determine the concentrations of both the amide product and the starting material, a fluorinated carbamate was used to follow the reaction using ^{19}F NMR spectroscopy (Scheme 2-9). An internal standard of α,α,α-trifluorotoluene was used to calibrate the axis to δ -63.72 ppm, and the carbamate (**1g**) and amide (**4f**) have a resonance at δ -121.91 ppm and δ -121.05 ppm respectively.

[79] (a) Burés, J. *Angew. Chem. Int. Ed.* **2016,** *55*, 2028. (b) Nielson, C. D.-T.; Burés, J. *Chem. Sci.* **2019,** *10*, 348.
[80] (a) Blackmond, D. G. *Angew. Chem. Int. Ed.* **2005**, *44*, 4302. (b) Blackmond, D. G. *J. Am. Chem. Soc.* **2015**, *137*, 10852.

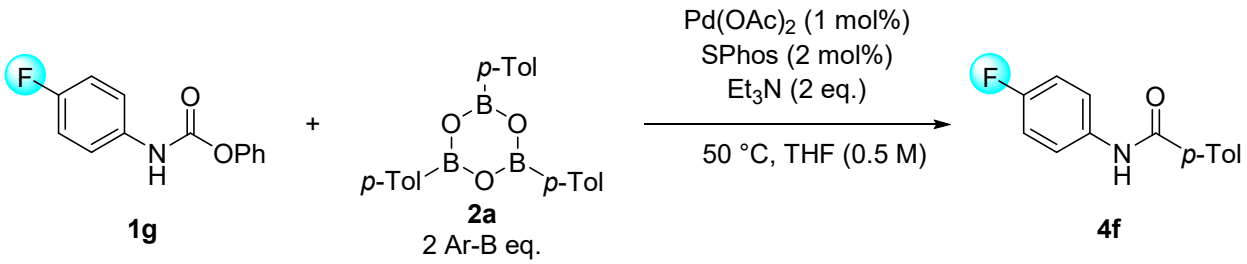

Scheme 2-9: Conditions for kinetic studv

Figuring out the optimal methodology for doing this kinetic study required some trial and error. First attempts were to do a control reaction to see what the isolated yield would be and then testing said reaction under different conditions. The first condition was to run the reaction in an NMR tube with a stir bar in an oil bath. With this methodology, there was a lot of tampering with the tube since the stir bar had to be removed for every time point for NMR analysis and seeing as this reaction is done under an argon atmosphere, this would not be a viable option. The second condition was performed on a larger scale and then taking aliquots out for every time point followed by a quench with THF. This methodology proved to be appropriate as a control reaction at room temperature showed that the progression is negligible (Table 4-2).

Preliminary studies in the determination of the order in **1g** and the catalyst were only including time points up to 6 hours (Figure 2-1). Experiments included varying the loadings of the catalysts including 0.50 mol% (•), 1.00 mol % (•), and 1.25 mol % (•) are plotted on Figure 2-1 (upper) for the determination of the order for the catalyst. Another set of experiments included difference concentrations of the carbamate (**1g**), namely at 0.50 M (•), 0.75 M (•), and 1.0 M (•) which are plotted on Figure 2-1 (lower). With this information, conclusions were drawn that each component had an order of zero as this was providing the best fit visually with the Burés[79] method. To better understand this kinetic behaviour, we sought out the expertise of Dr. Keillor. Further analysis showed that by limiting monitoring to before the reaction was completed was not indicative of the entire reaction. Dr. Keillor was in the midst of developing a mathematical algorithm that would yield the information typically provided that the Burés method[79] but wouldn't rely on the visual aspect of the analysis. The mathematical approached conceived by Dr. Keillor is based on the best possible fit, using an analysis where each possible multiplier is tested and analyzed, providing the user with a value with the highest correlation. Overall, it was felt that this quantitative approach would reduce the uncertainty that arose from a visual representation and

allow more certainty when there is little variation observed between similar values. With this, a collaboration emerged to test out Dr. Keillor's algorithm with the experimental data presented in this section. To offer the reasoning and context for applying this new methodology by Dr. Keillor, steps taken towards applying this approach will be given in the determination of the catalyst order. Then Dr. Keillor's mathematical approach will be used to determine the order regarding the carbamate and boroxine reagents.

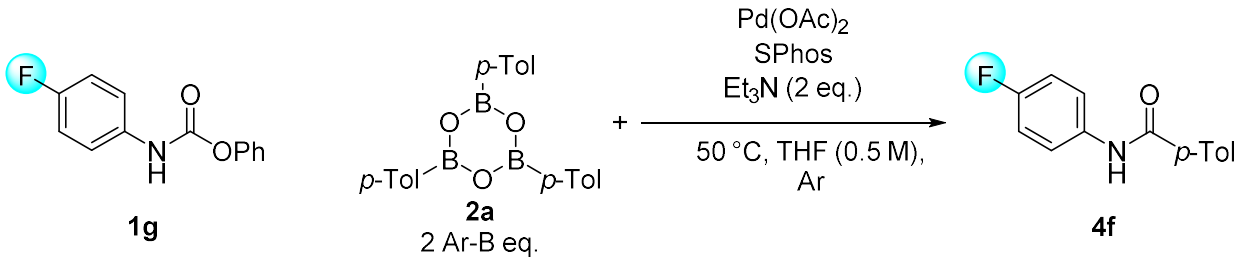

- :**1g** (0.6 mmol), **2a** (0.4 mmol, 2.0 Ar-B eq.), Et_3N (1.2 mmol), $Pd(OAc)_2$ (1 mol%), SPhos (2 mol%), THF (0.5 M), $PhCF_3$ (0.6 mmol), 50 °C, Ar.
- :**1g** (0.6 mmol), **2a** (0.4 mmol, 2.0 Ar-B eq.), Et_3N (1.2 mmol), $Pd(OAc)_2$ (0.5 mol%), SPhos (1 mol%).
- :**1g** (0.6 mmol), **2a** (0.4 mmol, 2.0 Ar-B eq.), Et_3N (1.2 mmol), $Pd(OAc)_2$ (1.25 mol%), SPhos (2.5 mol%).
- :**1g** (0.9 mmol), **2a** (0.4 mmol, 2.0 Ar-B eq.), Et_3N (1.2 mmol), $Pd(OAc)_2$ (0.5 mol%), SPhos (1 mol%).
- :**1g (1.2 mmol)**, **2a** (0.4 mmol, 2.0 Ar-B eq.), Et_3N (1.2 mmol), $Pd(OAc)_2$ (0.5 mol%), SPhos (1 mol%).

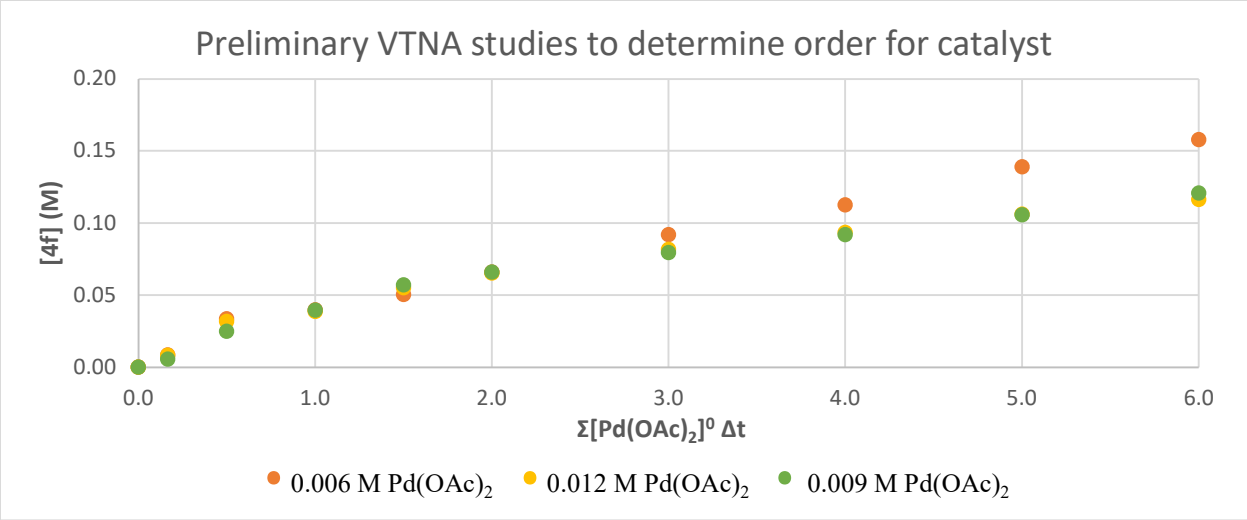

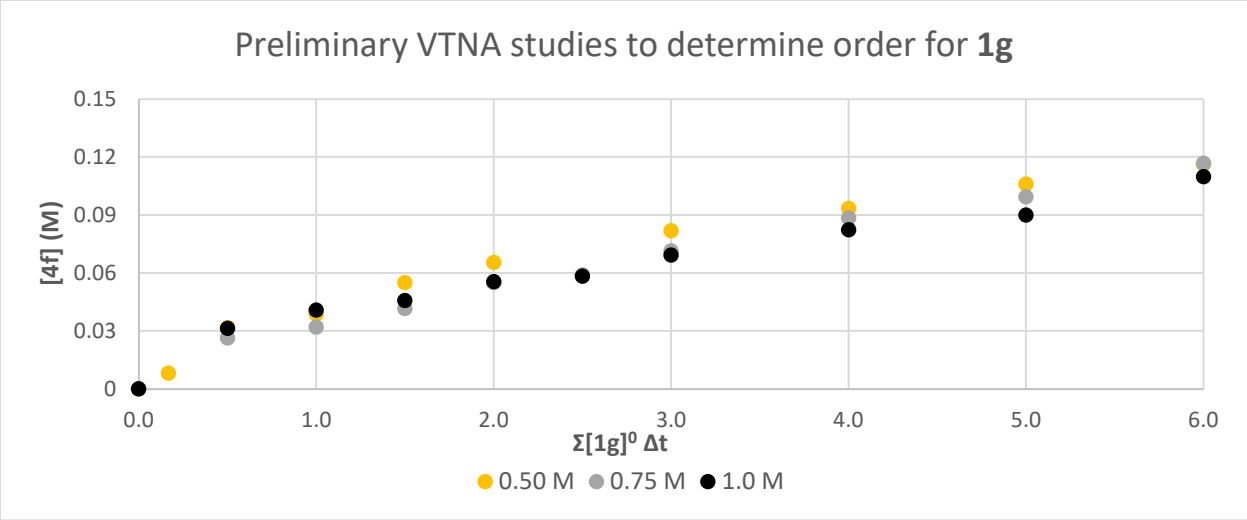

*Figure 2-1: Early studies visually showing the order in $Pd(OAc)_2$ (upper) and **1g** (lower) both being zero*

2.3.1: Kinetically probing the catalyst

While testing the applicability of this new methodology, various side-products were observed which consequently could form Pd(0). If a Pd(II)/(II) mechanism is operative, the formation of Pd(0) could be considered as a mode of catalyst decomposition. The Pd(0) that is formed must get oxidized back to Pd(II) as the yield of biaryl product supersedes the initial concentration of $Pd(OAc)_2$. Outlined in the Burés method,[79] an experiment exists which can probe for catalyst decomposition and/or product inhibition. The experiments done in Figure 2-2 are to show if there is catalyst decomposition or product inhibition. To probe for catalyst decomposition, experiments consisting of a control reaction using the optimized conditions and overlaying it with a truncated mmol of reagents but with the same mmol of catalyst as the control experiment. In an ideal case, the rate at which **1g** is consumed should not depend on the number of turnovers the catalyst has underwent or the amount of starting material present at one time. Experiment (■) represents a control experiment at a 1.0 mmol scale with 1 mol% of catalyst whereas experiment (♦) uses the same mmol of catalyst as (■) but with 0.3 mmol and 0.11 mmol less of the carbamate and boroxine respectively. As there is less **1g** in (♦) than (■), a three-hour time shift was performed to allow for the first point of (♦) to overlay with a point from (■). Since the traces do not fully overlay between (■) and (♦), a likely explanation is that either catalyst decomposition or product inhibition is operating as this could explain why the rate of **1g** consumption was different between the two experiments. To determine what is inhibiting the reaction, a third experiment (■) was run

which includes 0.3 mmol of **4f** which can answer the question if it is product inhibition or catalyst decomposition. If the product was inhibiting the reaction, the two traces would not overlay. With full overlay of (♦) and (■), it can be seen that the presence of the amide product **4f** doesn't impede catalyst performance which supports the conclusion that catalyst decomposition is occurring. This observation is consistent with the observation that a Pd(0) catalyst is formed by biaryl formation.

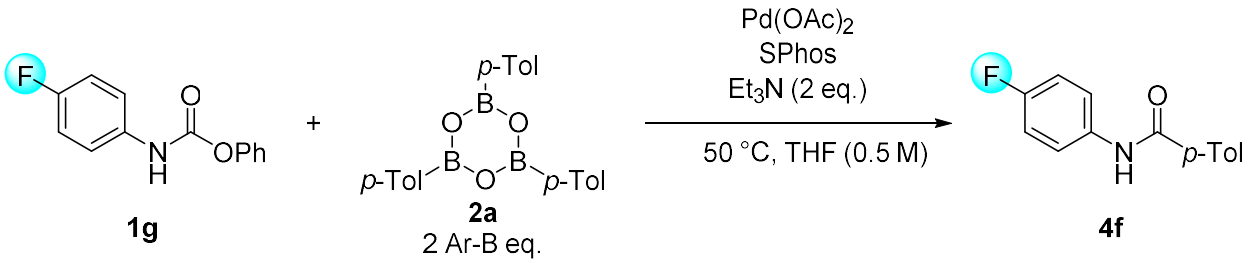

■ :**1g** (1.0 mmol), **2a** (0.67 mmol, 2.0 Ar-B eq.), Et_3N (2.0 mmol), $Pd(OAc)_2$ (1 mol%), SPhos (2 mol%), THF (0.5 M), $PhCF_3$ (1.0 mmol) 50 °C, Ar.
♦ :**1g** (0.7 mmol), **2a** (0.56 mmol, 1.7 Ar-B eq.)
■ :**1g** (0.7 mmol), **2a** (0.56 mmol, 1.7 Ar-B eq.), **4f** (0.3 mmol)

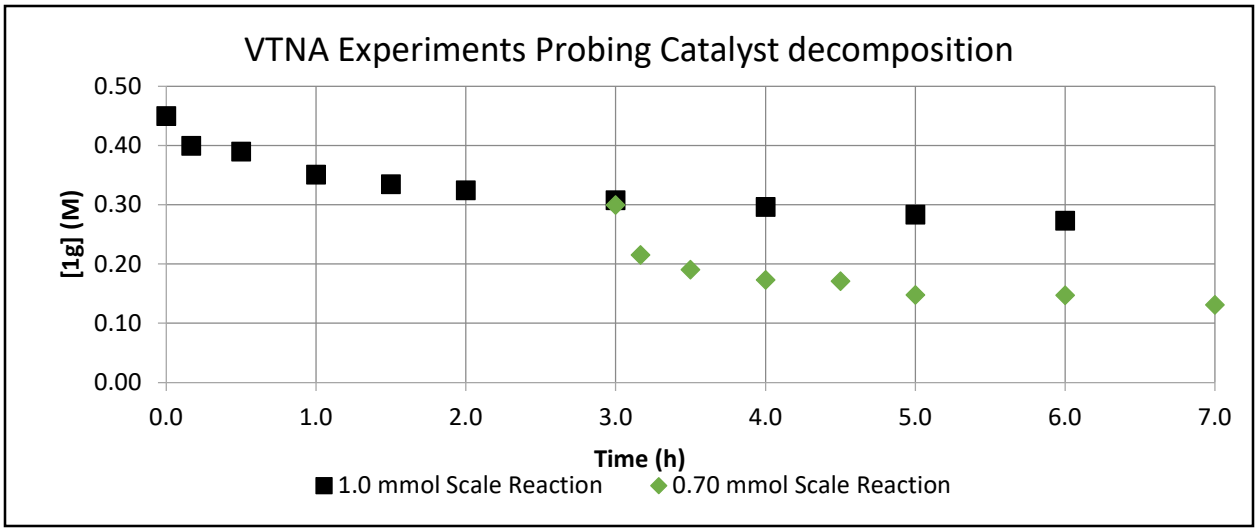

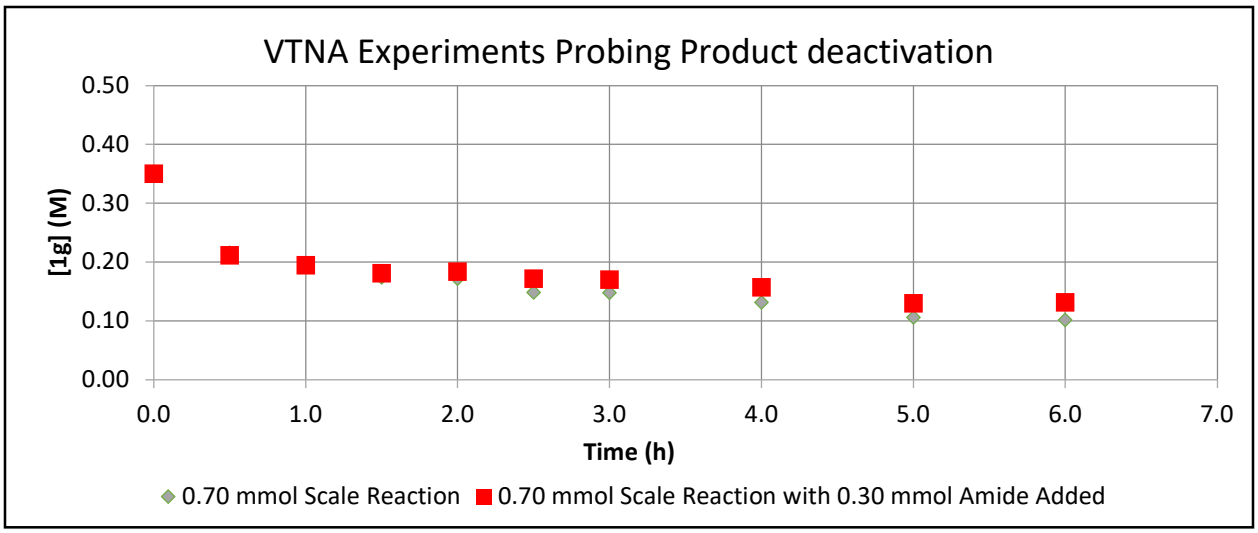

Figure 2-2: Experiments probing if catalyst decomposition (upper) or product deactivation

Although it was found that catalyst decomposition is occurring, determination of the order with respect to the catalyst can still be determined. To determine this, the catalyst concentration has to be assumed to be constant according to the Burés method.[79] The concentrations monitored to determine the order in catalyst were the carbamate (**1g**) and the amide (**4f**). The order can be determined using the VTNA method whilst changing the concentration of the catalyst and monitorring it kinetically. As the optimized conditions are 1 mol% of palladium, experiments varrying the loadings of palladium to 0.5 and 0.75 mol% were performed. As alluded to above early expeditions revealed a zereoth order in catalyst when the monitorring extended to only seven hours. Further experiments included time points up to and inlcuding 24 hours, although 24 hours wasn't included since product formation didn't increase past 16 hours (Table 4-5). Extending the monitoring to include data from the latter part of the reaction would likely target this shortcoming and provide kinetic data that is more indicative of the entire reaction. Figure 2-3 contains three traces each with different loadings of the palladium including 1 mol% (♦), 0.75 mol% (■), and 0.5 mol% (▲) which could give insight into how the concentration of the catalyst effects the reaction. The traces in Figure 2-3 include multipliers of 0, 0.5, and 1 which by using the VTNA methodology, this would illustrate the order of said reagent that displayed the greatest correlation. Examining the correlations in each of the traces in Figure 2-3, an order of zero visually would have the weakest correlation and would be safe to conclude that the order is non-zero. Building off of the early experiments that truncated the reaction time, it can be seen that allowing for the reaction to reach completion appears to have given a different order which should be more indicative of the

order of the entire reaction. As for determining a more precise order, manipulations with the multiplier showed that 0.5 and one gave a better overlay than zero. But this being limited to visually determining what the order may be, it would be difficult to be precise. With this, a strong conclusion stating that the order is nonzero can be drawn, but it is only possible to indicate that the order of catalyst appears to be between 0.5 and 1 with the data presented.

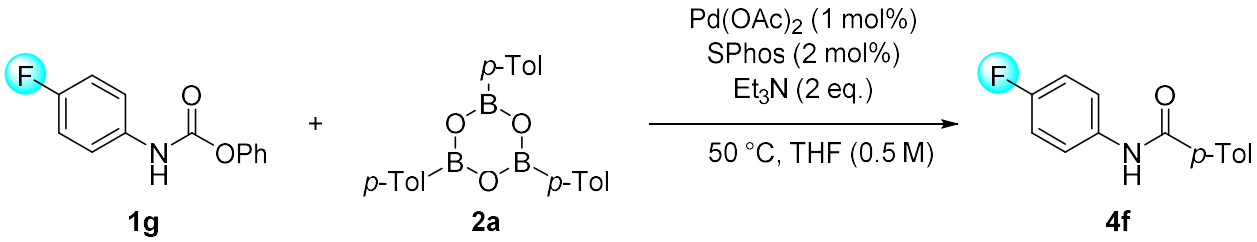

♦ :**1g** (0.6 mmol), **2a** (0.4 mmol, 2.0 Ar-B eq.), Et_3N (1.2 mmol), $Pd(OAc)_2$ (1 mol%), SPhos (2 mol%), THF (0.5 M), $PhCF_3$ (0.6 mmol), 50 °C, Ar.
■ : $Pd(OAc)_2$ (0.5 mol%), SPhos (1 mol%),
▲: $Pd(OAc)_2$ (0.75 mol%), SPhos (1.5 mol%),

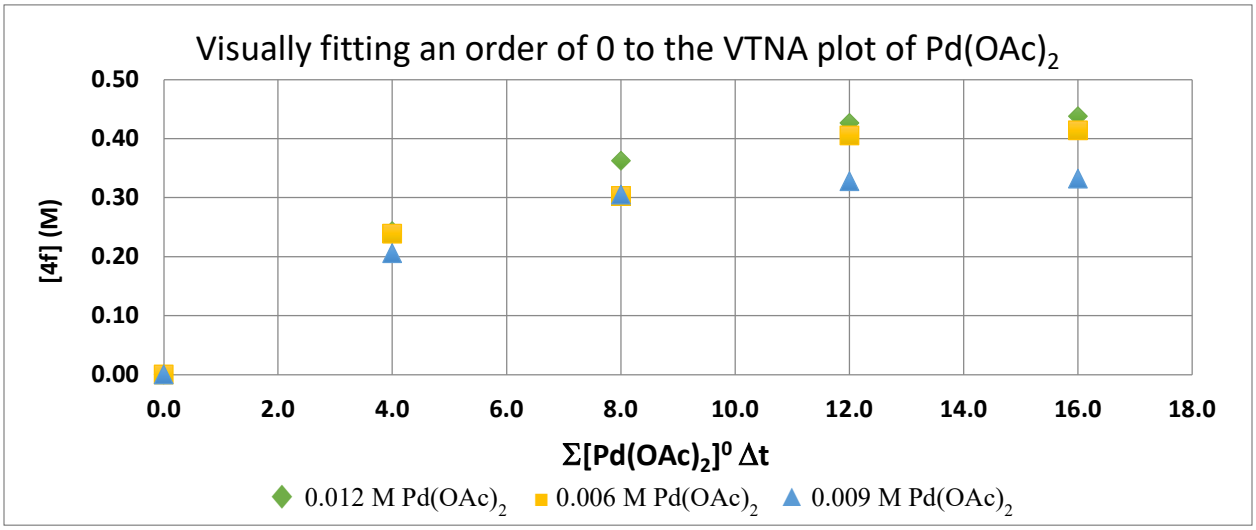

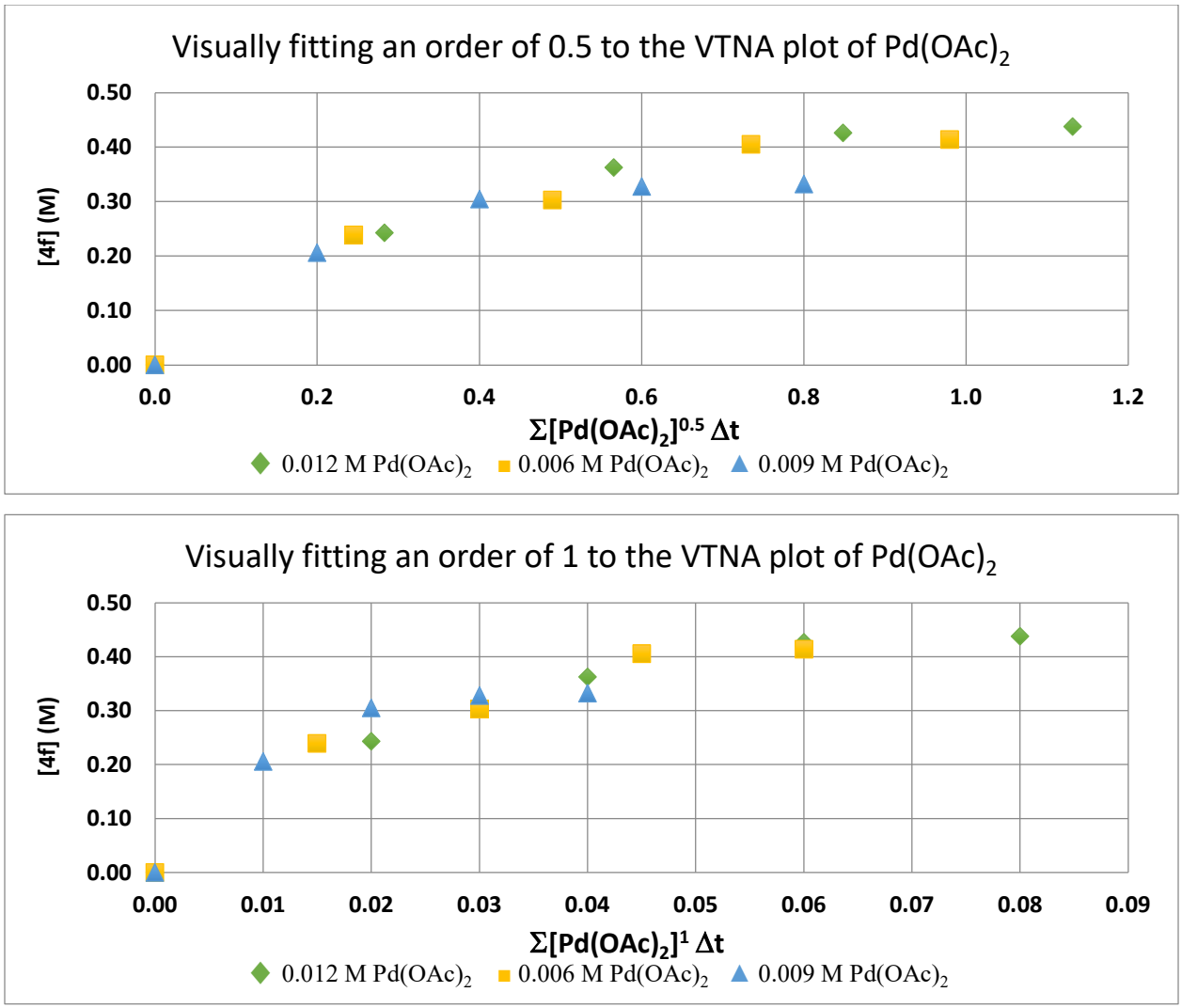

Figure 2-3: Determining the kinetic profile of the catalyst using the VTNA approach including 0 (upper), 0.5 (middle), and 1 (lower) as possible orders

Given this, we were attracted to Dr. Keillor's algorithm that would be able to test all possible multipliers and then produce the multiplier with the highest fit. As a trial run, Dr. Keillor tested his methodology on the data that was produced from this study and suggests that an order of 0.3 receives the highest correlation (Figure 2-4) although with the omission of the latter points in the (▲) trace. These points were omitted because the reaction likely didn't reach completion as the catalyst could have been deactivated due to various decomposition pathways touched upon above. Visually, it would be up to the interpreter to say if this multiplier does in fact produce greater than the traces outlined in Figure 2-4. Although there is decreased correlation in the latter part of the experiment, namely with the 0.5 mol% (▲) trace, if these points were to be omitted the lack of correlation at this point would not be present (Figure 4-1). Having a fractional order in the

rate law can mean that the catalyst must undergo a dissociation of a complex leading up to the rate determining step as well as having a positive order suggests that the catalyst is involved in the rate determining step.

As alluded to above, one of the inherent assumptions to study the order in catalyst was that the concentration of the catalyst does not change during the course of the experiment. Since the data shown in Figure 2-2 and biaryl formation show that there is indeed catalyst decomposition, the order in palladium that has been obtained from this study should only be taken quantitively. One method to determine the concentration of the catalyst would be to monitor the production of biaryl, although there is often a higher concentration of biaryl than the original concentration of $Pd(OAc)_2$ leading to the conclusion that the Pd must be re oxidized to Pd(II) by some means. With this, a more exhaustive analysis into the order of the catalyst would have to be done as there is likely more than one catalytic cycle that is operative.

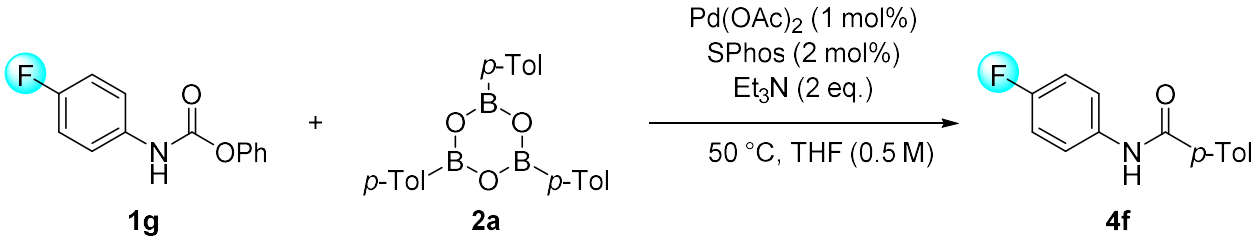

♦ :**1g** (0.6 mmol), **2a** (0.4 mmol, 2.0 Ar-B eq.), Et_3N (1.2 mmol), $Pd(OAc)_2$ (1 mol%), SPhos (2 mol%), THF (0.5 M), $PhCF_3$ (0.6 mmol), 50 °C, Ar.
■ : $Pd(OAc)_2$ (0.5 mol%), SPhos (1 mol%),
▲: $Pd(OAc)_2$ (0.75 mol%), SPhos (1.5 mol%),

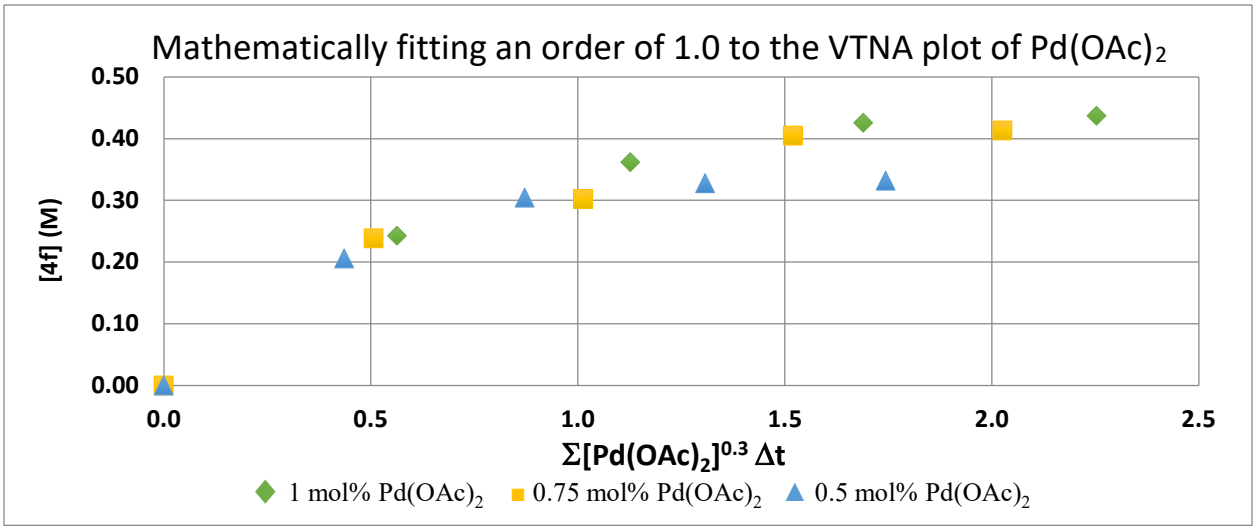

Figure 2-4: Analyzing the reaction profile of the catalyst using VTNA with Dr. Keillor's mathematical algorithm

2.3.2: Kinetically probing the reaction order in carbamate reagent

After analyzing the order of the catalyst, determining the order of the carbamate commenced. The reaction time, experimentation, and manipulation of the data was similar to that of the approach in determining the order in catalyst. With this, different concentrations of the carbamate (**1g**) were tested (Figure 2-5) including 0.625 (▲), 0.500 (♦), and 0.375 M (■) where the optimized conditions are at 0.500 M. Analyzing the data visually, the greatest correlation would result from a fitting with an order of 1 (Figure 2-5, upper). Although the fitting with a multiplier of 1 has good correlation, the algorithm developed by Dr. Kiellor was run on this set of data points and yielded an order of 0.97. Having an order of approximately 1 means that one equivalent of **1e** is present in the rate determining step of the reaction.

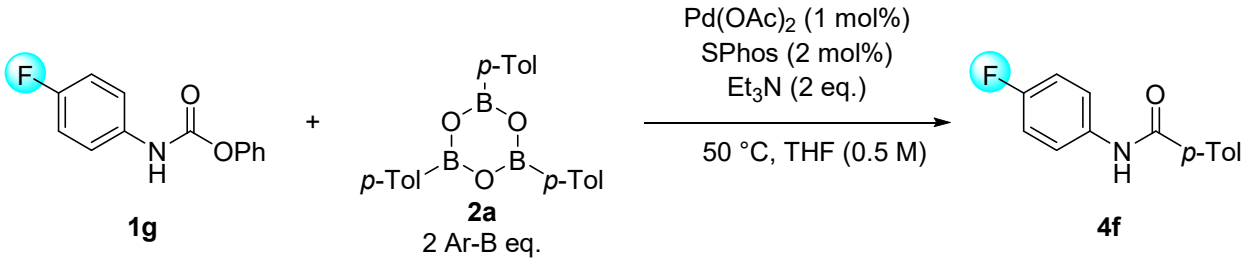

♦ :**1g** (0.6 mmol), **2a** (0.4 mmol, 2.0 Ar-B eq.), Et_3N (1.2 mmol), $Pd(OAc)_2$ (1 mol%), SPhos (2 mol%), THF (0.5 M), $PhCF_3$ (0.6 mmol), 50 °C, Ar.
■ :**1g** (0.45 mmol)
▲ :**1g** (0.75 mmol)

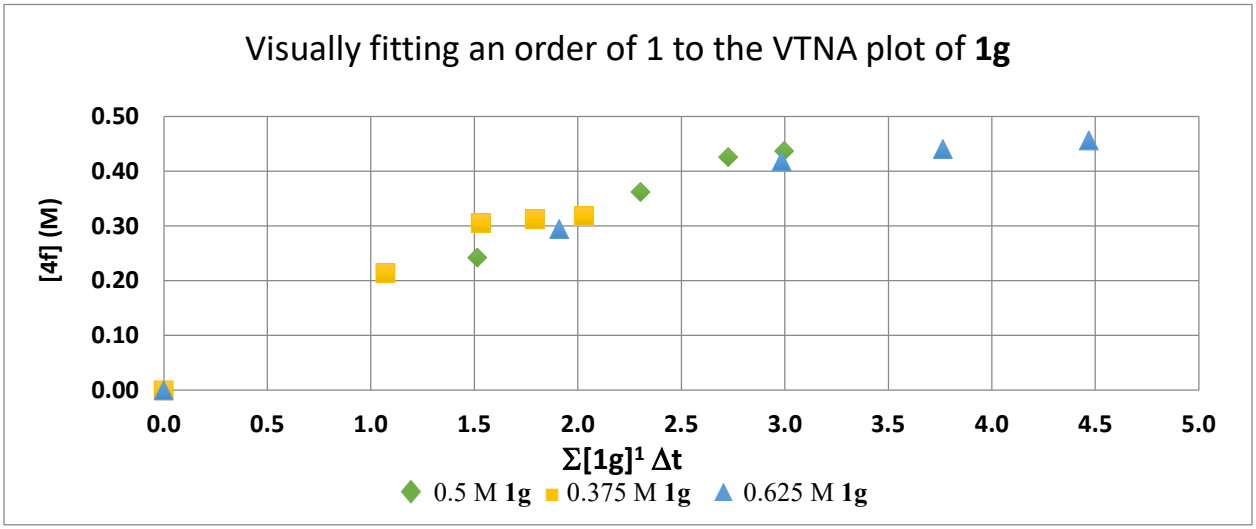

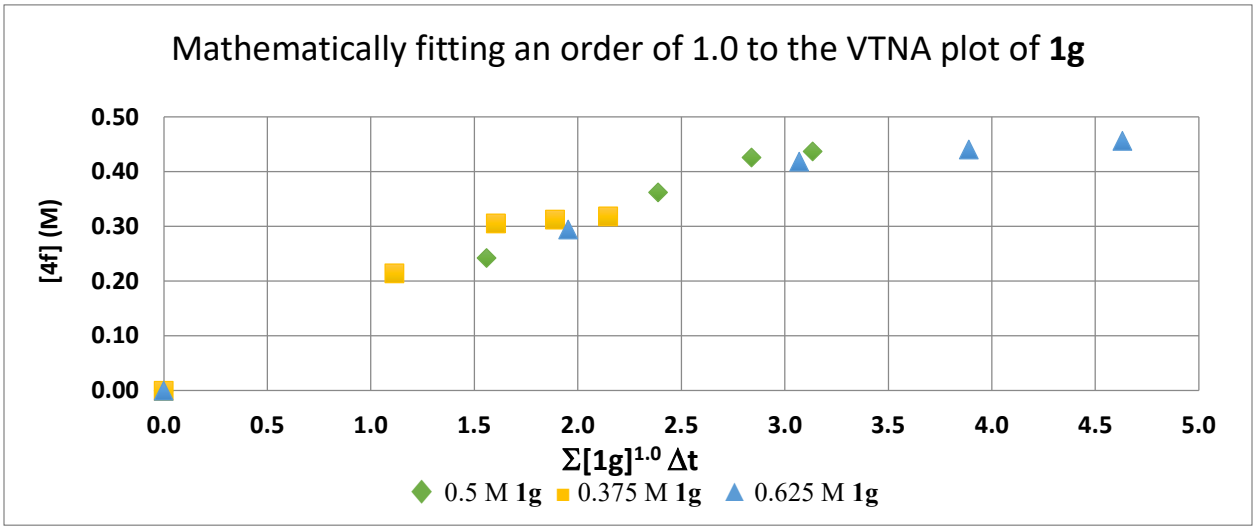

*Figure 2-5: Analyzing the reaction order for the carbamate reagent (**1g**) using VTNA contrasting between a visual (upper) and mathematical (lower) approach*

2.3.3: Kinetically probing the reaction order in boroxine reagent

The next logical step in doing this kinetic study would be to analyze how the concentration of boroxine effects the reaction. With analyzing the catalyst, the catalyst concentration was assumed to be constant throughout the whole experiment which meant it was not directly monitored. With analyzing the carbamate (**1g**), the concentration could be directly measured as it was tagged with a fluorine atom. The concentration of the boroxine could very well be monitored this way by tagging it with a fluorine atom which would allow for a direct analysis. Although, the boroxine that is being used is presumed to be only the dehydrated counterpart, it is difficult to fully dehydrate it as there will always be a small concentration of the boronic acid in solution which could skew the true concentration. With this, directly monitoring the boroxine by ^{19}F NMR was not done which results in the concentration of the boroxine dependent on the concentration of **4f**. Assumptions have to be made to do this effectively, including assuming that there is a 1:1 stoichiometry between the **4f** and the Ar-B substrate. With these assumptions, kinetic studies were performed (Figure 2-6) varying the concentration of the Ar-B equivalent including 1.0 M (♦), 0.875 M (■), and 0.7 M (▲) where the optimized conditions are at 1.0 M (♦). Concentrations above 1.0 M were not performed because solubility started becoming an issue when concentrations supersede 1.0 M. Analyzing the data visually, the strongest correlation was found to be with **2a** being first order. To gain a more precise determination of the order, the algorithm developed by Dr. Keillor was performed on this data set alluding to an order of 1.06. Having an order of approximately 1, conclusions can be made that one equivalent of the Ar-B equivalent is present in the rate determining step.

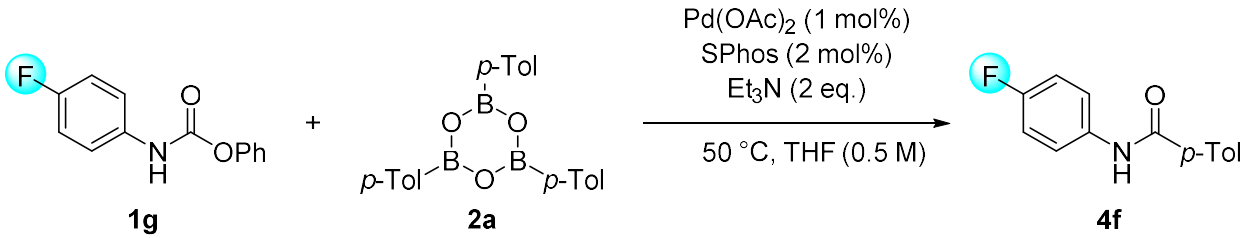

♦ :**1g** (0.6 mmol), **2a** (0.4 mmol, 2.0 Ar-B eq.), Et_3N (1.2 mmol), $Pd(OAc)_2$ (1 mol%), SPhos (2 mol%), THF (0.5 M), 50 °C, Ar.
■ :**2a** (0.35 mmol, 1.75 Ar-B eq.)
▲:**2a** (0.30 mmol, 1.50 Ar-B eq.)

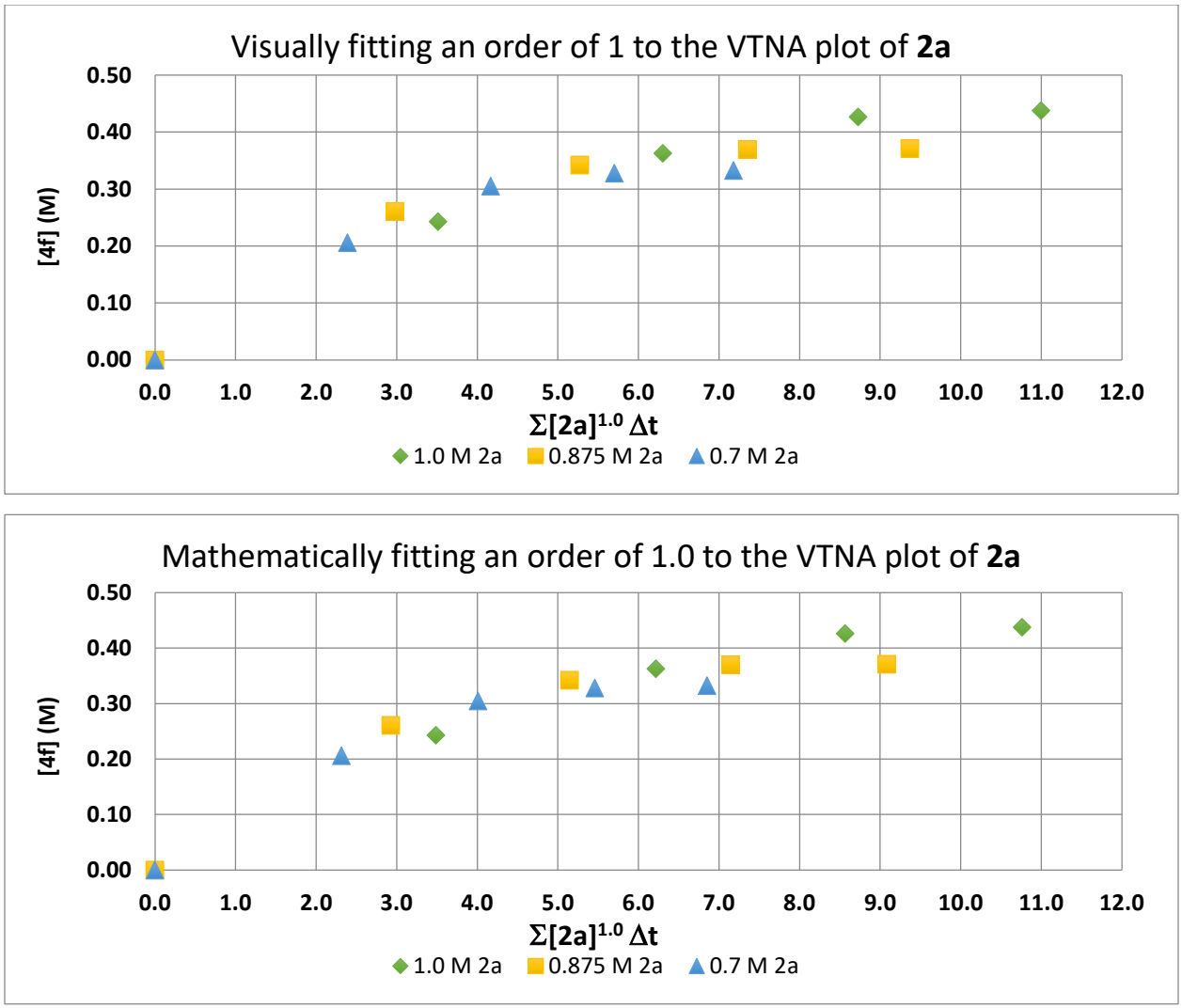

*Figure 2-6: Analyzing the reaction order for the boroxine reagent (**2a**) using VTNA contrasting between a visual (upper) and mathematical (lower) approach*

2.3.4: Tracing the kinetic results to the mechanism

Looking at the kinetic studies described in section 2.3, conclusions were drawn that there was in fact catalyst decomposition, along with the orders of the catalyst, carbamate, and boroxine. With all three components analyzed giving an order that is positive and non-zero, it can be proposed that the rate determining step must involve each of these components. If the Pd(0)/(II) mechanism (Scheme 2-4) is operative, there must be a step that involves all three components. The step that fits this requirement would be the transmetallation step between the carbamoyl palladium and the aryl boroxine nucleophile. If the Pd(II)/(II) mechanism (Scheme 2-7) is operative, the insertion step would be rate determining as this intermediate consists of all three components.

Linking this to previous control experiments where **1a-Me** failed to provide the desired product (Scheme 2-3) suggesting that the oxidative insertion type mechanism is inoperative. With this, the rate determining step is most likely the insertion into the isocyanate and the transmetallation and deblocking are relatively facile steps under the reaction conditions.

As a primary focus of doing this kinetic study was to determine the rate determining step to see if there was hope for moving forward with a C-H functionalization type pathway rather than a boron nucleophile. If the rate determining step was in fact the transmetallation, slowing this down further with a less nucleophilic C-H would likely limit this extension. But since the results obtained suggest a rate limiting insertion, forming the nucleophile is not the limiting factor which means there is room for manipulation.

Chapter 3:

Summary and outlook

In conclusion, the objective described in Chapter 2 was expanding the use of masked isocyanates in catalysis for amide formation which has largely been achieved and shows promise for further developments. Various mechanistic studies were performed including control reactions and kinetic reactions in hopes of gathering evidence for what mechanism may be active.

As described in Chapter 1, limited use of masked isocyanates in catalysis has been documented for the synthesis of amides with only the use of a rhodium catalyst in two reports. This work stemmed from the work that Mr. Joshua Derasp was doing during his Ph. D. on the rhodium-catalyzed addition of boron nucleophiles to masked isocyanates. In efforts to extend this methodology, he tried a palladium catalyst and it proved to be fruitful as early results with Buchwald ligands proved to be effective in amide formation. Out of the ligands scanned, SPhos proved unique enabling reactivity whereas more traditional ligands lacked the desired reactivity. Further optimization resulted in a decrease of catalyst loading as well as decreasing the need for high excess of the reagents used.

Figure 3-1: Summary of Project

With the optimized conditions in hand, the impact of the aryl boroxine nucleophile and masked isocyanate on the reactivity was evaluated. The use of both electron deficient and rich aryl boroxines were competent under the reaction conditions. Electron rich aryl masked isocyanates provided the parent amide in excellent yields, whereas electron deficient masked isocyanates required more forcing conditions to promote reactivity. Alkyl masked isocyanates yielded the desired amide product with only moderate decreases in reactivity. Although the palladium system gave excellent reactivity for the substrates evaluated, it did fall short in contrast to the rhodium system. This can be seen by the halide bearing substrates not being compatible such as **3i**, **4k**, and **4l** as well as heterocyclic based boron nucleophiles lacking the desired reactivity.

During the course of evaluating the reactivity of this methodology, urea and homocoupled biaryl products were observed deriving from off-cycle pathways which sparked interest into probing the mechanism. These products can however offer insight into the various pathways that

may be operative since their production involves the changing of oxidation state of the catalyst. The reduction of Pd(II) to Pd(0) can be largely attributed to the formation of a homocoupled biaryl product, but pathways that could be responsible for oxidation were discussed and have promise. Although there is literature precedence for an oxidative insertion type mechanism with similar substrates, the lack of reactivity observed when using **3a-Me** in Scheme 2-3 suggested that Pd(0) was not responsible for the activation of the carbamate. A kinetic study using a VTNA methodology was done and indicated a positive order arising from the $Pd(OAc)_2$ (order = 0.3), blocked isocyanate (order = 1.0), and boroxine (order = 1.0). In addition, results showed that catalyst decomposition was occurring making the result obtained for the obtained in palladium only a qualitative measurement. Overall, these results appear consistent with a rate-determining insertion step, but additional experiments and potentially DFT calculations could be used to secure additional support. Coupled with the reactivity and the mechanism being evaluated, this palladium-catalyzed amide formation methodology holds promise for expanding the applicability of masked isocyanates in catalysis.

Chapter 4:

Supporting information

4.1: General information

Purification of reaction products was carried out by flash column chromatography using SiliCycle silica gel (40-63 μm), unless otherwise noted. Analytical thin layer chromatography (TLC) was performed on aluminum, cut to size. Visualization was accomplished with UV light followed by staining with a potassium permanganate solution and heating.

^{1}H, ^{13}C, and ^{19}F NMR spectra were recorded on Bruker AVANCE 300 MHz, 400 MHz, and 500 MHz spectrometers at ambient temperature, unless otherwise indicated. Spectral data was reported in ppm using solvent as the reference ($CDCl_3$ at 7.26 ppm or DMSO-*d6* at 2.50 ppm for ^{1}H NMR, $CDCl_3$ at 77.2 ppm or DMSO-d_6 at 39.5 for ^{13}C NMR and $C_6H_5CF_3$ at -63.7 ppm for ^{19}F NMR). ^{1}H NMR data was reported as: multiplicity (br = broad, s = singlet, d = doublet, t = triplet, q = quartet, quint. = quintet, sext. = sextuplet, sept = septuplet, m = multiplet), integration and coupling constant(s) in Hz. Carbon resonances were assigned using dept 135 spectra. Infrared (IR) spectra were obtained on neat samples using an Attenuated Total Reflectance Fourier transform infrared spectrometer (ATR-FTIR). High-resolution mass spectroscopy (HRMS) was performed on a Kratos Concept-11A mass spectrometer with an electron beam of 70 eV (EI) or Micromass Q-TOFI- Time of Flight Electrospray Ionization mass spectrometer (ESI) at the Ottawa-Carleton Mass Spectrometry Centre.

4.2: Supporting information for Chapter 2

Unless otherwise noted, all commercially available materials were purchased from commercial sources and used without further purification. Tetrahydrofuran (THF) and α,α,α-triflourotoluene ($PhCF_3$) were passed through an activated alumina column embedded in a solvent purification system by LC Technology solutions. Masked (blocked) isocyanates **1c, d, f, h, l, m** were prepared by known methods following literature procedures.[65] Masked (blocked) isocyanates with different blocking groups **1aa**,[81] **1ab**,[82] **1ac**,[83] **1ad**,[84] **1ah**,[85] and **1ai**[86] were prepared by known procedures. Aryl boroxines were readily prepared using literature procedures.[69] Masked (blocked)

---

[81] Houlden, C. E.; Lloyd-Jones, G. C.; Brooker-Milburn, K. I. *Org. Lett.* **2010,** *12*, 3090.
[82] Geffken, D.; Froböse, J. *J. Prakt. Chem.* **1993,** *335*, 555.
[83] Kothandaraman, H.; Nasar, A. S. *J. Indian Chem. Soc.* **1992,** *69*, 869.
[84] Yamasaki, R.; Honjo, Y.; Ito, A.; Fukuda, K.; Okamoto, I. *Chem. Pharm. Bull.* **2018,** *66*, 880.
[85] Ricard, S.; Gagnon, A.; Daoust, B. *ChemistrySelect* **2018,** *3*, 4923.
[86] Chen, M.; Ren, Z.-H.; Wang, Y.-Y.; Guan, Z.-H. *J. Org. Chem.* **2015,** *80*, 1258.

isocyanate **1a-Me** was readily prepared using literature procedures.[87] Aryl boronic acids were heated to 110 ℃ overnight under reduced pressure and the corresponding boroxine were stored in a desiccator. Recrystallization of the boronic acid in water before dehydration allowed for more reproducible results. Aryl boronic esters **2ab,**[88] **2ac,**[89] **2ad,**[90] **2ae**[91] were synthesized according to literature procedures. Aryl boroxine **2k** was obtained via recrystallization and dehydration of the corresponding boronic acid that was synthesized according to literature procedure.[92]

4.2.1: Starting material synthesis

General procedure A: $NaHCO_3$ (11.0 mmol, 1.10 equiv.) was added to a round bottom flask containing THF:H_2O (33.3 mL, 3:1) followed by the addition of the amine (10.0 mmol, 1.00 equiv.) The temperature of the solution was brought to 0 ℃ upon which the addition of phenyl chloroformate (10.5 mmol, 1.05 equiv.) was added dropwise. The solution was allowed to warm to room temperature and subsequently monitored for the disappearance of starting material (generally 0.5 to 2 hours). Upon completion, the reaction was diluted with EtOAc (120 mL), then extracted with water (1 x 100 mL) and brine (1 x 100 mL). The organic layer was collected, dried over Na_2SO_4, and concentrated under reduced pressure. The crude extract was purified by silica gel chromatography to give the corresponding product.

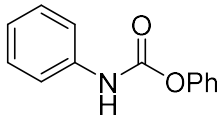

Phenyl phenylcarbamate (1a): Synthesized according to general procedure **A** using aniline (0.88 mL, 10 mmol), phenyl chloroformate (1.32 mL, 10.5 mmol), and $NaHCO_3$ (0.924 g, 11.0 mmol). The reaction reached completion within 2 hours. The desired product was extracted pure from the reaction mixture yielding an amorphous white solid (2.09 g, 97%). TLC R_F = 0.53 in 60% CH_2Cl_2/Hexanes. ^{1}H NMR (500 MHz, $CDCl_3$) δ 6.88 – 7.04 (br s, 1H), 7.11 (td, *J* = 7.4, 1.2 Hz,

[87] Jacquemard, U.; Bénéteau, V.; Lefoix, M.; Routier, S.; Mérour, J.-Y.; Coudert, G. *Tetrahedron* **2004,** *60*, 10039.
[88] Powell, C. R.; Dillon, K. M.; Wang, Y.; Carrazzone, R. J.; Matson, J. B. *Angew. Chem. Int. Ed.* **2018,** *57*, 6324.
[89] Ronson, T. O.; Renders, E.; Van Steijvoort, B. F.; Wang, X.; Wybon, C. C. D.; Prokopcová, H.; Meerpoel, L.; Maes, B. U. W. *Angew. Chem. In. Ed.* **2018,** *58*, 482.
[90] Lew, T. T. S.; Lim, D. S. W.; Zhang, Y. *Green Chem.* **2015,** *17*, 5140.
[91] Oh, S.-W.; Weis, J. W. E.; Kerneghan, P. A.; Korobkov, I.; Maly, K. E.; Bryce, D. L. *Magn. Reson. Chem.* **2012,** *50*, 388.
[92] Yang, Y. G.; Chen, H.; Tang, G.; Wen, J. X. *Mol. Cryst. Liq. Cryst.* **2010,** *373*, 1.

1H), 7.18 – 7.22 (m, 2H), 7.22 – 7.25 (m, 1H), 7.30 – 7.37 (m, 2H), 7.37 – 7.43 (m, 2H), 7.45 (d, J = 8.0 Hz, 2H). ^{13}C NMR (126 MHz, $CDCl_3$) δ 118.8 (CH), 121.7 (CH), 125.8 (CH), 129.2 (CH), 129.5 (CH), 137.4 (C), 150.6 (C), 151.7 (C). Data is consistent with literature.[87]

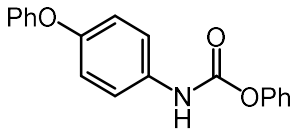

Phenyl (4-phenoxyphenyl)carbamate (1b): Synthesized according to general procedure **A** using 4-phenoxyaniline (0.556 g, 3.00 mmol), phenyl chloroformate (0.395 mL, 3.15 mmol), and $NaHCO_3$ (0.277 g, 0.330 mmol). The reaction reached completion within 2 hours. The crude mixture was recrystallized in ether/Hexanes providing the desired product as a crystalline off white solid (0.800 g, 88%). M.P. 156.7-157.0 °C. TLC R_F = 0.5 in 80% Hexanes/EtOAc. ^{1}H NMR (500 MHz $CDCl_3$) δ 6.88-6.94 (1H, br s), 6.97-7.02 (4H, m), 7.09 (1H, t, J = 7.4 Hz), 7.18-7.21 (2H, m), 7.22-7.25 (1H, m), 7.30-7.35 (2H, m), 7.37-7.44 (4H, m). ^{13}C NMR (125 MHz $CDCl_3$) δ 118.5 (CH), 119.9 (CH), 120.6 (CH), 121.7 (CH), 123.2 (CH), 125.8 (CH), 129.7 (CH), 129.9 (CH), 133.0 (C), 150.7 (C), 151.9 (C), 153.4 (C), 157.7 (C). IR (film): 3392, 3343, 3059, 2112, 1711, 1614, 1589 cm^{-1}. HRMS (EI): Exact mass calcd for $C_{19}H_{15}NO_3$ $[M]^+$: 305.1052. Found: 305.1065.

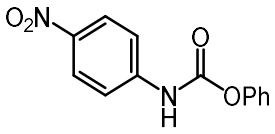

Phenyl(4-nitrophenyl)carbamate (1d): Synthesized according to general procedure **A** using 4-nitroaniline (0.414 g, 3.00 mmol), phenyl chloroformate (0.395 mL, 3.15 mmol), and $NaHCO_3$ (0.277 g, 0.330 mmol). The reaction reached completion within 2 hours. The crude mixture was recrystallized in ether/Hexanes providing the desired product as a crystalline off-white solid (0.628 g, 81%). M.P. 170.9-171.2 °C. TLC R_F = 0.16 in 80% Hexanes/EtOAc. ^{1}H NMR (500 MHz $CDCl_3$) δ 7.16-7.21 (1H, m), 7.26-7.30 (1H, m), 7.34-7.37 (1H br s), 7.39-7.45 (1H, m), 7.58-7.62 (1H, m), 8.19-8.23 (1H, m). ^{13}C NMR (125 MHz $CDCl_3$) δ 118.2 (CH), 121.6 (CH), 125.4 (CH), 126.4 (CH), 129.7 (CH), 143.5 (C), 143.6 (C), 150.2 (C), 151.3 (C). IR (film): 3321, 3120, 2113, 1741, 1719, 1614, 1595 cm^{-1}. HRMS (EI): Exact mass calcd for $C_{13}H_{10}N_2O_4$ $[M]^+$: 258.0641 Found: 258.0666. Under 1.0% relative abundance. Exact mass calcd for isocyanate $C_7H_4N_2O_3$

[M]$^+$: 164.0222. Found: 164.0234. Exact mass calcd for phenol C_6H_6O [M]$^+$: 94.0419. Found: 94.0414. Data consistent with literature.[93]

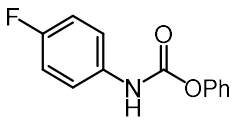

Phenyl (4-fluorophenyl)carbamate (1g): Synthesized according to general procedure **A** using 4-fluoroaniline (0.947 mL, 10.0 mmol), phenyl chloroformate (1.32 mL, 10.5 mmol), and $NaHCO_3$ (0.924 g, 10.5 mmol). The reaction reached completion within 1 hour. The desired product was recrystallized (20% EtOAc/Hexanes) 3 times yielding a white solid (2.02 g, 87 % yield). TLC R_F = 0.73 in CH_2Cl_2. 1H NMR (500 MHz, $CDCl_3$) δ 6.97-7.06 (m, 3H), 7.20-7.17 (m, 2H), 7.25 (tt, 7.2, 1.3 Hz, 1H) 7.39 (tt, *J* = 7.5, 2.3 Hz, 4H). ^{13}C NMR (126 MHz, $CDCl_3$) δ 115.9 (CH, d, *J* = 22.7 Hz), 120.7 (CH), 121.8 (CH), 125.9 (CH), 129.6 (CH), 133.5 (C), 150.6 (C), 152.0 (C), 159.3 (C, d, *J* = 241.1 Hz). ^{19}F NMR (471 MHz, $CDCl_3$) δ -119.90. Data is consistent with literature.[94]

General procedure B: An amine (3.00 mmol, 1.00 equiv.), CH_2Cl_2 (0.3 M), and Et_3N (3.30 mmol, 1.10 equiv.) were added to a dry round bottom flask. The temperature of the solution was brought to 0 ℃ upon which phenyl chloroformate (3.15 mmol, 1.05 equiv.) was added dropwise. The solution was warmed to room temperature and subsequently monitored for the disappearance of starting material. The reaction was concentrated under reduced pressure, resuspended in EtOAc (40 mL) and extracted with water (1 x 30 mL) and brine (1 x 30 mL). The organic layer was collected, dried over sodium sulfate, and concentrated under reduced pressure. The crude extract was purified by silica gel chromatography to give the corresponding products.

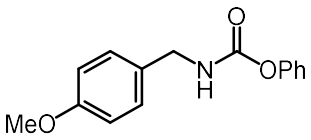

Phenyl (4-methoxybenzyl)carbamate (1i): Synthesized according to general procedure **B** using 4-methoxybenzylamine (0.39 mL, 3.0 mmol), phenyl chloroformate (0.41 mL, 3.3 mmol), and Et_3N (0.47 mL, 0.34 mmol). The reaction reached completion within 2 hours. The desired product

[93] Zhang, L.; Xia, W.; Wang, B. Luo, Y.; Lu, W.; *Synth. Commun.* **2011**, *41*, 3140.
[94] Darvesh, S.; MacDonald, I.; Martin, E.; Pottie, I. Carbamate Compounds and Methods of Use in Disease of the Nervous System. U.S. Patent WO2014039526, March 3, 2014.

was purified by column chromatography (70% Hexanes/EtOAc) yielding an amorphous white solid (0.467 g, 61% yield). TLC R_F = 0.50 in 70% Hexanes/EtOAc. ^{1}H NMR (300 MHz $CDCl_3$) δ 3.82 (3H, s), 4.39 (2H, d, *J* = 5.8 Hz), 6.86-6.92 (2H, m), 7.10-7.23 (3H, m), 7.26-7.40 (4H, m). ^{13}C NMR (100 MHz $CDCl_3$) δ 44.9 (CH_2), 55.4 (CH_3), 114.3 (CH), 121.7 (CH), 125.4 (CH), 129.3 (CH), 129.4 (CH), 130.3 (C), 151.2 (C), 154.7 (C), 159.3 (C). IR (film): 3287.0, 3059, 2959, 2836, 1699, 1612, 1531 cm^{-1}. HRMS (ESI): Exact mass calcd for $C_{15}H_{15}NO_3Na$ $[M+Na]^+$: 280.0942. Found: 280.0950.

General procedure C: An oven-dried microwave vial equipped with a magnetic stir bar and fitted with a microwave cap was charged with diphenyl carbonate (6.00 mmol, 2.00 equiv.) and heated to 70 °C until the diphenyl carbonate had turned into a liquid. Subsequently, the corresponding amine (3.00 mmol, 1.00 equiv.) was added dropwise to the vial and stirred for an additional 10 minutes at 70 °C. The reaction mixture was then cooled to room temperature, diluted with EtOAc (10 mL) and extracted 1M NaOH (1 x 20 mL), saturated $NaHCO_3$ (1 x 20 mL), and brine (1 x 20 mL). The organic layer was collected, dried over Na_2SO_4, and concentrated under reduced pressure. The crude mixture was purified by silica gel chromatography providing the desired product.

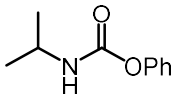

Phenyl isopropylcarbamate (1j): Synthesized according to general procedure **C** using isopropylamine (0.257 mL, 3.00 mmol), diphenyl carbonate (0.642 g, 3.00 mmol). The desired product was purified by column chromatography (90% Hexanes/EtOAc) yielding an amorphous white solid (0.188 g, 35% yield). TLC R_F = 0.40 in 90% Hexanes/EtOAc. ^{1}H NMR (300 MHz, DMSO-*d*$_6$): 1H NMR (300 MHz $CDCl_3$) δ 1.24 (1H, d, *J* = 6.6 Hz), 3.89 (1H, m, *J* = 6.9 Hz), 4.75-4.86 (1H, br s), 7.09-7,15 (1H, m), 7.18 (1H, app t, *J* = 7.4 Hz), 7.35 (1H, t, *J* = 7.9 Hz). ^{13}C NMR (125 MHz $CDCl_3$) δ 23.0 (CH_3), 43.6 (CH), 121.8 (CH), 125.3 (CH), 129.4 (CH), 151.2 (C), 153.8 (C). Data consistent with literature.[95]

[95] Tanwar, D. K.; Ratan, A.; Gill, M. S. *Org. Biomol. Chem.* **2017**, *15*, 4992

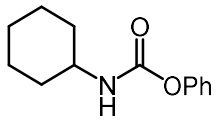

Phenyl isopropylcarbamate (1k): Synthesized according to general procedure **C** using cyclohexylamine (0.541 mL, 8.00 mmol) and diphenyl carbonate (1.80 g, 8.40 mmol). The reaction reached completion within 2 hours. The desired product was dry loaded onto silica gel (MeOH) and purified by column chromatography (90% Hexanes/EtOAc) yielding an amorphous white solid (1.04 g, 59% yield). TLC R_F = 0.27 in 90% Hexanes/EtOAc. ^{1}H NMR (500 MHz $CDCl_3$) δ 1.14-1.27 (1H, m), 1.32-1.42 (1H, m), 1.59-1.65 (1H, m), 1.69-1.78 (1H, m), 1.97-2.07 (1H, m), 3.52-3.61 (1H, m), 4.53-5.00 (1H, br s), 7.13 (1H, d, *J* = 7.9 Hz), 7.18 (1H, t, *J* = 7.3 Hz), 7.35 (1H, t, *J* = 7.8 Hz). ^{13}C NMR (125 MHz $CDCl_3$) δ 24.9 (CH_2), 25.6 (CH_2), 33.4 (CH_2), 50.3 (CH), 121.8 (CH), 125.3 (CH), 129.4 (CH), 151.3 (C), 153.8 (C). Data consistent with literature.[96]

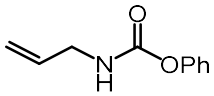

Phenyl allylcarbamate (1n): Synthesized according to general procedure **C** using allylamine (0.220 mL, 3.00 mmol) and diphenyl carbonate (1.28 g, 6.00 mmol). The reaction reached completion within 1 hour. The desired product was purified by column chromatography (90% Hexanes/EtOAc) yielding a viscous oil (0.422 g, 79% yield). TLC R_F = 0.19 in 90% Hexanes/EtOAc. ^{1}H NMR (500 MHz, $CDCl_3$) δ 3.66 – 4.10 (m, 2H). 4.82 - 5.15 (br. s, 1H), 5.15 – 5.30 (m, 2H), 5.90 (ddt, *J* = 16.1, 10.8, 5.7 Hz, 1H), 7.09 – 7.16 (m, 2H), 7.20 (t, *J* = 7.4 Hz, 1H), 7.36 (t, *J* = 7.8 Hz, 2H). ^{13}C NMR (126 MHz, $CDCl_3$) δ 43.8 (CH_2), 116.7 (CH_2), 121.7 (CH), 125.4 (CH), 129.4 (CH), 134.2 (CH), 151.1 (C), 154.6 (C). Data is consistent with literature.[97]

General Procedure D: According to literature procedure.[98] An oven dried microwave vial equipped with a magnetic stir bar and fitted with a microwave cap was charged with the corresponding phenol (5.00 mmol, 1 equiv.) and purged under a stream of argon for a total of 2 minutes. Phenyl isocyanate (5.00 mmol, 1equiv.) was added dropwise addition via syringe and

[96] Bianco, A.; Bonadies, F.; Napolitano, R.; Ortaggi, G. *Org. Process. Res. Dev.* **2004**, *2*, 141.
[97] Moineau, C.; Mele, G.; Alper, H. *Can. J. Chem.* **2001**, *79*, 587.
[98] Maghsoodlou, M. T.; Saravani, H.; Shokouhian, M.; Mofarrah, E. *Phosphorous, Sulfur, and Silicon.* **2015,** *190*, 1450.

stirred for 6 hours at room temperature. After completion, the crude mixture was purified by column chromatography.

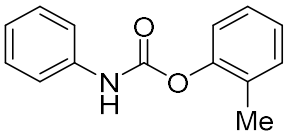

***o*-Tolyl phenylcarbamate** (**1ae**): Synthesised according to general procedure **D** using *o*-cresol (0.52 mL, 5.00 mmol) and phenyl isocyanate (0.55 mL, 5.00 mmol). The reaction reached completion within 6 hours. The desired product was purified by column chromatography (80 % Hexanes/EtOAc) yield an amorphous white solid (0.796 g, 70 %). TLC R_F = 0.63 in 70% Hexanes/EtOAc. ^{1}H NMR (500 MHz, $CDCl_3$) δ 2.27 (s, 3H), 6.90 - 7.02 (br. s, 1H), 7.06 – 7.19 (m, 3H), 7.20 – 7.25 (m, 2H), 7.32 – 7.41 (m, 2H), 7.47 (d, *J* = 8.0 Hz, 2H). ^{13}C NMR (101 MHz, $CDCl_3$) δ 16.3 (CH_3), 118.7 (CH), 122.3 (CH), 123.9 (CH), 126.1 (CH), 127.0 (CH), 129.2 (CH), 130.8 (C), 131.3 (CH), 137.6 (C), 149.1 (C), 151.6 (C). HRMS (EI): Exact mass calcd for $C_{14}H_{13}NO_2$ $[M]^+$: 227.0946. Found: 227.0947.

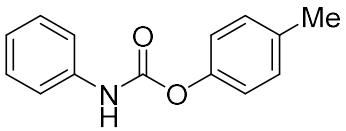

***p*-Tolyl phenylcarbamate** (**1af**): Synthesised according to general procedure **D** using *p*-cresol (0.52 mL, 5.00 mmol) and phenyl isocyanate (0.55 mL, 5.00 mmol). The reaction reached completion within 6 hours. The desired product was purified by column chromatography (80 % hexanes/EtOAc) yield an amorphous white solid (0.796 g, 70 %). TLC R_F = 0.63 in 70% Hexanes/EtOAc. ^{1}H NMR (500 MHz, $CDCl_3$) δ 2.35 (s, 3H), 6.84 – 6.94 (br. s, 1H), 7.04 – 7.14 (m, 2H), 7.19 (dd, J = 8.7, 0.8 Hz, 1H), 7.31 – 7.38 (m, 1H), 7.45 (d, J = 8.4 Hz, 1H). ^{13}C NMR (101 MHz, $CDCl_3$) δ 21.0 (CH_3), 118.8 (CH), 124.0 (CH), 129.3 (CH), 130.1 (CH), 137.6 (C), 148.4 (C), 152.0 (C). Data is consistent with literature.[99]

[99] Inaloo, I. D.; Majnooni, S. *New J. Chem.* **2018,** *42*, 13249.

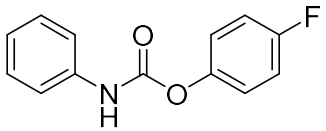

4-Fluorophenyl phenylcarbamate (**1ag**): Synthesized according to general procedure **D** using *p*-fluorophenol (0.304 g, 2.71 mmol) and phenyl isocyanate (0.29 mL, 2.71 mmol). The reaction reached completion within 6 hours. The desired product was purified by recrystallization (Ether/Hexanes) yielding an amorphous white solid (0.349 g, 56%). TLC R_F 0.63 in 70% Hexanes/EtOAc. ^{1}H NMR (500 MHz, $CDCl_3$) δ 6.92 (br. s, 1H), 7.04 – 7.20 (m, 5H), 7.32 – 7.39 (m, 2H), 7.44 (d, J = 8.4 Hz, 2H). ^{13}C NMR (126 MHz, $CDCl_3$) δ 115.91 (C, d, J = 23.6 Hz), 118.7 (CH), 123.0 (CH, d, J = 8.6 Hz), 124.0 (CH), 129.1 (CH), 137.1 (C), 146.3 (C, d, J = 2.7 Hz), 151.5 (C), 160.1 (C, d, J = 243.9 Hz). ^{19}F NMR (470 MHz, $CDCl_3$) δ -118.2 (s). HRMS (EI): Exact mass calcd for $C_{13}H_{10}FNO_2$ $[M]^+$: 231.0696. Found: 231.0697.

4.2.2: Supplementary optimization data

General procedure E: An oven-dried microwave vial equipped with a magnetic stir bar was cooled under a stream of argon followed by the addition of $Pd(OAc)_2$ ($2.00x10^{-3}$ mmol, 0.0100 equiv.) and SPhos (0.040 mmol, 0.020 equiv.). The microwave vial was then sealed and purged under a stream of argon for a total of 2 minutes and subsequently anhydrous THF (0.4 mL) was added. The resulting mixture was stirred under argon at room temperature for 5 minutes.

A second oven-dried microwave vial equipped with a magnetic stir bar was cooled under a stream of argon followed by the addition of the corresponding carbamate (0.200 mmol, 1.00 equiv.) and arylboroxine (0.130 mmol, 2.00 ‘Ar-B’ equiv.). The microwave vial was then sealed and purged under a stream of argon for a total of 2 minutes. The catalyst solution was then transferred to the vial via syringe and then let stir at room temperature for 5 minutes then subsequent addition of Et_3N (0.40 mmol, 2.0 equiv.) via syringe. The microwave vial was then heated to 50 ℃ for 24 h. Upon completion, the reaction was concentrated under reduced pressure. The yields were then determined through the use of an internal standard.

Table 4-1: Boron equivalent[a]

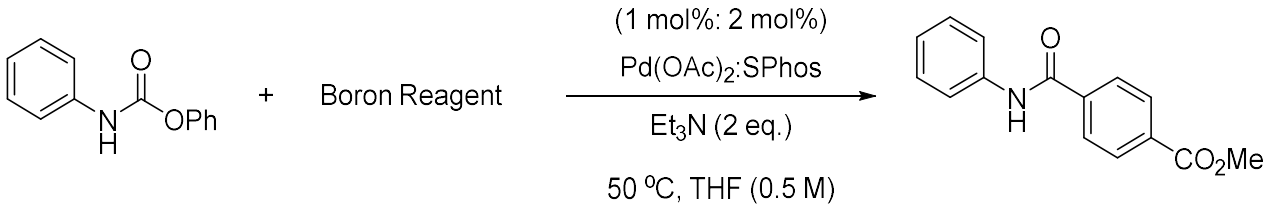

Entry	Boron Reagent	Yield (%)
1	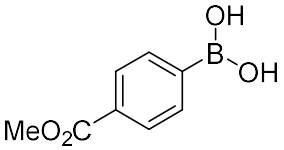	0
2	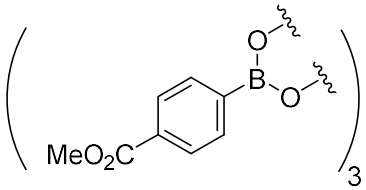	60

[a]Conditions: **1a** (0.2 mmol), **31a** (0.13 mmol, 2.0 'Ar-B' equiv), $Pd(OAc)_2$ (1.0 mol%), SPhos (2.0 mol%), Et_3N (0.4 mmol), THF (0.5 M), 50 °C. ^1H NMR yield determined using 1,3,5-trimethoxybenzene as internal standard.

Table 4-2: Temperature dependence[a]

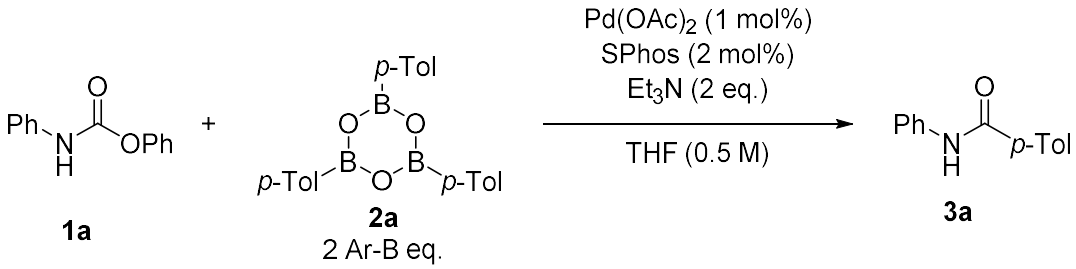

Entry	Temperature (°C)	Yield (%)
1	20	3.7
2	50	88
3	70	85
4	100	63

[a]Conditions: **1a** (0.2 mmol), **31a** (0.13 mmol, 2.0 'Ar-B' equiv), $Pd(OAc)_2$ (1.0 mol%), SPhos (2.0 mol%), Et_3N (0.4 mmol), THF (0.5 M), 50 °C. ^1H NMR yield determined using 1,3,5-trimethoxybenzene as internal standard.

4.2.3: Synthesis of substrates from tables Table 2-6 and Table 2-7

General procedure F: An oven-dried microwave vial equipped with a magnetic stir bar was cooled under a stream of argon followed by the addition of $Pd(OAc)_2$ ($6.00x10^{-3}$ mmol, 0.0100 equiv.) and SPhos (0.0120 mmol, 0.020 equiv.). The microwave vial was then sealed and purged under a stream of argon for a total of 2 minutes and subsequently anhydrous THF (1.2 mL) was added. The resulting mixture was stirred under argon at room temperature for 5 minutes.

A second oven-dried microwave vial equipped with a magnetic stir bar was cooled under a stream of argon followed by the addition of the corresponding carbamate (0.600 mmol, 1.00 equiv.) and arylboroxine (0.400 mmol, 2.00 'Ar-B' equiv.). The microwave vial was then sealed and purged under a stream of argon for a total of 2 minutes. The catalyst solution was then transferred to the vial via syringe and then let stir at room temperature for 5 minutes then subsequent addition of Et_3N (1.20 mmol, 2.00 equiv.) via syringe. The microwave vial was then heated to 50 ℃ for 24 h. Upon completion, the reaction was concentrated under reduced pressure, diluted with EtOAc (40 mL) and extracted 1M NaOH (1 x 30mL), saturated $NaHCO_3$ (1 x 30 mL), and brine (1 x 30 mL). The organic layer was collected, dried over Na_2SO_4, and concentrated under reduced pressure. The crude mixture was purified by silica gel column chromatography providing the desired product.

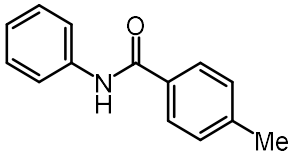

4-Methyl-*N*-phenylbenzamide (Table 2-6, 3a): Synthesized according to general procedure **F** using masked isocyanate **1a** (0.128 g, 0.600 mmol), arylboroxine **2a** (0.141 g, 0.400 mmol, 2.00 equiv "Ar-B"), Et_3N (0.167 mL, 1.20 mmol), $Pd(OAc)_2$ (1.3 mg, $6.0x10^{-3}$ mmol), and SPhos (4.9 mg, 0.012 mmol). The desired product was purified by column chromatography (75% CH_2Cl_2/Hexanes to 100% CH_2Cl_2) yielding an amorphous white solid (0.112 g, 89% yield). TLC R_F = 0.42 in 99% CH_2Cl_2/Et_3N. ^1H NMR (500 MHz $CDCl_3$) δ 2.42 (3H, s), 7.14 (1H, t, *J* = 7.4 Hz), 7.28 (1H, d, *J* = 7.9 Hz), 7.37 (1H, t, *J* = 7.9 Hz), 7.64 (1H, d, *J* = 7.8 Hz), 7.77 (1H, d, *J* = 8.1 Hz), 7.79-7.84 (1H, br s). ^{13}C NMR (125 MHz $CDCl_3$) δ 21.6 (CH_3), 120.3 (CH), 124.6 (CH),

127.2 (CH), 129.2 (CH), 129.6 (CH), 132.3 (C), 138.2 (C), 142.5 (C), 165.8 (C). Data is consistent with literature.[100]

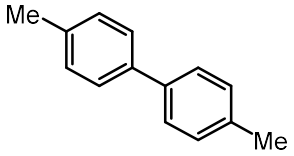

4,4'-Dimethyl-1,1'-biphenyl (Scheme 2-1, 5a): Isolated during the isolation of **3a**. The desired product was purified by column chromatography (60% CH_2Cl_2/Hexanes) yielding an amorphous white solid (0.009 g, 8% yield). TLC R_F = 0.80 in 60% CH_2Cl_2/Hexanes. ^{1}H NMR (400 MHz, $CDCl_3$) δ 2.38 (s, 6H) 7.22 (d, *J* = 7.8 Hz, 4H), 7.46 (d, *J* = 8.2 Hz, 4H). ^{13}C NMR (101 MHz, $CDCl_3$) δ 21.1 (CH_3), 126.8 (CH), 129.4 (CH), 136.7 (C), 138.3 (C). Data consistent with literature.[101]

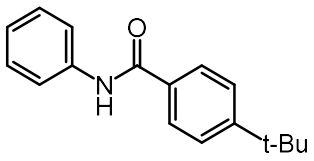

4-(*tert*-Butyl)-*N*-phenylbenzamide (Table 2-6, 3b): Synthesized according to general procedure **F** using masked isocyanate **1a** (0.128 g, 0.600 mmol), arylboroxine **2b** (0.192 g, 0.400 mmol, 2.00 equiv "Ar-B"), Et_3N (0.167 mL, 1.20 mmol), $Pd(OAc)_2$ (1.3 mg, 6.0x10^{-3} mmol), and SPhos (4.9 mg, 0.012 mmol). The reaction reached completion within 20 hours. The desired product was purified by column chromatography (40% Hexanes/CH_2Cl_2) yielding an amorphous white solid (0.126 g, 83% yield). TLC R_F = 0.33 in 40% Hexanes/CH_2Cl_2. ^{1}H NMR (400 MHz, DMSO-d_6) δ 1.28 (s, 9H), 7.05 (tt, *J* = 7.3, 1.2 Hz, 1H), 7.26 – 7.35 (m, 2H), 7.47 – 7.54 (m, 2H), 7.72 – 7.79 (m, 2H), 7.83 – 7.90 (m, 2H), 10.14 (s, 1H). ^{13}C NMR (101 MHz, DMSO-d_6) δ 31.4 (CH_3), 35.1 (C), 120.7 (CH), 124.0 (CH), 125.6 (CH), 128.0 (CH), 129.0 (CH), 132.8 (CH), 139.8 (C), 154.8 (C), 166.0 (C). Data is consistent with literature.[102]

---

[100] Wan, Y.; Alterman, M.; Larhead, M.; Hallberg, A. *J. Org. Chem.* **2002**, *67*, 6232.
[101] Dong-Hwan, L.; Minkee, C.; Byung-Woo, Y.; Ryong, R.; Abu, T.; Shahin, H.; Myung-Jong, J. *Adv. Synth. Catal.* **2009**, *351*, 2912.
[102] Zhang, J.; Ma, Y.; Ma, Y. *Eur. J. Org. Chem.* **2018**, *2018*, 1720.

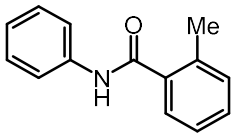

2-Methyl-*N*-phenylbenzamide (Table 2-6, 3c): Synthesized according to general procedure **F** using masked isocyanate **1a** (0.128 g, 0.600 mmol), arylboroxine **2d** (0.141 g, 0.400 mmol, 2.00 equiv "Ar-B"), Et_3N (0.167 mL, 1.20 mmol), $Pd(OAc)_2$ (1.3 mg, $6.0x10^{-3}$ mmol), and SPhos (4.9 mg, 0.012 mmol). The desired product was purified by column chromatography (80% Hexanes/EtOAc) yielding an amorphous off-white solid (0.104 g, 82% yield). TLC R_F = 0.50 in 80% Hexanes/EtOAc. ^{1}H NMR (300 MHz $CDCl_3$) δ 2.52 (1H, s), 7.16 (1H, t, *J* = 7.4 Hz), 7.23-7.30 (2H, m), 7.33-7.45 (4H, m), 7.49 (2H, d, *J* = 7.3 Hz), 7.62 (2H, d, *J* = 7.8 Hz). ^{13}C NMR (100 MHz $CDCl_3$) δ 19.9 (CH_3), 120.0 (CH), 124.7 (CH), 126.0 (CH), 126.7 (CH), 129.2 (CH), 130.4 (CH), 131.4 (CH), 136.5 (C), 136.6 (C), 138.1 (C), 168.2 (C). Data consistent with literature.[103]

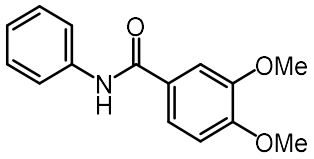

3,4-Dimethoxy-*N*-phenylbenzamide (Table 2-6, 3d): Synthesized according to general procedure **F** using masked isocyanate **1a** (0.128 g, 0.600 mmol), arylboroxine **2c** (0.197 g, 0.400 mmol, 2.00 equiv "Ar-B"), Et_3N (0.167 mL, 1.20 mmol), $Pd(OAc)_2$ (1.3 mg, $6.0x10^{-3}$ mmol), and SPhos (4.9 mg, 0.012 mmol). The reaction reached completion within 20 hours. The desired product was purified by column chromatography (100% CH_2Cl_2 to 5% EtOAc/CH_2Cl_2) yielding an amorphous white solid (0.122 g, 79% yield). TLC R_F = 0.33 in 95% CH_2Cl_2/EtOAc. ^{1}H NMR (400 MHz, DMSO-d_6) δ 3.84 (s, 3H), 3.85 (s, 3H), 7.09 (dd, *J* = 6.3, 7.9 Hz, 2H), 7.35 (dd, *J* = 7.3, 8.5 Hz, 2H), 7.55 (d, *J* = 2.1 Hz, 1H), 7.63 (dd, *J* = 2.1, 8.4 Hz, 1H), 7.77 (dd, *J* = 1.3, 8.6 Hz, 2H), 10.08 (s, 1H). ^{13}C NMR (101 MHz, DMSO-d_6) δ 56.10 (CH_3), 56.13 (CH_3), 111.4 (CH), 111.5 (CH), 121.0 (CH), 121.5 (CH), 123.9 (CH), 127.5 (C), 129.0 (CH), 139.8 (C), 148.8 (C), 152.1 (C), 165.4 (C). Data is consistent with literature.[104]

---

[103] Rauf, W.; Brown, J. M. *Angew. Chem., Int. Ed.* **2008**, *47*, 4228.
[104] Kumar, K. N.; Sreeramamurthy, K.; Palle, S.; Mukkanti, K.; Das, P. *Tetrahedron Lett.* **2010**, *51*, 899.

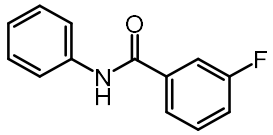

3-Fluoro-*N*-phenylbenzamide (Table 2-6, 3e): Synthesized according to general procedure **F** using masked isocyanate **1a** (0.128 g, 0.600 mmol), arylboroxine **2e** (0.146 g, 0.400 mmol, 2.00 equiv "Ar-B"), Et_3N (0.167 mL, 1.20 mmol), $Pd(OAc)_2$ (1.3 mg, $6.0x10^{-3}$ mmol), and SPhos (4.9 mg, 0.012 mmol). The reaction reached completion within 20 hours. The desired product was purified by column chromatography (75% CH_2Cl_2/ Hexanes) yielding an amorphous white solid (0.102 g, 79% yield). TLC R_F = 0.22 in 60% CH_2Cl_2/Hexanes. ^1H NMR (400 MHz, DMSO-d_6) δ 7.08 (tt, *J* = 7.4, 1.2 Hz, 1H), 7.28 – 7.36 (m, 2H), 7.40 (tdd, *J* = 8.5, 2.7, 1.0 Hz, 1H), 7.55 (td, *J* = 8.0, 5.8 Hz, 1H), 7.71 – 7.81 (m, 4H), 10.28 (s, 1H). ^{13}C NMR (101 MHz, DMSO-d_6) δ 115.0 (CH, d, *J* = 22.8 Hz), 118.9 (CH, d, *J* = 21.2 Hz), 120.9 CH, 124.3 (CH), 129.1 (CH), 131.0 (CH, d, *J* = 8.0 Hz), 137.7 (C, d, *J* = 6.7 Hz), 139.4 (C), 162.4 (C, d, *J* = 244.3 Hz),164.6 (C, d, *J* = 2.5 Hz). Data consistent with literature.[105]

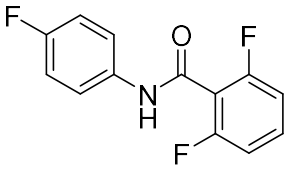

2,6-difluoro-N-(4-fluorophenyl)benzamide (Table 2-6, 3f) Synthesized according to general procedure **F** using masked isocyanate **1g** (0.138 g, 0.600 mmol), arylboroxine **2k** (0.167 g, 0.400 mmol, 2.00 equiv "Ar-B"), Et_3N (0.167 mL, 1.20 mmol), $Pd(OAc)_2$ (1.3 mg, $6.0x10^{-3}$ mmol), and SPhos (4.93 mg, 0.012 mmol). The desired product was purified by column chromatography (60% CH_2Cl_2/Hexanes) yielding an amorphous white solid (0.144 g, 96% yield). TLC R_F 0.37 in 60% CH_2Cl_2/Hexanes. ^1H NMR (400 MHz, $CDCl_3$) δ 6.99 (ap t, *J* = 8.3 Hz, 2H), 7.06 (ap t, *J* = 8.8 2H), 7.41 (tt, *J* = 6.3, 8.5 Hz, 1H), 7.59 (ddd, *J* = 6.3, 8.0, 8.4, 2H), 7.66 – 7.74 (br. s, 1H). 13C NMR (101 MHz, $CDCl_3$) δ 112.1 – 112.6 (CH, m), 114.3 (C, t, J = 19.4 Hz), 115.9 (CH, d, J = 22.7 Hz), 122.2 (CH, d, J = 8.1 Hz), 132.4 (CH, t, J = 10.3 Hz), 133.4 (C, d, J = 2.9 Hz), 158.5 (C), 159.9 (C, d, J = 244.7 Hz), 160.2 (C, dd, J = 6.7, 253.0 Hz). ^{19}F NMR (471 MHz, $CDCl_3$) δ -

[105] Guo, X.; Tang, L.; Yang, Y.; Zha, Z.; Wang, Z. *Green Chem.* **2014**, *16*, 2443.

121.90 (tt, J = 4.6, 8.2 Hz, 1F), -116.82 (dtd, J = 1.4, 3.6, 6.4 Hz, 2F). IR (film) 3215, 2922, 1649, 1622, 1588, 1537, 1506, 1462 cm^{-1}. HRMS (ESI): Exact mass calcd for $C_{13}H_8F_3NONa$ [M+Na]: 274.0456. Found 274.0465.

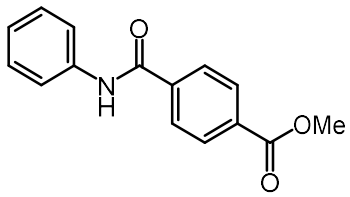

Methyl 4-(phenylcarbamoyl)benzoate (Table 2-6, 3g): Synthesized according to general procedure **F** using masked isocyanate **1a** (0.128 g, 0.600 mmol), arylboroxine **2f** (0.192 g, 0.400 mmol, 2.00 equiv "Ar-B"), Et_3N (0.167 mL, 1.20 mmol), $Pd(OAc)_2$ (1.3 mg, $6.0x10^{-3}$ mmol), and SPhos (4.9 mg, 0.012 mmol). The reaction reached completion within 40 hours. The desired product was recrystallized in a 50% EtOAc/Hexanes mixture providing the desired compound as a crystalline white solid (0.091 g, 60% yield). ^1H NMR (500 MHz $CDCl_3$) δ 3.96 (3H, s), 7.18 (1H, t, J = 7.41 Hz), 7.39 (2H, t, J = 7.88 Hz), 7.65 (2H, d, J = 7.92 Hz), 7.80-7.87 (1H, br s), 7.93 (2H, d, J = 8.27 Hz), 8.15 (2H, d, J = 8.30 Hz). ^{13}C NMR (100 MHz $CDCl_3$) δ 52.6 (CH_3), 120.4 (CH), 125.1 (CH), 127.2 (CH), 129.3 (CH), 130.2 (CH), 133.2 (C), 137.7 (C), 139.0 (C), 165.5 (C), 166.3 (C). Data is consistent with literature.[106]

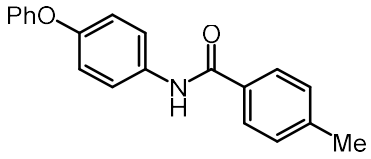

4-Methyl-*N*-(4-phenoxyphenyl)benzamide (Table 2-7, 4a): Synthesized according to general procedure **F** using masked isocyanate **1b** (0.183 g, 0.600 mmol), arylboroxine **2a** (0.141 g, 0.400 mmol, 2.00 equiv "Ar-B"), Et_3N (0.167 mL, 1.20 mmol), $Pd(OAc)_2$ (1.3 mg, $6.0x10^{-3}$ mmol), and SPhos (4.9 mg, 0.012 mmol). The desired product was purified by column chromatography (70% Hexanes/EtOAc) yielding an amorphous white solid (0.135 g, 75% yield). TLC R_F = 0.20 in 70% Hexanes/EtOAc. ^1H NMR (400 MHz, $CDCl_3$) δ 2.43 (3H, s), 6.97-7.12 (5H, m), 7.26-7.36 (4H,

[106] Perry, R. J.; Wilson, B. D. *J. Org. Chem.* **1996**, *61*, 7482.

m), 7.56-7.63 (2H, m), 7.72-7.76 (1H br s.), 7.74-7.79 (2H, m). ^{13}C NMR (100 MHz $CDCl_3$) δ 21.6 (CH_3), 118.6 (CH), 119.8 (CH), 122.1 (CH), 123.2 (CH), 127.2 (CH), 129.6 (CH), 129.9 (CH), 132.1 (C), 133.7 (C), 142.5 (C), 153.8 (C), 157.7 (C), 165.8 (C). IR (film): 3394, 3358, 3062, 1713, 1651, 1589, 1603 cm^{-1}. HRMS (ESI-TOF): Exact mass calcd for $C_{20}H_{17}NO_2Na$ $[M+Na]^+$: 326.1157. Found: 326.1157.

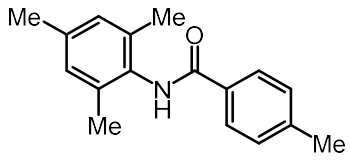

***N*-Mesityl-4-methylbenzamide (Table 2-7, 4b):** Synthesized according to general procedure **F** using masked isocyanate **1e** (0.153 g, 0.600 mmol), arylboroxine **2a** (0.141 g, 0.400 mmol, 2.00 equiv "Ar-B"), Et_3N (0.167 mL, 1.20 mmol), $Pd(OAc)_2$ (1.3 mg, $6.0x10^{-3}$ mmol), and SPhos (4.9 mg, 0.012 mmol). The desired product was purified by column chromatography (CH_2Cl_2 to 5% EtOAc/CH_2Cl_2) yielding an amorphous white solid (0.102 g, 67% yield). TLC R_F = 0.16 in CH_2Cl_2. ^{1}H NMR (400 MHz $CDCl_3$) δ 2.23 (6H, s), 2.29 (3H, s), 2.43 (3H, s), 6.93 (2H, s), 7.29 (2H, d, *J* = 8.0 Hz), 7.81 (2H, d, *J* = 8.1 Hz). ^{13}C NMR (100 MHz $CDCl_3$) δ 18.5 (CH_3), 21.1 (CH_3), 21.6 (CH_3), 31.0 (CH_3), 127.3 (CH), 129.1 (CH), 129.5 (CH), 131.4 (C), 131.9 (C), 135.4 (C), 137.1 (C), 142.3 (C), 166.0 (C). Data is consistent with literature.[65]

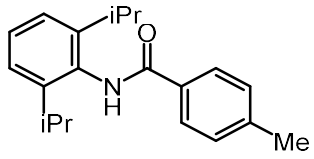

***N*-(2,6-Diisopropylphenyl)-4-methylbenzamide (Table 2-7, 4c):** Synthesized according to general procedure **F** using masked isocyanate **1f** (0.178 g, 0.600 mmol), arylboroxine **2a** (0.141 g, 0.400 mmol, 2.00 equiv "Ar-B"), Et_3N (0.167 mL, 1.20 mmol), $Pd(OAc)_2$ (1.3 mg, $6.0x10^{-3}$ mmol), and SPhos (4.9 mg, 0.012 mmol). The desired product was purified by column chromatography (20% EtOAc/ Hexanes) yielding an amorphous white solid (0.047 g, 26% yield). TLC R_F = 0.27 in 15% EtOAc/Hexanes. ^{1}H NMR (300 MHz $CDCl_3$) δ 1.22 (12H, d, *J* = 6.88 Hz), 2.45 (3H, s), 3.14 (2H, m, *J* = 6.92 Hz), 7.19-7.24 (2H, m), 7.29-7.37 (3H, m), 7.82-7.85 (2H, m). ^{13}C NMR (125 MHz $CDCl_3$) δ 21.6 (CH_3), 23.8 (CH_3), 29.0 (CH), 123.7 (CH), 127.3 (CH), 128.6

(CH), 129.6 (CH), 131.4 (C), 131.9 (C), 142.4 (C), 146.5 (C), 166.9 (C). Data consistent with literature.[107]

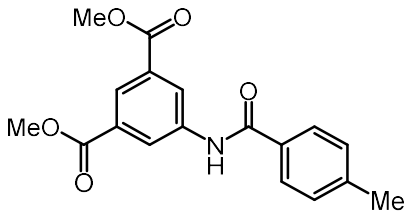

Dimethyl-5-(4-methylbenzamido)isophthalate (Table 2-7, 4d): Synthesized according to general procedure **F** using masked isocyanate **1c** (0.214 g, 0.600 mmol), arylboroxine **2a** (0.141 g, 0.400 mmol, 2.00 equiv "Ar-B"), Et_3N (0.167 mL, 1.20 mmol), $Pd(OAc)_2$ (1.3 mg, $6.0x10^{-3}$ mmol), and SPhos (4.9 mg, 0.012 mmol). The desired product was purified by column chromatography (80% Hexanes/EtOAc) yielding an amorphous white solid (0.124 g, 64% yield). TLC R_F = 0.24 in 80% Hexanes/EtOAc. ^{1}H NMR (500 MHz $CDCl_3$) δ 2.44 (3H, s), 3.95 (6H, s), 7.32 (2H, d, *J* = 8.0 Hz), 7.80 (2H, d, *J* = 8.1 Hz), 7.95-7.99 (1H, br s), 8.46-8.47 (1H, m), 8.51-8.53 (2H, m). ^{13}C NMR (125 MHz $CDCl_3$) δ 21.7 (CH_3), 52.6 (CH_3), 125.3 (CH), 126.6 (CH), 127.3 (CH), 129.7 (CH), 131.4 (C), 131.6 (C), 138.8 (C), 143.1 (C), 165.9 (C), 166.1 (C). Data consistent with literature.[65]

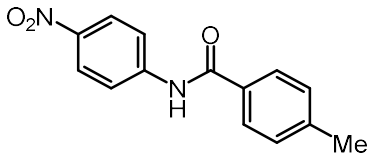

4-Methyl-*N*-(4-nitrophenyl)benzamide (Table 2-7, 4e): Synthesized according to general procedure **F** using masked isocyanate **1d** (0.154 g, 0.600 mmol), arylboroxine **2a** (0.141 g, 0.400 mmol, 2.00 equiv "Ar-B"), Et_3N (0.167 mL, 1.20 mmol), $Pd(OAc)_2$ (1.3 mg, $6.0x10^{-3}$ mmol), and SPhos (4.9 mg, 0.012 mmol). The desired product was purified by column chromatography (80% Hexanes/EtOAc) yielding an amorphous white solid (0.092 g, 60% yield). TLC R_F = 0.26 in 80% Hexanes/EtOAc. ^{1}H NMR (500 MHz DMSO-*d*$_6$) δ 2.40 (3H, s), 7.37 (2H, d, *J* = 8.0 Hz), 7.90 (2H, d, *J* = 8.1 Hz), 8.06 (2H, d, *J* = 9.2 Hz), 8.26 (2H, d, *J* = 9.2 Hz), 10.67-10.75 (1H, br s). ^{13}C

[107] Boeré, R. T.; Klassen, V.; Wolmershäuser, G. *J. Chem. Soc., Dalton Trans.* **1998**, 4147.

NMR (500 MHz DMSO-d_6) δ 21.0 (CH_3), 120.0 (CH), 124.8 (CH), 128.0 (CH), 129.0 (CH), 131.3 (C), 142.4 (C), 145.63 (C), 166.05 (C). Data consistent with literature.[108]

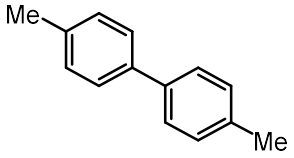

4,4'-Dimethyl-1,1'-biphenyl (Scheme 2-1, 5a): Isolated during the isolation of **4e** yielding an amorphous white solid (0.003 g, 3% yield). Data consistent with literature.[101]

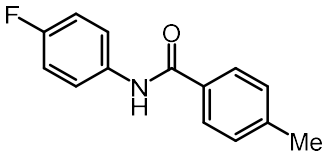

***N*-(4-Fluorophenyl)-4-methylbenzamide (Table 2-7, 4f):** Synthesized according to general procedure **F** using masked isocyanate **1g** (0.138 g, 0.600 mmol), boroxine **2a** (0.141 g, 0.400 mmol), Et_3N (0.167 mL, 1.20 mmol), $Pd(OAc)_2$ (1.3 mg, $6.0x10^{-3}$ mmol), and SPhos (4.9 mg, 0.0120 mmol). The reaction reached completion within 16 hours. The crude mixture was dry loaded onto silica gel (acetone) and purified by column chromatography (75% CH_2Cl_2/Hexanes) white solid (0.954 g, 70% yield). TLC R_F = 0.18 in 75% CH_2Cl_2/ Hexanes. ^{1}H NMR (300 MHz, acetone-d_6) δ 2.37 (s, 3H), 6.80 – 7.20 (m, 2H), 7.29 (dd, J = 7.9, 0.7 Hz, 2H), 7.51- 8.49 (m, 4H), 9.49 (br. s, 1H). ^{13}C NMR (126 MHz, Acetone-d_6) δ 21.4 (CH_3), 115.9 (CH, d, J = 22.3 Hz), 122.8 (CH, d, J = 7.7 Hz), 128.4 (CH), 129.9 (CH), 133.3 (C), 136.7 (d, J = 2.7 Hz), 159.8 (C, d, J = 240.2 Hz), 142.8 (C), 166.1 (C). Data consistent with literature.[109]

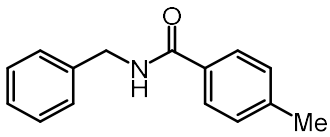

***N*-Benzyl-4-methylbenzamide (Table 2-7, 4g):** Synthesized according to general procedure **F** using masked isocyanate **1h** (0.136 g, 0.600 mmol), arylboroxine **2a** (0.141 g, 0.400 mmol, 2.00

[108] Alapati, M.; L.; P.; R.; Abburu, S. R.; Mutyala, K.; R.; Mukkamala, S.; B. *Synth. Commun.* **2016**, *46*, 1242.
[109] Sharma, R.; Vishwakarma, R. A.; Bharate, S. B. *Adv. Synth. Catal.* **2016**, *358*, 3027.

equiv "Ar-B"), Et_3N (0.167 mL, 1.20 mmol), $Pd(OAc)_2$ (1.3 mg, $6.0x10^{-3}$ mmol), and SPhos (4.9 mg, 0.012 mmol). The desired product was purified by column chromatography (CH_2Cl_2) yielding an amorphous white solid (0.102 g, 75% yield). TLC R_F = 0.17 in CH_2Cl_2. ^1H NMR (300 MHz $CDCl_3$) δ 2.40 (3H, s), 4.65 (2H, d, *J* = 5.7 Hz), 6.26-6.37 (1H, br s), 7.19-7.25 (2H, m), 7.27-7.38 (5H, m), 7.69 (1H, d, *J* = 8.4 Hz). ^{13}C-NMR (125 MHz $CDCl_3$) δ 21.6 (CH_3), 44.3 (CH_2), 127.1 (CH), 127.8 (CH), 128.1 (CH), 128.9 (CH), 129.4 (CH), 131.7 (C), 138.5 (C), 142.1 (C), 167.4 (C).Data is consistent with literature.[110]

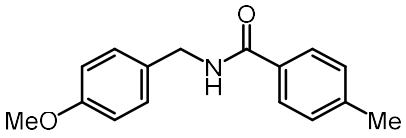

***N*-(4-Methoxybenzyl)-4-methylbenzamide (Table 2-7, 4h):** Synthesized according to general procedure **F** using masked isocyanate **1i** (0.154 g, 0.600 mmol), arylboroxine **2a** (0.141 g, 0.400 mmol, 2.00 equiv "Ar-B"), Et_3N (0.167 mL, 1.20 mmol), $Pd(OAc)_2$ (1.3 mg, $6.0x10^{-3}$ mmol), and SPhos (4.9 mg, 0.012 mmol). The reaction reached completion within 16 hours. The desired product was purified by column chromatography (80% Hexanes/EtOAc) yielding an amorphous white solid (0.090 g, 59% yield). TLC R_F = 0.16 80% Hexanes/EtOAc. ^1H NMR (500 MHz, $CDCl_3$) δ 2.38 (3H, s), 3.79 (3H, s), 4.54 (2H, d, *J* = 5.6 Hz), 6.50 (1H, br s.), 6.86 (2H, td, *J* = 2.5, 9.5 Hz), 7.20 (2H, d, *J* = 7.9 Hz), 7.26 (2H, d, *J* = 8.7 Hz), 7.68 (2H, d, *J* = 8.2 Hz). ^{13}C NMR (125 MHz) δ 21.5 (CH_3), 43.6 (CH_2), 55.3 (CH_3), 114.13 (CH), 127.0 (CH), 129.2 (CH), 129.3 (CH) 130.5 (C), 131.6 (C), 141.9 (C), 159.1 (C), 167.3 (C). Data consistent with literature.[111]

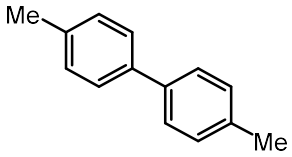

4,4'-Dimethyl-1,1'-biphenyl (Scheme 2-1, 5a): Isolated during the isolation of **4e** yielding an amorphous white solid (0.003 g, 3% yield). Data was consistent with literature.[101]

[110] Aqwada, V. C. *J. Chem. Eng. Data* **1982**, *27*, 479.
[111] Katritzky, A. R.; Zhang, S.; Wang, M.; Kolb, H. C.; Steel, P, J. *J. Heterocycl. Chem.* **2002**, *39*, 759.

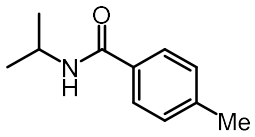

***N*-Isopropyl-4-methylbenzamide (Table 2-7, 4i):** Synthesized according to general procedure **F** using masked isocyanate **1J** (0.107 g, 0.600 mmol), arylboroxine **2a** (0.141 g, 0.400 mmol, 2.00 equiv "Ar-B"), Et_3N (0.167 mL, 1.20 mmol), $Pd(OAc)_2$ (1.3 mg, $6.0x10^{-3}$ mmol), and SPhos (4.9 mg, 0.012 mmol). The desired product was purified by column chromatography (80% Hexanes/EtOAc) yielding an amorphous white solid (0.061 g, 57% yield). TLC R_F = 0.32 in 80% Hexanes/EtOAc. ^1H NMR (500 MHz $CDCl_3$) δ 1.25 (6H, d, *J* = 6.6 Hz), 2.38 (3H, s), 4.28 (1H, m, *J* = 6.7 Hz), 5.81-5.94 (1H, br s), 7.21 (2H, d, *J* = 7.9 Hz), 7.64 (2H, d, *J* = 8.0 Hz). ^{13}C NMR (500 MHz $CDCl_3$) δ 21.6 (CH_3), 23.1 (CH_3), 41.9 (CH), 126.9 (CH), 129.3 (CH), 132.3 (C), 141.8 (C), 166.7 (C). Data consistent with literature.[112]

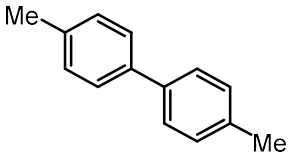

4,4'-Dimethyl-1,1'-biphenyl (Scheme 2-1, 5a): Isolated during the isolation of **4i** yielding an amorphous white solid (0.004 g, 3% yield). Data was consistent with literature.[101]

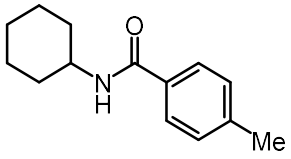

***N*-Cyclohexyl-4-methylbenzamide (Table 2-7, 4j):** Synthesized according to general procedure **F** using masked isocyanate **1k** (0.131 g, 0.600 mmol), arylboroxine **2a** (0.141 g, 0.400 mmol, 2.00 equiv "Ar-B"), Et_3N (0.167 mL, 1.20 mmol), $Pd(OAc)_2$ (1.3 mg, $6.0x10^{-3}$ mmol), and SPhos (4.93 mg, 0.012 mmol). The desired product was purified by column chromatography (20% EtOAc/CH_2Cl_2) yielding an amorphous white solid (0.093 g, 71% yield). TLC R_F = 0.20 in 20% EtOAc/Hexanes. ^1H NMR (500 MHz $CDCl_3$) δ 1.14-1.27 (3H, m), 1.37-1.48 (2H, m), 1.60-1.69

[112] Rolfe, A.; Probst, D. A.; Volp, K. A.; Omar, I.; Flynn, D. L.; Hanson, P. R. *J. Org. Chem.* **2008**, *73*, 8785.

(1H, m), 1.70-1.79 (2H, m), 1.98-2.06 (2H, m), 2.38 (3H, s), 3.94-4.01 (1H, m), 5.87-5.98 (1H, br s), 7.21 (2H, d, J = 7.9), 7.64 (2H, d, J = 7.9). ^{13}C NMR (125 MHz $CDCl_3$) δ 21.5 (CH_3), 25.1 (CH_2), 25.7 (CH_2), 33.4 (CH_2), 48.7 (CH), 126.9 (CH), 129.3 (CH), 132.4 (C), 141.7 (C), 166.6 (C). Data consistent with literature.[113]

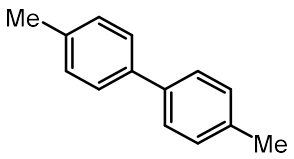

4,4'-Dimethyl-1,1'-biphenyl (Scheme 2-1, 5a): Isolated during the isolation of **4j** yielding an amorphous white solid (0.009 g, 8% yield). Data was consistent with literature.[101]

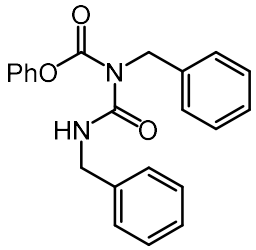

Phenyl benzyl(benzylcarbamoyl)carbamate (Table 2-8, 5b): Isolated during small scale reactions probing alternative arylboronic acid ester derivatives. Synthesized according to general procedure **E** using masked isocyanate **1g** (0.043 g, 0.200 mmol), Et_3N (0.056 mL, 0.40 mmol), $Pd(OAc)_2$ (0.45 mg, 2.0x10^{-3} mmol), and SPhos (4.0x10^{-3} mmol, 1.6 mg). The desired product was purified by column chromatography (80% Hexanes/EtOAc) yielding an amorphous white solid. TLC R_F = 0.48 in 80% Hexanes/EtOAc. ^{1}H NMR (300 MHz $CDCl_3$) δ 4.53 (2H, d, J = 6.21 Hz), 5.19 (2H, s), 6.95 (2H, d, J = 7.5 Hz), 7.27-7.45 (13H, m), 8.85-8.94 (1H, br s). ^{13}C NMR (125 MHz $CDCl_3$) δ 45.2 (CH_2), 47.4 (CH_2), 121.7 (CH), 126.6 (C), 127.6 (C), 127.6 (C), 127.8 (C), 128.0 (C), 128.7 (C), 128.8 (C), 129.7 (C), 138.1 (C), 138.1 (C), 150.1 (C), 154.3 (C), 155.3 (C). IR (film): 3227, 2968, 2923, 2872, 1657, 1613, 153.8, 1510 cm^{-1}. HRMS (ESI-TOF): Exact mass calcd for $C_{22}H_{20}N_2O_3Na$ [M+Na]: 383.1364. Found: 383.1372.

[113] Shaabani, A.; Soleimani, E.; Rezayan, A. H. *Tetrahedron Lett.* **2007**, *48*, 6137.

4.2.4: Supplemental data for kinetic studies

General procedure G: An oven-dried microwave vial equipped with a magnetic stir bar was cooled under a stream of argon followed by the addition of $Pd(OAc)_2$ ($6.00x10^{-3}$ mmol, 0.0100 equiv.) and SPhos (0.0120 mmol, 0.0200 equiv.). The microwave vial was then sealed and purged under a stream of argon for a total of 2 minutes and subsequently anhydrous THF (1.2 mL) was added. The resulting mixture was stirred under argon at room temperature for 5 minutes.

A second oven-dried microwave vial equipped with a magnetic stir bar was cooled under a stream of argon followed by the addition of the corresponding carbamate (0.600 mmol, 1.00 equiv.) and arylboroxine (0.400 mmol, 2.00 'Ar-B' equiv.). The microwave vial was then sealed and purged under a stream of argon for a total of 2 minutes. The catalyst solution was then transferred to the vial via syringe and then let stir at room temperature for 5 minutes then subsequent addition of Et_3N (1.2 mmol, 2.0 equiv.) and $PhCF_3$ (0.6 mmol, 1.0 equiv.) via syringe. The microwave vial was then heated to 50 °C for 24 h. At each time point described, 0.1 mL aliquots were withdrawn via syringe followed by the quenching with 0.4 mL THF which was then sealed and analyzed via ^{19}F NMR. The yields were then determined through the use of an internal standard. Please see tables below for variations of each reagent to generate tables below.

Table 4-3: Supplemental data for Figure 2-1

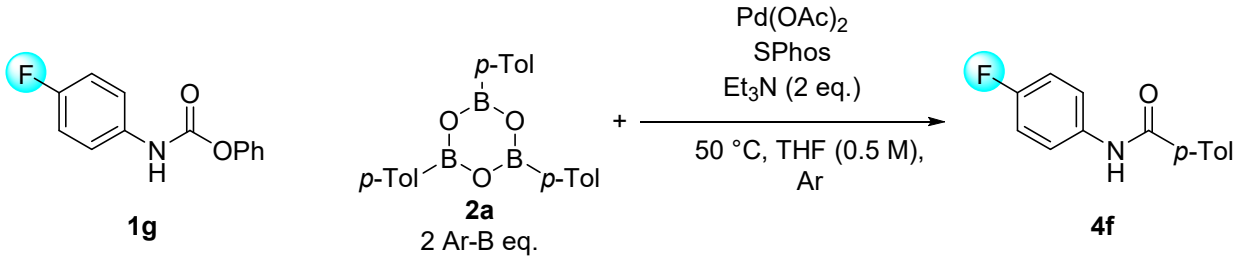

- :**1g** (0.6 mmol), **2a** (0.4 mmol, 2.0 Ar-B eq.), Et_3N (1.2 mmol), $Pd(OAc)_2$ (1 mol%), SPhos (2 mol%), THF (0.5 M), $PhCF_3$ (0.6 mmol), 50 °C, Ar.
- :**1g** (0.6 mmol), **2a** (0.4 mmol, 2.0 Ar-B eq.), Et_3N (1.2 mmol), $Pd(OAc)_2$ (0.5 mol%), SPhos (1 mol%).
- :**1g** (0.6 mmol), **2a** (0.4 mmol, 2.0 Ar-B eq.), Et_3N (1.2 mmol), $Pd(OAc)_2$ (1.25 mol%), SPhos (2.5 mol%).
- :**1g** (0.9 mmol), **2a** (0.4 mmol, 2.0 Ar-B eq.), Et_3N (1.2 mmol), $Pd(OAc)_2$ (0.5 mol%), SPhos (1 mol%).
- :**1g (1.2 mmol)**, **2a** (0.4 mmol, 2.0 Ar-B eq.), Et_3N (1.2 mmol), $Pd(OAc)_2$ (0.5 mol%), SPhos (1 mol%).

Time (h)	Experiment (•)	Experiment (•)	Experiment (•)	Experiment (•)	Experiment (•)
0	0	0	0	0	0
0.17	0.009	0.008	0.006	0.026	0.031
0.50	0.034	0.032	0.025	0.032	0.041
1.00	0.040	0.039	0.040	0.042	0.046
1.50	0.050	0.055	0.057	0.055	0.056
2.00	0.066	0.065	0.066	0.059	0.058
3.00	0.092	0.082	0.079	0.071	0.069
4.00	0.113	0.093	0.092	0.088	0.082
5.00	0.139	0.106	0.106	0.099	0.090
6.00	0.158	0.116	0.121	0.117	0.110

Table 4-4: Raw data for inhibition studies (Figure 2-2)[a]

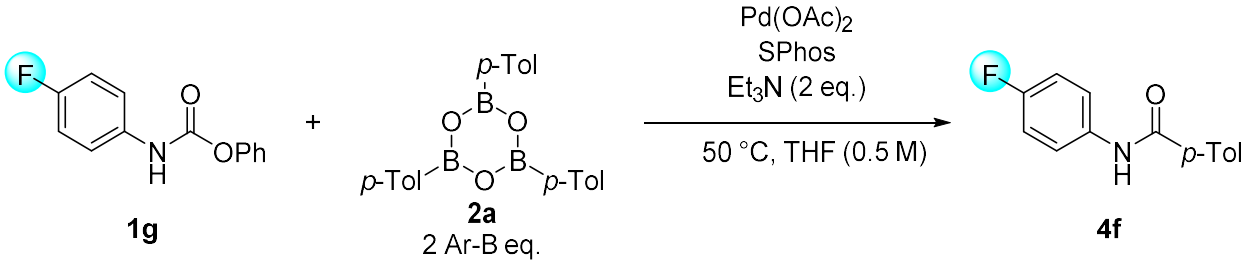

■ :**1g** (1.0 mmol), **2a** (0.67 mmol, 2.0 Ar-B eq.), Et_3N (2.0 mmol), $Pd(OAc)_2$ (1 mol%), SPhos (2 mol%), THF (0.5 M), $PhCF_3$ (1.0 mmol) 50 °C, Ar.

♦ :**1g** (0.7 mmol), **2a** (0.56 mmol, 1.7 Ar-B eq.)

■ :**1g** (0.7 mmol), **2a** (0.56 mmol, 1.7 Ar-B eq.), **4f** (0.3 mmol)

Time (h)	Experiment (■) 1g (M)	Experiment (♦) 1g (M)	Experiment (■) 1g (M)
0.00	0.450	0.300	0.300
0.17	0.400	-	-
0.50	0.390	0.216	0.211
1.00	0.351	0.191	0.195
1.50	0.335	0.1739	0.181
2.00	0.325	0.172	0.183
2.50	-	0.148	0.172
3.00	0.308	0.148	0.170
4.00	0.297	0.131	0.157
5.00	0.284	0.106	0.130
6.00	0.274	0.101	0.132

[a] Reactions were based off a 1.0 mmol scale rather than a 0.6 mmol scale.

Table 4-5: Raw data for determination of the order in catalyst (Figure 2-3)

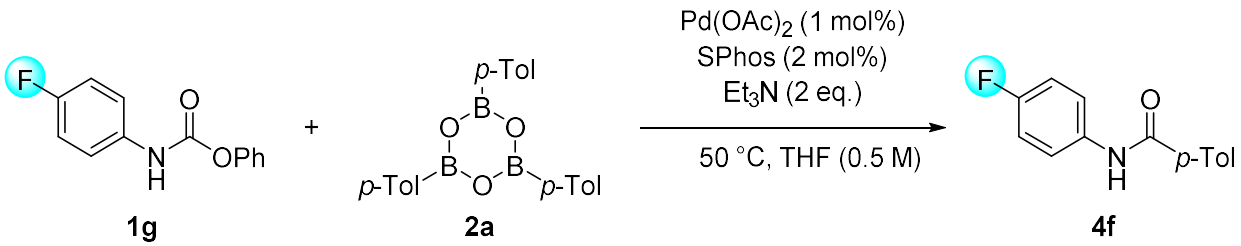

♦ :**1g** (0.6 mmol), **2a** (0.4 mmol, 2.0 Ar-B eq.), Et_3N (1.2 mmol), $Pd(OAc)_2$ (1 mol%), SPhos (2 mol%), THF (0.5 M), $PhCF_3$ (0.6 mmol), 50 °C, Ar.
■ : $Pd(OAc)_2$ (0.5 mol%), SPhos (1 mol%),
▲: $Pd(OAc)_2$ (0.75 mol%), SPhos (1.5 mol%),

Time (h)	Experiment (♦) 0.012 M $Pd(OAc)_2$		Experiment (■) 0.006 M $Pd(OAc)_2$		Experiment (▲) 0.009 M $Pd(OAc)_2$	
	1g (M)	4f (M)	1g (M)	4f (M)	1g (M)	4f (M)
0.00	0.500	0.000	0.500	0.000	0.500	0.000
4.00	0.257	0.243	0.294	0.206	0.261	0.239
8.00	0.138	0.363	0.195	0.305	0.197	0.303
12.00	0.074	0.426	0.172	0.328	0.095	0.405
16.00	0.062	0.438	0.168	0.332	0.086	0.414

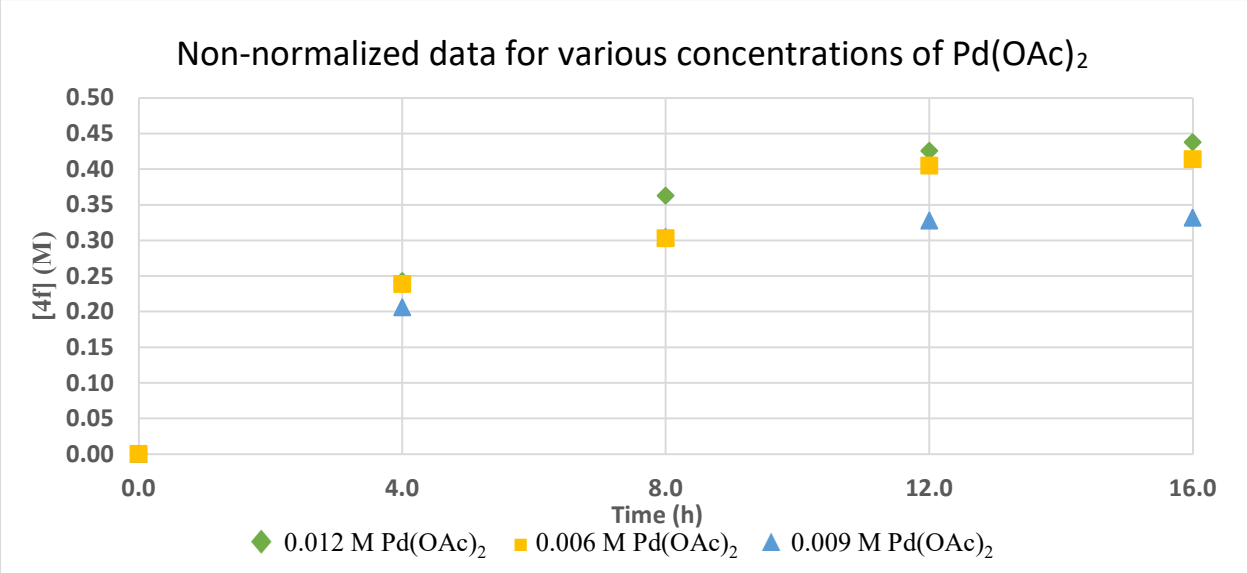

*Table 4-6: Raw data for determination of order in **1g** (Figure 2-5)*

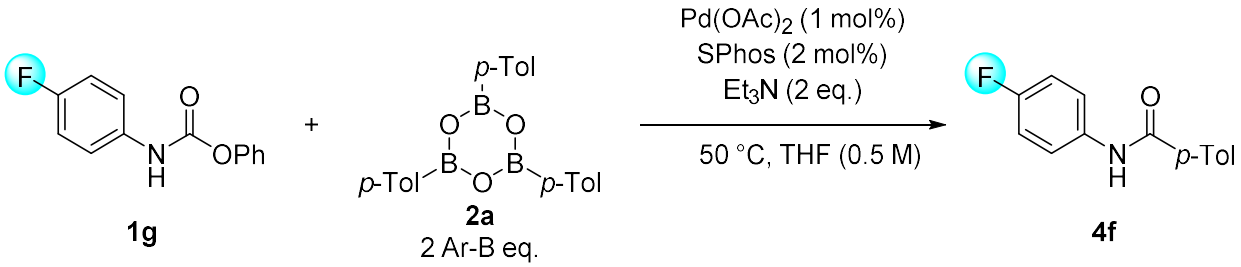

♦ :**1g** (0.6 mmol), **2a** (0.4 mmol, 2.0 Ar-B eq.), Et_3N (1.2 mmol), $Pd(OAc)_2$ (1 mol%), SPhos (2 mol%), THF (0.5 M), $PhCF_3$ (0.6 mmol), 50 °C, Ar.
■ :**1g** (0.45 mmol)
▲:**1g** (0.75 mmol)

Time (h)	Experiment (♦) 1.0 eq. (1g)		Experiment (■) 0.75 eq. (1g)		Experiment (▲) 1.25 eq. (1g)	
	1g (M)	4f (M)	1g (M)	4f (M)	1g (M)	4f (M)
0.00	0.500	0.000	0.375	0.000	0.625	0.000
4.00	0.257	0.243	0.161	0.214	0.330	0.295
8.00	0.138	0.363	0.069	0.306	0.206	0.419
12.00	0.074	0.426	0.062	0.313	0.184	0.441
16.00	0.062	0.438	0.056	0.319	0.168	0.457

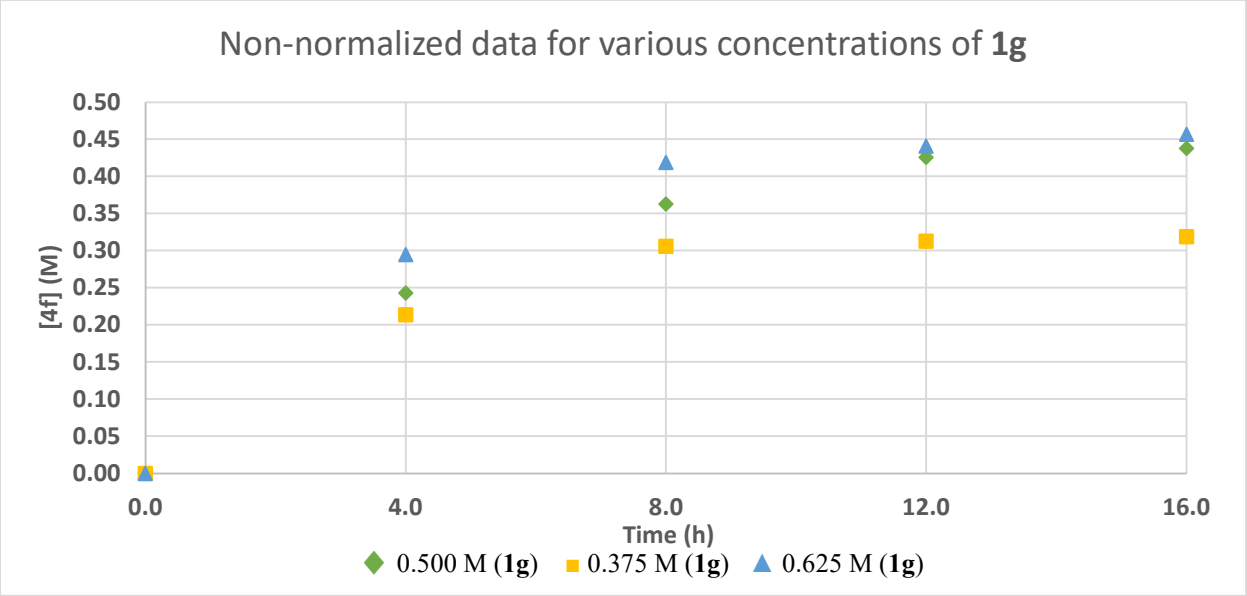

*Table 4-7: Raw data for determination of order in **2a** (Figure 2-6)*

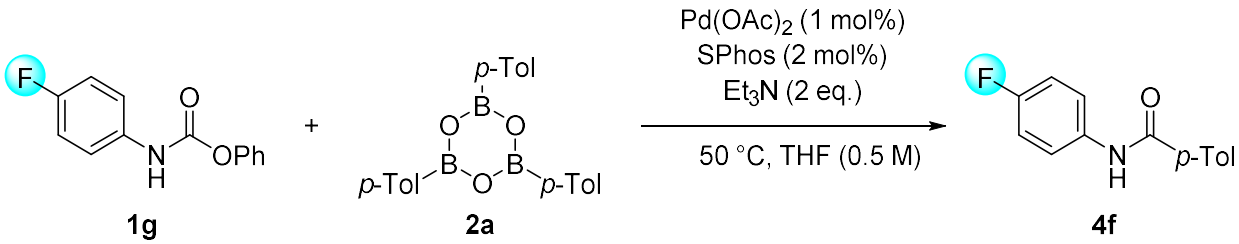

♦ :**1g** (0.6 mmol), **2a** (0.4 mmol, 2.0 Ar-B eq.), Et_3N (1.2 mmol), $Pd(OAc)_2$ (1 mol%), SPhos (2 mol%), THF (0.5 M), $PhCF_3$ (0.6 mmol), 50 °C, Ar.
■ :**2a** (0.35 mmol, 1.75 Ar-B eq.)
▲ :**2a** (0.30 mmol, 1.50 Ar-B eq.)

Time (h)	**Experiment (♦), 2.0 Ar-B eq.**		
	4f (M)	**1g (M)**	**2a (M)**
0.00	0.000	0.500	1.000
4.00	0.243	0.257	0.757
8.00	0.363	0.138	0.638

12.00	0.426	0.074	0.574
16.00	0.438	0.062	0.562

Time (h)	**Experiment (■), 1.75 Ar-B eq.**		
	4f (M)	**1g (M)**	**2a (M)**
0.00	0.000	0.500	0.875
4.00	0.261	0.239	0.614
8.00	0.342	0.158	0.533
12.00	0.370	0.130	0.505
16.00	0.371	0.129	0.504

Time (h)	**Experiment (▲), 1.50 Ar-B eq.**		
	4f (M)	**1g (M)**	**2a (M)**
0.00	0.000	0.500	0.700
4.00	0.206	0.294	0.494
8.00	0.305	0.195	0.395
12.00	0.328	0.172	0.372
16.00	0.332	0.168	0.368

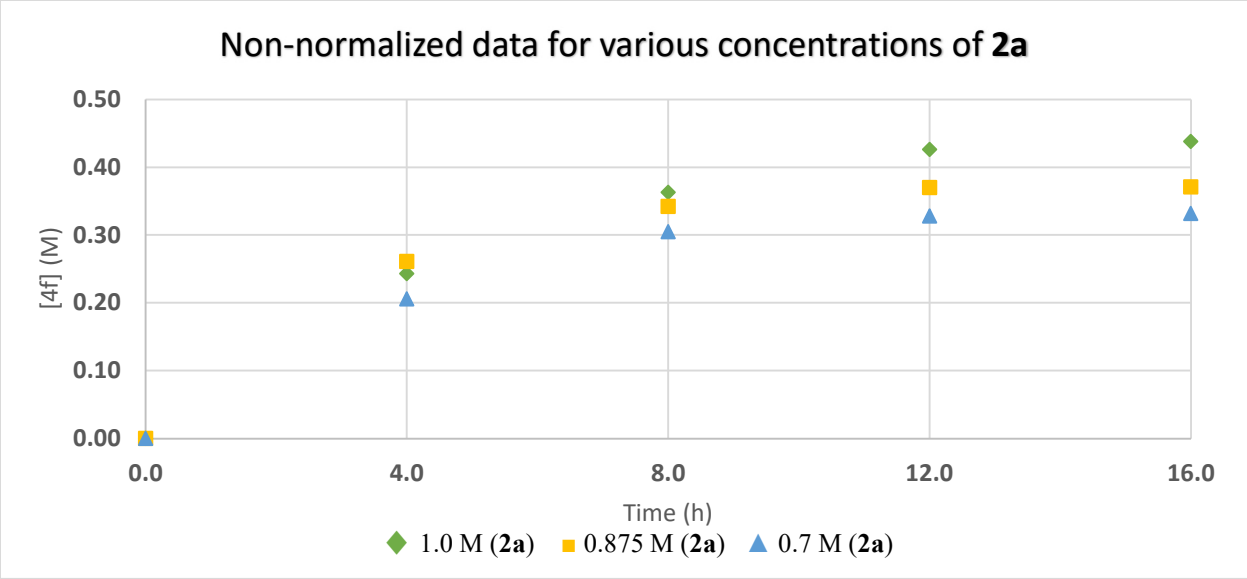
Non-normalized data for various concentrations of 2a
0.50
0.40
0.30
0.20
0.10
0.00
[4f] (M)
0.0
4.0
8.0
12.0
16.0
Time (h)
1.0 M (2a)
0.875 M (2a)
0.7 M (2a)

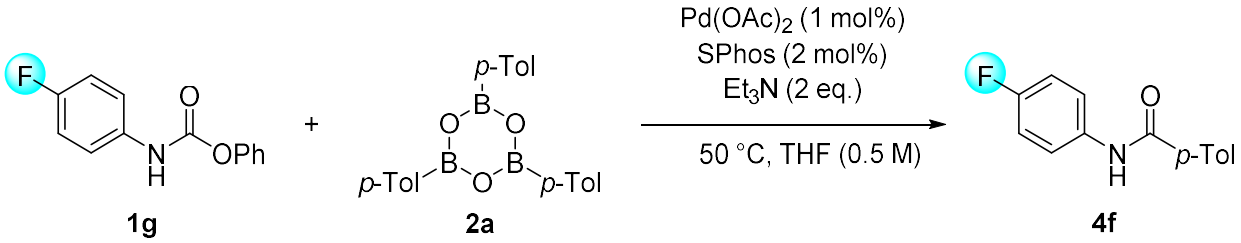

1g **2a** **4f**

♦ :**1g** (0.6 mmol), **2a** (0.4 mmol, 2.0 Ar-B eq.), Et_3N (1.2 mmol), $Pd(OAc)_2$ (1 mol%), SPhos (2 mol%), THF (0.5 M), $PhCF_3$ (0.6 mmol), 50 °C, Ar.
■ : $Pd(OAc)_2$ (0.5 mol%), SPhos (1 mol%),
▲: $Pd(OAc)_2$ (0.75 mol%), SPhos (1.5 mol%),

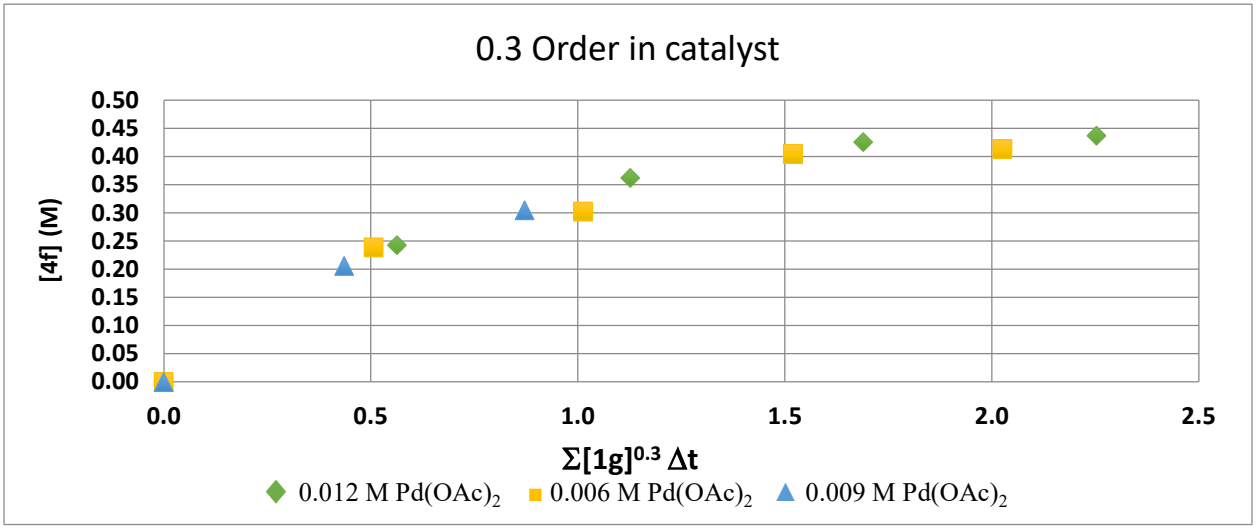

Figure 4-1: Order in catalyst with points omitted

Appendix I

Claims to Original Research

1) Completed optimization and developed a Pd-catalyzed amide forming reaction involving aromatic boroxines and phenyl carbamates as masked isocyanate reagents.
2) Performed kinetic studies indicating that there is catalyst degradation and that the rate determining step involves the catalyst, the masked isocyanates (1st order), and the organoboron reagent (1st order).
3) Proposed mechanisms to explain the reactivity and re-oxidations of Pd(0) to Pd(II) under the reaction conditions.

Presentations from this work

Poster Presentation

- **David D. Brzezinski,** Joshua S. Derasp, André M. Beauchemin; (June 3-7, 2019) Palladium-Catalyzed Synthesis of Amides from Blocked Isocyanates and Aryl Boroxines. 102nd Canadian Chemistry Conference and Exhibition (CCCE).

Spectra

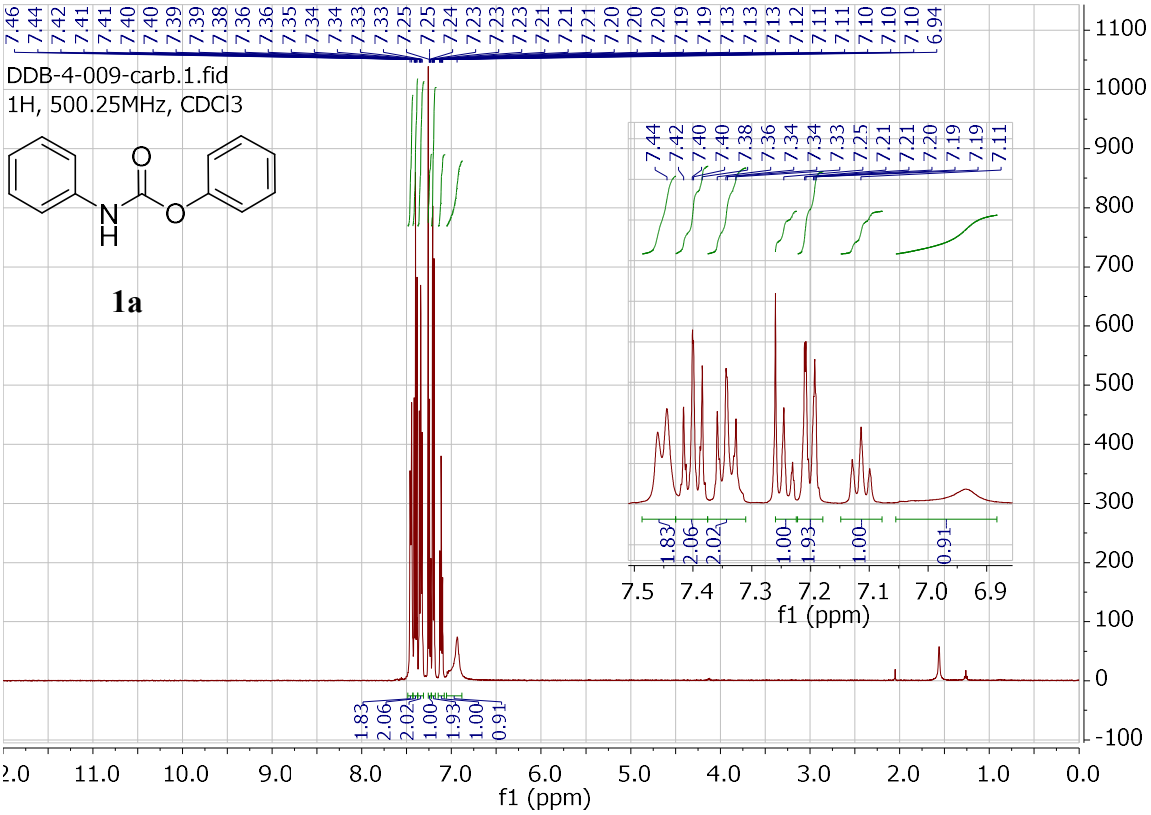
DDB-4-009-carb.1.fid
1H, 500.25MHz, CDCl3
1a
f1 (ppm)

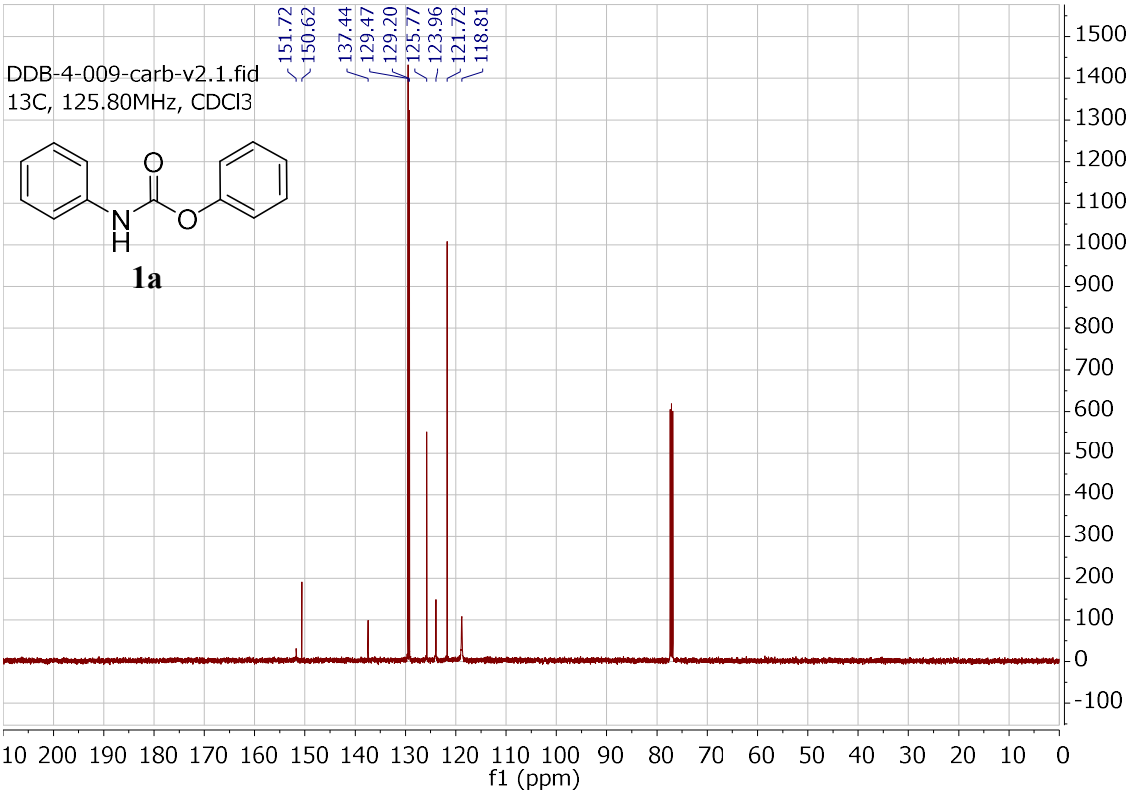
DDB-4-009-carb-v2.1.fid
13C, 125.80MHz, CDCl3
1a
f1 (ppm)

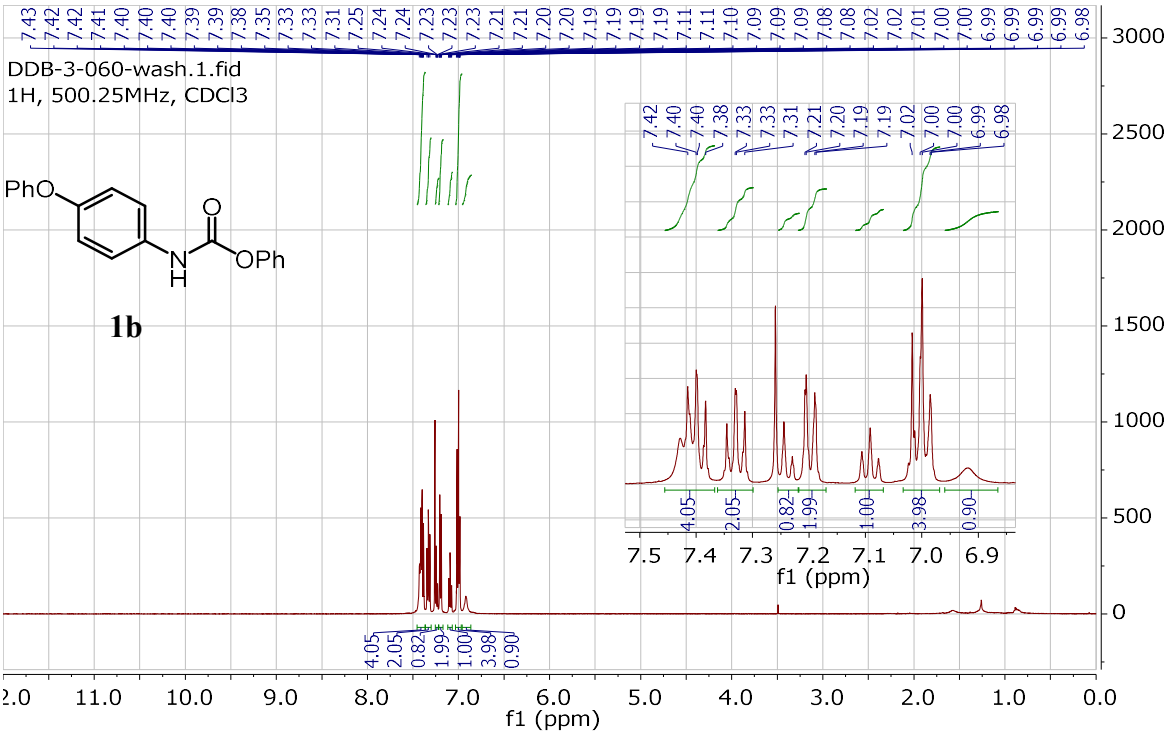
DDB-3-060-wash.1.fid
1H, 500.25MHz, CDCl3
PhO
O
N
H
OPh
1b
f1 (ppm)

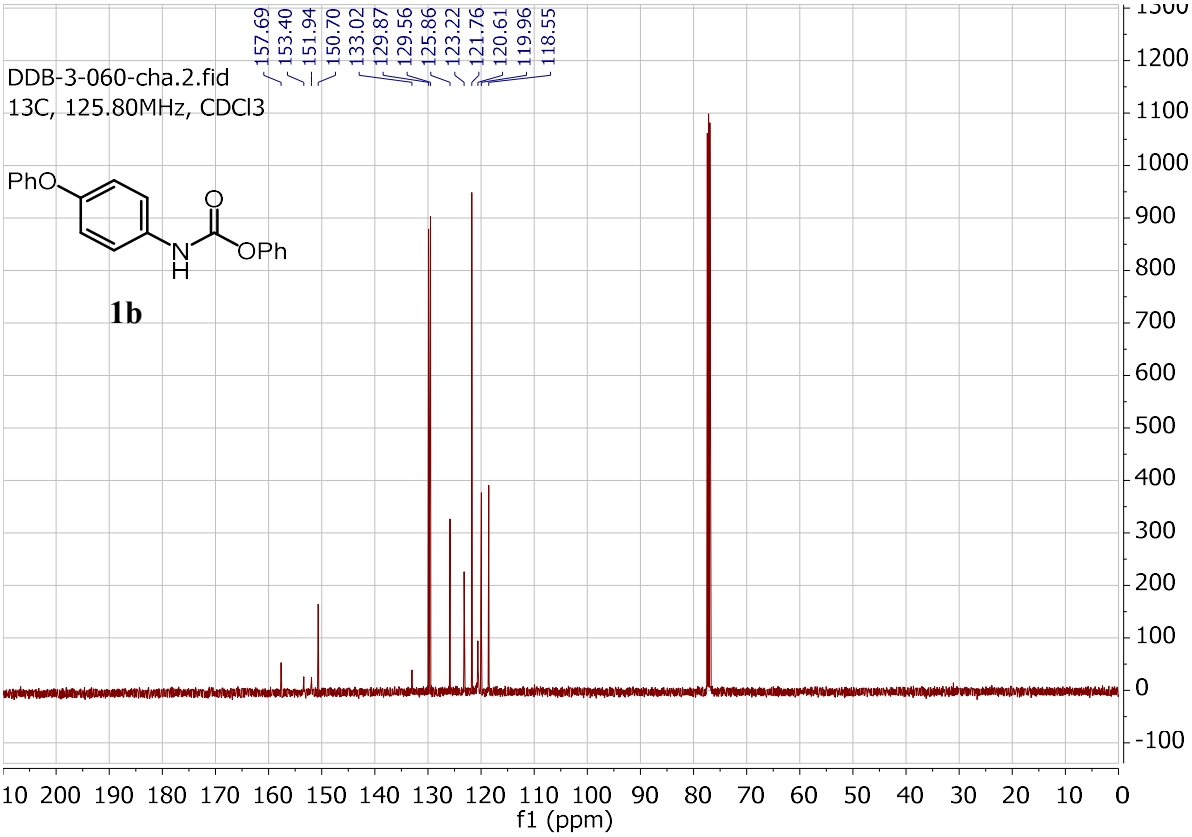
DDB-3-060-cha.2.fid
13C, 125.80MHz, CDCl3
PhO
O
N
H
OPh
1b
f1 (ppm)

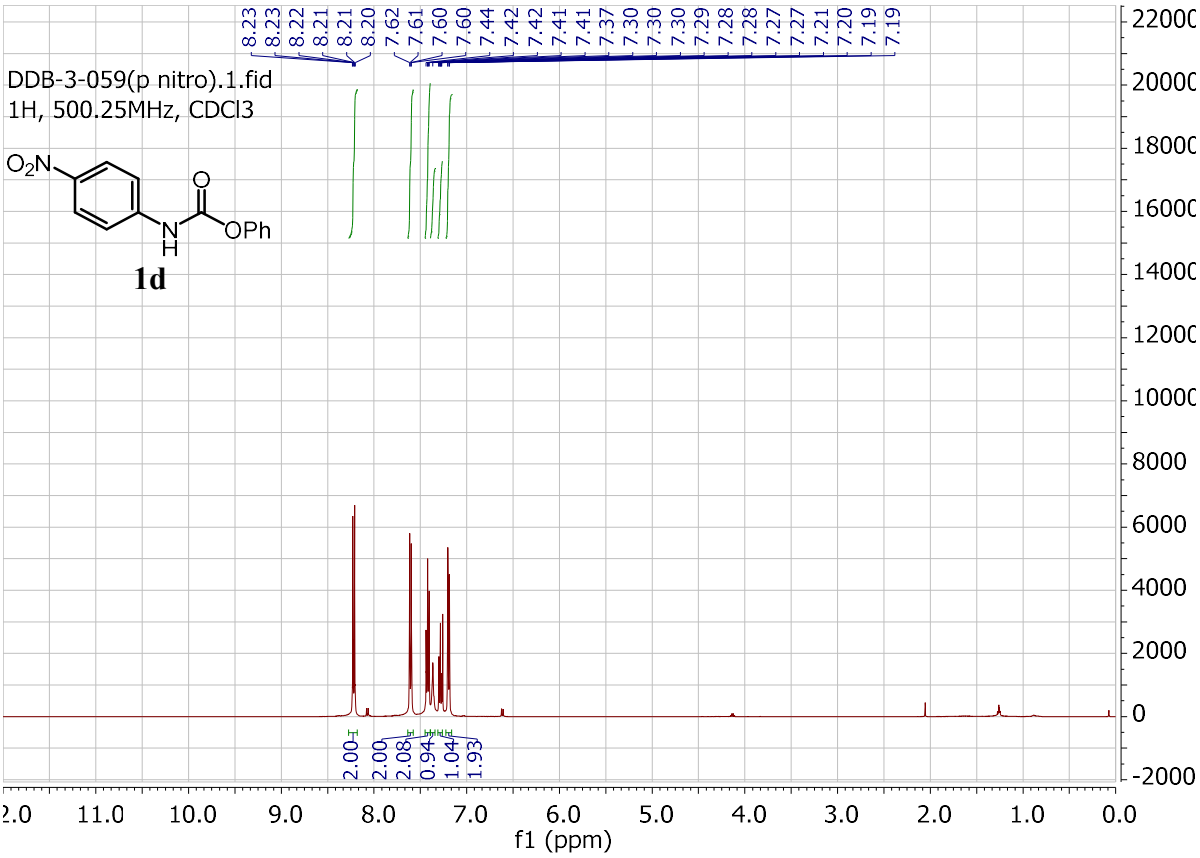
8.23
8.23
8.22
8.21
8.21
8.20
7.62
7.61
7.60
7.60
7.44
7.42
7.42
7.41
7.41
7.37
7.30
7.30
7.30
7.29
7.28
7.28
7.27
7.27
7.21
7.20
7.19
7.19
DDB-3-059(p nitro).1.fid
1H, 500.25MHz, CDCl3
O2N
O
N
H
OPh
1d
2.00
2.00
2.08
0.94
1.04
1.93
22000
20000
18000
16000
14000
12000
10000
8000
6000
4000
2000
0
-2000
2.0
11.0
10.0
9.0
8.0
7.0
6.0
5.0
4.0
3.0
2.0
1.0
0.0
f1 (ppm)

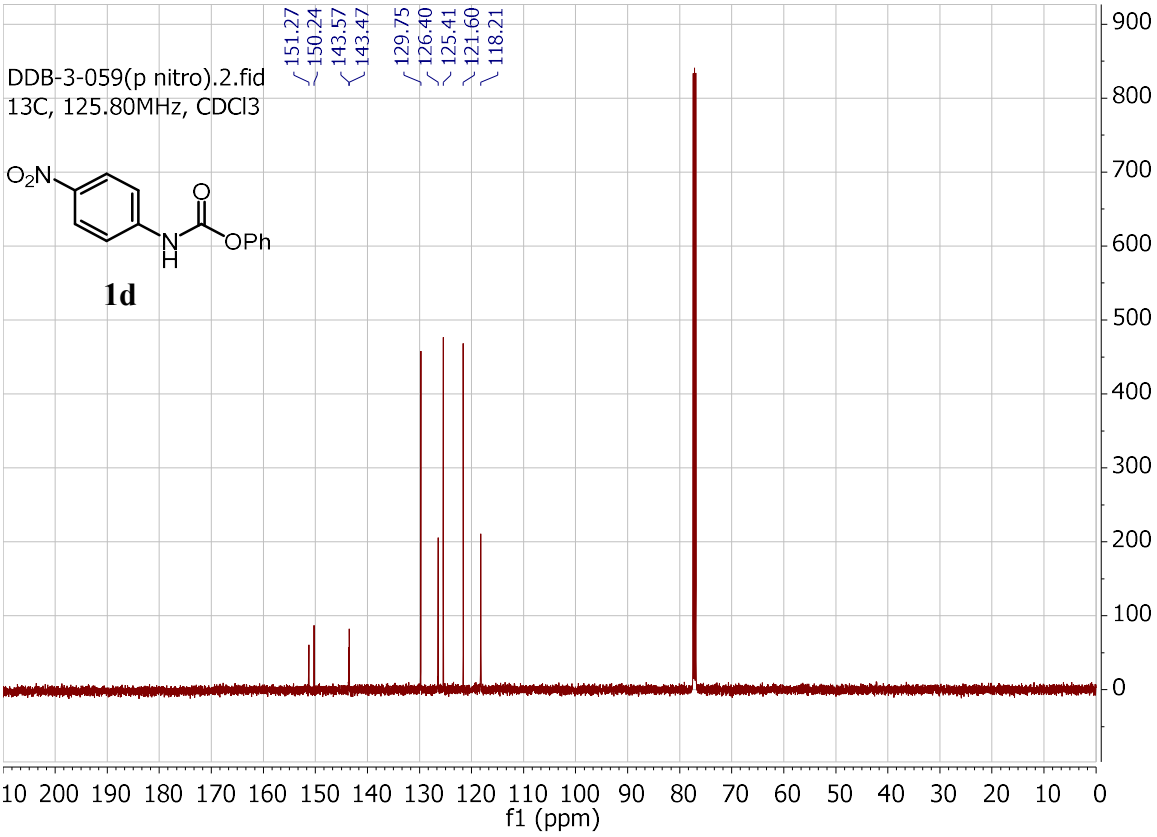
151.27
150.24
143.57
143.47
129.75
126.40
125.41
121.60
118.21
DDB-3-059(p nitro).2.fid
13C, 125.80MHz, CDCl3
O2N
O
N
H
OPh
1d
900
800
700
600
500
400
300
200
100
0
10 200 190 180 170 160 150 140 130 120 110 100 90 80 70 60 50 40 30 20 10 0
f1 (ppm)

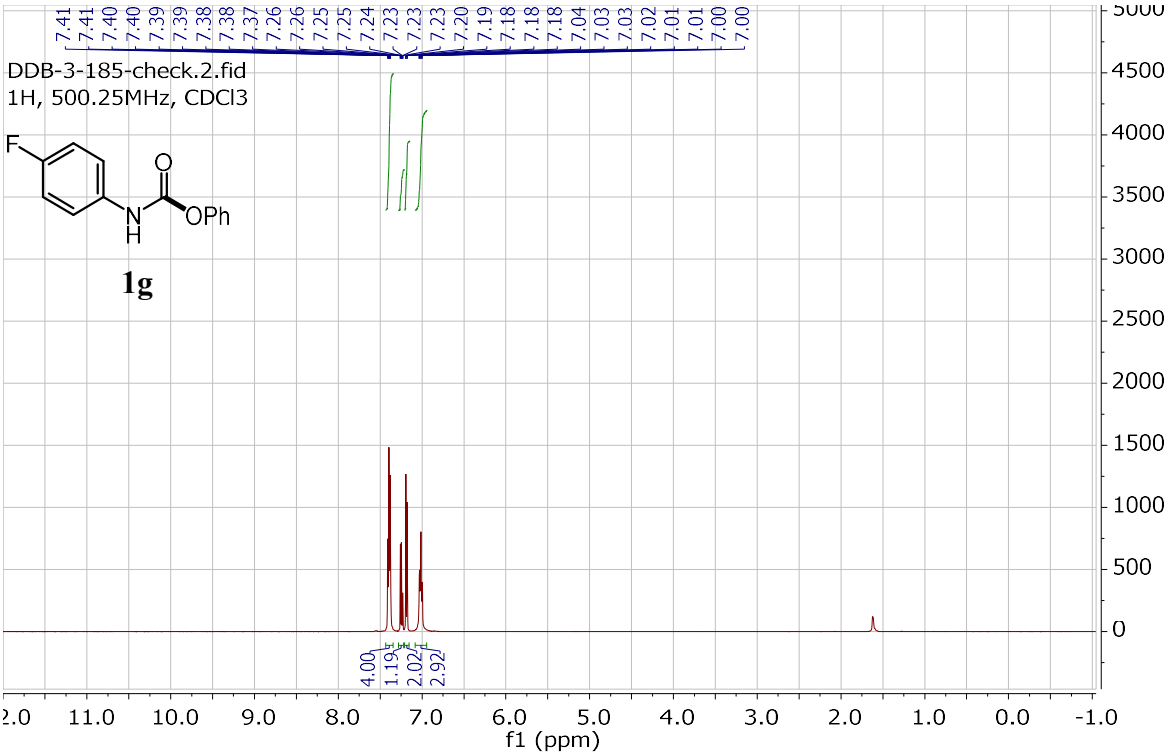
DDB-3-185-check.2.fid
1H, 500.25MHz, CDCl3
F
O
N
H
OPh
1g
7.41 7.41 7.40 7.40 7.39 7.39 7.38 7.38 7.37 7.26 7.26 7.25 7.25 7.24 7.23 7.23 7.23 7.20 7.19 7.18 7.18 7.18 7.04 7.03 7.03 7.02 7.01 7.01 7.00 7.00
4.00 1.19 2.02 2.92
f1 (ppm)

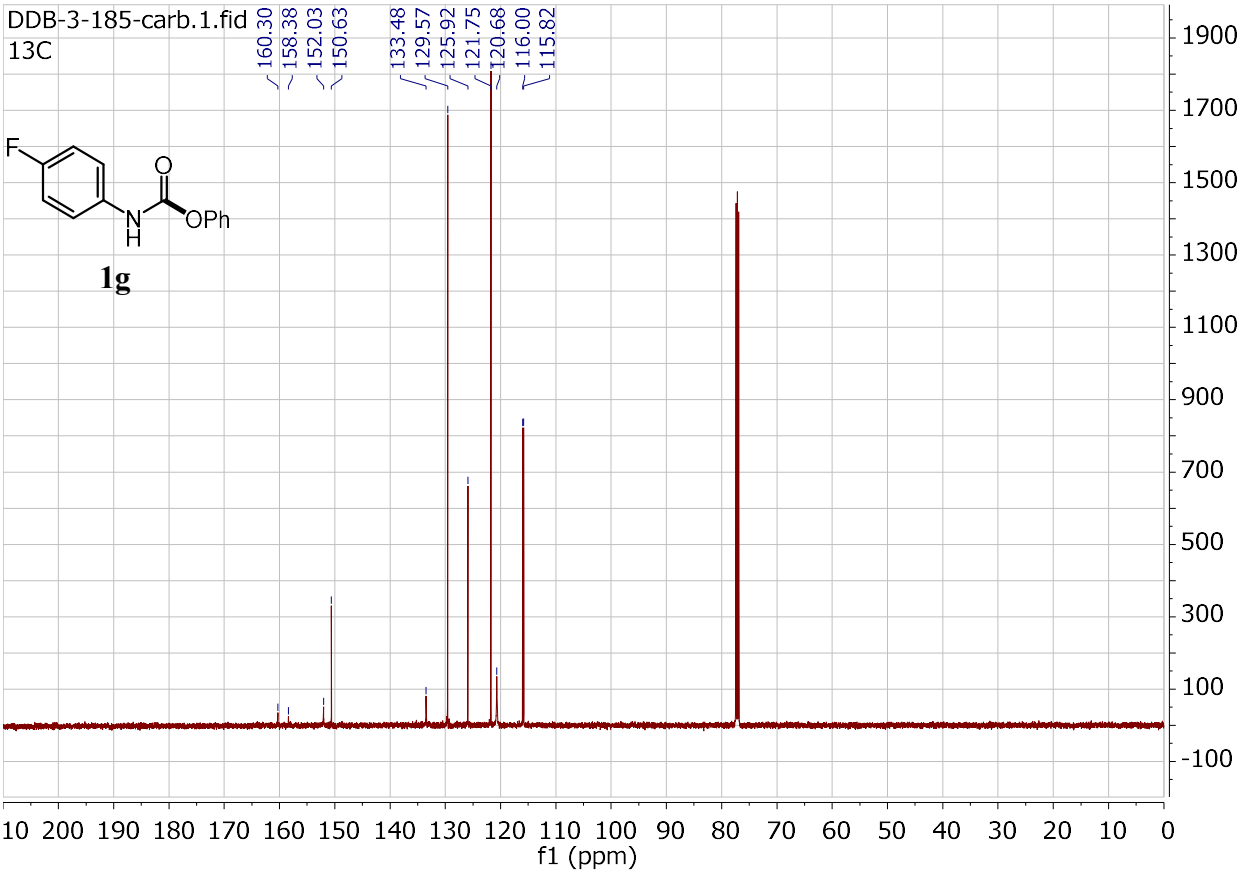
DDB-3-185-carb.1.fid
13C
F
O
N
H
OPh
1g
160.30 158.38 152.03 150.63 133.48 129.57 125.92 121.75 120.68 116.00 115.82
f1 (ppm)

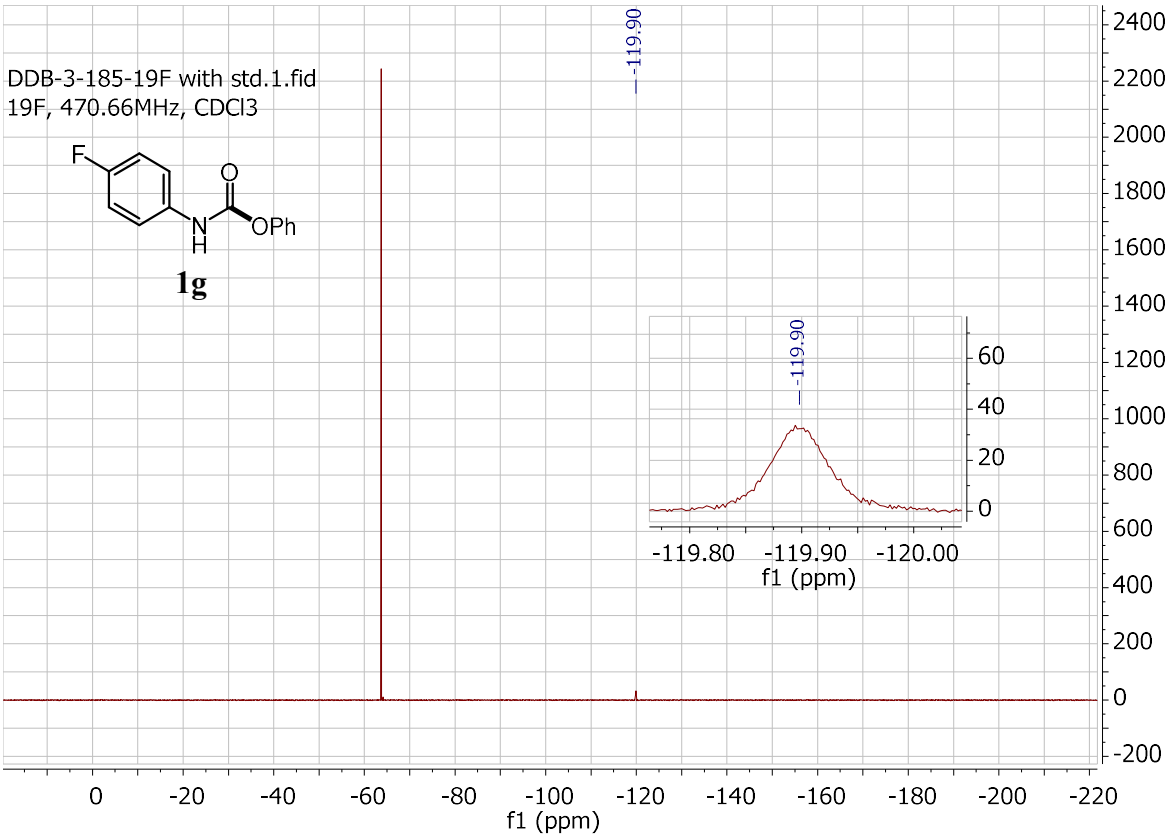
DDB-3-185-19F with std.1.fid
19F, 470.66MHz, CDCl3
F
O
N
H
OPh
1g
-119.90
-119.90
-119.80
-119.90
-120.00
f1 (ppm)
f1 (ppm)

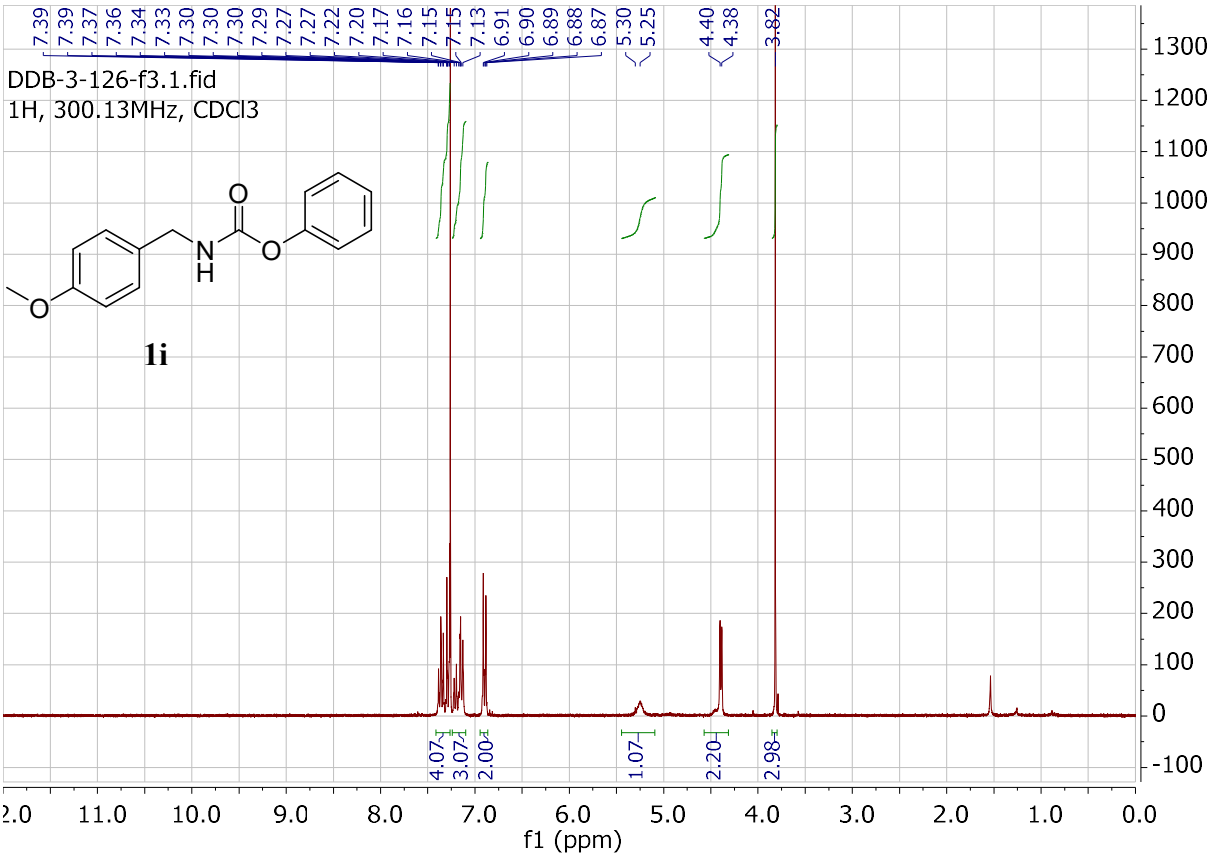
DDB-3-126-f3.1.fid
1H, 300.13MHz, CDCl3
7.39 7.39 7.37 7.36 7.34 7.33 7.30 7.30 7.30 7.29 7.27 7.27 7.22 7.20 7.17 7.16 7.15 7.15 7.13 6.91 6.90 6.89 6.88 6.87 5.30 5.25 4.40 4.38 3.82
4.07 3.07 2.00 1.07 2.20 2.98
f1 (ppm)

1i

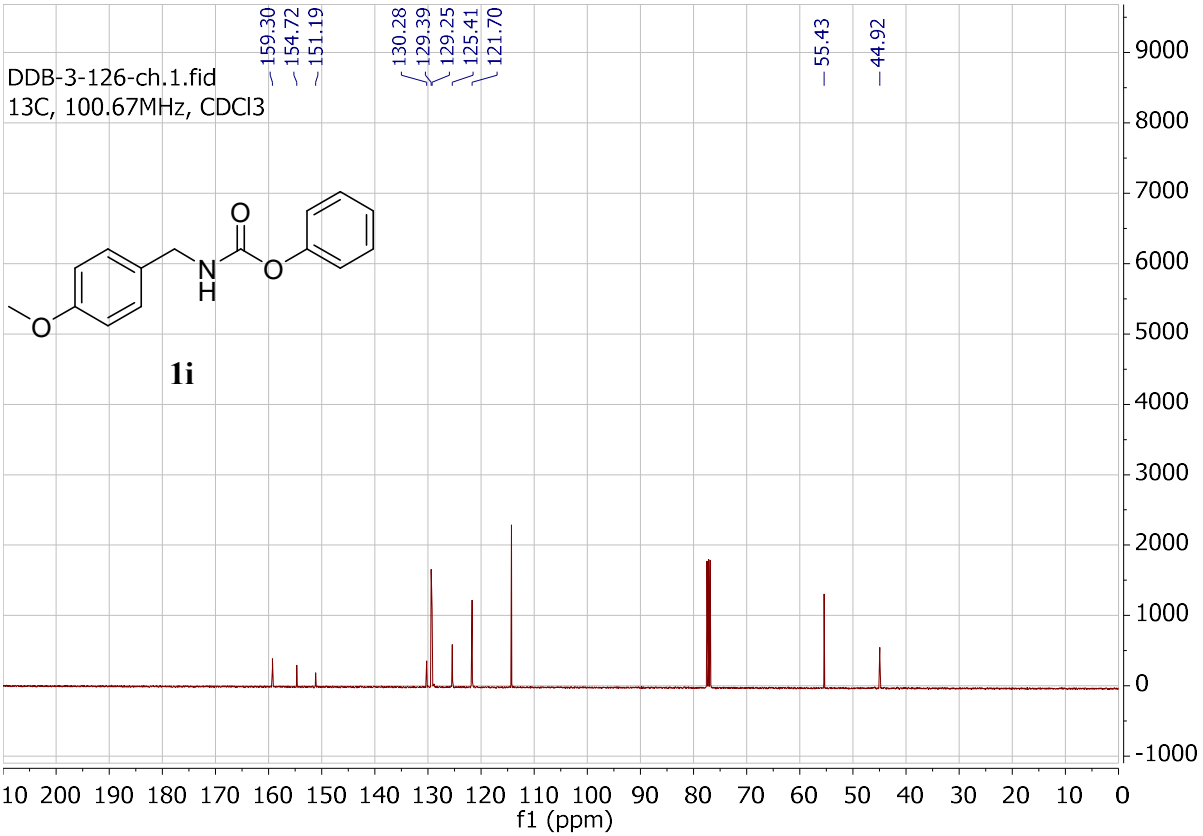
DDB-3-126-ch.1.fid
13C, 100.67MHz, CDCl3
159.30 154.72 151.19 130.28 129.39 129.25 125.41 121.70 55.43 44.92
f1 (ppm)

1i

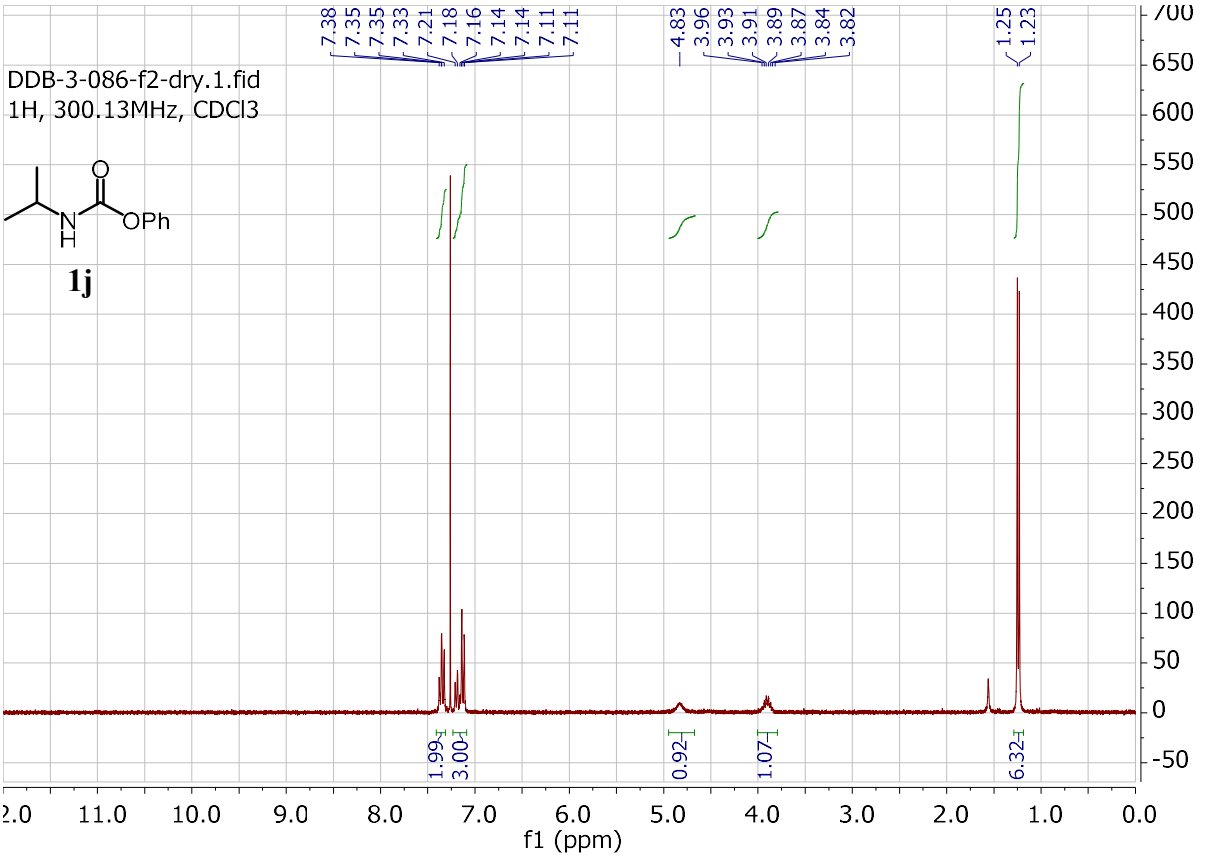
DDB-3-086-f2-dry.1.fid
1H, 300.13MHz, CDCl3
1j
7.38
7.35
7.35
7.33
7.21
7.18
7.16
7.14
7.14
7.11
7.11
4.83
3.96
3.93
3.91
3.89
3.87
3.84
3.82
1.25
1.23
1.99
3.00
0.92
1.07
6.32
f1 (ppm)

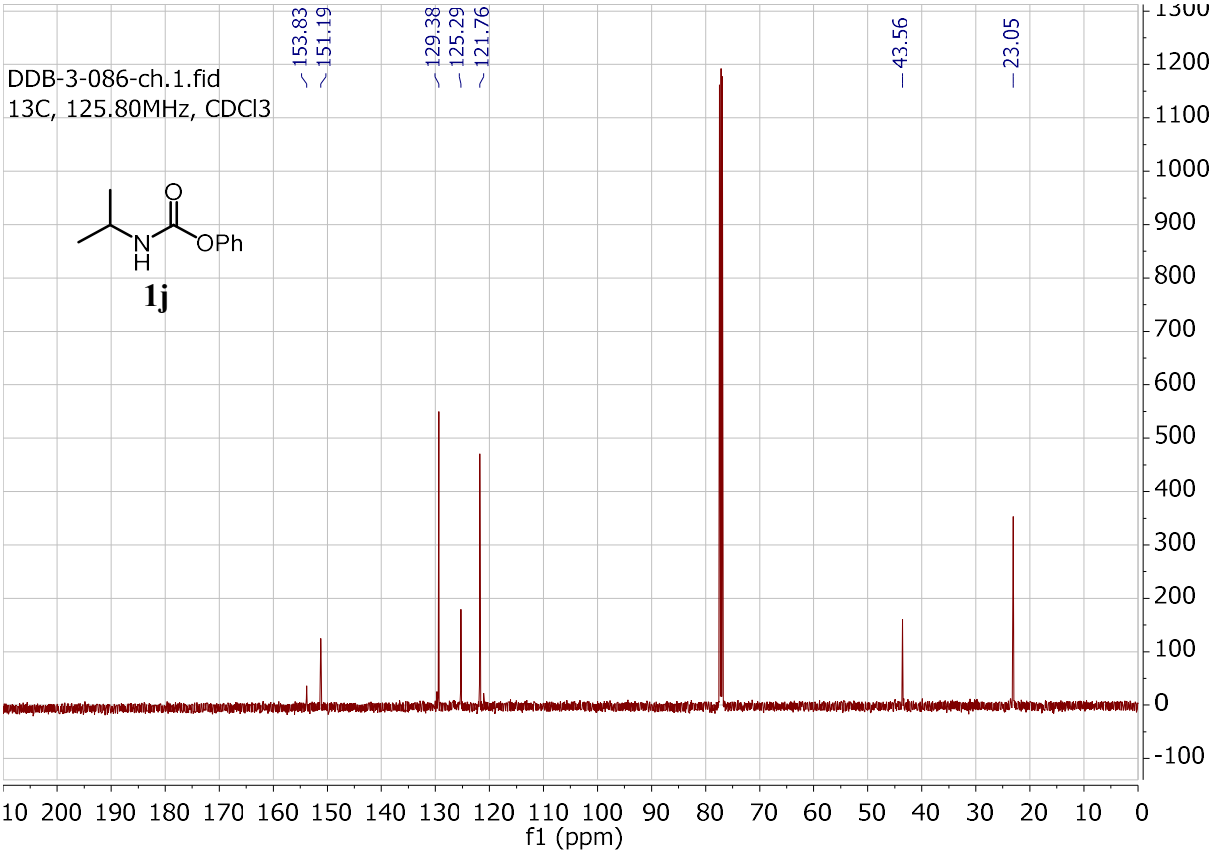
DDB-3-086-ch.1.fid
13C, 125.80MHz, CDCl3
1j
153.83
151.19
129.38
125.29
121.76
43.56
23.05
f1 (ppm)

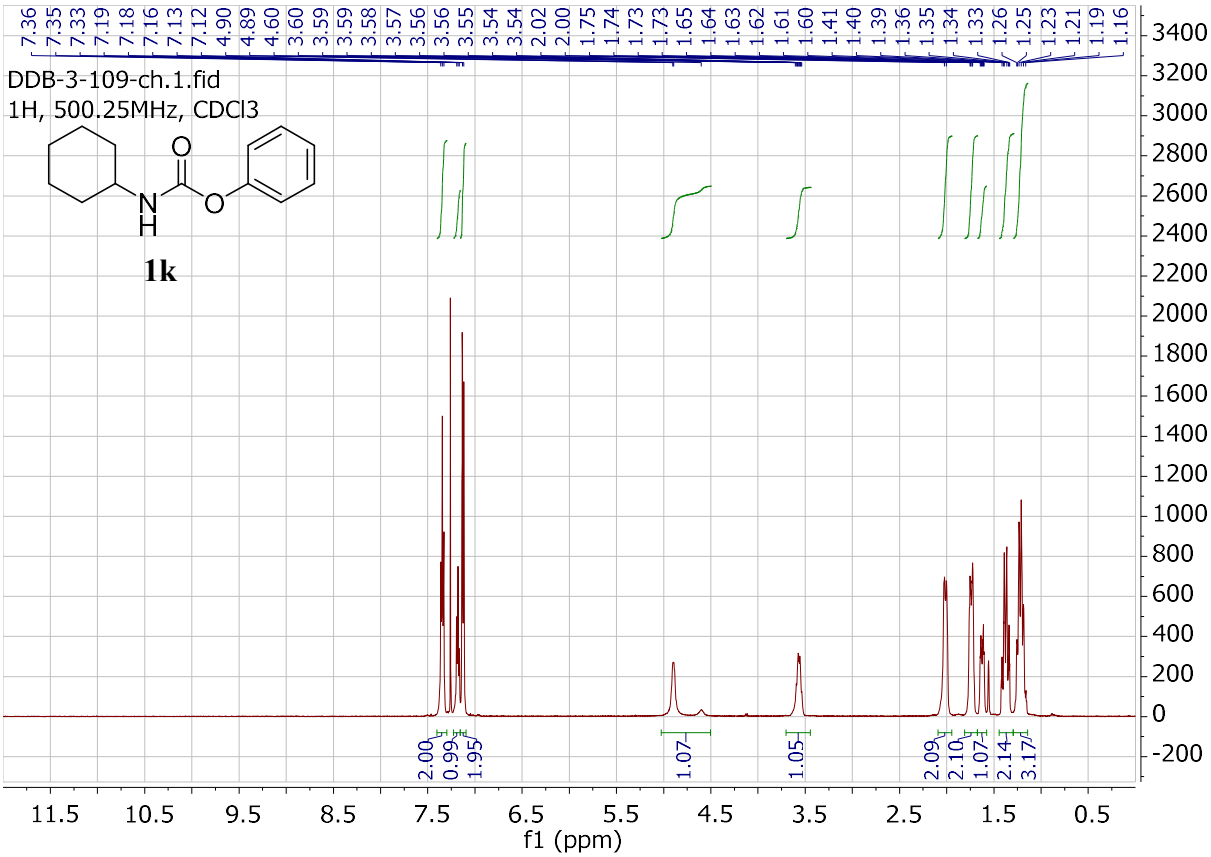
DDB-3-109-ch.1.fid
1H, 500.25MHz, CDCl3
1k
f1 (ppm)

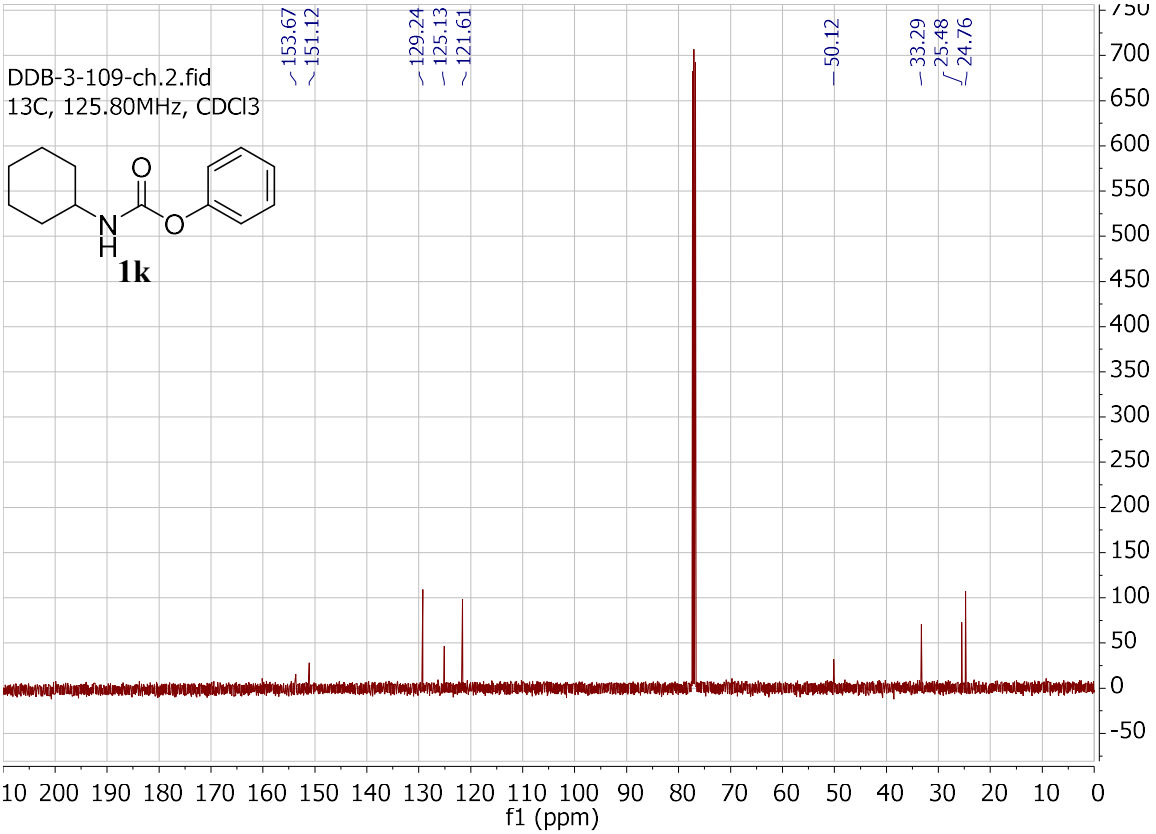
DDB-3-109-ch.2.fid
13C, 125.80MHz, CDCl3
1k
f1 (ppm)

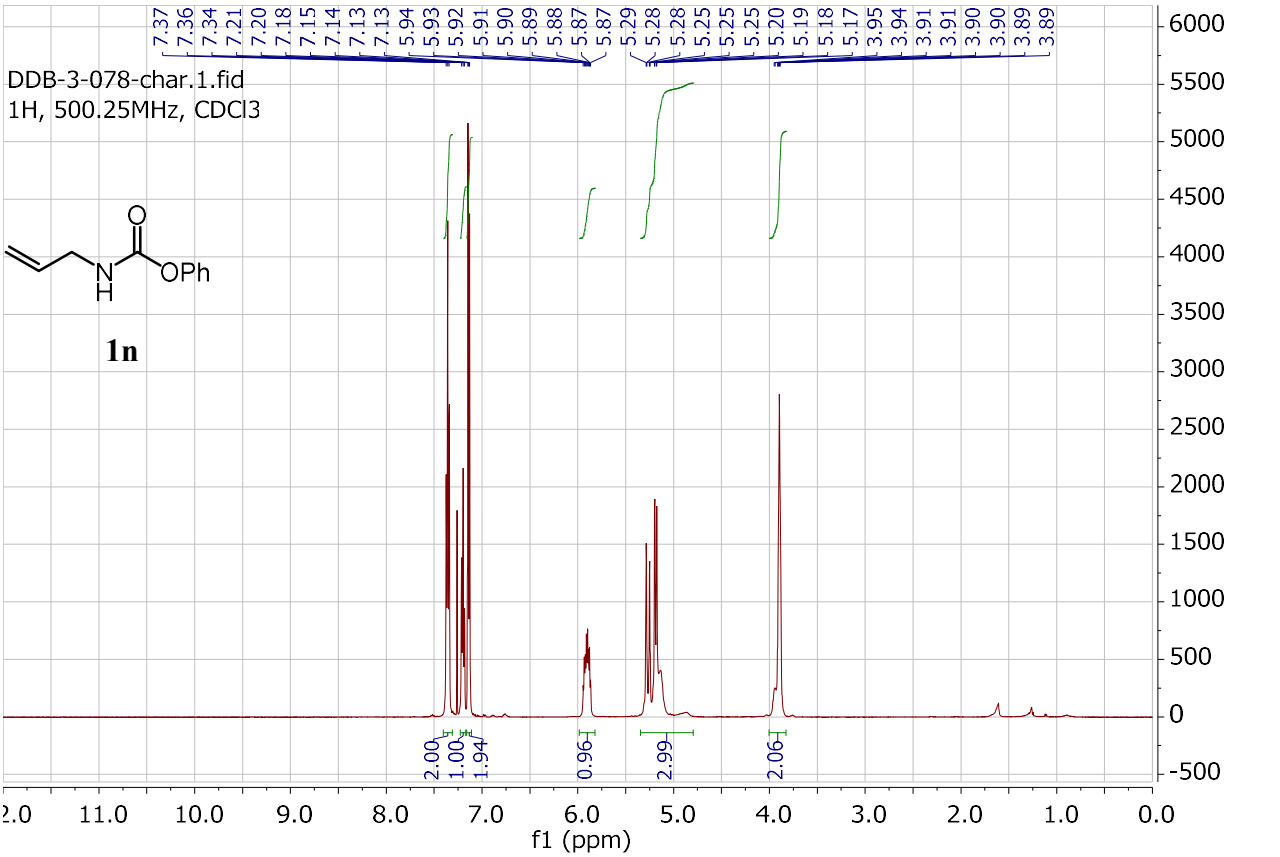
DDB-3-078-char.1.fid
1H, 500.25MHz, CDCl3
1n
f1 (ppm)

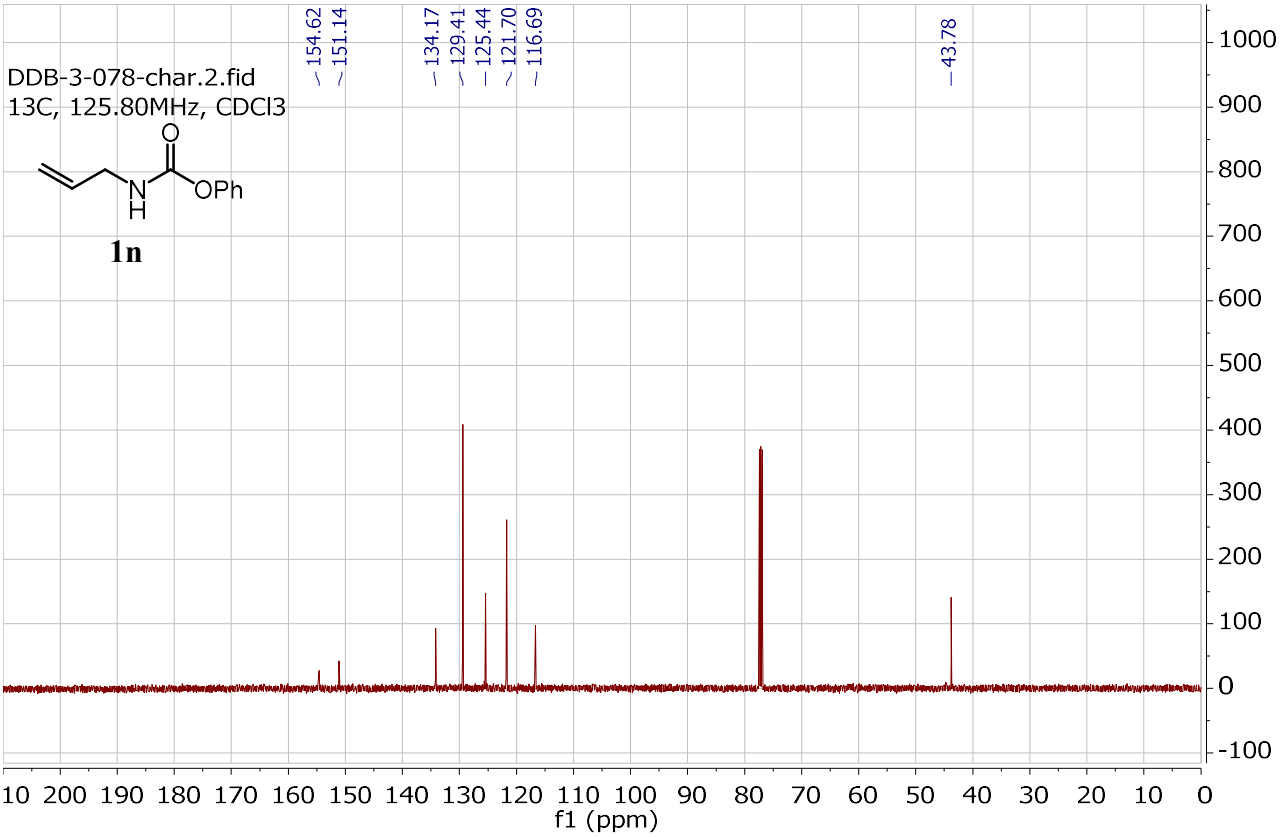
DDB-3-078-char.2.fid
13C, 125.80MHz, CDCl3
1n
f1 (ppm)

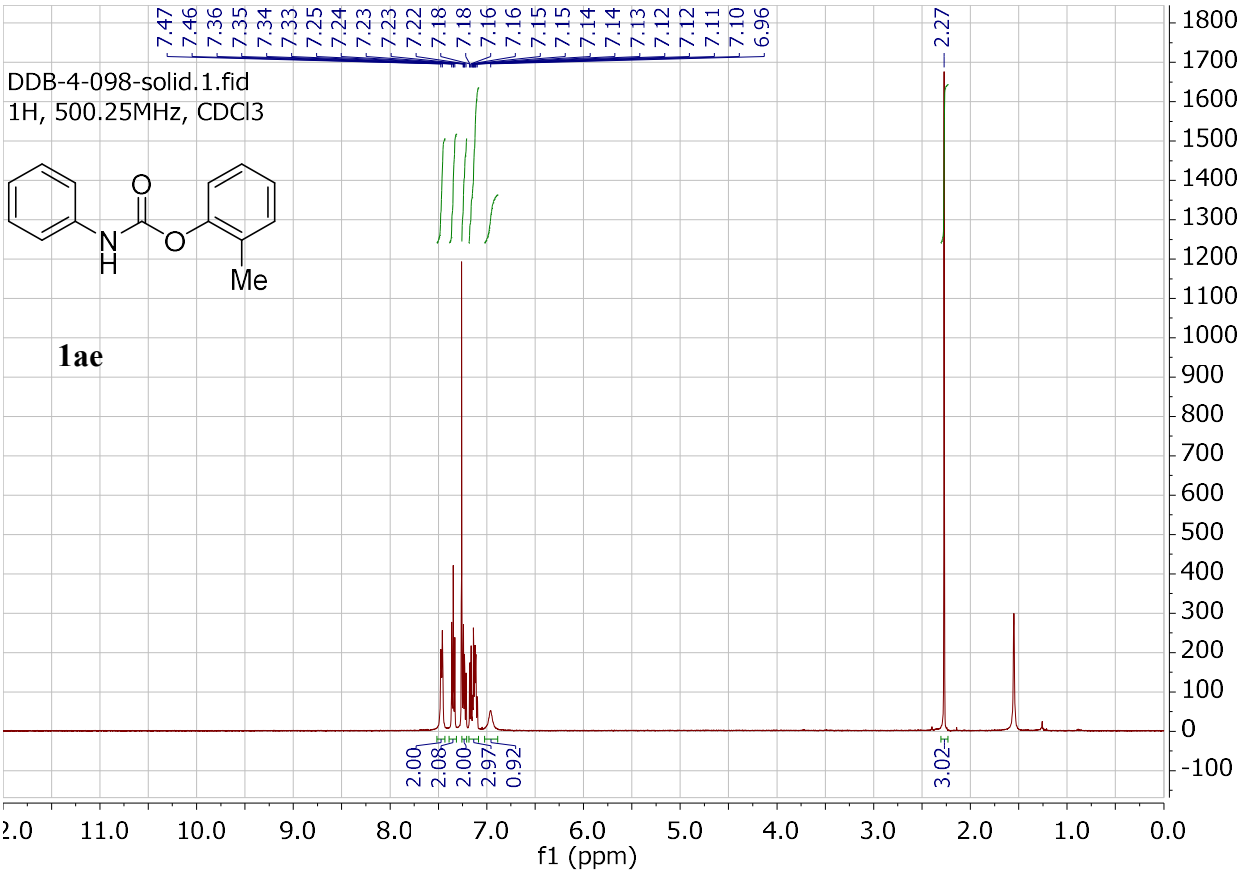
DDB-4-098-solid.1.fid
1H, 500.25MHz, CDCl3
1ae
f1 (ppm)

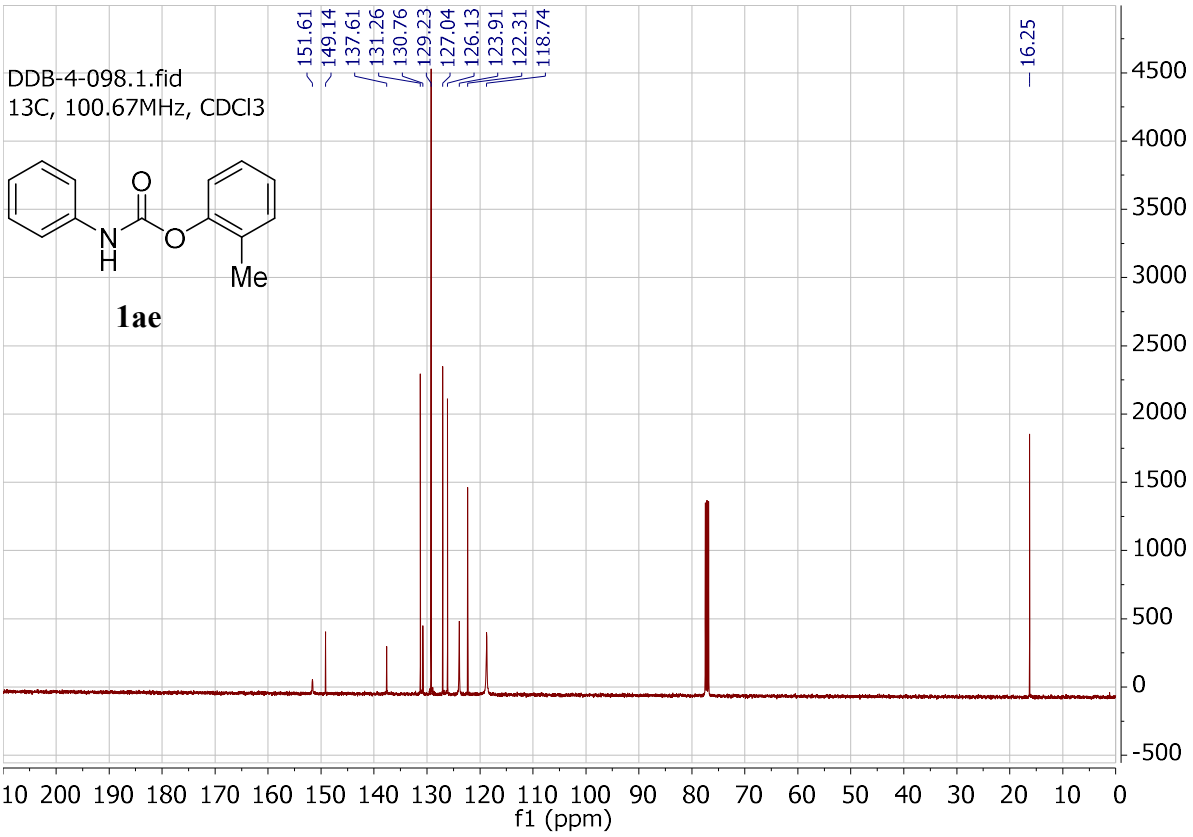
DDB-4-098.1.fid
13C, 100.67MHz, CDCl3
1ae
f1 (ppm)

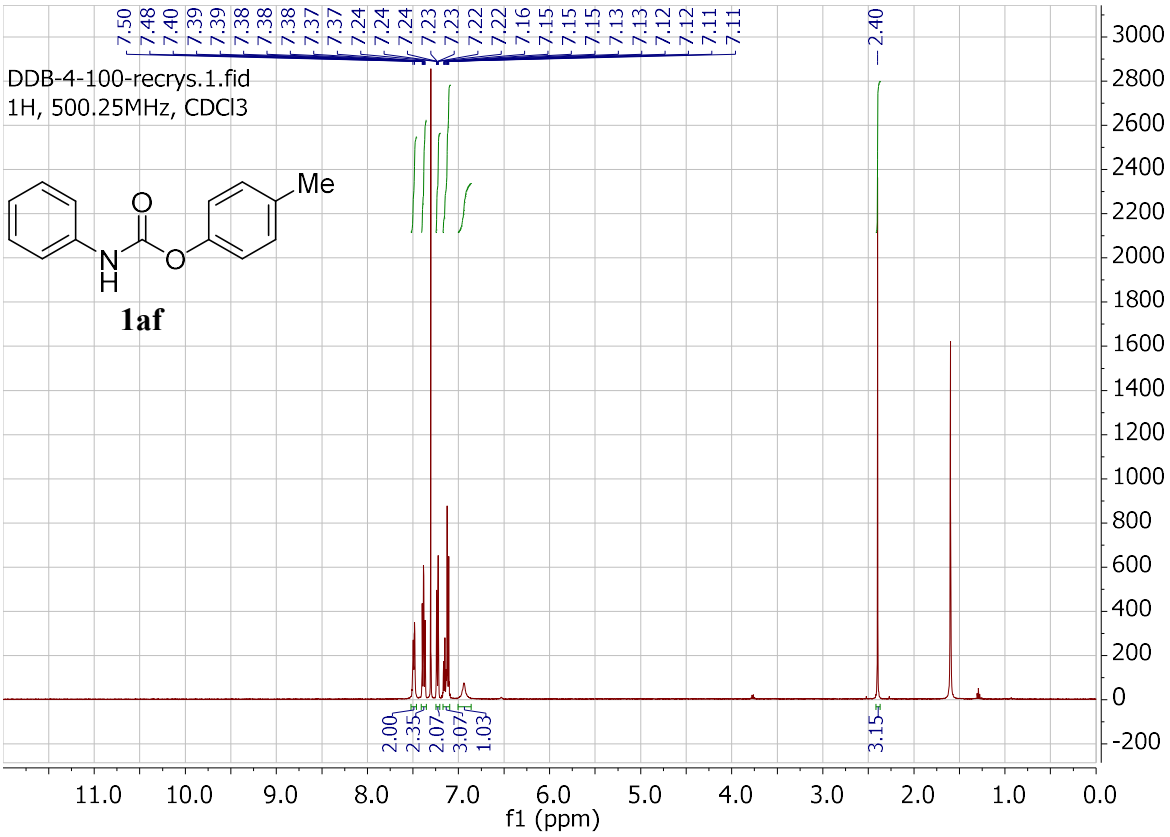
DDB-4-100-recrys.1.fid
1H, 500.25MHz, CDCl3
Me
O
N
H
O
1af
7.50 7.48 7.40 7.39 7.39 7.38 7.38 7.38 7.37 7.37 7.24 7.24 7.24 7.23 7.23 7.22 7.22 7.16 7.15 7.15 7.15 7.13 7.13 7.12 7.12 7.11 7.11
2.40
2.00 2.35 2.07 3.07 1.03
3.15
f1 (ppm)

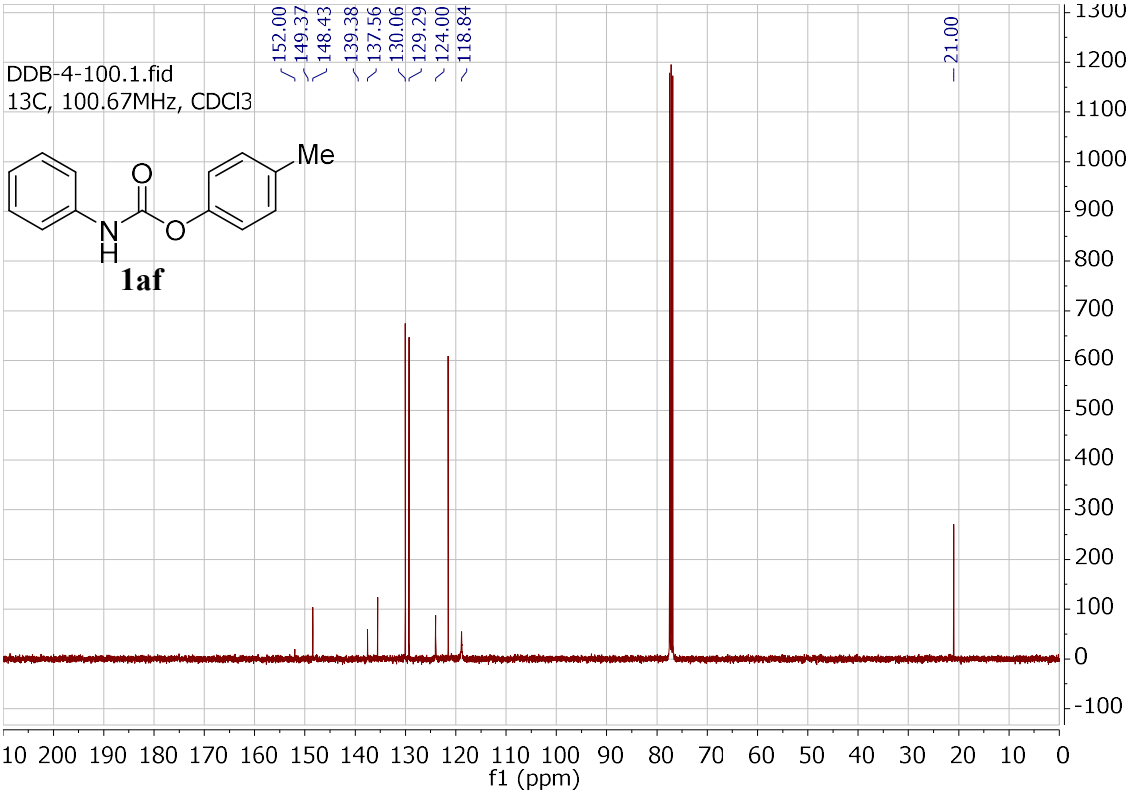
DDB-4-100.1.fid
13C, 100.67MHz, CDCl3
Me
O
N
H
O
1af
152.00 149.37 148.43 139.38 137.56 130.06 129.29 124.00 118.84
21.00
f1 (ppm)

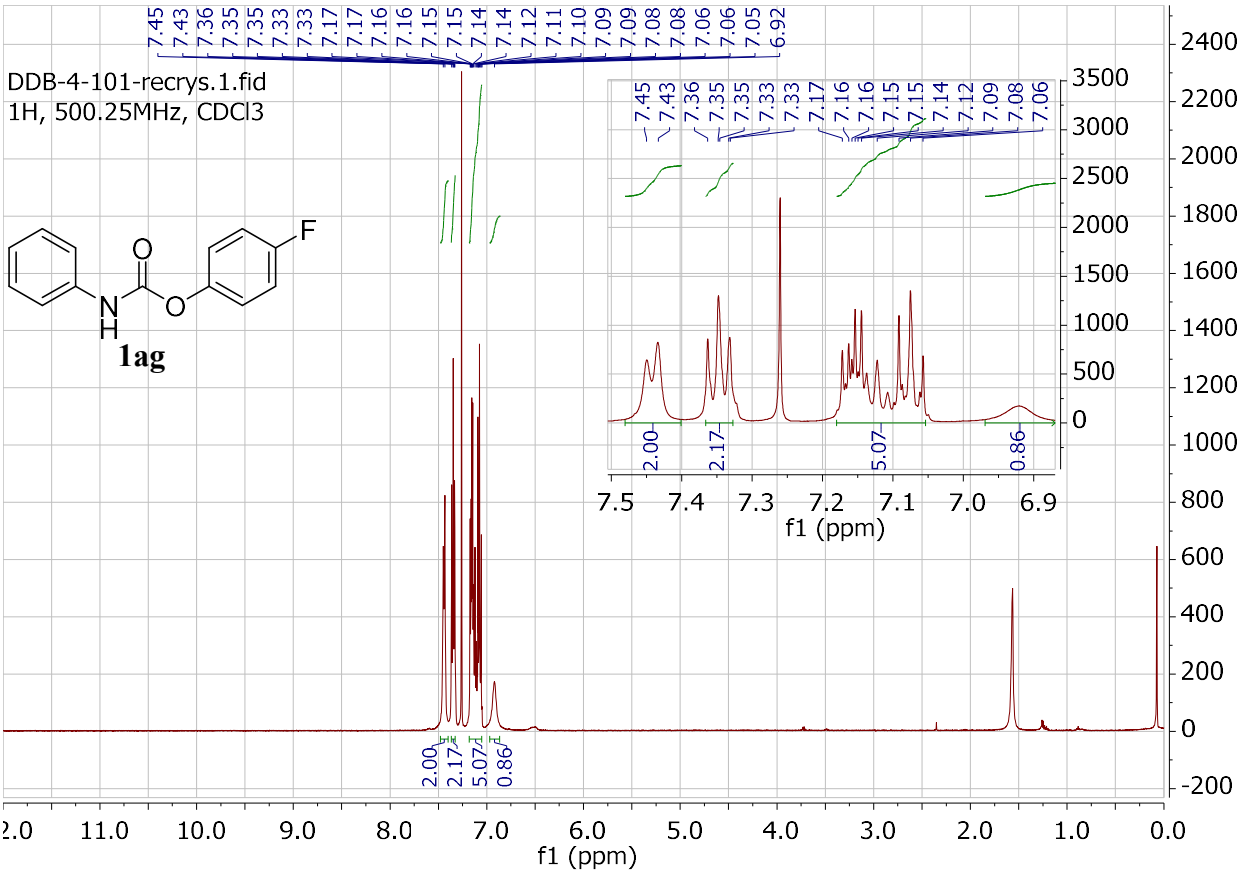
DDB-4-101-recrys.1.fid
1H, 500.25MHz, CDCl3
1ag
f1 (ppm)

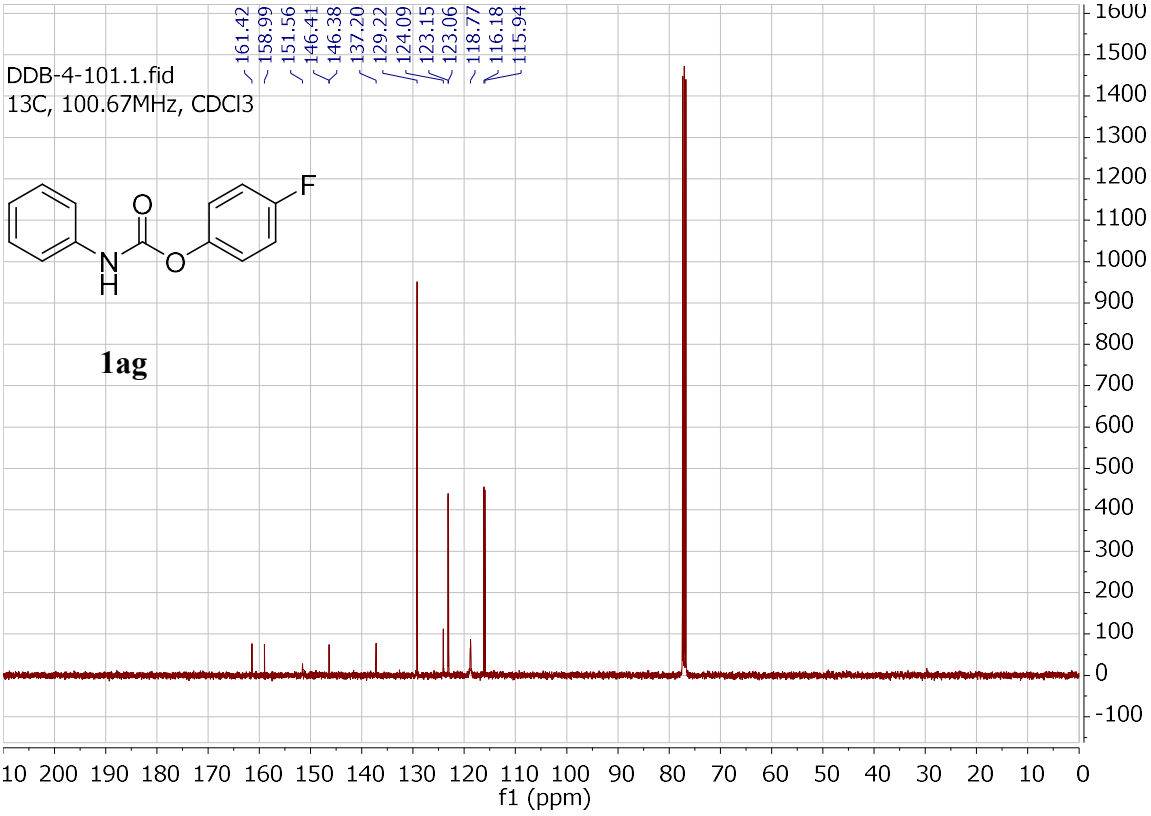
DDB-4-101.1.fid
13C, 100.67MHz, CDCl3
1ag
f1 (ppm)

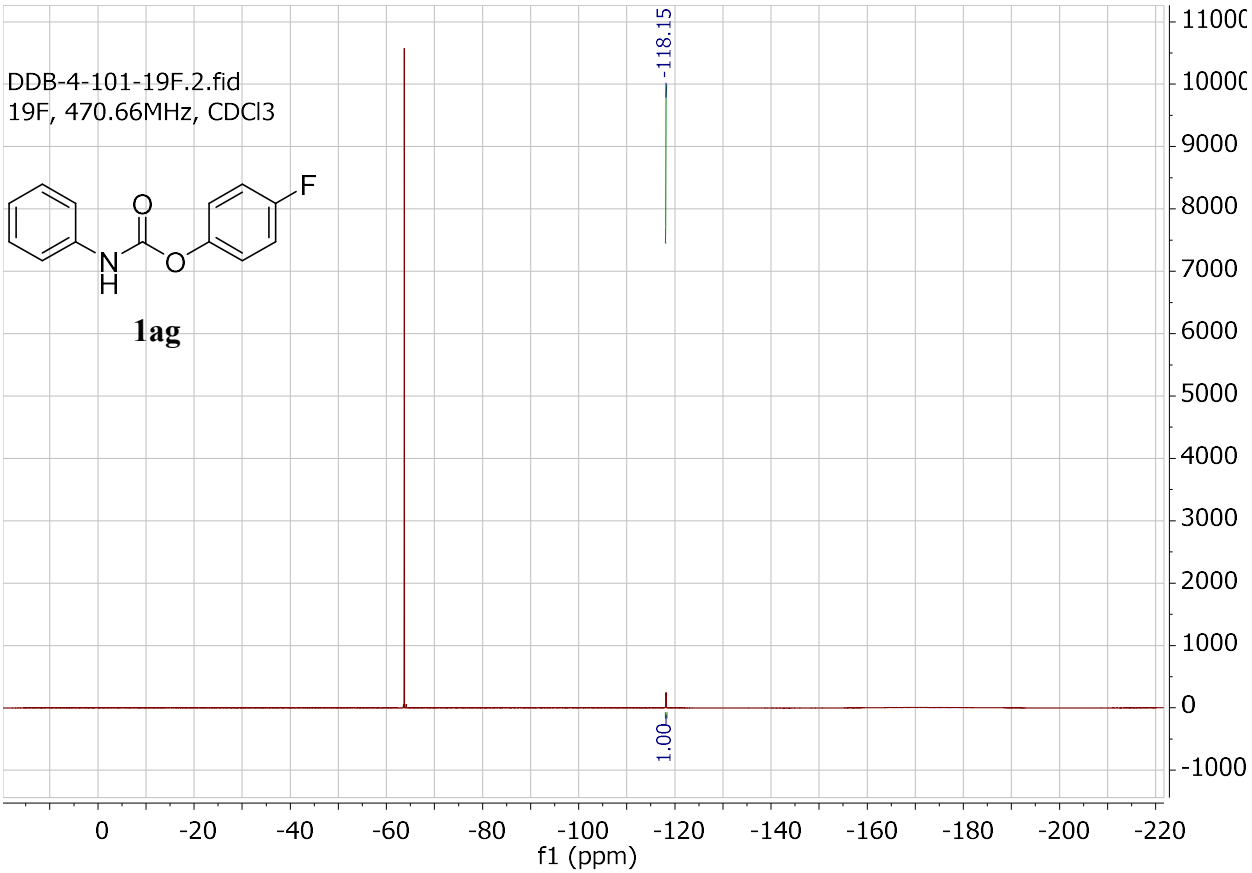
DDB-4-101-19F.2.fid
19F, 470.66MHz, CDCl3
F
O
N
H
O
1ag
118.15
1.00
11000
10000
9000
8000
7000
6000
5000
4000
3000
2000
1000
0
-1000
0
-20
-40
-60
-80
-100
-120
-140
-160
-180
-200
-220
f1 (ppm)

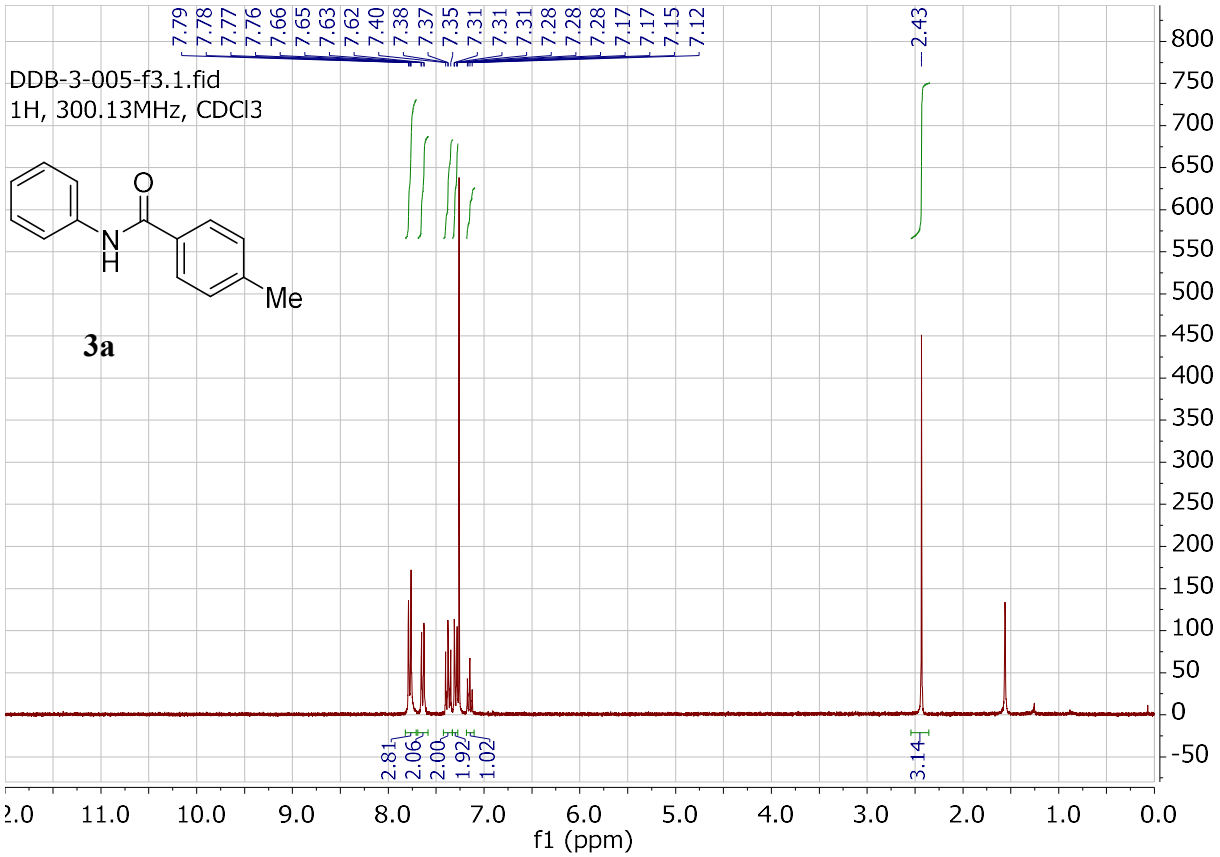
7.79
7.78
7.77
7.76
7.66
7.65
7.63
7.62
7.40
7.38
7.37
7.35
7.31
7.31
7.31
7.28
7.28
7.28
7.17
7.17
7.15
7.12
2.43
DDB-3-005-f3.1.fid
1H, 300.13MHz, CDCl3
O
N
H
Me
3a
2.81
2.06
2.00
1.92
1.02
3.14
f1 (ppm)

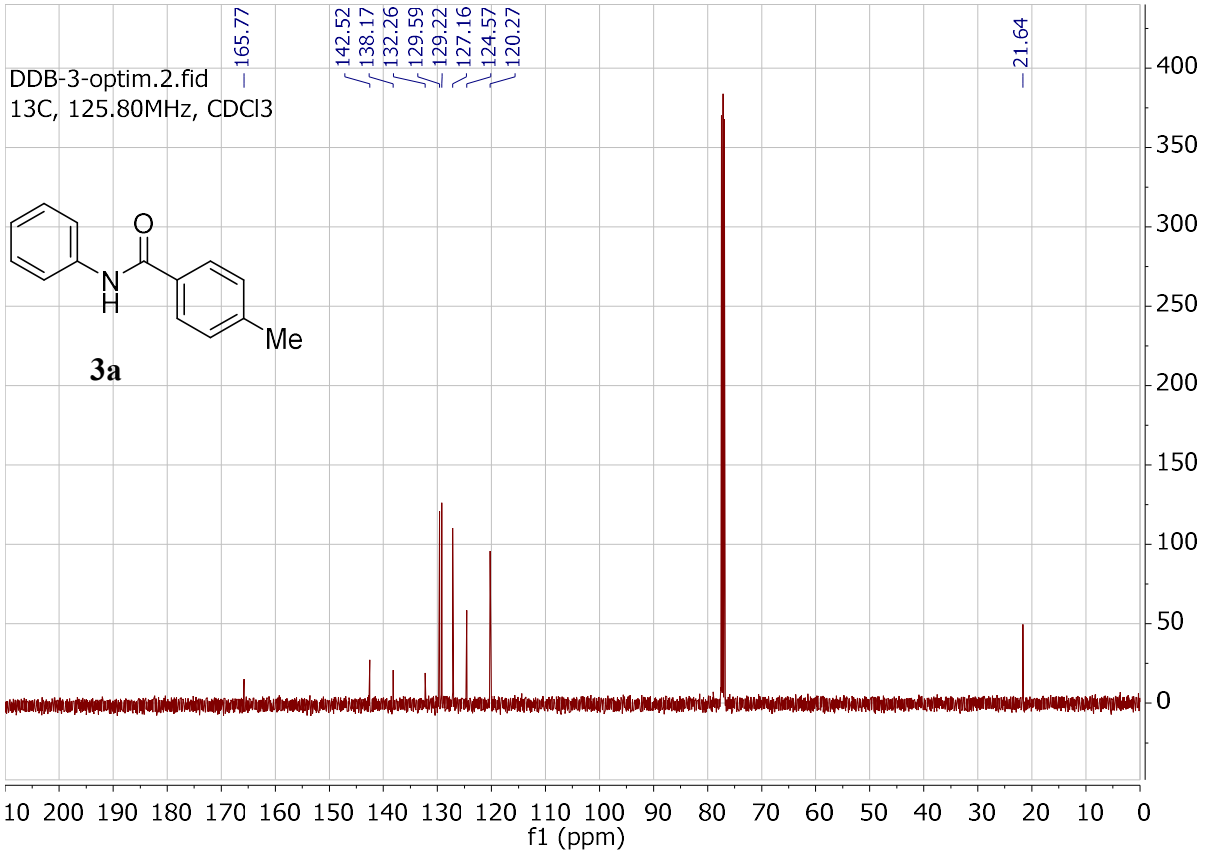
165.77
142.52
138.17
132.26
129.59
129.22
127.16
124.57
120.27
21.64
DDB-3-optim.2.fid
13C, 125.80MHz, CDCl3
O
N
H
Me
3a
f1 (ppm)

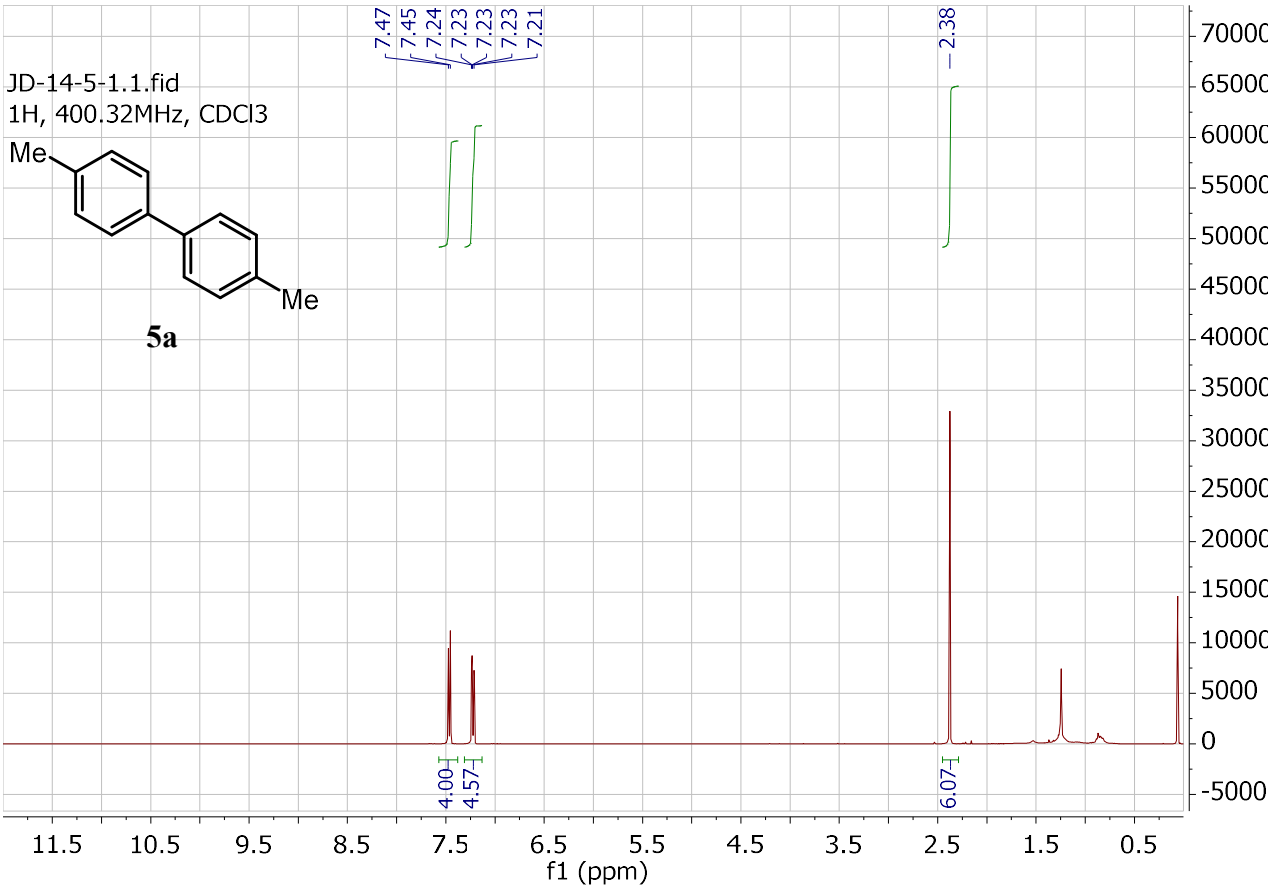
JD-14-5-1.1.fid
1H, 400.32MHz, CDCl3
Me
Me
5a
7.47
7.45
7.24
7.23
7.23
7.23
7.21
2.38
4.00
4.57
6.07
f1 (ppm)

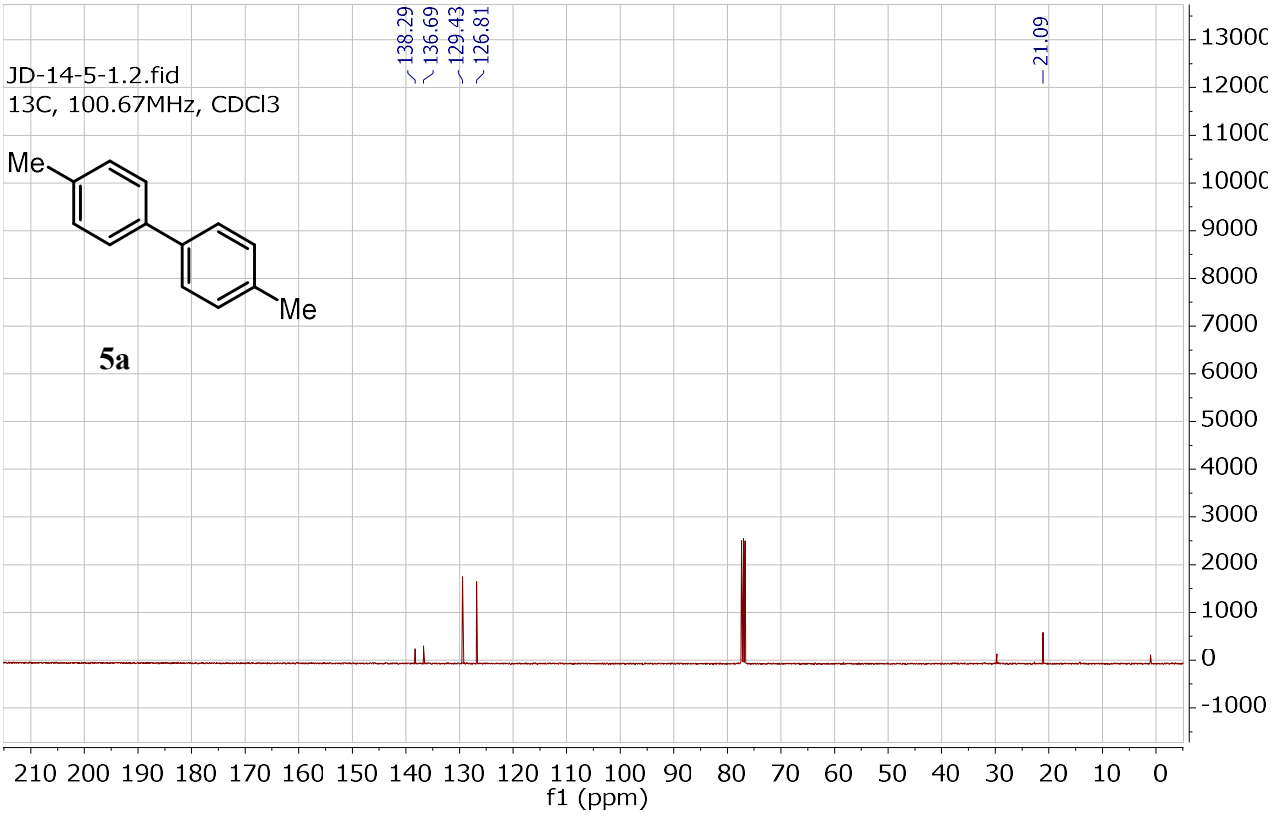
JD-14-5-1.2.fid
13C, 100.67MHz, CDCl3
Me
Me
5a
138.29
136.69
129.43
126.81
21.09
f1 (ppm)

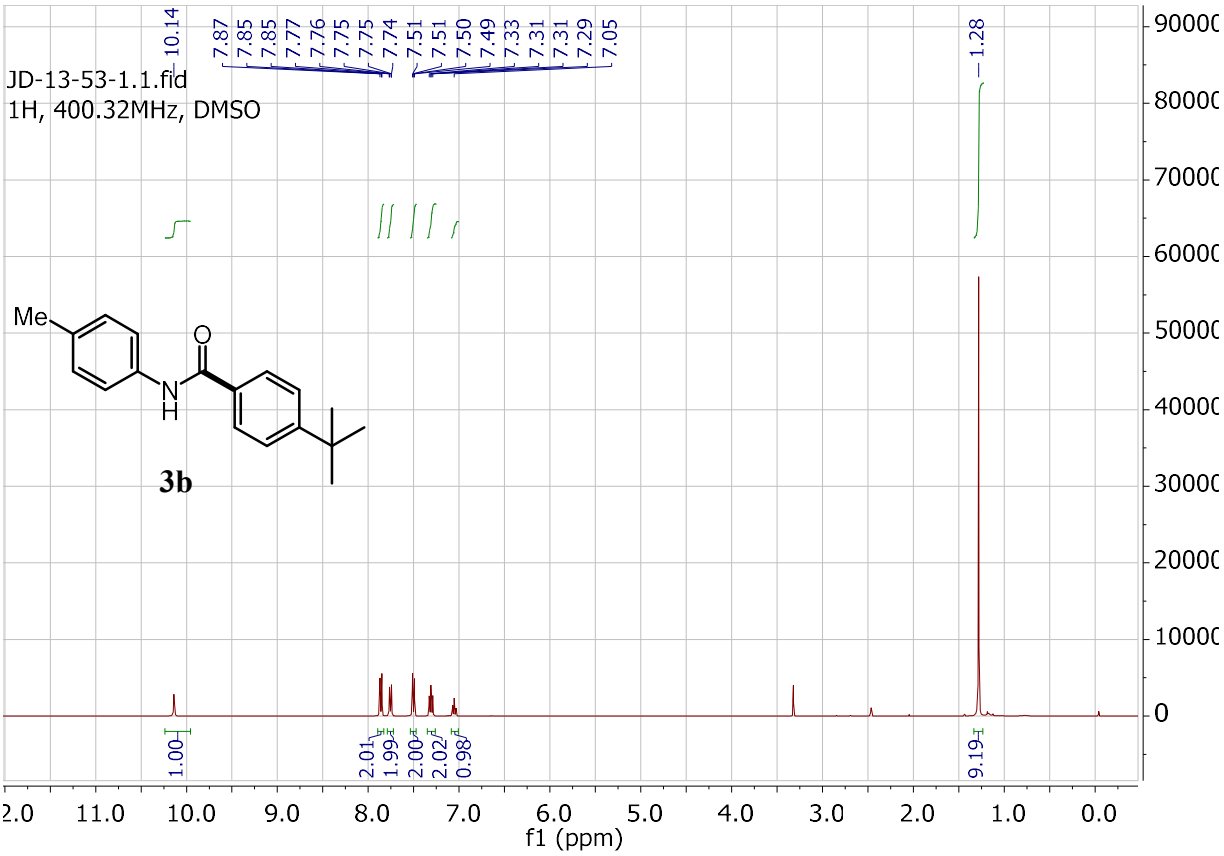
JD-13-53-1.1.fid
1H, 400.32MHz, DMSO
10.14
7.87
7.85
7.85
7.77
7.76
7.75
7.75
7.74
7.51
7.51
7.50
7.49
7.33
7.31
7.31
7.29
7.05
1.28
Me
O
N
H
3b
1.00
2.01
1.99
2.00
2.02
0.98
9.19
f1 (ppm)

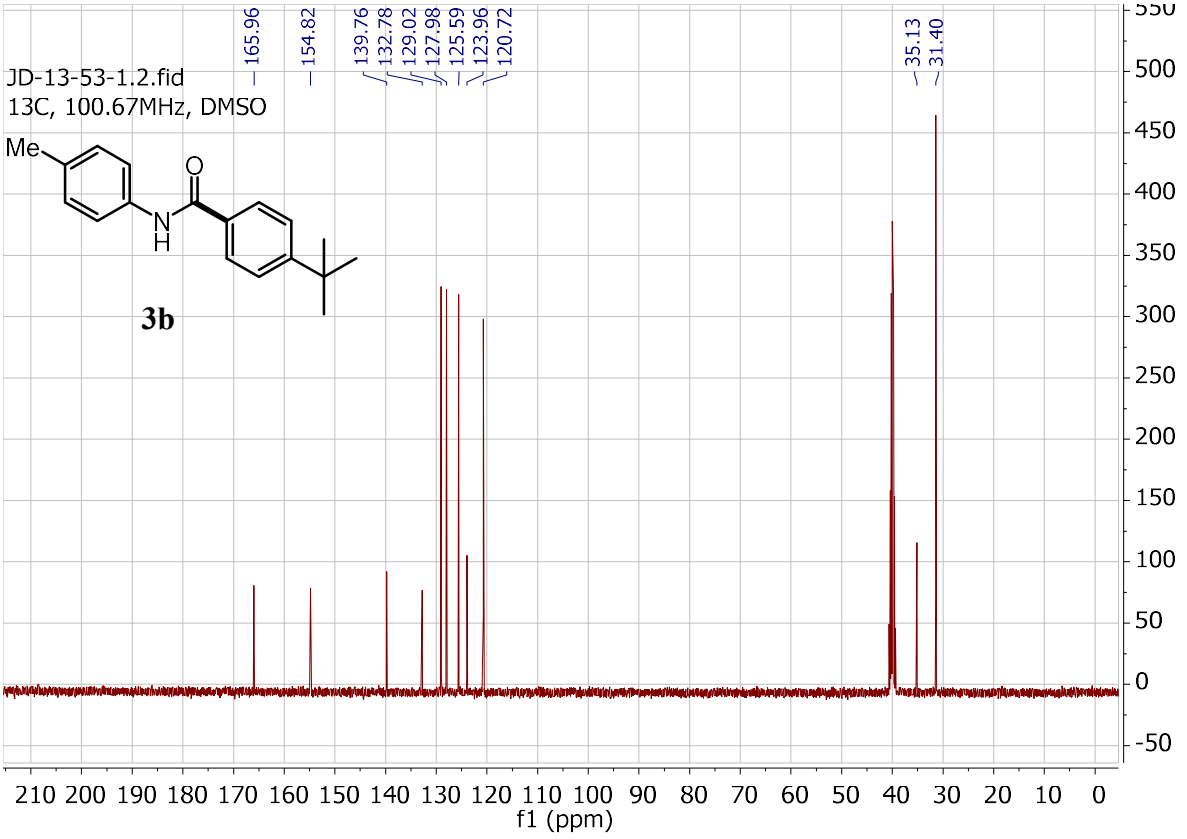
JD-13-53-1.2.fid
13C, 100.67MHz, DMSO
165.96
154.82
139.76
132.78
129.02
127.98
125.59
123.96
120.72
35.13
31.40
Me
O
N
H
3b
f1 (ppm)

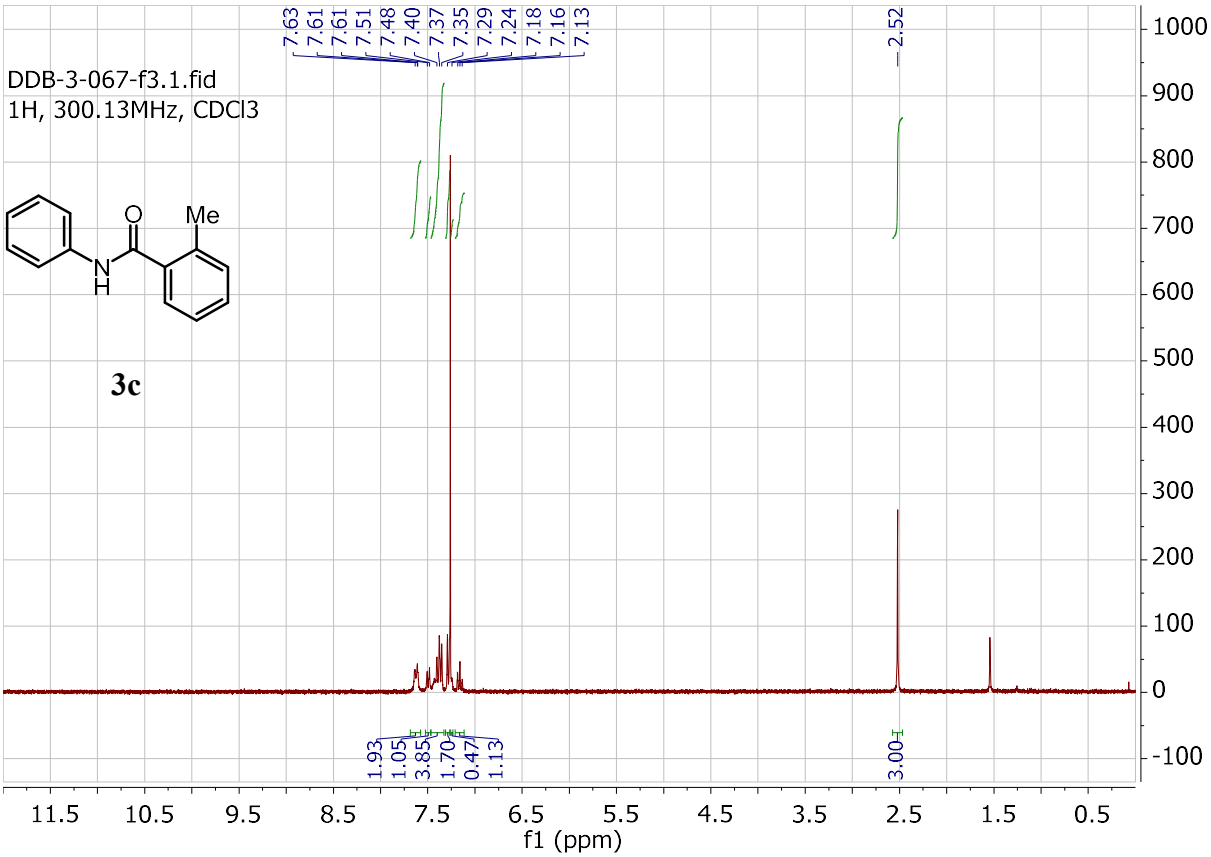
DDB-3-067-f3.1.fid
1H, 300.13MHz, CDCl3
3c
7.63
7.61
7.61
7.51
7.48
7.40
7.37
7.35
7.29
7.24
7.18
7.16
7.13
2.52
1.93
1.05
3.85
1.70
0.47
1.13
3.00
f1 (ppm)

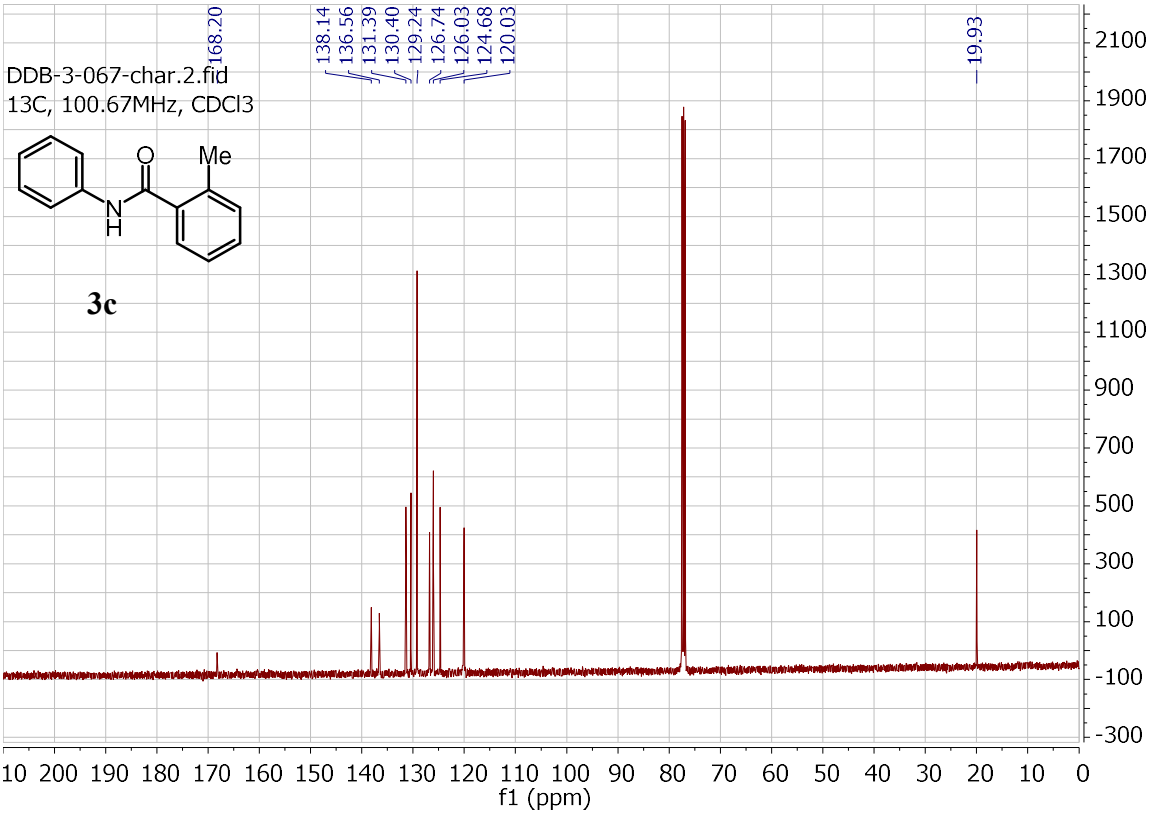
DDB-3-067-char.2.fid
13C, 100.67MHz, CDCl3
3c
168.20
138.14
136.56
131.39
130.40
129.24
126.74
126.03
124.68
120.03
19.93
f1 (ppm)

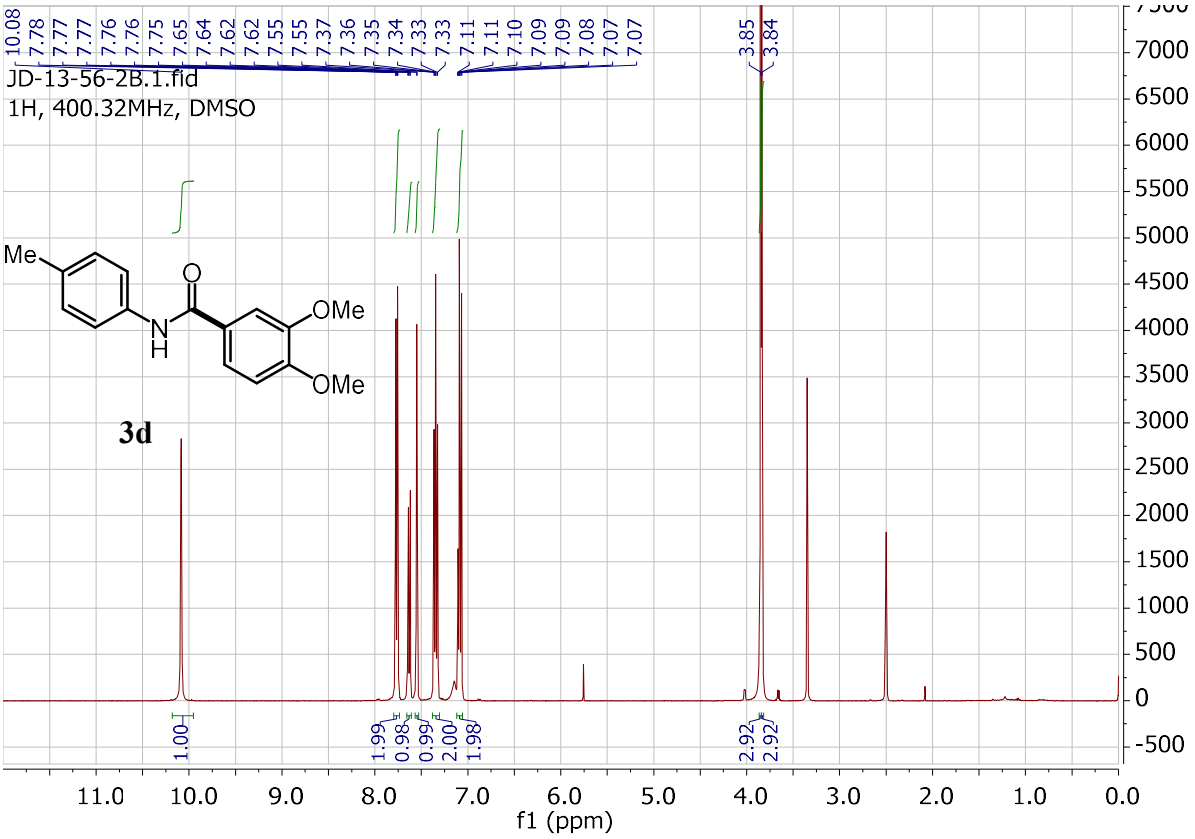
JD-13-56-2B.1.fid
1H, 400.32MHz, DMSO
10.08
7.78
7.77
7.77
7.76
7.76
7.75
7.65
7.64
7.62
7.62
7.55
7.55
7.37
7.36
7.35
7.34
7.33
7.33
7.11
7.10
7.09
7.09
7.08
7.07
7.07
3.85
3.84
Me
O
N
H
OMe
OMe
3d
1.00
1.99
0.98
0.99
2.00
1.98
2.92
2.92
f1 (ppm)

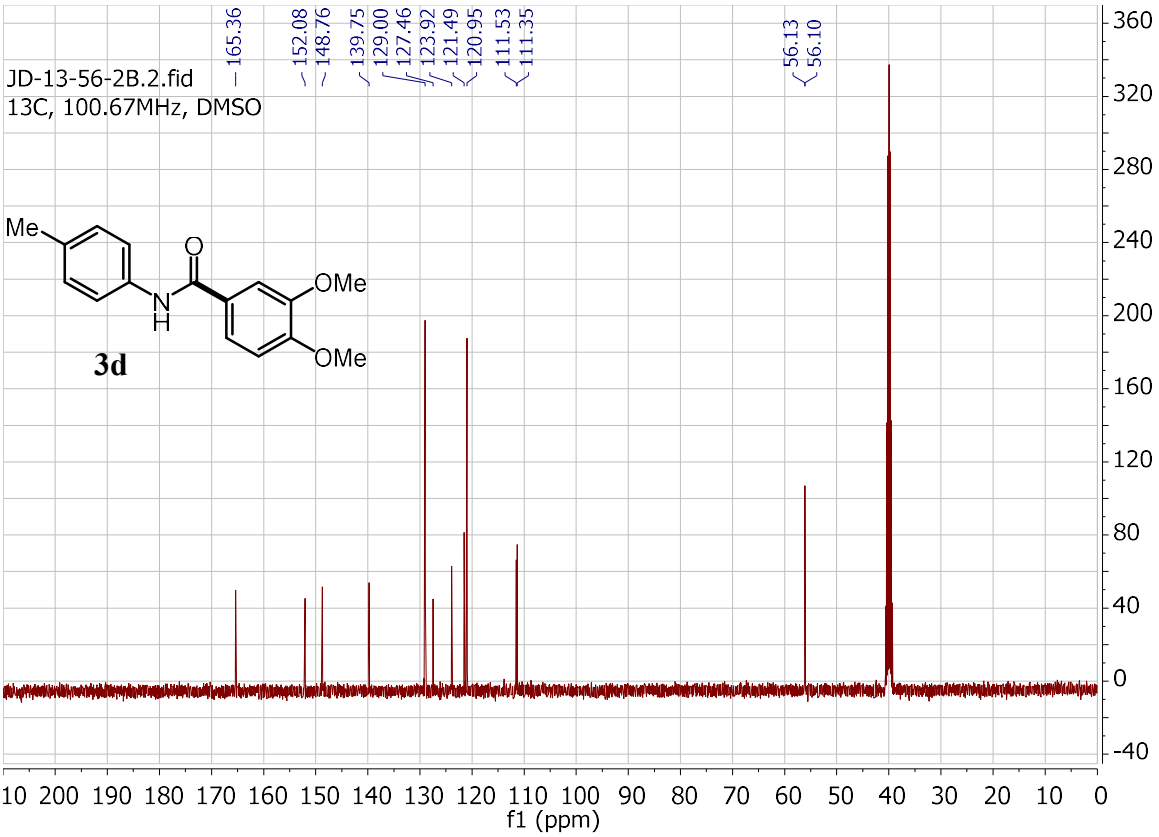
JD-13-56-2B.2.fid
13C, 100.67MHz, DMSO
165.36
152.08
148.76
139.75
129.00
127.46
123.92
121.49
120.95
111.53
111.35
56.13
56.10
Me
O
N
H
OMe
OMe
3d
f1 (ppm)

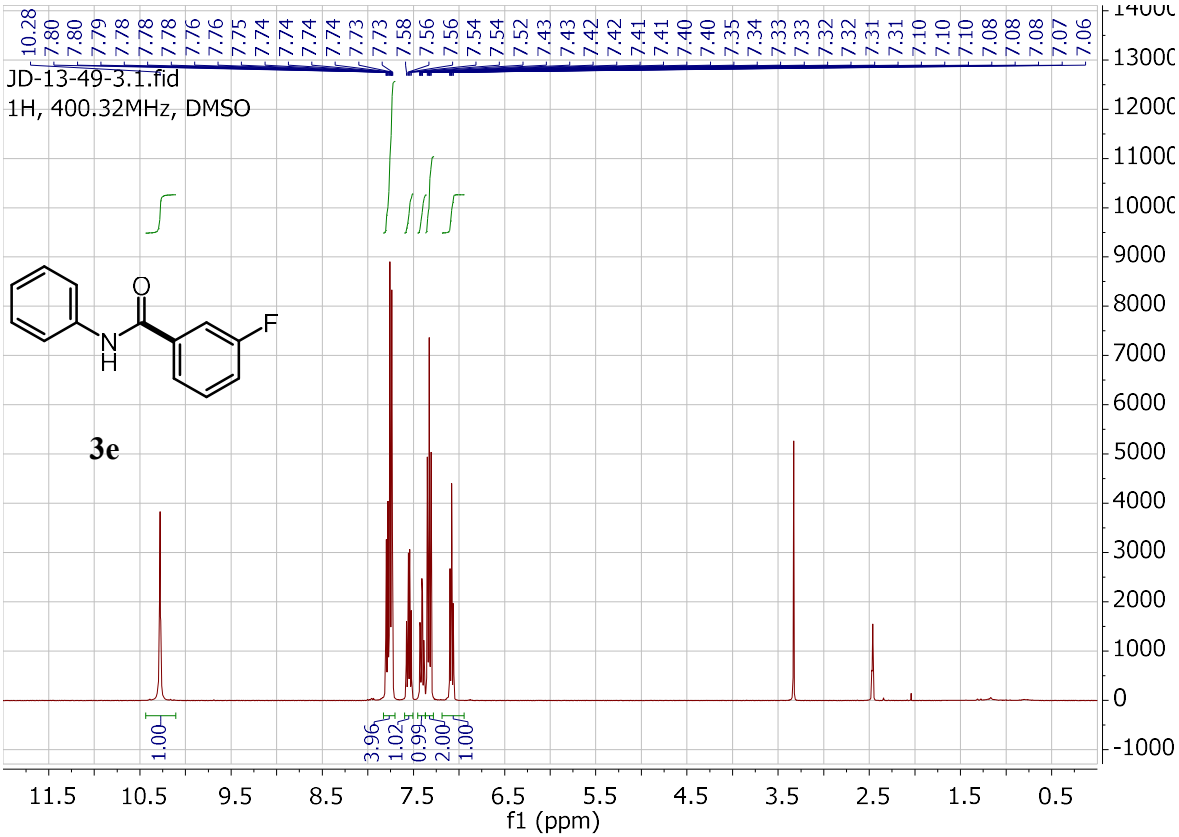
JD-13-49-3.1.fid
1H, 400.32MHz, DMSO
3e
f1 (ppm)

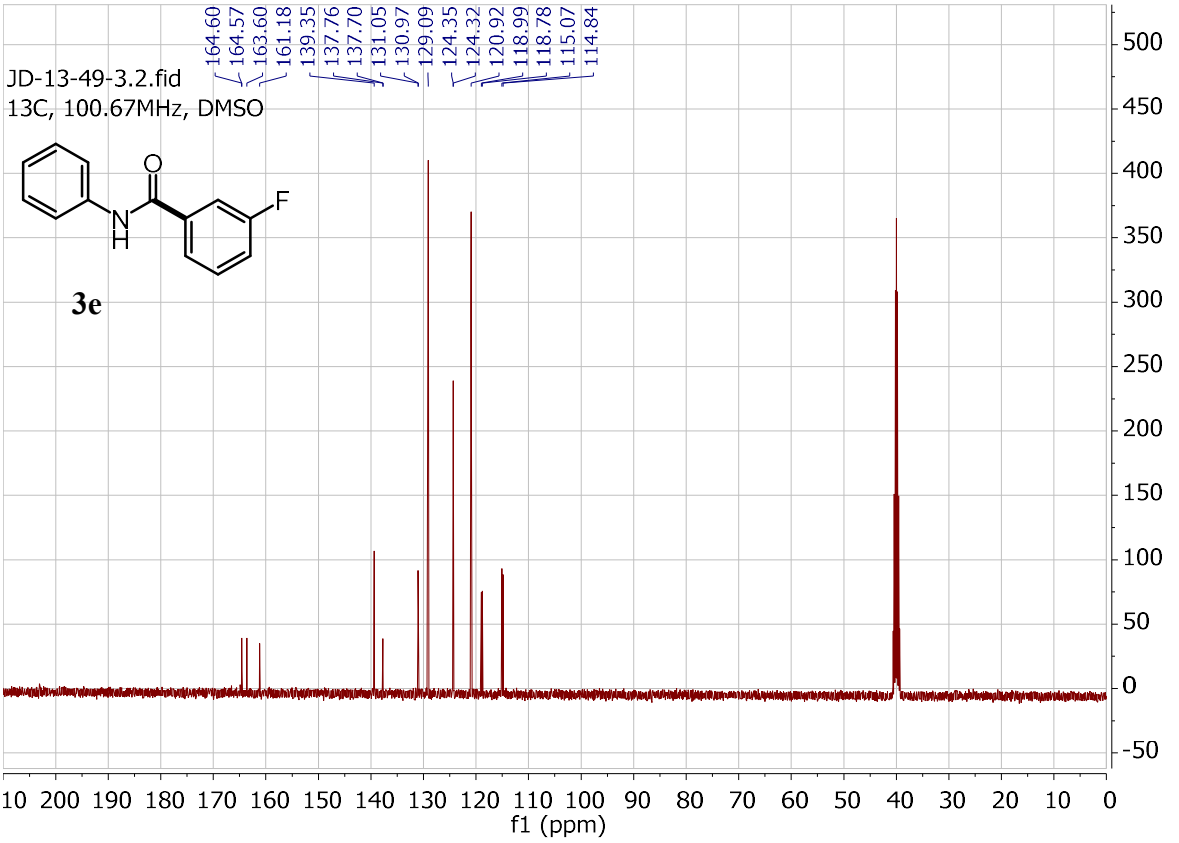
JD-13-49-3.2.fid
13C, 100.67MHz, DMSO
3e
f1 (ppm)

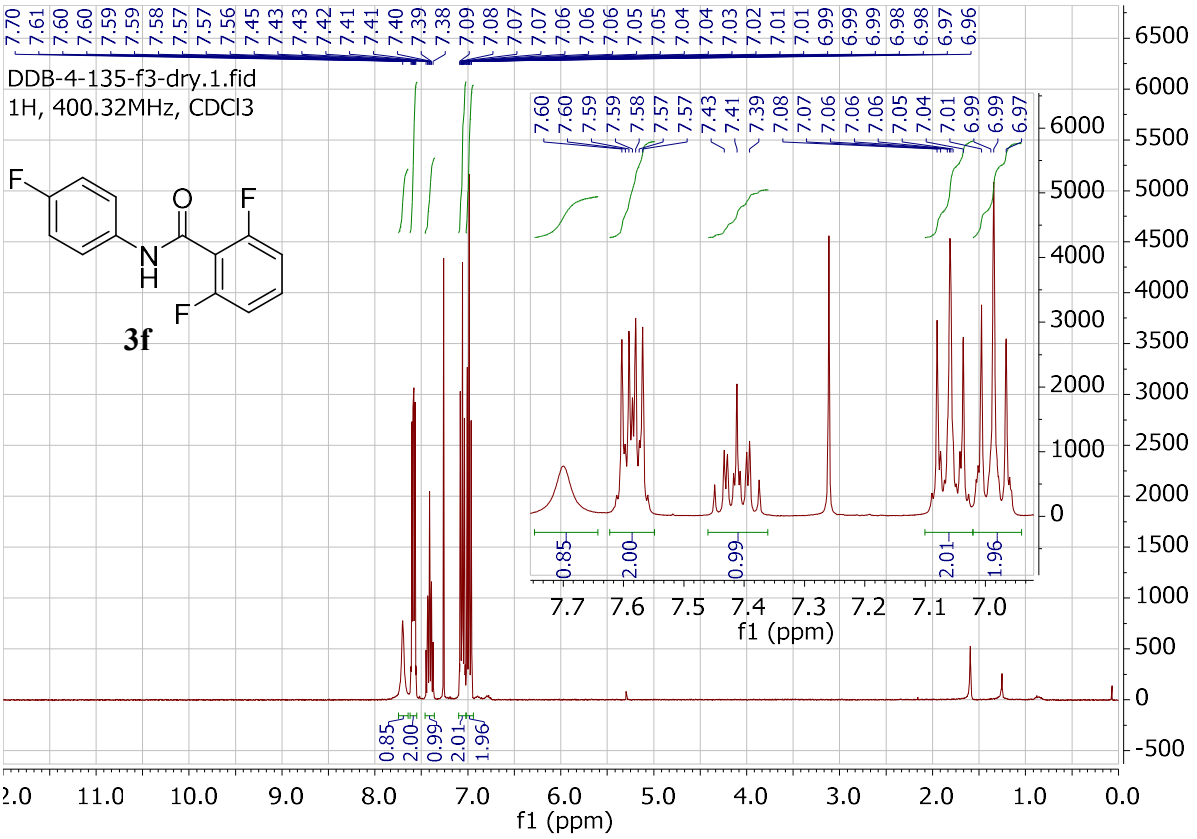
DDB-4-135-f3-dry.1.fid
1H, 400.32MHz, CDCl3
3f
f1 (ppm)

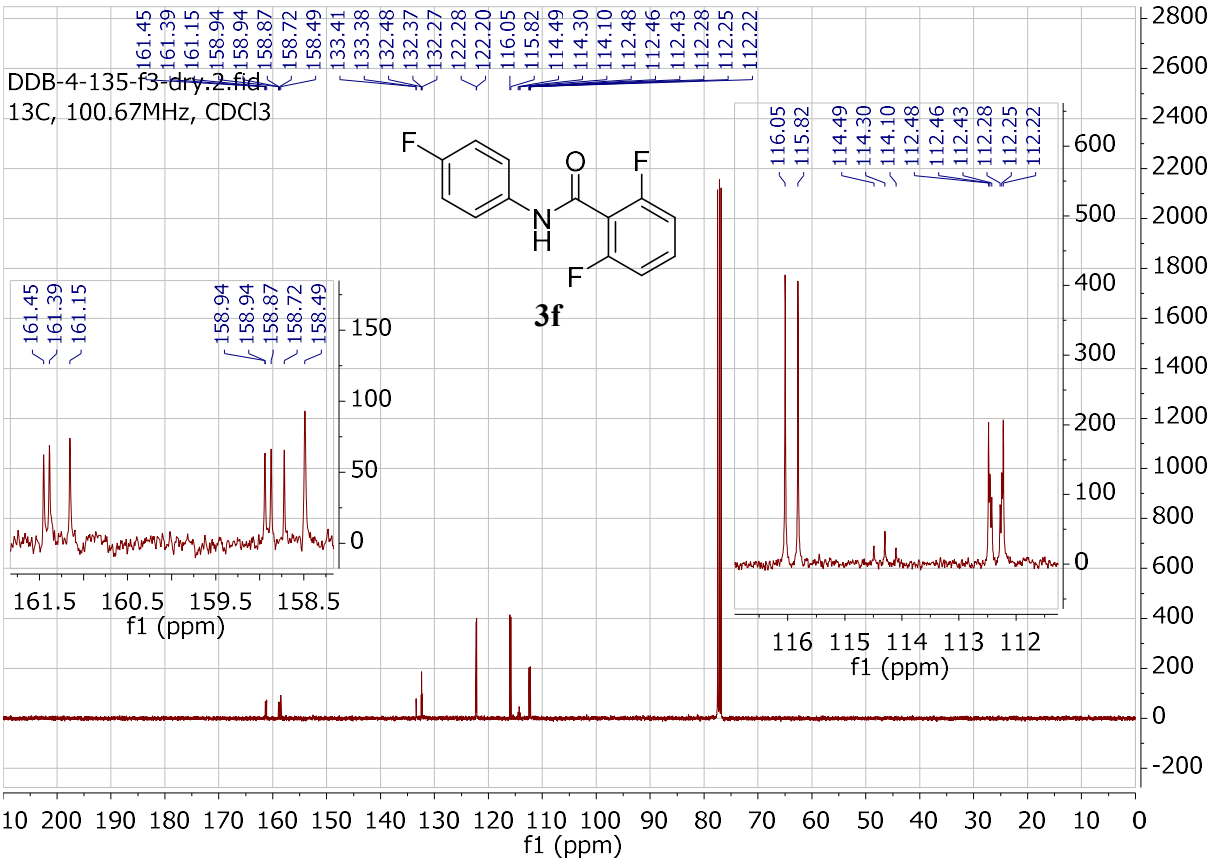
DDB-4-135-f3-dry.2.fid
13C, 100.67MHz, CDCl3
3f
f1 (ppm)

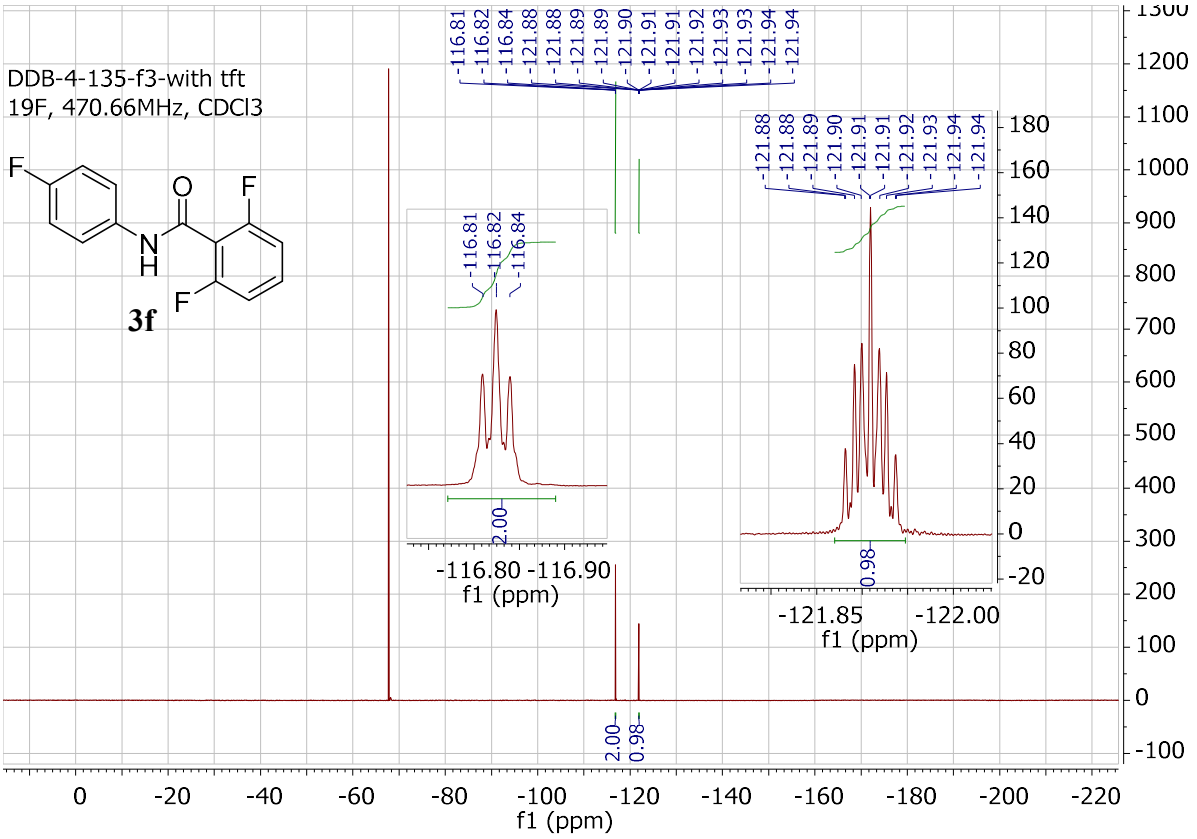
DDB-4-135-f3-with tft
19F, 470.66MHz, CDCl3
3f
-116.81
-116.82
-116.84
-121.88
-121.88
-121.89
-121.89
-121.90
-121.91
-121.91
-121.92
-121.93
-121.93
-121.94
-121.94
2.00
0.98
-116.80 -116.90
f1 (ppm)
-121.85 -122.00
f1 (ppm)
f1 (ppm)

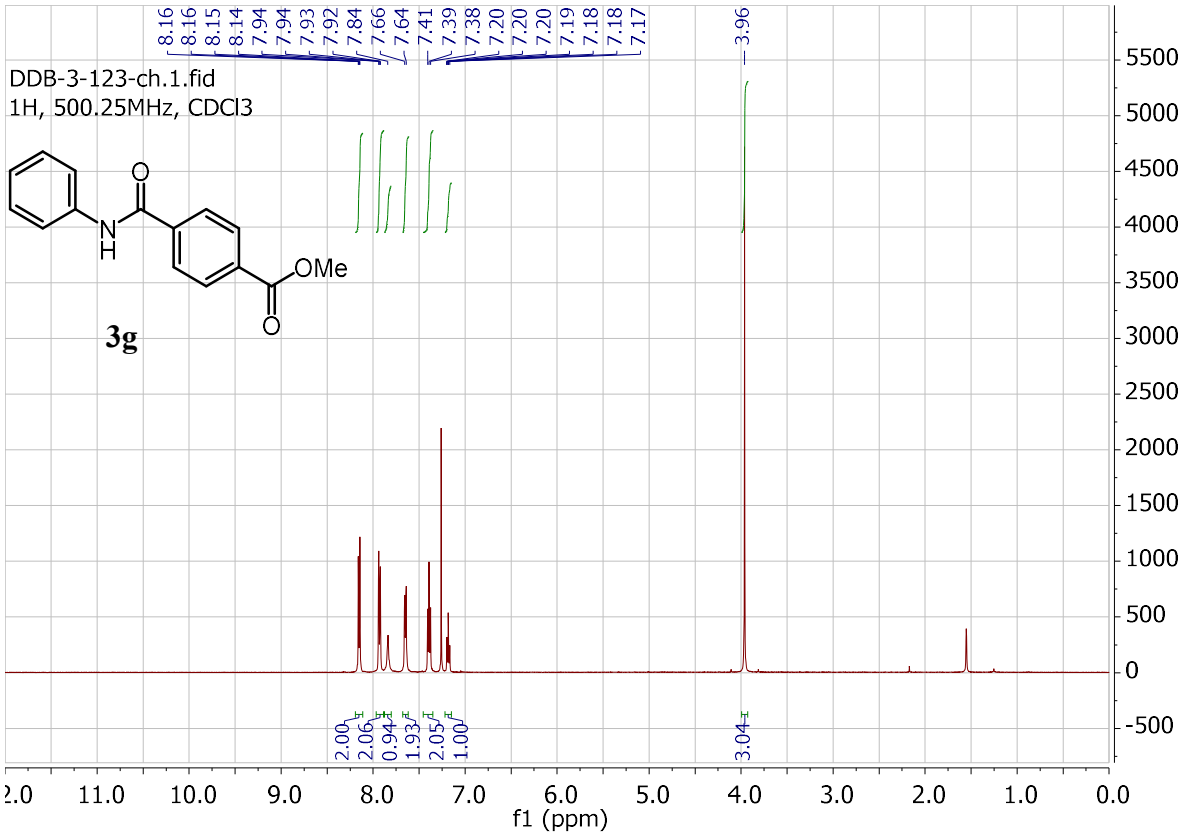
8.16
8.16
8.15
8.14
7.94
7.94
7.93
7.92
7.84
7.66
7.64
7.41
7.39
7.38
7.20
7.20
7.19
7.18
7.18
7.17
3.96
DDB-3-123-ch.1.fid
1H, 500.25MHz, CDCl3
O
N
H
OMe
O
3g
5500
5000
4500
4000
3500
3000
2500
2000
1500
1000
500
0
-500
2.00
2.06
0.94
1.93
2.05
1.00
3.04
2.0
11.0
10.0
9.0
8.0
7.0
6.0
5.0
4.0
3.0
2.0
1.0
0.0
f1 (ppm)

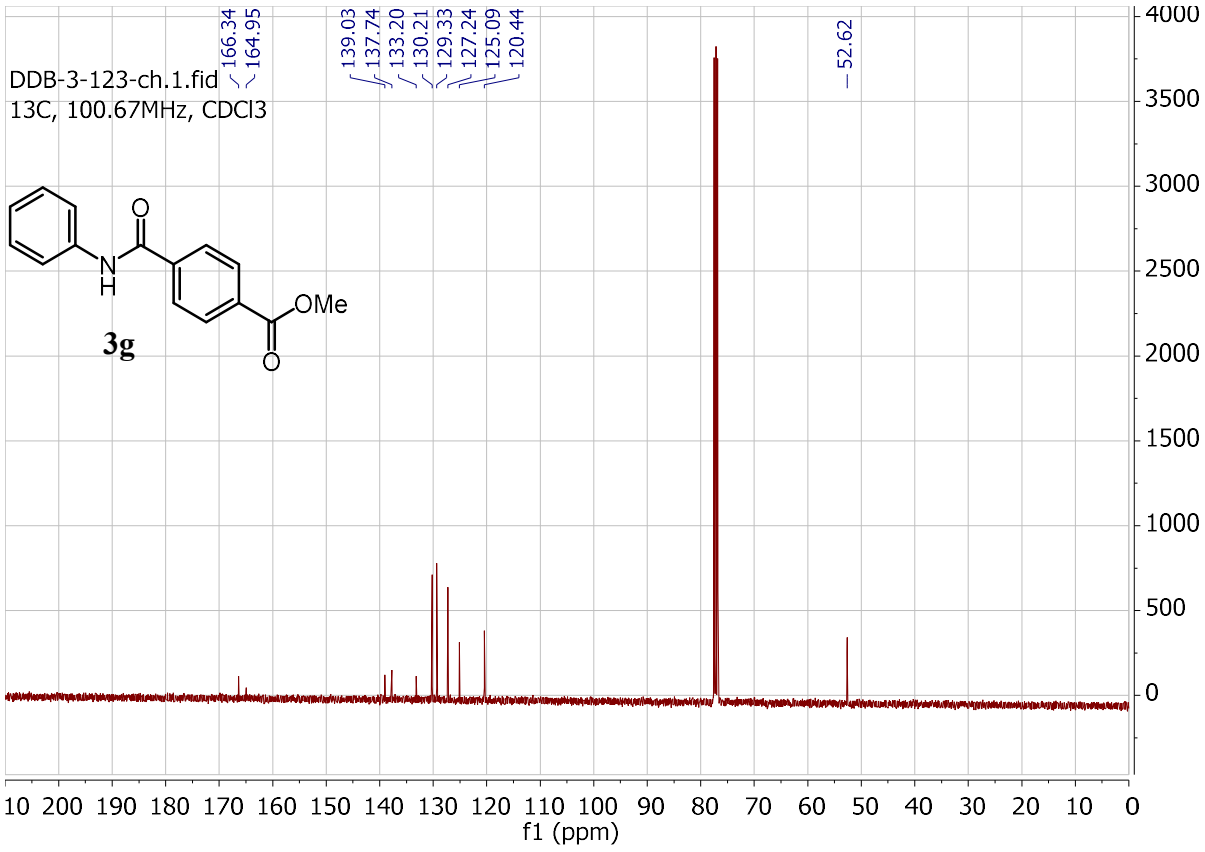
166.34
164.95
139.03
137.74
133.20
130.21
129.33
127.24
125.09
120.44
52.62
DDB-3-123-ch.1.fid
13C, 100.67MHz, CDCl3
O
N
H
OMe
O
3g
4000
3500
3000
2500
2000
1500
1000
500
0
10 200 190 180 170 160 150 140 130 120 110 100 90 80 70 60 50 40 30 20 10 0
f1 (ppm)

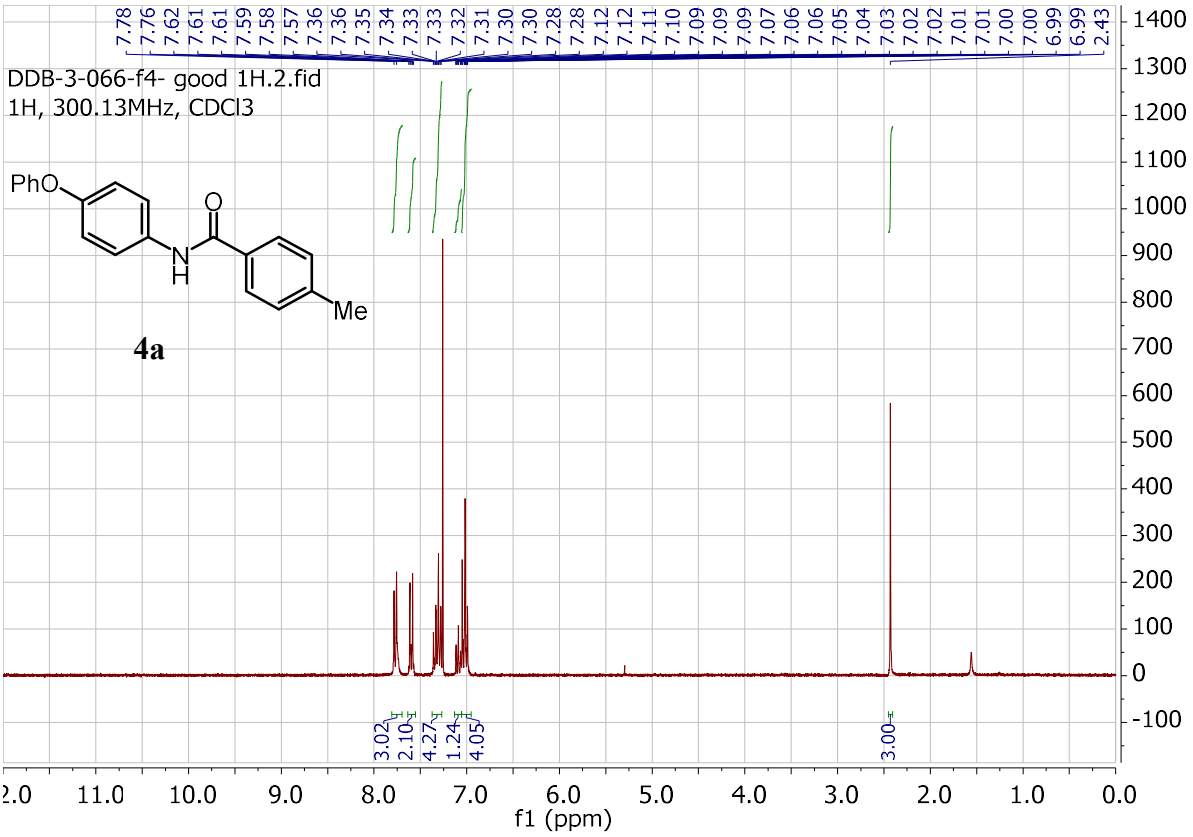
DDB-3-066-f4- good 1H.2.fid
1H, 300.13MHz, CDCl3
PhO
O
N
H
Me
4a
7.78 7.76 7.62 7.61 7.61 7.59 7.58 7.57 7.36 7.36 7.35 7.34 7.33 7.33 7.32 7.31 7.30 7.30 7.28 7.28 7.12 7.12 7.11 7.10 7.09 7.09 7.09 7.07 7.06 7.06 7.05 7.04 7.03 7.02 7.02 7.01 7.01 7.00 7.00 6.99 6.99 2.43
3.02 2.10 4.27 1.24 4.05 3.00
f1 (ppm)

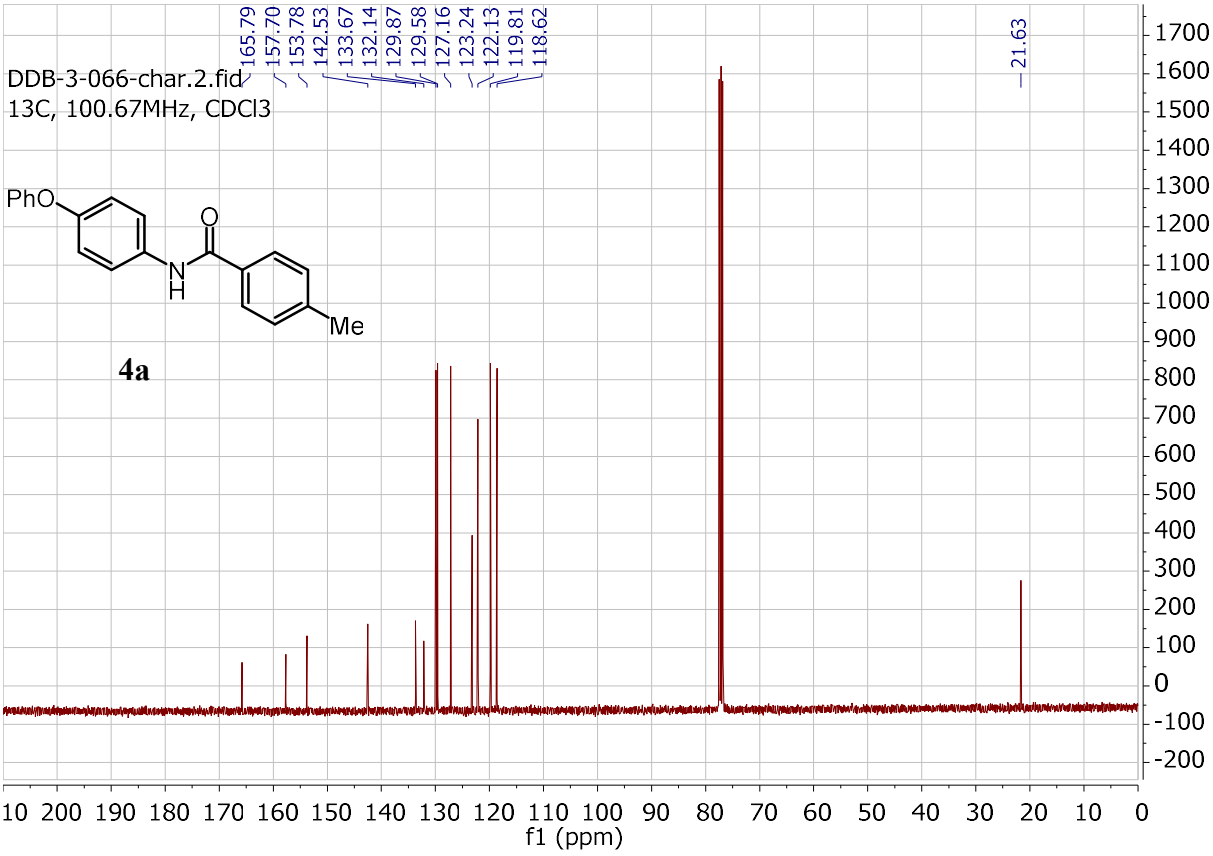
DDB-3-066-char.2.fid
13C, 100.67MHz, CDCl3
PhO
O
N
H
Me
4a
165.79 157.70 153.78 142.53 133.67 132.14 129.87 129.58 127.16 123.24 122.13 119.81 118.62
21.63
f1 (ppm)

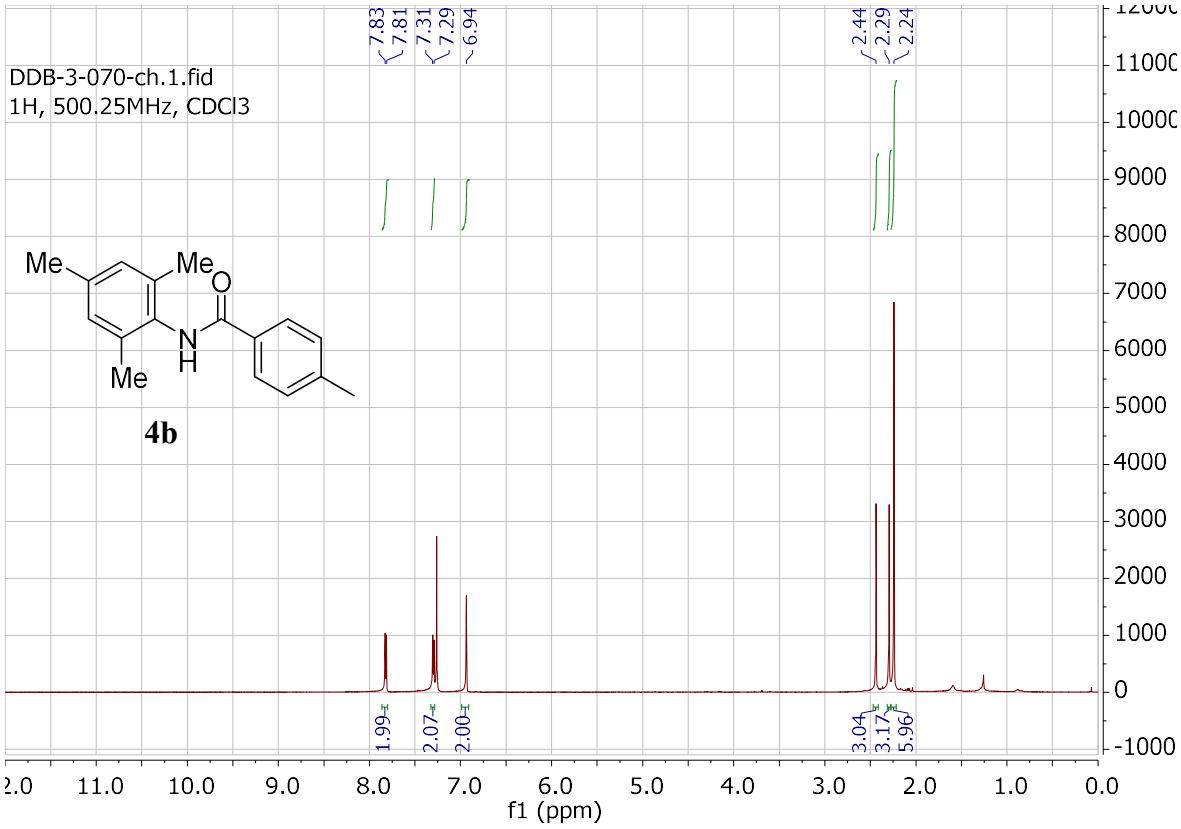
DDB-3-070-ch.1.fid
1H, 500.25MHz, CDCl3
7.83
7.81
7.31
7.29
6.94
2.44
2.29
2.24
Me
Me
O
N
H
Me
4b
1.99
2.07
2.00
3.04
3.17
5.96
f1 (ppm)

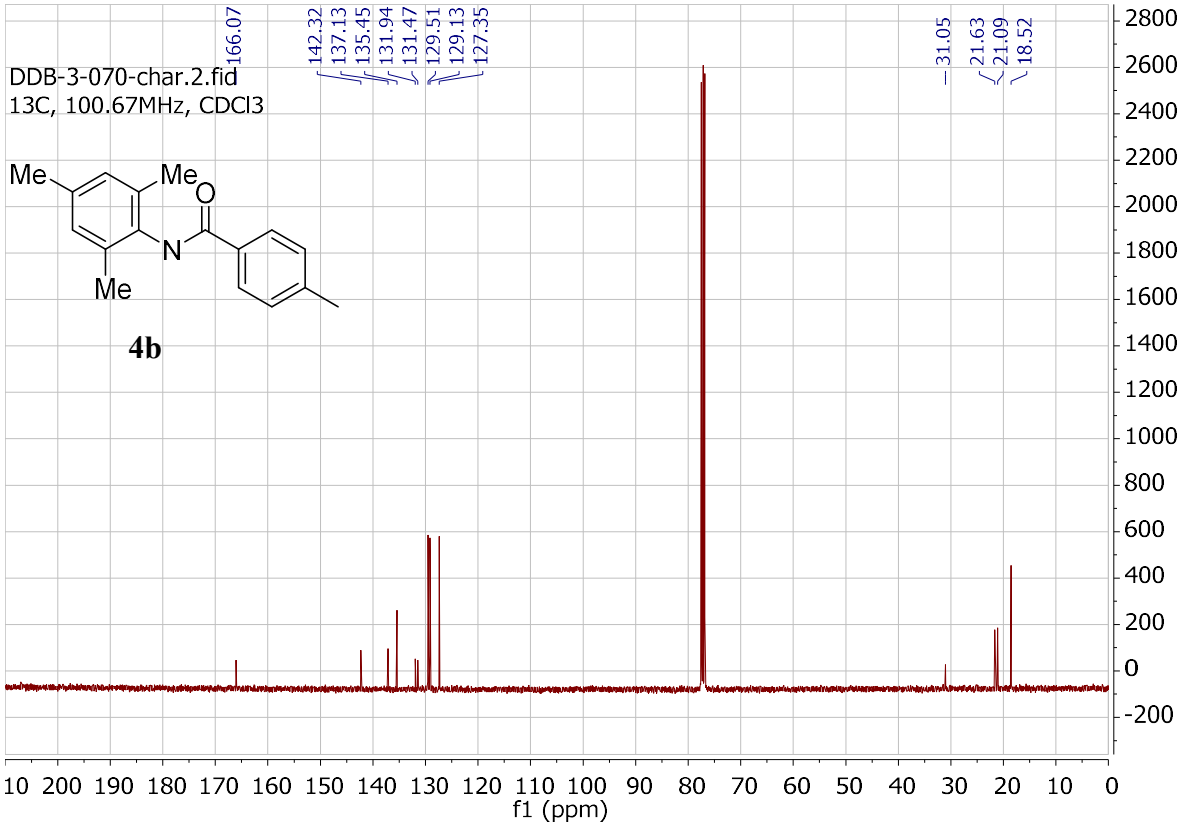
DDB-3-070-char.2.fid
13C, 100.67MHz, CDCl3
166.07
142.32
137.13
135.45
131.94
131.47
129.51
129.13
127.35
31.05
21.63
21.09
18.52
Me
Me
O
N
Me
4b
f1 (ppm)

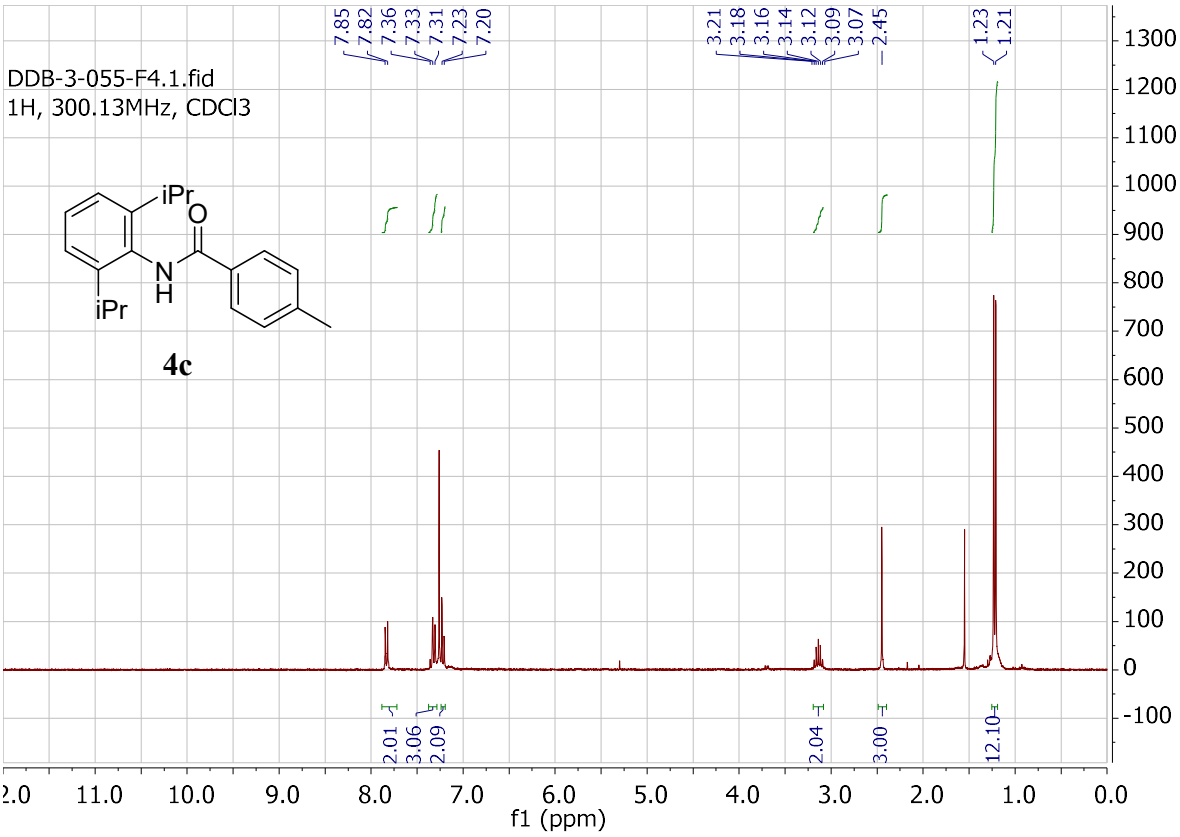
DDB-3-055-F4.1.fid
1H, 300.13MHz, CDCl3
7.85
7.82
7.36
7.33
7.31
7.23
7.20
3.21
3.18
3.16
3.14
3.12
3.09
3.07
2.45
1.23
1.21
2.01
3.06
2.09
2.04
3.00
12.10
iPr
O
N
H
iPr
4c
f1 (ppm)

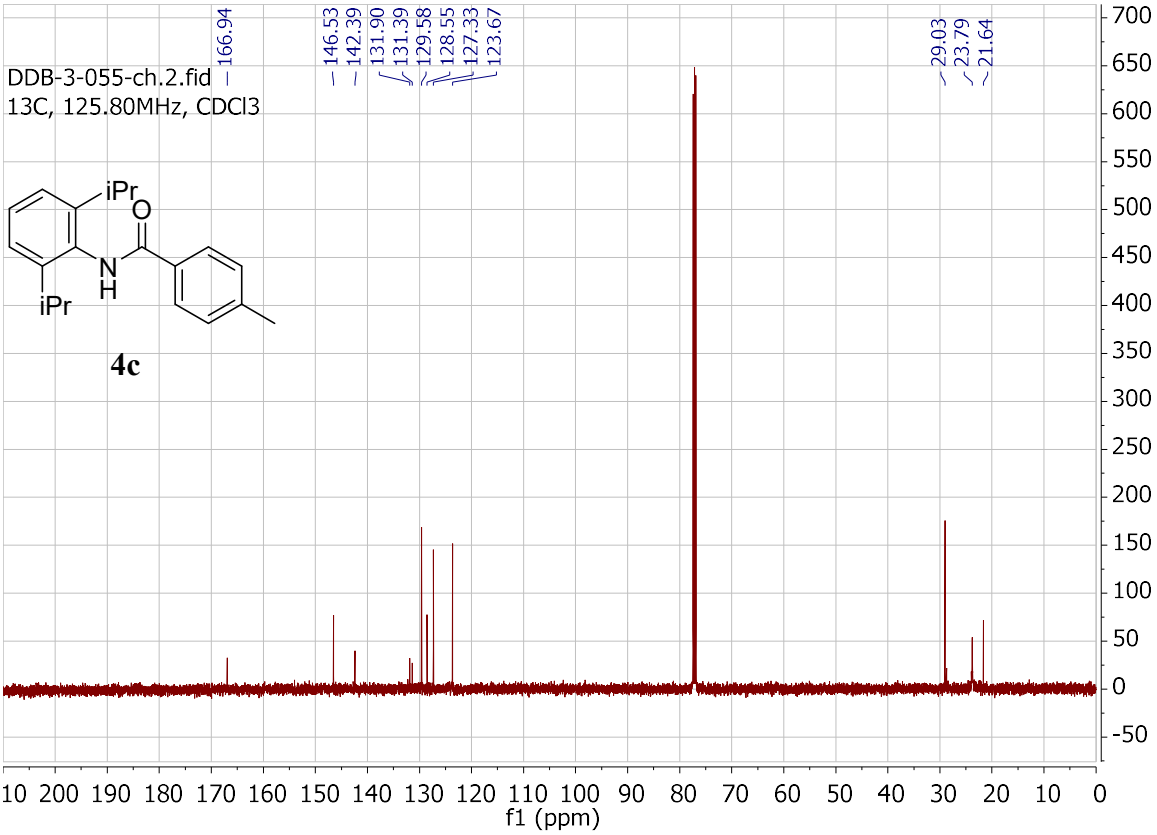
DDB-3-055-ch.2.fid
13C, 125.80MHz, CDCl3
166.94
146.53
142.39
131.90
131.39
129.58
128.55
127.33
123.67
29.03
23.79
21.64
iPr
O
N
H
iPr
4c
f1 (ppm)

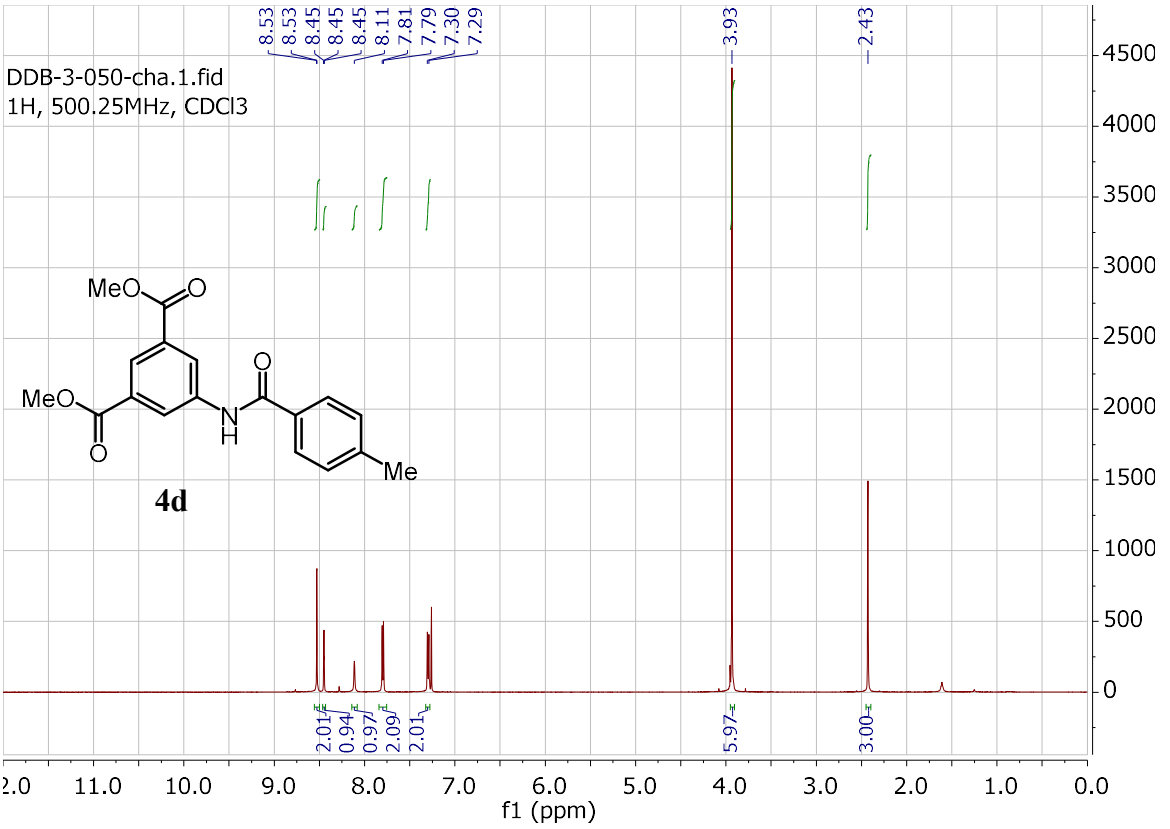
DDB-3-050-cha.1.fid
1H, 500.25MHz, CDCl3
8.53
8.53
8.45
8.45
8.45
8.11
7.81
7.79
7.30
7.29
3.93
2.43
MeO
O
MeO
O
N
H
O
Me
4d
2.01
0.94
0.97
2.09
2.01
5.97
3.00
4500
4000
3500
3000
2500
2000
1500
1000
500
0
2.0
11.0
10.0
9.0
8.0
7.0
6.0
5.0
4.0
3.0
2.0
1.0
0.0
f1 (ppm)

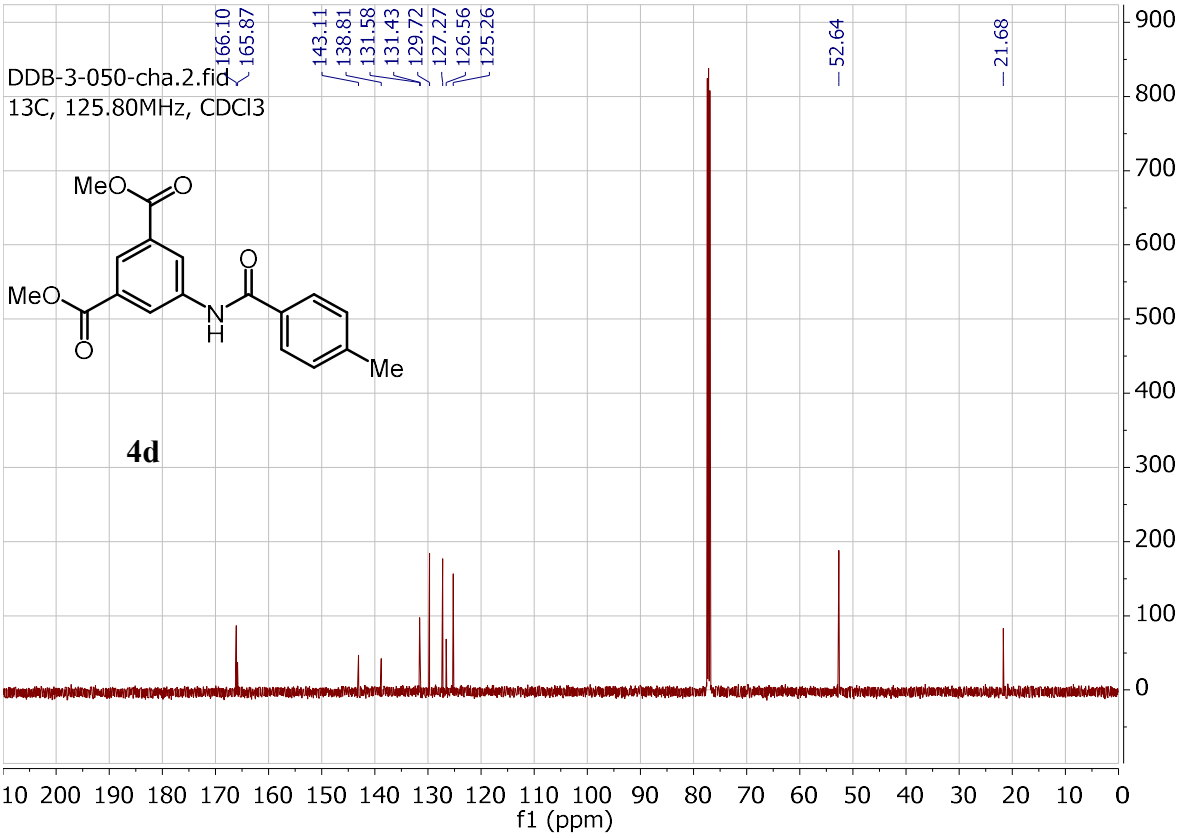
DDB-3-050-cha.2.fid
13C, 125.80MHz, CDCl3
166.10
165.87
143.11
138.81
131.58
131.43
129.72
127.27
126.56
125.26
52.64
21.68
MeO
O
MeO
O
N
H
O
Me
4d
900
800
700
600
500
400
300
200
100
0
10 200 190 180 170 160 150 140 130 120 110 100 90 80 70 60 50 40 30 20 10 0
f1 (ppm)

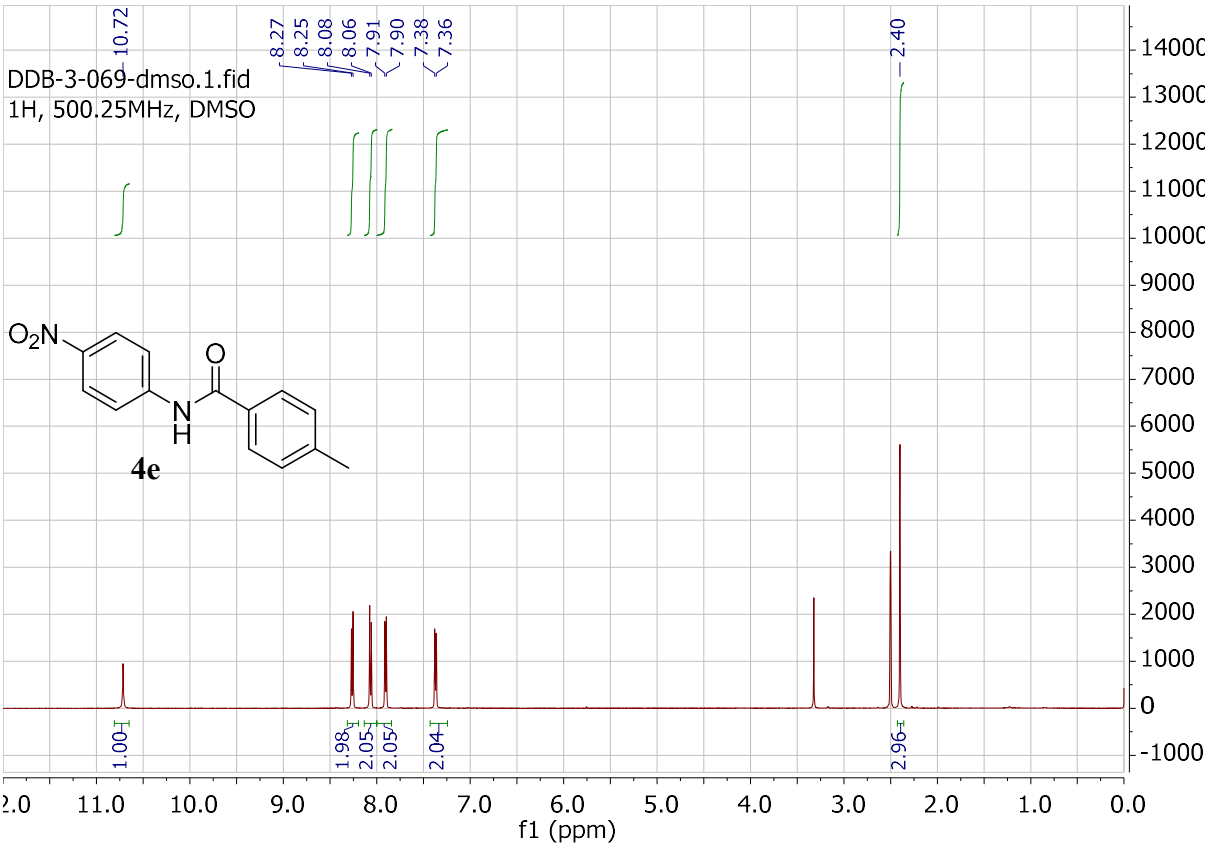
DDB-3-069-dmso.1.fid
1H, 500.25MHz, DMSO
10.72
8.27
8.25
8.08
8.06
7.91
7.90
7.38
7.36
2.40
1.00
1.98
2.05
2.05
2.04
2.96
4e
f1 (ppm)

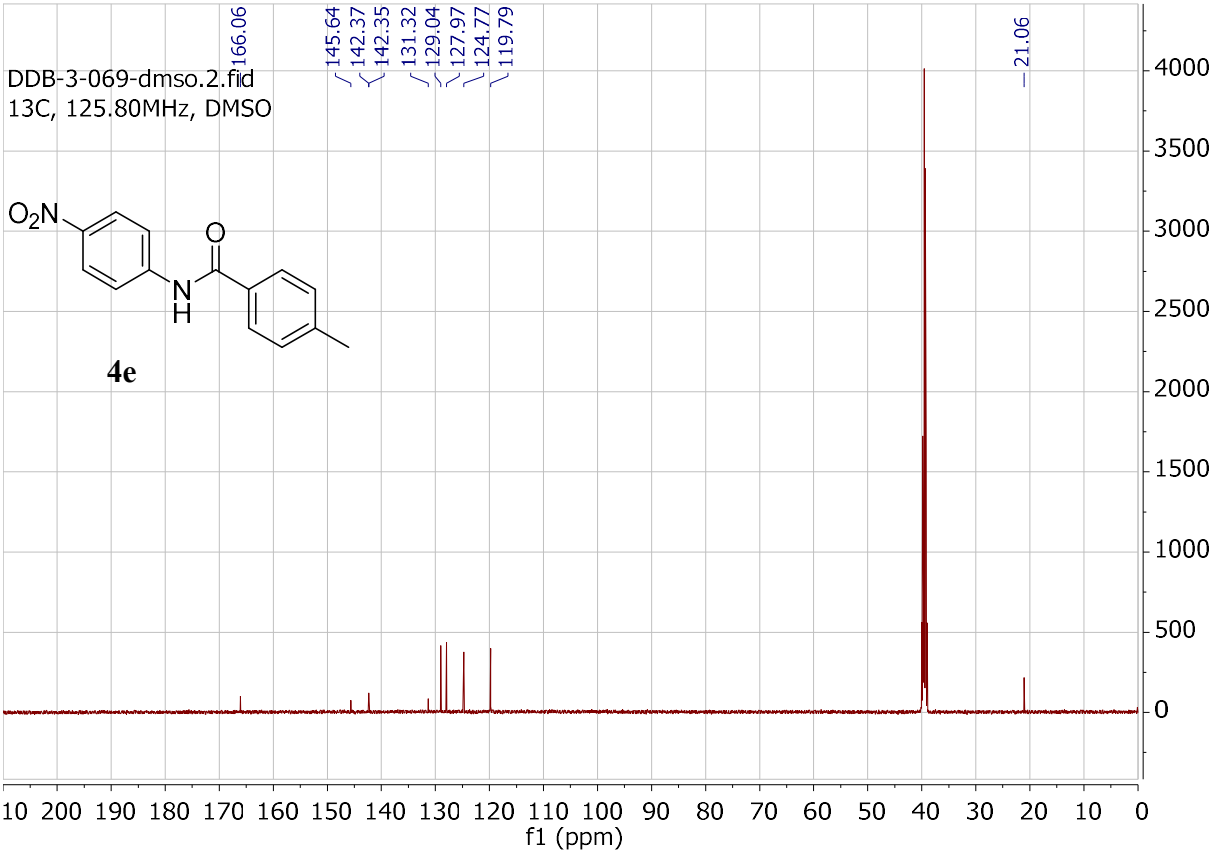
DDB-3-069-dmso.2.fid
13C, 125.80MHz, DMSO
166.06
145.64
142.37
142.35
131.32
129.04
127.97
124.77
119.79
21.06
4e
f1 (ppm)

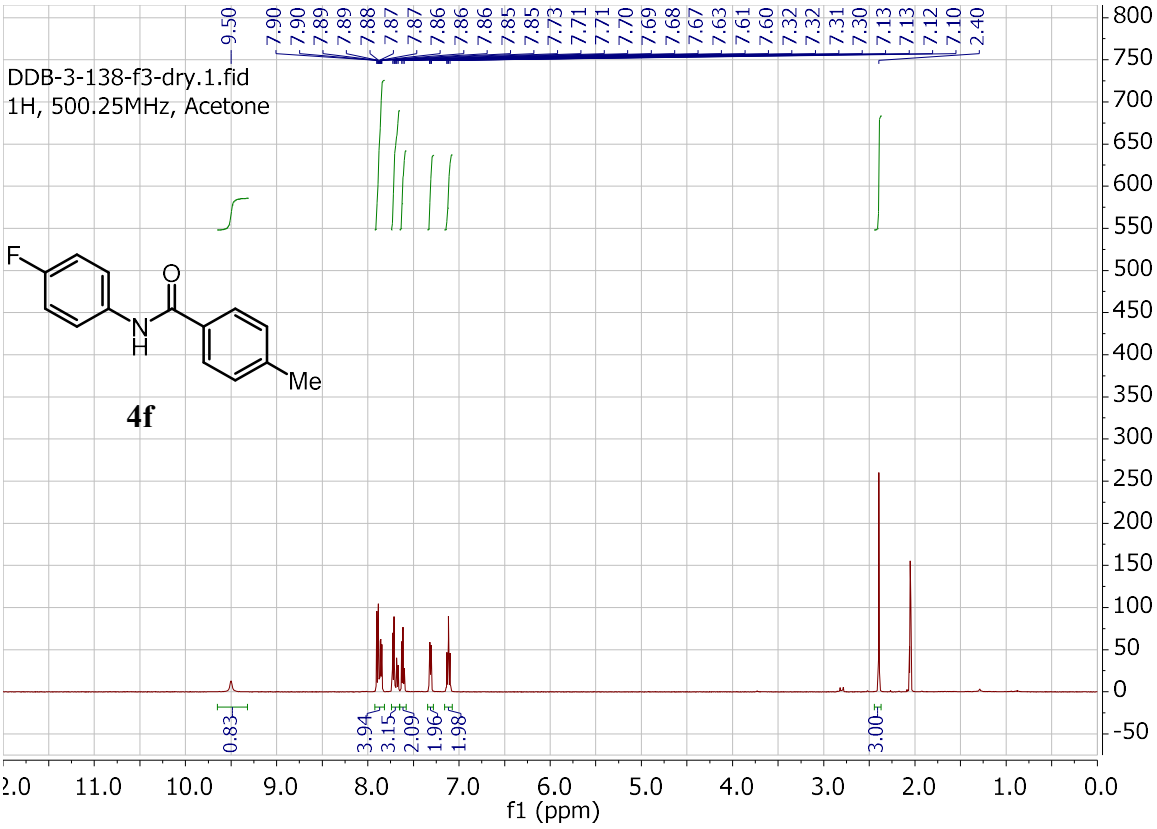
DDB-3-138-f3-dry.1.fid
1H, 500.25MHz, Acetone
F
O
N
H
Me
4f
9.50
7.90
7.90
7.89
7.89
7.88
7.87
7.87
7.86
7.86
7.86
7.85
7.85
7.73
7.71
7.71
7.70
7.69
7.68
7.67
7.63
7.61
7.60
7.32
7.32
7.31
7.30
7.13
7.13
7.12
7.10
2.40
0.83
3.94
3.15
2.09
1.96
1.98
3.00
f1 (ppm)

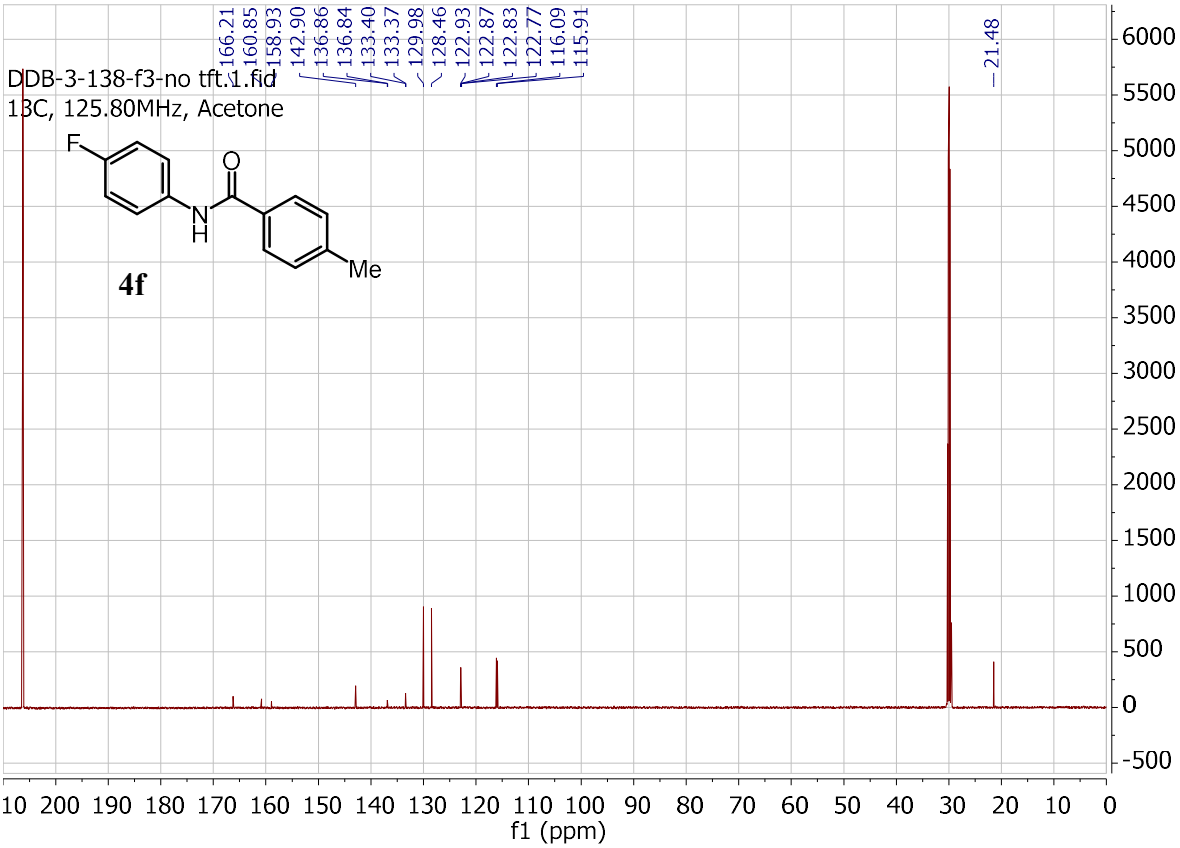
DDB-3-138-f3-no tft.1.fid
13C, 125.80MHz, Acetone
F
O
N
H
Me
4f
166.21
160.85
158.93
142.90
136.86
136.84
133.40
133.37
129.98
128.46
122.93
122.87
122.83
122.77
116.09
115.91
21.48
f1 (ppm)

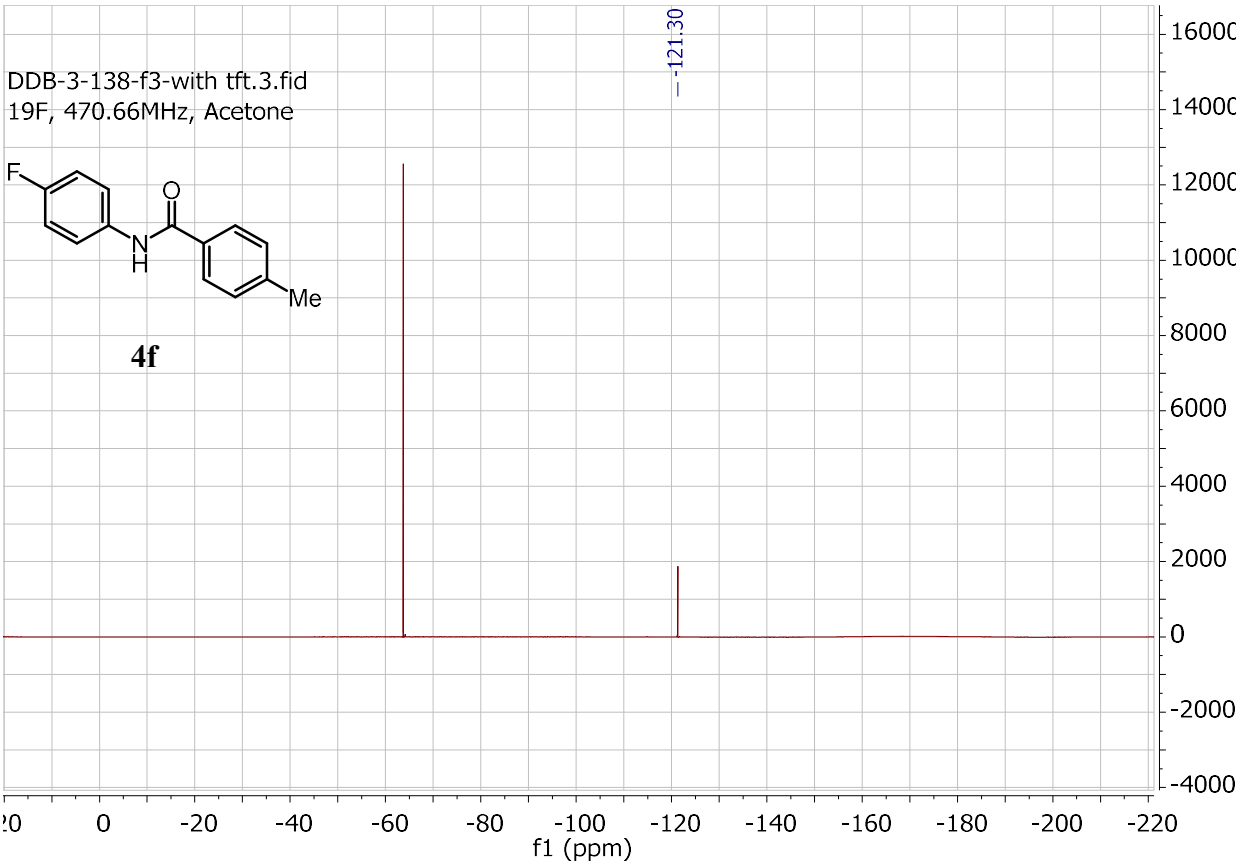
DDB-3-138-f3-with tft.3.fid
19F, 470.66MHz, Acetone
F
O
N
H
Me
-121.30
4f
16000
14000
12000
10000
8000
6000
4000
2000
0
-2000
-4000
0
-20
-40
-60
-80
-100
-120
-140
-160
-180
-200
-220
f1 (ppm)

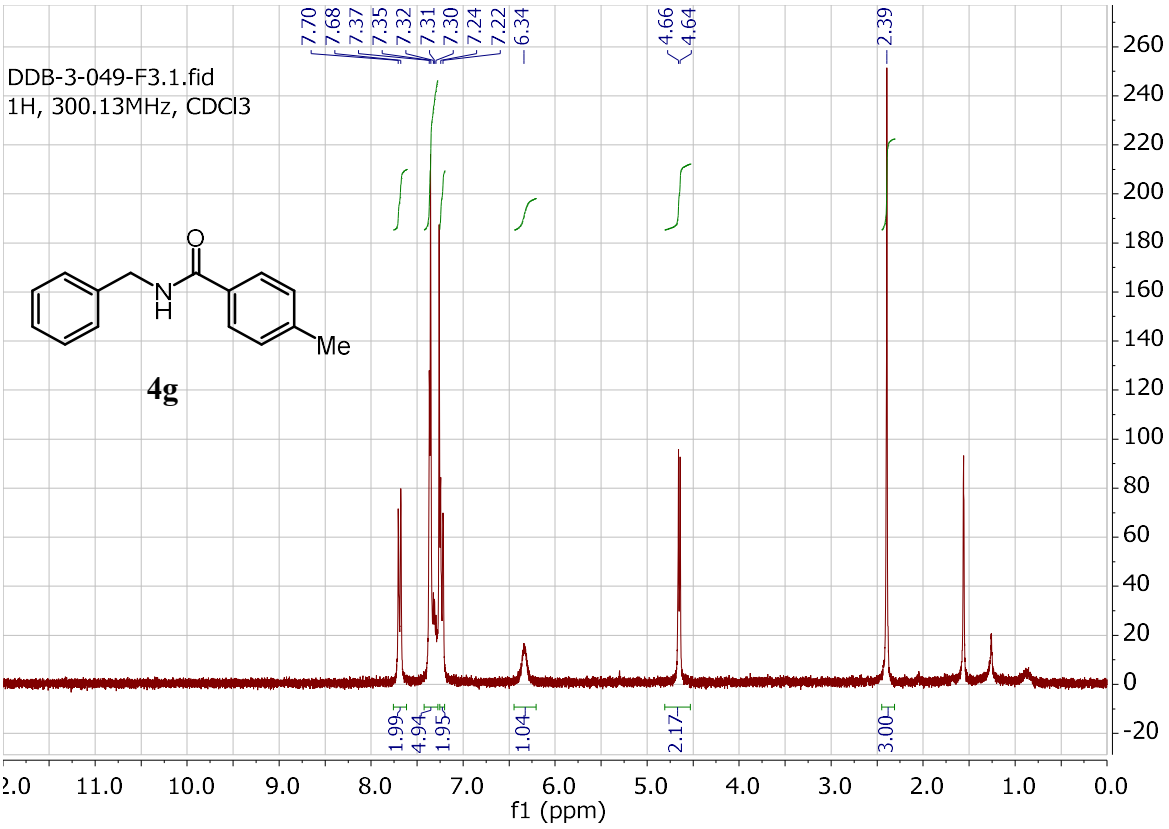
DDB-3-049-F3.1.fid
1H, 300.13MHz, CDCl3
7.70
7.68
7.37
7.35
7.32
7.31
7.30
7.24
7.22
6.34
4.66
4.64
2.39
1.99
4.94
1.95
1.04
2.17
3.00
Me
4g
f1 (ppm)

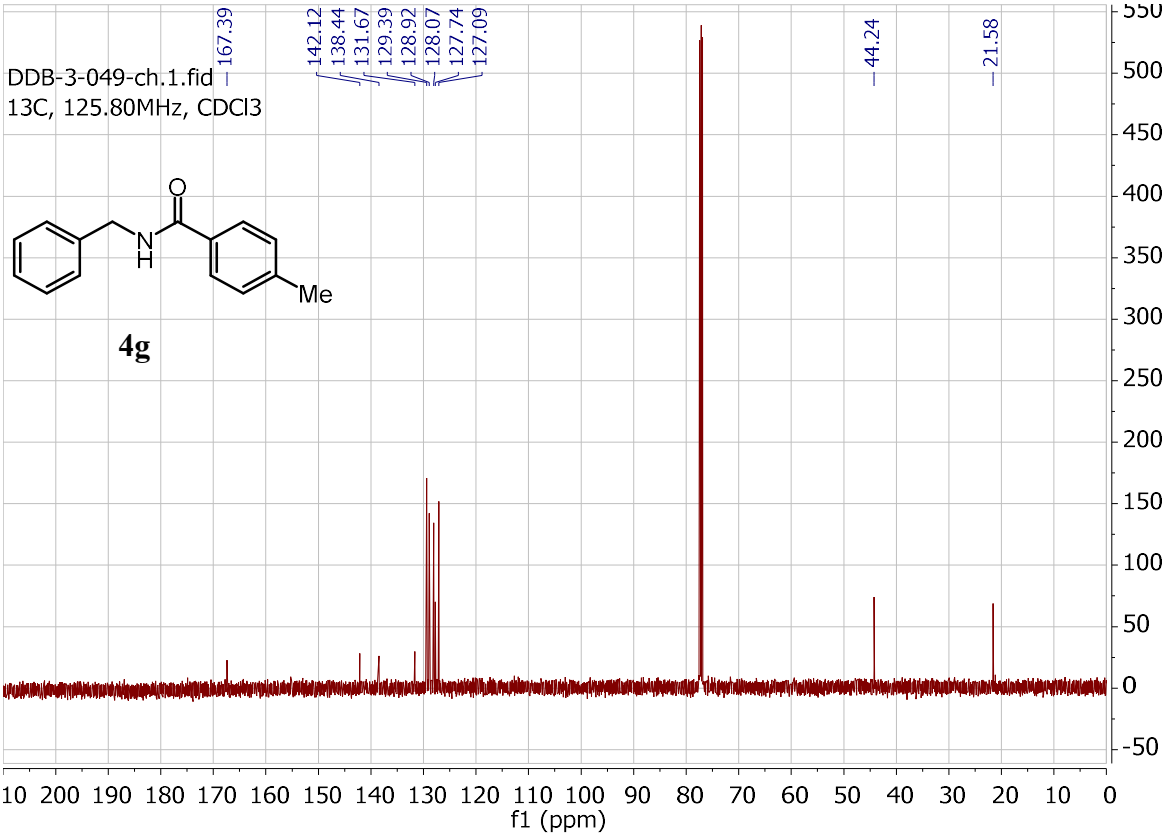
DDB-3-049-ch.1.fid
13C, 125.80MHz, CDCl3
167.39
142.12
138.44
131.67
129.39
128.92
128.07
127.74
127.09
44.24
21.58
Me
4g
f1 (ppm)

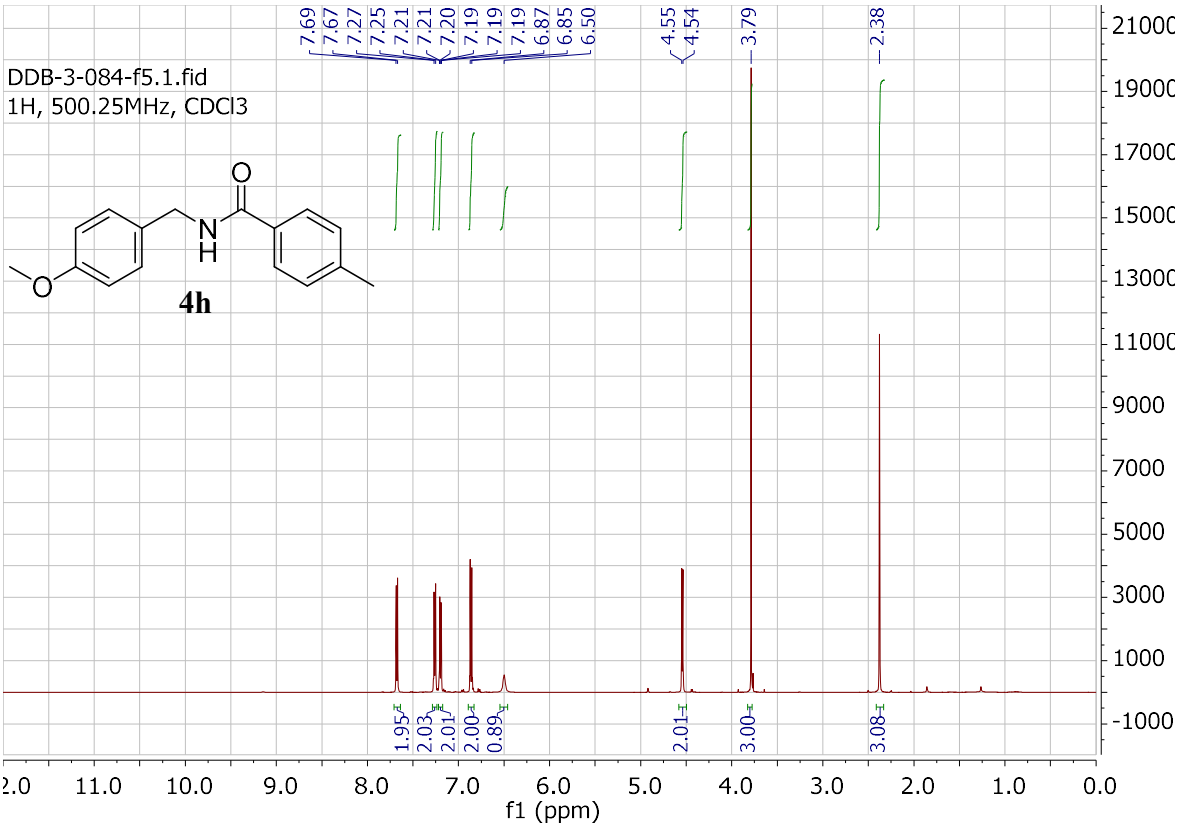
DDB-3-084-f5.1.fid
1H, 500.25MHz, CDCl3
4h
7.69
7.67
7.27
7.25
7.21
7.21
7.20
7.19
7.19
7.19
6.87
6.85
6.50
4.55
4.54
3.79
2.38
1.95
2.03
2.01
2.00
0.89
2.01
3.00
3.08
f1 (ppm)

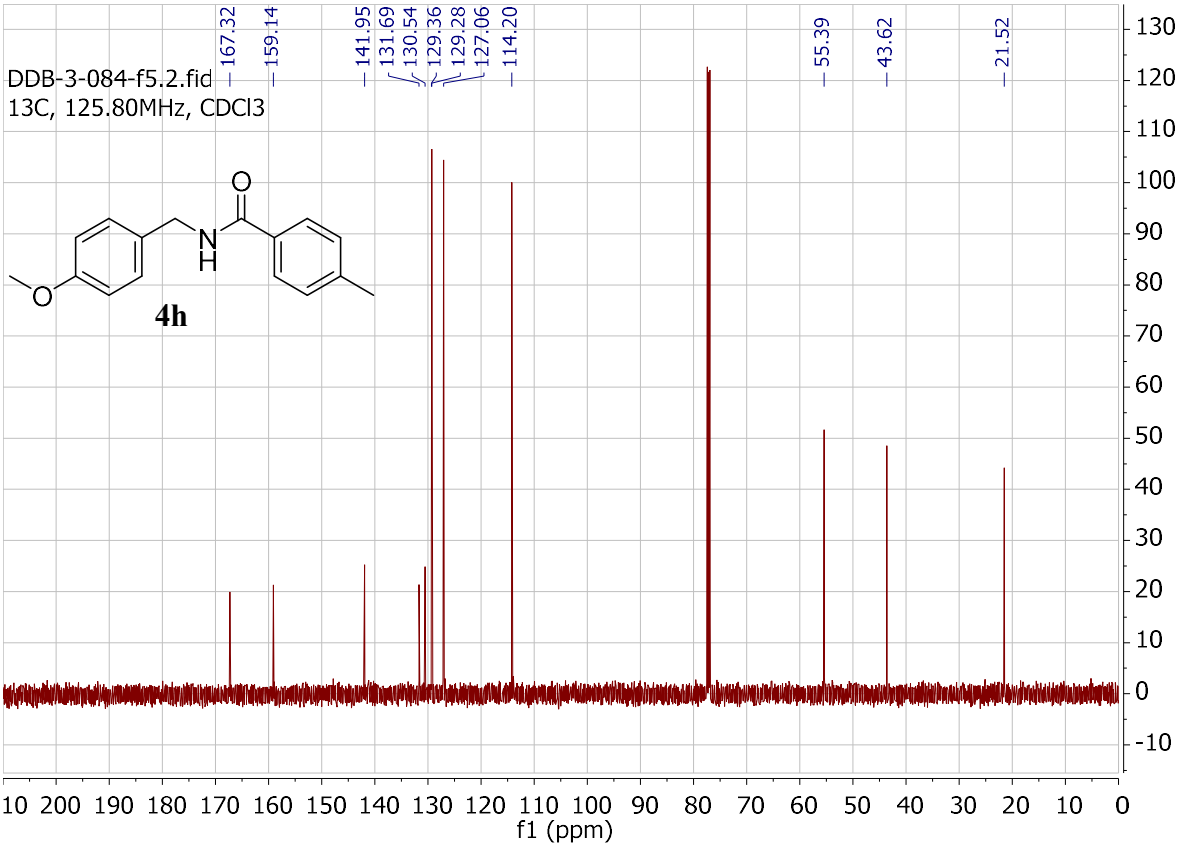
DDB-3-084-f5.2.fid
13C, 125.80MHz, CDCl3
4h
167.32
159.14
141.95
131.69
130.54
129.36
129.28
127.06
114.20
55.39
43.62
21.52
f1 (ppm)

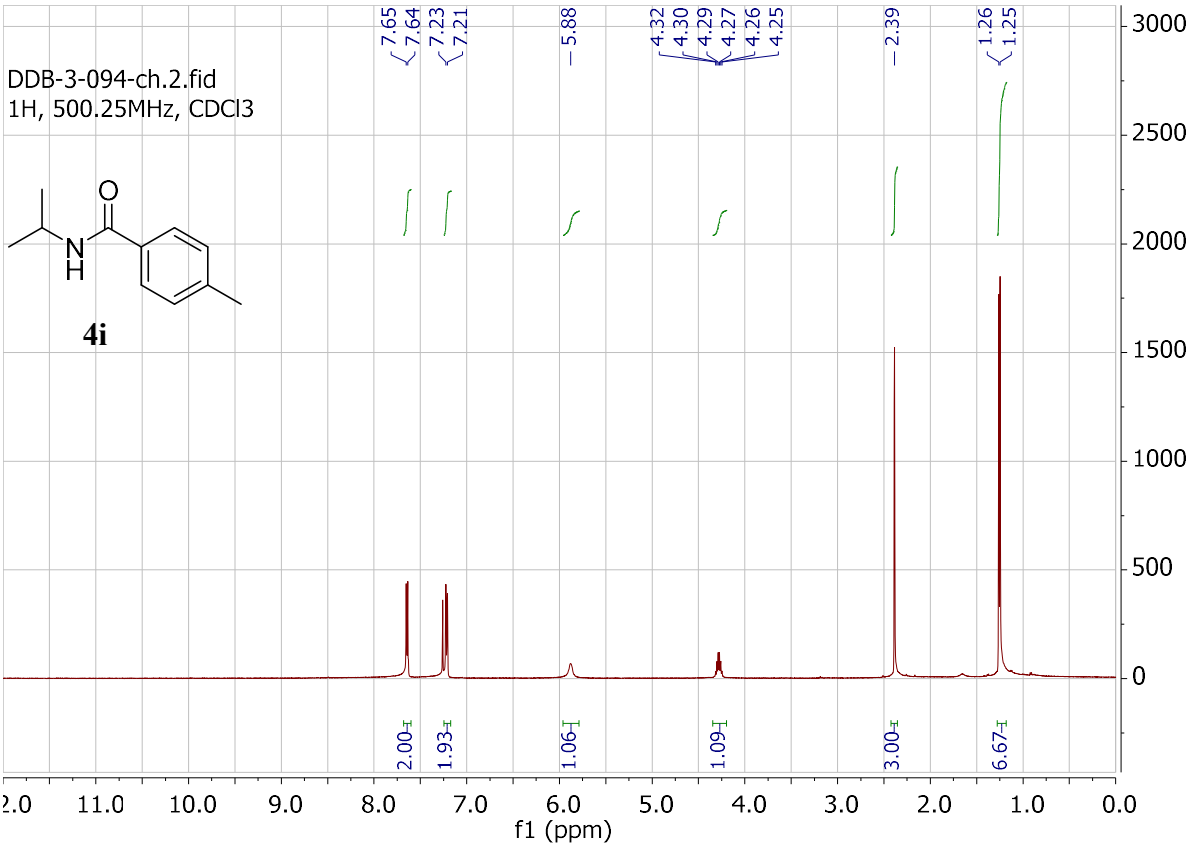
DDB-3-094-ch.2.fid
1H, 500.25MHz, CDCl3
4i
7.65
7.64
7.23
7.21
5.88
4.32
4.30
4.29
4.27
4.26
4.25
2.39
1.26
1.25
2.00
1.93
1.06
1.09
3.00
6.67
f1 (ppm)

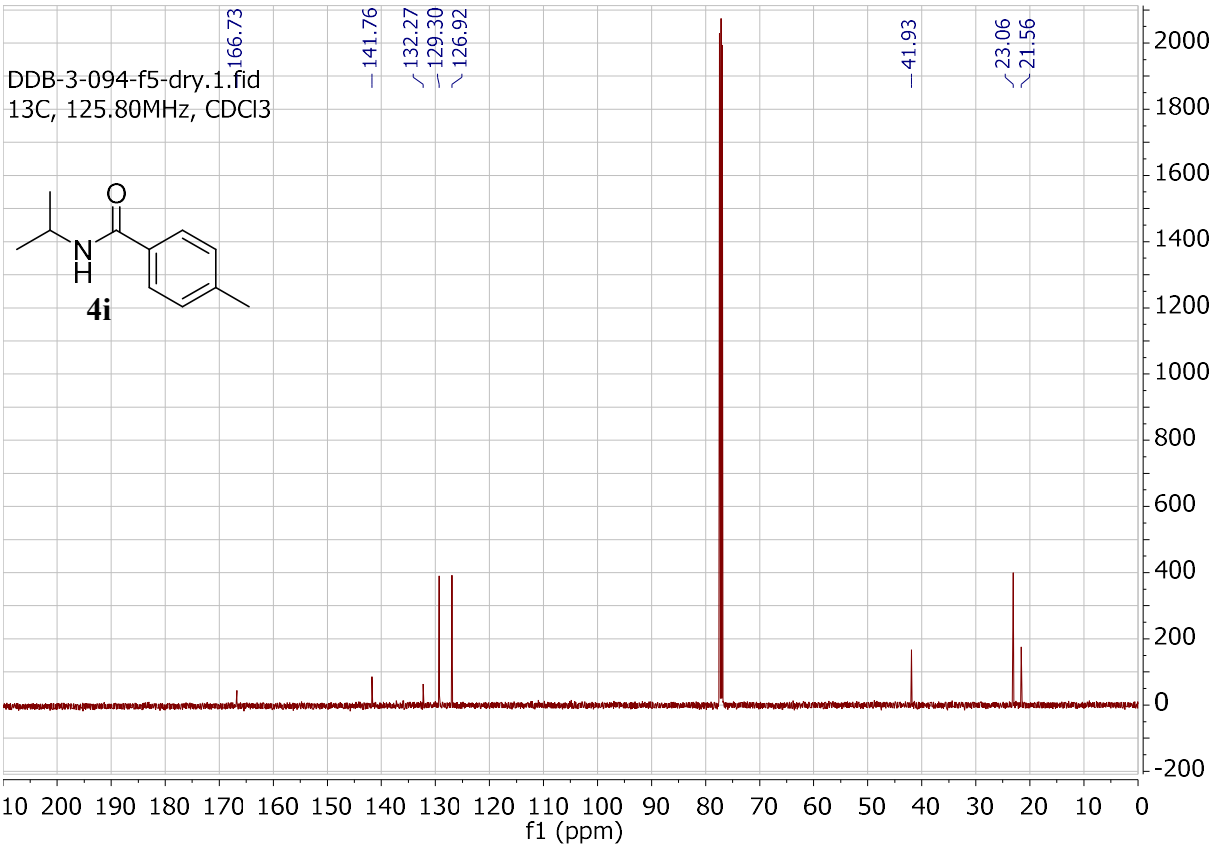
DDB-3-094-f5-dry.1.fid
13C, 125.80MHz, CDCl3
4i
166.73
141.76
132.27
129.30
126.92
41.93
23.06
21.56
f1 (ppm)

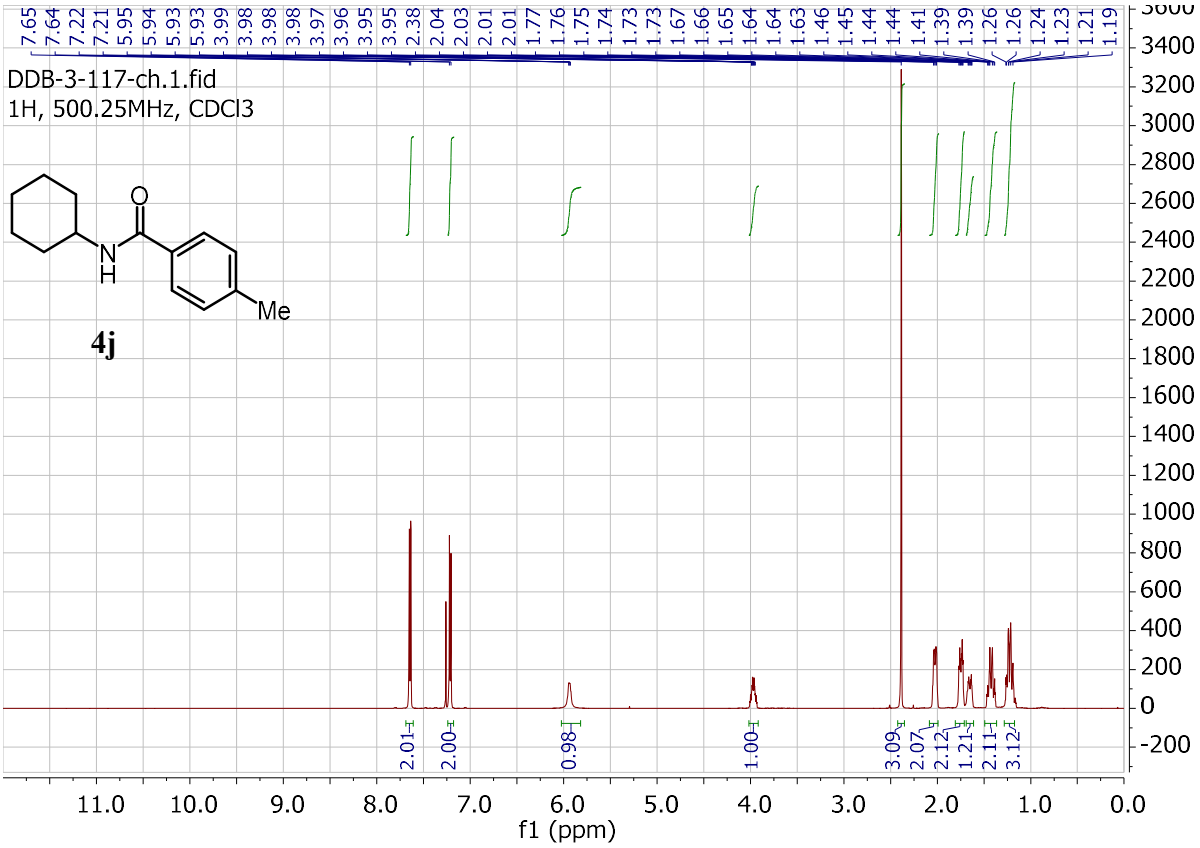
DDB-3-117-ch.1.fid
1H, 500.25MHz, CDCl3
4j
f1 (ppm)

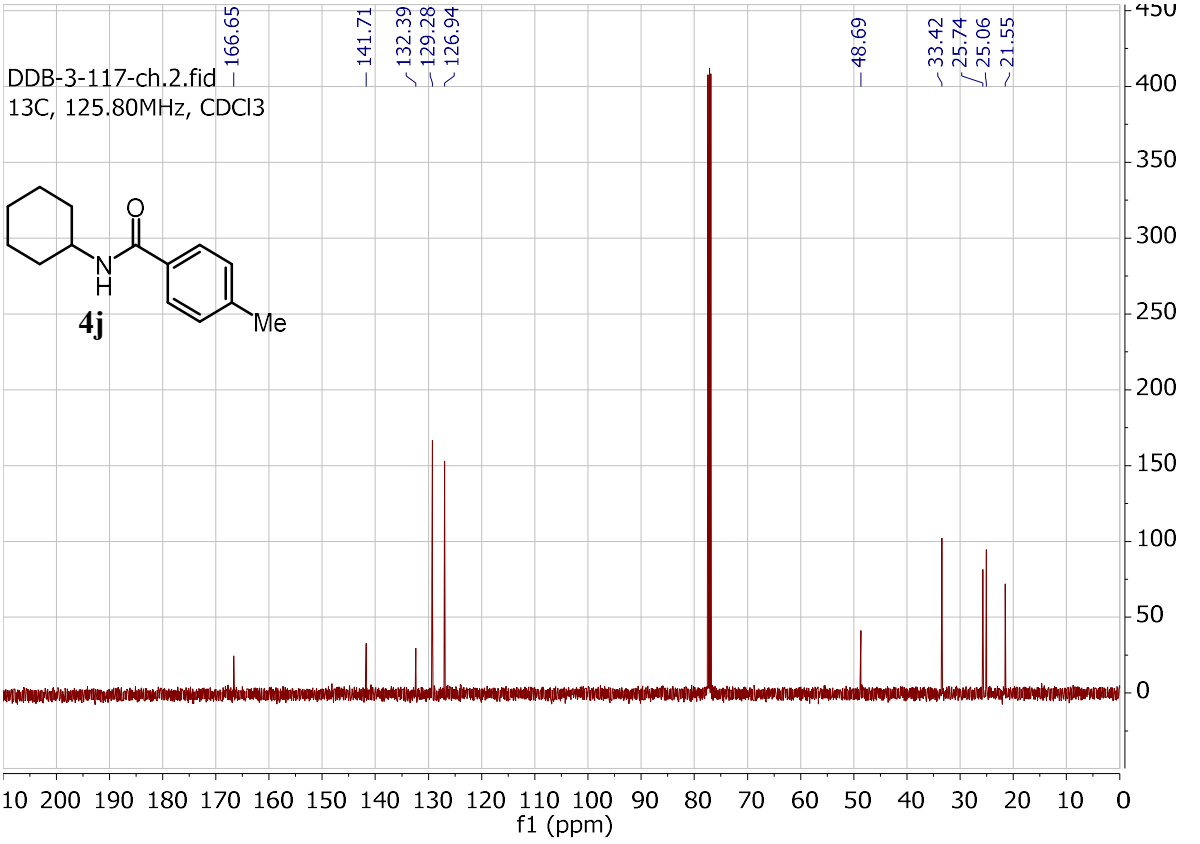
DDB-3-117-ch.2.fid
13C, 125.80MHz, CDCl3
4j
f1 (ppm)

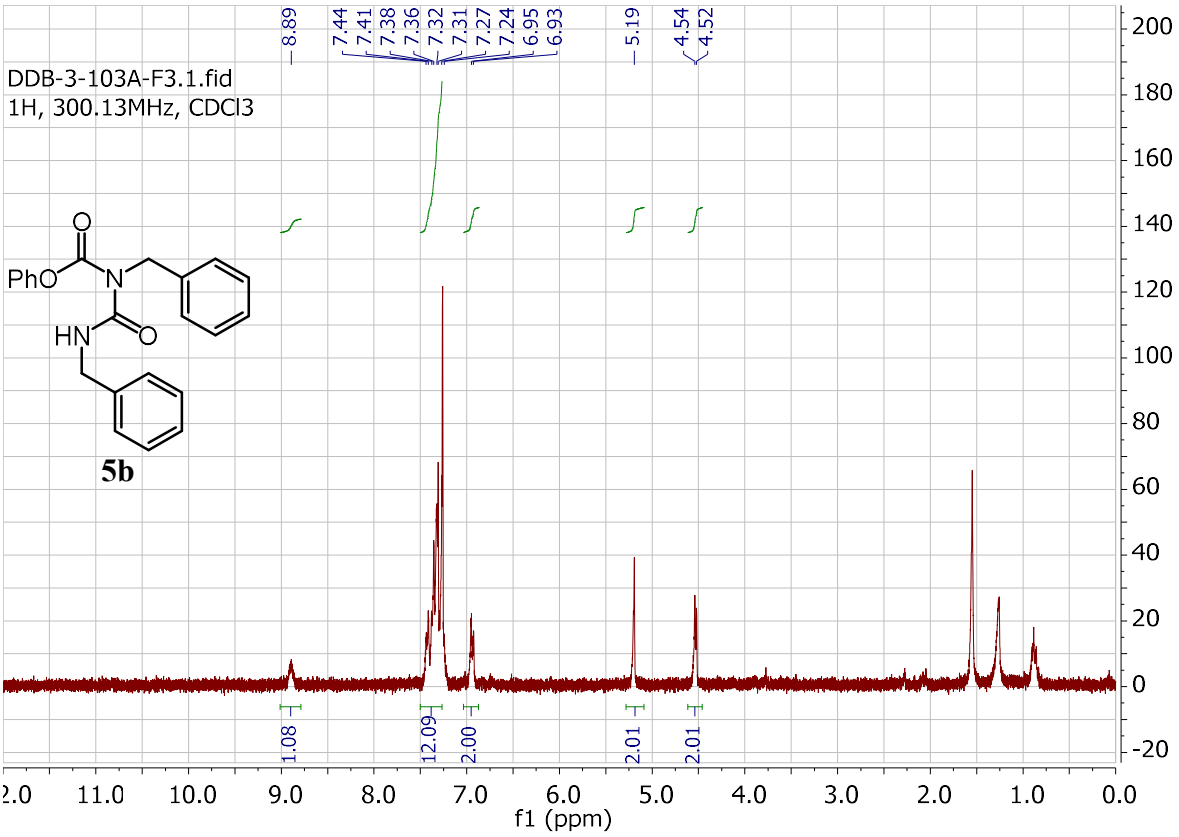
DDB-3-103A-F3.1.fid
1H, 300.13MHz, CDCl3
8.89
7.44
7.41
7.38
7.36
7.32
7.31
7.27
7.24
6.95
6.93
5.19
4.54
4.52
PhO
N
HN
O
5b
1.08
12.09
2.00
2.01
2.01
f1 (ppm)

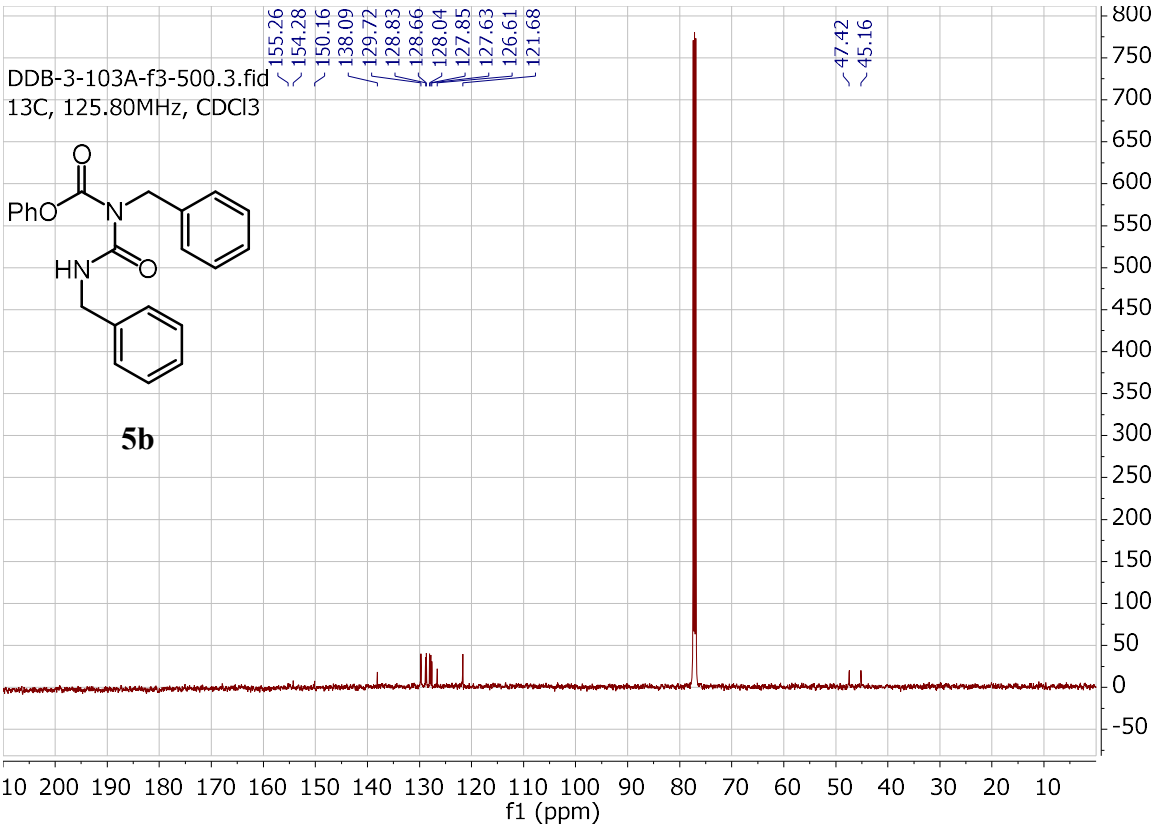
DDB-3-103A-f3-500.3.fid
13C, 125.80MHz, CDCl3
155.26
154.28
150.16
138.09
129.72
128.83
128.66
128.04
127.85
127.63
126.61
121.68
47.42
45.16
PhO
N
HN
O
5b
f1 (ppm)

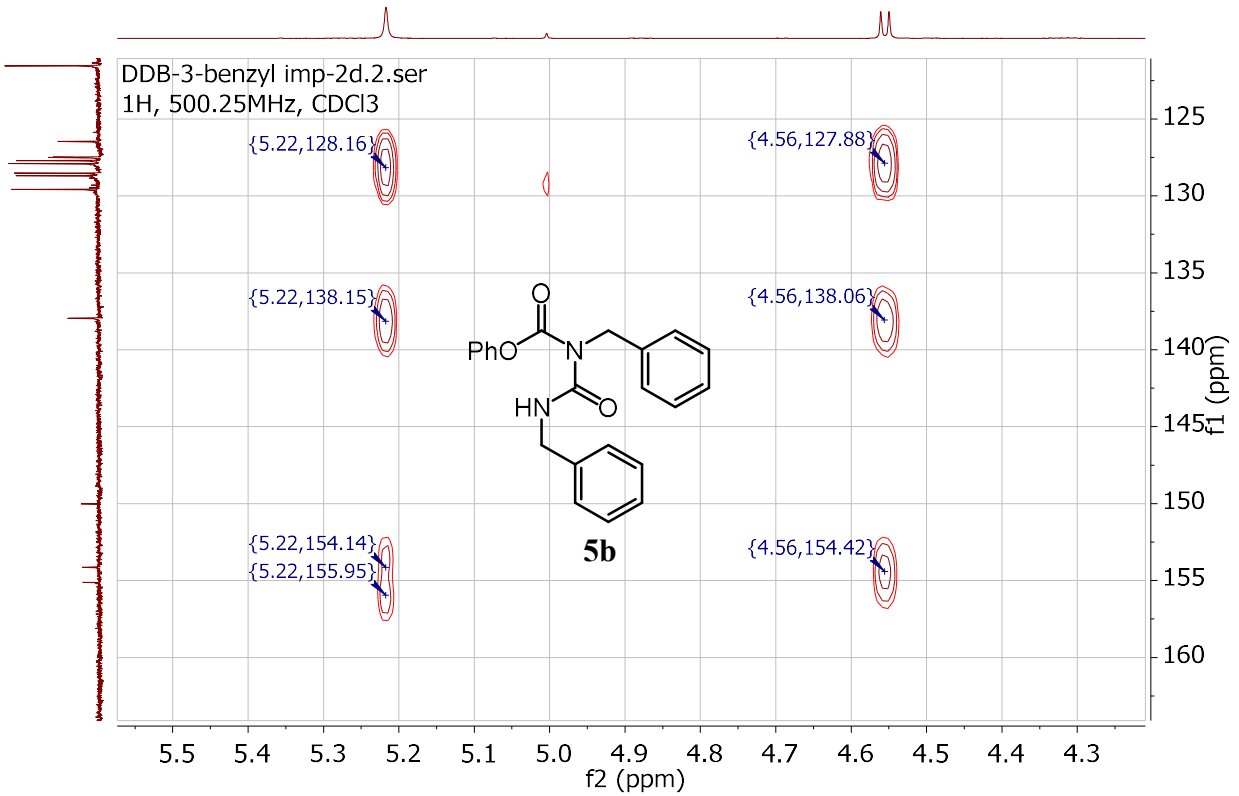
DDB-3-benzyl imp-2d.2.ser
1H, 500.25MHz, CDCl3
{5.22,128.16}
{4.56,127.88}
{5.22,138.15}
{4.56,138.06}
{5.22,154.14}
{5.22,155.95}
{4.56,154.42}
PhO
N
HN
O
O
5b
125
130
135
140
145
150
155
160
f1 (ppm)
5.5
5.4
5.3
5.2
5.1
5.0
4.9
4.8
4.7
4.6
4.5
4.4
4.3
f2 (ppm)